NCHRP

REPORT 449

NATIONAL COOPERATIVE HIGHWAY RESEARCH PROGRAM

Elastomeric Bridge Bearings: Recommended Test Methods

TRANSPORTATION RESEARCH BOARD

NATIONAL RESEARCH COUNCIL

NATIONAL COOPERATIVE HIGHWAY RESEARCH PROGRAM

NCHRP REPORT 449

Elastomeric Bridge Bearings: Recommended Test Methods

J. YURA, A. KUMAR, A. YAKUT, C. TOPKAYA, E. BECKER, AND J. COLLINGWOOD
University of Texas at Austin
Austin, TX

SUBJECT AREAS
Bridges, Other Structures, and Hydraulics and Hydrology • Materials and Construction

Research Sponsored by the American Association of State Highway and Transportation Officials
in Cooperation with the Federal Highway Administration

TRANSPORTATION RESEARCH BOARD — NATIONAL RESEARCH COUNCIL

NATIONAL ACADEMY PRESS
WASHINGTON, D.C. — 2001

NATIONAL COOPERATIVE HIGHWAY RESEARCH PROGRAM

Systematic, well-designed research provides the most effective approach to the solution of many problems facing highway administrators and engineers. Often, highway problems are of local interest and can best be studied by highway departments individually or in cooperation with their state universities and others. However, the accelerating growth of highway transportation develops increasingly complex problems of wide interest to highway authorities. These problems are best studied through a coordinated program of cooperative research.

In recognition of these needs, the highway administrators of the American Association of State Highway and Transportation Officials initiated in 1962 an objective national highway research program employing modern scientific techniques. This program is supported on a continuing basis by funds from participating member states of the Association and it receives the full cooperation and support of the Federal Highway Administration, United States Department of Transportation.

The Transportation Research Board of the National Research Council was requested by the Association to administer the research program because of the Board's recognized objectivity and understanding of modern research practices. The Board is uniquely suited for this purpose as it maintains an extensive committee structure from which authorities on any highway transportation subject may be drawn; it possesses avenues of communications and cooperation with federal, state and local governmental agencies, universities, and industry; its relationship to the National Research Council is an insurance of objectivity; it maintains a full-time research correlation staff of specialists in highway transportation matters to bring the findings of research directly to those who are in a position to use them.

The program is developed on the basis of research needs identified by chief administrators of the highway and transportation departments and by committees of AASHTO. Each year, specific areas of research needs to be included in the program are proposed to the National Research Council and the Board by the American Association of State Highway and Transportation Officials. Research projects to fulfill these needs are defined by the Board, and qualified research agencies are selected from those that have submitted proposals. Administration and surveillance of research contracts are the responsibilities of the National Research Council and the Transportation Research Board.

The needs for highway research are many, and the National Cooperative Highway Research Program can make significant contributions to the solution of highway transportation problems of mutual concern to many responsible groups. The program, however, is intended to complement rather than to substitute for or duplicate other highway research programs.

Note: The Transportation Research Board, the National Research Council, the Federal Highway Administration, the American Association of State Highway and Transportation Officials, and the individual states participating in the National Cooperative Highway Research Program do not endorse products or manufacturers. Trade or manufacturers' names appear herein solely because they are considered essential to the object of this report.

NCHRP REPORT 449

Project D10-51 FY '97

ISSN 0077-5614

ISBN 0-309-06667-0

Library of Congress Control Number 2001-131319

Price $34.00

NOTICE

The project that is the subject of this report was a part of the National Cooperative Highway Research Program conducted by the Transportation Research Board with the approval of the Governing Board of the National Research Council. Such approval reflects the Governing Board's judgment that the program concerned is of national importance and appropriate with respect to both the purposes and resources of the National Research Council.

The members of the technical committee selected to monitor this project and to review this report were chosen for recognized scholarly competence and with due consideration for the balance of disciplines appropriate to the project. The opinions and conclusions expressed or implied are those of the research agency that performed the research, and, while they have been accepted as appropriate by the technical committee, they are not necessarily those of the Transportation Research Board, the National Research Council, the American Association of State Highway and Transportation Officials, or the Federal Highway Administration, U.S. Department of Transportation.

Each report is reviewed and accepted for publication by the technical committee according to procedures established and monitored by the Transportation Research Board Executive Committee and the Governing Board of the National Research Council.

Published reports of the

NATIONAL COOPERATIVE HIGHWAY RESEARCH PROGRAM

are available from:

Transportation Research Board
National Research Council
2101 Constitution Avenue, N.W.
Washington, D.C. 20418

and can be ordered through the Internet at:

http://www4.nationalacademies.org/trb/homepage.nsf

Printed in the United States of America

FOREWORD

By Staff
Transportation Research Board

This report contains the findings of a study undertaken to develop performance-related specifications for elastomeric bridge bearings. The report includes recommended specifications and three new test methods for evaluating essential properties of elastomeric bearings. The material in this report will be of immediate interest to bridge designers and materials engineers.

Elastomeric bridge bearings have generally performed satisfactorily under current AASHTO and state DOT materials-test methods and requirements. Nevertheless, there has been concern that bearings are being unnecessarily rejected because of noncompliance with testing requirements that may not be essential or appropriate. Although specifications exist for the materials, design, and construction of elastomeric bearings, little information has been available on the relationship between test results and field performance. Additionally, some current materials-test requirements are thought to be inappropriate for bearing applications. If tests that are accurate and essential predictors of field performance can be employed, testing requirements and elastomeric bearing costs can be reduced.

Under NCHRP Project 10-51, the University of Texas at Austin addressed these concerns. Through laboratory testing and mathematical analysis, 8 of the 15 existing required tests were demonstrated to be unnecessary. Three new tests were developed to replace existing tests for creep, shear modulus, and compressive strain. This report provides full details of the research methods and the new test methods and presents recommended specifications for the acceptance testing of elastomeric bearings.

CONTENTS

AUTHOR ACKNOWLEDGMENTS

The research was performed at the Department of Civil Engineering and the Department of Engineering Mechanics at the University of Texas at Austin. The experimental portion was conducted at the Ferguson Structural Engineering Laboratory, J.J. Pickle Research Campus, the University of Texas at Austin.

Joseph A. Yura, the Warren S. Bellows Centennial Professor in Civil Engineering, was a co-principal investigator in overall charge of the project. He directly supervised Alok Kumar, private consultant and Ph.D. candidate, who conducted the aging, creep and static analyses phases of the research; Ahmet Yakut, research assistant and Ph.D. candidate, who was responsible for the low temperature phase; and Cem Topkaya, research assistant and M.S. student (currently Ph.D. candidate), who developed the shear modulus test phase. Eric Becker, Professor of Engineering Mechanics, a co-principal investigator in charge of the crack growth studies, supervised Jerry P. Collingwood, research assistant and M.S. student, who conducted the fatigue studies. All of the members of the research team contributed to the authorship of this report.

Phoenix National Laboratories, Inc., in Tempe, Arizona, provided data related to the commercial testing of elastomeric materials.

ELASTOMERIC BRIDGE BEARINGS: RECOMMENDED TEST METHODS

SUMMARY

Plain and steel-laminated elastomeric bearings have had an exemplary performance record over the past 40 years. Recently, increased testing requirements have been imposed that now make the testing of the elastomeric bearings one of the major costs of the supports. Currently, 15 different tests are required for elastomeric bearings. It is not clear whether all these tests are necessary or, in fact, are even related to the actual performance of an elastomeric bridge bearing. Historically, many of the tests have been used for much smaller products that are loaded mainly in tension. A bridge bearing is loaded mainly in shear; therefore, research was undertaken to evaluate the various tests and to determine whether or not they were important or even related to the performance of the bridge bearing. A secondary purpose was to develop new test methods that would be more cost-effective.

As a result of the research, eight different test methods were found to have little effect on the bearing behavior. Past research and some additional crack growth studies examining the fatigue behavior of elastomeric bearings reported herein determined that the ozone test was unnecessary and so the test could be eliminated. The ozone test caused some manufacturers to add antiozanant waxes that bloom to the bearing surface to provide protection. The viscous layer of wax is responsible for a significant number of serious slipping problems: in some cases, the bearings "walked out" of the support area. It is expected that waxes will no longer be added, thus improving the slip resistance. Accelerated aging tests (heat resistance) were examined because bearings taken out of service were found to perform very well with very little deterioration in their characteristics. Accelerated aging tests were conducted at two different elevated temperatures on samples loaded in shear—not tension, as required by the standard tests. This was done because the elastomeric bridge bearing is loaded mainly in shear. The research showed that the sample size was very important in establishing the significance of aging. Current test methods use very thin specimens and the results generally show significant changes because of aging. However, when even a relatively small bearing was tested in shear in this program, it was found that it would take hundreds of years of service to change the bearing stiffness by 10 percent. It was established that the aging tests are unnecessary for elastomeric bridge bearing. The compression set test, which is remotely related to creep, was replaced by a stress relaxation test that could be directly related to

creep deformation. Finite element analysis was used to determine the stress state at the bond line between the elastomer and the steel laminate. All along the bond line, the stress was compressive, which is opposite to the tension present in the peel test that purports to measure bond stress. A new bond test was developed that more closely represents the actual stress state. A full-scale bearing shear test at low temperature had performance limits that were unrealistic and was causing conflicts with other low temperature requirements as shown in the low temperature phase of the research program; therefore, this test was removed in the draft test document that was prepared.

Shear modulus is the most important physical property of the elastomer in bridge bearings. Currently, two tests are used to establish the shear modulus in the AASHTO specifications; these are known as the quad shear test and the full-scale shear test. The quad shear test requires destruction of a bearing in order to fabricate a small specimen cut from the full-size bearing. An alternative setup, which enables the full-size bearing to be tested, requires a test setup that is generally too costly for many DOTs. A new test, called the inclined compression test, was developed. This test only uses a compression test machine. The test results from the new test compared favorably with values of the shear modulus from more traditional testing methods. Both full-size bearings and samples cut from bearings were equally acceptable, and adjustment factors were developed to correlate very small samples with the full-size results. The advantage of the inclined compression test is that it can also function for several of the other tests currently required. For example, the inclined compression test can also be used to check the shear bond by merely taking the test to higher shear strains beyond service load. Similarly, a short-term compression test at 1.5 times the service load currently required for one out of every five bearings to check for shim misalignment could also use the inclined compression test.

A phase of this project was devoted to the performance of elastomeric bearings under cold temperatures. The current test methods tend to indicate that bearings fabricated in the past would fail the recently established test requirements, even though there are no reported instances of poor performance in low temperature regions. A performance-based procedure was developed in which the behavioral history of various bearings was established on the assumption that these bearings with measured material properties had been installed about 50 years ago in four different cites. It was determined that the bearings would, in fact, behave satisfactorily, even though the bearings in many instances fail the current test procedures. This indicates that the current performance requirements related to cold temperature testing are not satisfactory. A procedure was developed to determine the performance requirements at any location. In order to implement the results in design, a low temperature design criteria map will have to be developed using the procedure developed and illustrated in this report.

Steel-laminated elastomeric bearings are sometimes rejected at the manufacturing stage because of failure to comply with fabrication tolerances in the AASHTO specifications. Bearings may be rejected that, in fact, would show excellent performance in service. Therefore, a theoretical study was undertaken in which the locations of the shims in a steel-laminated bearing were varied to determine their effect on various internal stresses and deformations in the bearing. It was established that current tolerances are very conservative and some flexibility in the tolerances is warranted. A formula was developed related to the various types of shim misalignment, which would not alter the eight different performance standards by more than 10 percent.

This research has recommended that eight different elastomeric bearing tests be eliminated. Their elimination should not reduce the quality or performance of elastomeric bearings. There will be a significant reduction in testing costs if the recommendations contained herein are adopted.

CHAPTER **1**

INTRODUCTION AND RESEARCH APPROACH

BACKGROUND

Elastomeric bridge bearings, which have been used since 1950, have had remarkably good performance records. A recent survey (Chen and Yura, 1995) of all state DOTs established only a few instances of poor performance. Some pad deterioration, resulting from large shear strains on plain pads, was generally dismissed as poor initial design and not the result of problems with the elastomer material or fabrication of the bearing. There were no reported problems related to fatigue or low temperature behavior. The most common performance problem was slip when the pad was not directly connected to the pier using sole plates or other mechanical devices. Repeated slip that has resulted in the "walking out" of the bearing has been traced to excessive paraffin wax in the rubber that has been added for ozone protection (Muscarella and Yura, 1995; McDonald, 1999).

Although performance problems are rare, more frequently, bearings are rejected at the manufacturing stage because of failure to meet specified material test criteria and geometric tolerances. A summary of the test requirements from AASHTO M251-97, *Standard Specification for Plain and Laminated Elastomeric Bridge Bearings*, is given in Figure 1. There are two levels of testing, depending on the magnitude of the compressive stress. Most of these material tests were developed for rubber products that are very different from bulky bridge bearings. The tensile strength test and the percent elongation at break are considered quality control tests, even though there is very little tension within the main body of the bearing because bearings are primarily subjected to compression and shear. The main physical property that controls the behavior under this combination of stress is the shear modulus, the slope of the stress-strain curve of an elastomer subjected to shear. Currently, a shear modulus test is only required if a bearing is subjected to high compressive stresses or if bearings have been ordered for a specific modulus. All bearings are required to have a hardness (durometer) test. Prior to 1985, bearings were specified by durometer, which is a surface hardness measurement. There is a very crude relationship between rubber hardness and shear modulus. Both the *AASHTO LRFD Bridge Design Specifications* and the *AASHTO 1998 Interim Bridge Design Specifications* require that bearings specified by hardness fall within a certain range of shear moduli, and vice versa. The duality in the material requirements can cause rejection of a bearing that will otherwise perform satisfactorily.

Since the adoption of the *AASHTO Standard Specification for Highway Bridges* (AASHTO, 1992), bearings have been specified by a grade that is related to the 50-year low temperature. Two new low temperature tests were introduced—crystallization and instantaneous stiffening—both of which require new equipment and test setups. One of these tests can require 1 month to perform, which can cause construction delays and result in a significant testing cost. AASHTO M251-97 requires that Level II testing also include all Level I test requirements. The Level II test for crystallization is a shear test, which has very different test methods than the Level I shear test. It would be very difficult to satisfy both criteria. Recently, a multimillion-dollar claim was filed because bearings were not delivered on time, thereby causing construction delays. Numerous bearings had been rejected that had satisfied Level II but not Level I criteria. In the *AASHTO LRFD Bridge Construction Specifications*, only the Level II test is specified. The AASHTO M251-92 materials testing specification had, for many years, used the Level I test. That there are two AASHTO documents that define elastomeric bearing test methods (i.e., the *AASHTO Bridge Construction Specifications* and the *AASHTO Materials and Testing Specifications*) causes confusion and, in the case cited, significant costs. This situation needs to be rectified.

The overall external dimensions of a bearing are relatively easy to control, but failure to satisfy the fabrication tolerances shown in Figure 1 related to the position of the internal steel laminates is one of the most frequent reasons for bearing rejection. There is strong suspicion that small variations beyond the stated tolerances have no significant effect on bearing performance. However, there has been no documented study to evaluate these tolerances. Such a study could significantly reduce bearing rejection.

Over the past decade, significant changes have occurred in the AASHTO design, construction, and materials specifications related to elastomeric bridge bearings, even though there have been few reported performance problems. These changes have generally reduced the design compressive stress for many typical bearings, tightened fabrication tolerances on the placement of the steel laminates, and required more testing. For example, a typical 50 durometer bearing design with two steel laminates, three equal elastomer layers 12 mm (0.5 in.) thick, and a shape factor of 6 could support 5.5 MPa (800 psi) based on the *AASHTO Standard Specifications for Highway Bridges*,

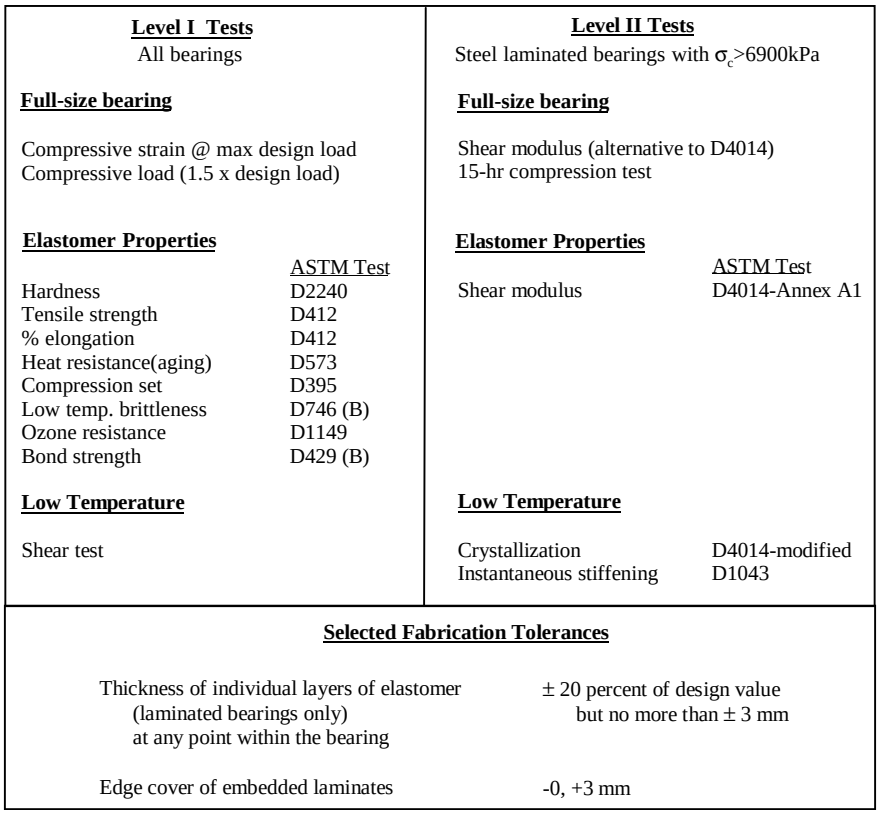

Figure 1. AASHTO M251-97 testing requirements and selected fabrication tolerances.

11th Edition (AASHTO, 1973). The 16th Edition of this specification (AASHTO, 1996) reduced this design stress by 46 percent, or 11 percent if the bearing is subjected to more rigorous testing. In order to qualify for the higher stress level that is still lower than that of the 11th Edition of this AASHTO specification, two additional tests would have to be performed: a shear modulus test and a 15-hr compression test. It is not clear that the additional testing is cost-effective or that it significantly affects bearing performance.

OBJECTIVE AND SCOPE

There is concern that bearings are being unnecessarily rejected because of noncompliance with testing requirements and fabrication tolerances that may not be essential or appropriate. In other words, despite failing current requirements, such bearings would have performed adequately for their intended purpose and design life if placed into service. Therefore, the objectives of this research are to (1) evaluate current test procedures and fabrication tolerances with respect to their effect on the performance of full-size bearings; (2) develop new cost-effective test methods, where appropriate, along with performance criteria that reflect actual behavior; (3) reorganize the various AASHTO documents that relate to elastomeric bearing materials and fabrication; and (4) eliminate incompatibilities and unnecessary redundancy of provisions. The research will concentrate on the performance of full-size bearings that generally meet the AASHTO bridge design criteria. The research will not be directed toward bearing design requirements and methods. Flat (no taper) plain and flat steel-laminated elastomeric bearings are considered. The research was limited to polychloroprene (neoprene) and polyisoprene (natural rubber) as currently permitted for bridge bearings designed in accordance with AASHTO specifications. Bearings with fabric laminates were not tested.

OVERVIEW OF CURRENT AASHTO TEST METHODS

In this section, the various AASHTO test requirements for elastomeric bearings will be critiqued (except for tensile strength and elongation at break because these are considered normal quality control tests). Because an elastomeric bearing is a relatively bulky product compared with most other rubber products, the applicability of some of the tests to bridge bearings is questionable. Many of the tests have different procedures and failure criteria for neoprene and for natural rubber, which appear illogical. It is well recognized that the

shear modulus is the most important physical property of the elastomer that affects bearing performance.

Hardness

Durometer hardness had been used as the specified elastomer material property in bridge bearings up until 1985. The specified hardness was required to be in the range of 50 to 70 (60 to 70 before 1973) with a tolerance of ±5. Other specified elastomer material requirements are independent of hardness except for elongation at break. The *AASHTO Standard Specification for Highway Bridges, Interim Revisions* (AASHTO, 1985) follows the recommendations given in *NCHRP Report 248* (Stanton and Roeder, 1982) and *NCHRP Report 298* (Roeder and Stanton, 1987). It was strongly suggested that bearings be specified by shear modulus because hardness is a surface measurement that only crudely represents the stress-strain relationship in shear. The interim revisions to the AASHTO standard specification (AASHTO, 1985), based on the research presented in *NCHRP Reports 248* and *298*, presents a range of shear modulus values corresponding to specific hardnesses of 50, 60, and 70 to be used when bearings are ordered by hardness rather than shear modulus. In such cases, the shear modulus, as determined by the test methods in AASHTO M251-97, must fall within the specified ranges or the lot is rejected.

Bearings with steel laminates currently are limited to hardness in the range of 50 to 60, even though much of the prior performance history included 70 durometer. The international railway specification (UIC Code 772, 1973) permits the use of natural rubber in the hardness range of 50 to 70. A bearing satisfying a specified shear modulus can still be rejected if the hardness is outside the 50 to 60 range. Shear modulus is the more important property for bearing design, and, while it is related to hardness, it may vary significantly among compounds of the same hardness.

Shear Modulus

In AASHTO M251-97, there are two test setups for determining the shear modulus: (1) a nondestructive test on a pair of full-size bearings sandwiched between three platens and (2) the ASTM D4014-89 quad shear test on small rubber samples cut from a bearing and cold-bonded to rigid plates. These are shown in Figure 2.

In the typical full-scale shear test setup, a compressive force is applied to the assemblage and is held constant during the test. A horizontal shear deformation is applied to the middle platen to simulate bridge movement resulting from temperature changes. The shear deformation can be applied in one or two directions.

In the quad shear test, the test piece is strained in a tension machine to an average 50-percent strain in each rubber block. Shear modulus values are calculated on the basis of the stress at 25-percent strain. In this test, the elastomer is strained in only one direction. In the cold temperature test procedure, the ASTM D4014-89 test method is specified, except that specimens are subjected to a cyclic strain of ±25 percent, a two-way test. Unfortunately, the quad shear specimen is potentially unstable when compression is applied, so the setup will become complex. In one laboratory that routinely conducts cold temperature tests, only a one-way tension test was performed—this does not satisfy the stated test requirement. The full-scale shear test setup shown in Figure 2 is the most realistic because bearings with and without sole plates can be tested, but it is also the most costly. A more cost-effective means of determining shear modulus in a finished bearing is needed.

Elastomers exhibit a nonlinear response under shear (as shown in Figure 3), so the value of the shear modulus changes with its definition. The bearing response shown was determined with the full-scale shear test setup after the specimen had been strained to the specified maximum strain a number of times to minimize stress softening, often called the Mullins effect (Mullins, 1987). Shear modulus is determined as the slope of a line between two points on the stress (load/area)-strain (displacement/total elastomer thickness) curve. Table 1 shows the relative values of shear modulus based on the various definitions that appear in the literature compared with the modulus from line d-e (secant modulus at 50-percent strain). The 50-percent secant modulus definition gives the correct value of the maximum shear force when the bearing is strained to the maximum design level, which is an important performance (design) limit. The ASTM quad shear definition at 0.25-percent strain gives a value that is 11-percent high, whereas the value based on the cold temperature test definition (line a-c) is 21-percent low. There is a 7-percent difference between the measured shear modulus based on maximum

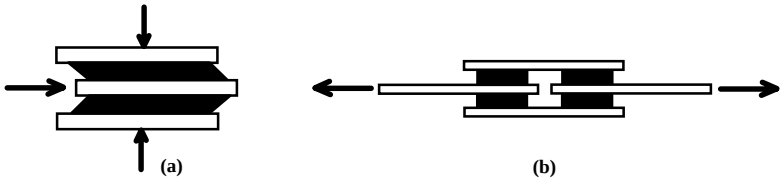

(a) Full-Scale Shear Test (b) ASTM D-4014 Quad Shear Test

Figure 2. Shear modulus test setups.

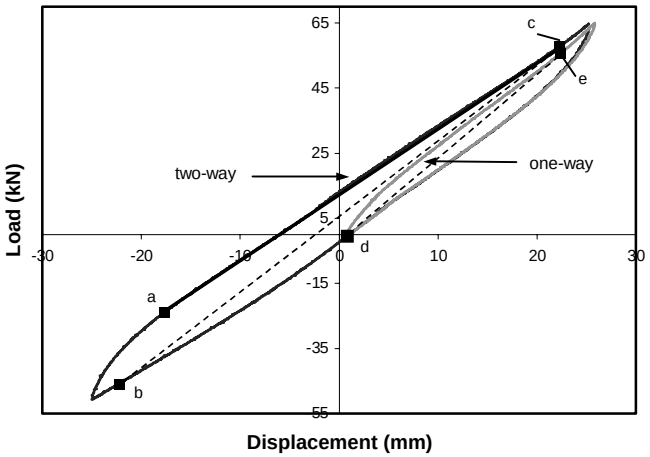

Figure 3. Typical load-displacement response of an elastomer under shear.

strain for either one-way or two-way behavior. Defining the shear modulus based on the flat portions of the stress-strain curve for either loading or unloading gives a lower shear modulus and unconservative estimates of the maximum anticipated shear force.

Throughout this report, the shear modulus reported will be based on the slope of a straight line drawn between the origin and the measured shear stress at the maximum specified shear strain for a one-way test, otherwise known as the secant shear modulus. For a two-way test, a secant line drawn between the positive and negative maximum specified strain will be used in calculations. All shear moduli will be based on the 50-percent secant definition unless otherwise stated because this definition will be recommended as the standard.

Heat Resistance

Aging of elastomers involves a progressive change in their physical and chemical properties, usually marked by deterioration. Factors that contribute to the deterioration of elastomers include ozone, heat, oxygen, sunlight, and humidity. However, in actual practice, the effects of heat and oxygen can hardly be separated. For this reason, the tests designed to determine heat resistance are normally carried out in air. Consequently, the property changes are caused by a combination of heat and oxygen. The long-term effects bring about major changes in the elastomeric material and are permanent. Such changes are caused by chemical reactions, normally leading to progressive increase or decrease in hardness and modulus with loss in tensile strength, elongation, and elastic properties.

TABLE 1 Shear modulus from different definitions

Definition of Shear Modulus	Test Direction	G / G_{d-e}
0-25 percent secant	One-way	1.11
0-50 percent secant (d-e)	One-way	1.00
+/- 50 percent secant (b-c)	Two-way	0.93
+/- 25 percent tangent	Two-way (Top line)	0.79
+/- 25 percent tangent	Two-way (Bottom line)	0.83
cold temperature (a-c)	Two-way (Top line)	0.79

Heat aging tests are carried out for the following purposes: to measure changes in the rubber vulcanite at the elevated service temperature (usually 70°C); as an accelerated test to estimate natural aging at normal ambient temperature; and as a quality control test. ASTM D573 is the test method that AASHTO uses for determining heat resistance or accelerated aging. This test determines the influence of elevated temperature on the physical properties (e.g., hardness, elongation at break, and tensile strength) of a small sample of vulcanized rubber. Small specimens of vulcanized rubber are exposed to the deteriorating influence of air at specified temperatures for known periods, after which the physical properties of the specimens are determined. The properties from the exposed specimens are compared with those of unaged specimens, and the changes must be less than the specified limits. AASHTO limits are greater than the ones required by Eurocode, British, and Australian codes. The test requirements and tolerances are different for natural rubber and neoprene.

Accelerated aging tests are best used only as a basis for comparison, because there is no known way of relating the test conditions to actual service life. Also, no correlation exists between accelerated aging and normal aging (Nagdi, 1993; Long, 1974). Because of the bulk and sheltered location of bearings, aging in practice is very slow, and readings after 5 years indicate very little change (Long, 1974). It is questionable that this test method gives any indication of the performance of the bearing. Given that the correlation between the test and the real situation is not known, it seems that the test is just a quality control test, not a performance test. It is also believed that there should be no distinction in test parameters and tolerances between neoprene and natural rubber because any bridge bearing must provide a certain performance during its service life. In this context, the necessity and validity of the heat resistance test for the aging of bridge bearings need to be investigated. A few studies (discussed later) have shown that the physical properties of bearings taken out of service after many years show little change.

Ozone Resistance

The aging resistance of natural rubber is not as good as neoprene but degradation resulting from heat, ozone, and oxygen attack can be prevented by the incorporation of protective compounds. Waxes are used in rubber to protect against oxygen and ozone attack. They bloom to the rubber

surface to create a physical barrier protecting the product from oxygen and ozone attack. Blooming of the wax to the exposed surface continues until the level of wax remaining is completely soluble in the rubber compound. As discussed earlier, a disadvantage of the blooming process is that bearing slip resistance can be reduced. Chemical antidegradants are also available to improve the resistance of rubber to environmental attack. Neoprene is highly resistant to oxidative aging and flex cracking and is almost completely ozone-resistant. In unstretched rubber, ozone degradation is confined to a thin surface layer, typically 0.5-microns thick, creating frosting, a white bloom-like appearance of the rubber (Lewis, 1986). Ozone attack is less apparent in unstretched rubber, because frosting is restricted to very slow uniform erosion of the surface with no visible cracks.

Rubber under tensile strain is susceptible to ozone cracking, a phenomenon that is much more serious and visible than frosting. Ozone cracks develop at right angles to the tensile strain. Ozone cracks are not simply unsightly, they degrade rubber tensile strength and may initiate fatigue growth that ultimately can lead to failure of the rubber product (Gent, 1992). Because cracks will only occur in regions where tensile stresses are induced, they are unable to penetrate very far into objects under compression where tensile forces only occur at the surface of the product. In objects mainly under compression or shear, growth ceases close to the surface because the cracks quickly encounter compressive rather than tensile stresses. Most researchers seem to agree that crack growth increases at higher strains (Gent, 1992; Lewis, 1986; Mathew, 1991).

All sources that evaluated the ozone test agreed that the ozone tests required by AASHTO are overly stringent for large, bulky rubber products, specifically bearing pads. Five research studies (Braden and Gent, 1960; Lake, 1970; Lewis, 1986; Roberts, 1988; Stevenson, 1985) contend that ozone damage is a serious concern in thin-walled products, but not in those rubber products with a large volume of rubber and relatively small surface area. In addition to finding that ozone degradation does not significantly affect the performance of a bulky product, the researchers cited above also contend that the ozone tests required by AASHTO cannot correctly evaluate an elastomer for use in a bearing pad. The ASTM ozone test does not accurately model the elastomer response to ozone attack in bearings because the test uses thin rubber test specimens in tension to evaluate bulky products in compression and shear, using elevated test temperatures and high ozone concentrations. Stevenson states that "accelerated tests exposing thin rubber sheets to elevated temperatures can give a misleadingly pessimistic view of longevity of rubber pads for civil engineering applications" (Stevenson, 1985). The researchers agree that ozone attack is much slower and less damaging than indicated by tensile tests. They also found that the performance of a bulky product like a bridge bearing is not affected by ozone attack.

However, the researchers did not study the problem of the exterior elastomer cover falling outside typical bearing pad specifications and lacking adequate thickness. If the bearing has a thin exterior layer, the stresses could be much larger. The failure mechanism could be an ozone crack exposing the steel shim and causing corrosion. Also the fatigue behavior of the bearings must be analyzed before coming to a firm conclusion. After performing analytical studies of the fatigue behavior, the effect of ozone on the bearings can be better understood. The results of additional research on crack growth may result in a modified ozone test procedure or even elimination of the test.

Low Temperature Behavior

When elastomers are exposed to low temperature, various types of stiffening take place. As an elastomer is cooled it becomes stiffer (instantaneous stiffening) and at very low temperatures becomes glass-like and brittle (glass transition temperature). Under static loading, the glass transition temperature is about −65°C and −45°C for natural rubber and neoprene, respectively (Long, 1974). If an elastomer is cooled to a moderately low temperature and held there for a period, it undergoes a phase change, a molecular realignment, and it becomes much stiffer. This change, called crystallization, is evident only after prolonged exposures. It may require days, weeks, or even months, depending on the exposure temperature and the composition of the elastomeric material. For each elastomer, there is a characteristic temperature at which crystallization takes place most rapidly. For unstrained elastomers, this temperature is near −10°C for neoprene and −25°C for natural rubber. Crystallization is slower above and below these temperatures. Application of stress usually increases the crystallization rate. Low temperature crystallization is not a problem if the elastomeric component is subject to frequent movements because heat generated during these movements will melt the crystals (Long, 1974). The low temperature stiffening effects are reversible; stiffening disappears when the elastomer warms up.

AASHTO M251-97 has four test procedures for the determination of low temperature properties of elastomeric bridge bearings—brittleness, instantaneous thermal stiffening, crystallization, and a shear test. These methods are employed to ensure that an elastomeric bearing would be satisfactory under a certain low temperature exposure during its service life. The temperature and exposure requirements for the AASHTO tests vary depending on the elastomer grade summarized in Table 2, based on the 50-year low temperature record. The required grade is based on the more severe of the two parameters, the lowest recorded temperature or the maximum number of consecutive days when the maximum temperature is below freezing (0°C). A brief description of these test methods is given below.

TABLE 2 AASHTO low temperature elastomer grades

Elastomer grade	0	2	3	4	5
50 year low temperature (˚C (˚F))	-18(0)	-29(-20)	-34(-30)	-43(-45)	all others
Maximum number of consecutive days that the high daily temperature is below 0˚C (32˚F)	3	7	14	N/A	N/A

Brittleness

The elastomeric bearing compounds are required to pass the ASTM D746-95, Procedure B, test to qualify for use at very low temperatures. No test is required for Grades 0 and 2 elastomers. Tests are required for Grades 3, 4, and 5 at temperatures of –40°C (–40°F), –48°C (–54°F), and –57°C (–71°F), respectively. The ASTM D746-95 test method basically addresses the determination of the temperature at which plastics and elastomers exhibit brittle failure under specified effect conditions. Five specimens are immersed in a bath where they are cooled by dry ice and liquid nitrogen. The specimens are held as cantilever beams. After being struck at a specified linear speed, the specimens are removed and examined. All specimens must pass the test. Failure is defined as the division of the specimen into two or more completely separated pieces or the formation of any crack in the specimen, which is visible to the unaided eye. Prior to 1992, all bearings had to pass ASTM D746-95 at –40°C (–40°F) as a quality control measure.

Instantaneous Thermal Stiffening

ASTM D1043-92 is employed to evaluate the amount of instantaneous stiffening at specified temperatures. Grades 0 and 2 bearings are tested at –32°C (–26°F). The test temperatures are specified to be –40°C (–40°F), –46°C (–51°F), and –54°C (–65°F) for Grades 3, 4, and 5, respectively. The elastomer compounds pass the test if the increase in stiffness is not more than 4 times the room temperature stiffness. This test method was developed to determine the stiffness characteristics of plastics by direct measurement of the shear modulus. The modulus value is obtained by measuring the angle of twist occurring when the specimen is subjected to an applied torque. Rectangular test specimens 63.5 mm by 6.35 mm (2.5 in. by 0.25 in.), having a thickness of 1 to 3 mm (0.04 to 0.12 in.) are cut from the bearing. The test specimen is mounted in the test apparatus that is capable of applying a torque sufficient to twist a test specimen through an angle between 5 deg and 100 deg. The specimen is conditioned at the specified test temperature for 3 min, +15 sec –0 sec, the torque is applied, and the angle of twist is noted. In ASTM D1043-92 the shear modulus is calculated as follows:

$$G = \frac{917TL}{uab^3\phi} \quad (1)$$

where

G is the shear modulus in Pa (or psi),
T is the applied torque in N-m (or lbf-in.),
L is the specimen length in mm (or in.),
a and b are the larger and smaller cross-sectional dimensions, respectively, in mm (or in.),
ϕ is the angle of twist in degrees, and
u is a constant that depends on the ratio of a to b.

The ratio of the two measured T/ϕ values, one at the specified low temperature, and one at room temperature, must be less than 4. Equation 1 is the same as the classic torsion equation, $T = GJ\phi/L$, where J is the torsion constant for a rectangular cross section. Equation 1 assumes that there is a proportional relationship between T and ϕ; this is not true for rubber, so the applicability of this method is questionable.

Low Temperature Crystallization

A test method was developed by Roeder et al. in *NCHRP Report 325* (Roeder et al., 1989) to evaluate the stiffness of an elastomeric bearing at a certain temperature for a specified period. AASHTO M251-97 requires no test for Grade 0 bearings, but Grades 2, 3, 4, and 5 bearings are required to be tested after being subjected to exposures of 7 days at –18°C (0°F), 14 days at –26°C (–15°F), 21 days at –37°C (–35°F), and 28 days at –37°C (–35°F), respectively. The stiffness is specified to be less than 4 times the room temperature stiffness. The room temperature stiffness is determined by the quad shear test of ASTM D4014-89, Annex A. The specimen is subjected to six load cycles at 50-percent shear strain with each cycle applied in 30 to 60 sec. The shear modulus is calculated from the force-deflection curve at the sixth cycle using the data at 25-percent strain. The shear modulus test procedure at low temperatures is different from the one at room temperature. The stiffness is measured with a quad shear test rig in an enclosed freezer; however, the specimen is subjected to a ±25-percent strain cycle with a complete cycle of strain applied within a period of 100 sec. The first 0.75 cycle of strain is discarded and the stiffness is determined from the slope of the force-deflection curve for the next 0.5 cycle of loading as shown by line a-c in Figure 3.

The test procedure described in Annex A of ASTM D4014-89 is a one-way test developed for room temperature stiffness measurements, whereas the AASHTO low temperature crystallization test specifies a two-way test. This can lead

to confusion for personnel conducting the test. The testing facility that conducted the certification tests of the bearings ordered for this research was visited to find out how the test was carried out. The researchers observed that the cold temperature tests were done in one direction only (one-way test).

Shear Test

The Level I shear test, described in AASHTO M251-97, requires that at least two pads per lot be tested. The bearing is conditioned at –29°C (–20°F) for 96 hr. The conditioned bearing is tested in open air with a compressive stress of 3.45 MPa (500 psi) applied. The bearing is then sheared to 25-percent maximum shear strain and held at this strain for 15 min. After this period, the shear stress is measured. The test is required to be completed within 30 min after the specimen is removed from the cold environment. For a bearing constructed with 50 durometer elastomer, the measured stress at 25-percent strain must be less than 0.35 MPa (50 psi) for neoprene and 0.21 MPa (30 psi) for natural rubber. These stress levels give maximum permissible low temperature secant shear moduli of 1.38 MPa (200 psi) and 0.83 MPa (120 psi) for neoprene and natural rubber, respectively. This test does not appear to have a rational performance criterion because G at room temperature can be greater than 0.83 MPa (120 psi) and there are no requirements for bearings with a durometer hardness greater than 50.

Creep and Compression Set

Creep and compression set are methods of evaluating the long-term effects of an applied stress or strain. Creep is the measurement of the increase of strain with time under constant force while compression set is the measurement of recovery after the removal of an applied stress or strain. In a creep test, a constant force is applied to the rubber and the change in deformation with time, is monitored. Detailed procedures were not standardized internationally until ISO 8013 was published (ISO 8013, 1988) and there is still no general ASTM method. AASHTO has no creep test, even though AASHTO specifications require an evaluation of long-term deflection. When test data are not available (the usual case), the AASHTO bridge design specifications estimate the creep deflection as 25 percent, 35 percent, and 45 percent for an elastomer hardness of 50, 60, and 70, respectively. Further discussion of creep test methods is given in Chapter 2.

Compression set, rather than creep, is generally given more attention. This is partly because of the relatively simple apparatus required and because it appears that set is the important parameter when judging sealing efficiency. Set correlates with relaxation only generally and it is actually the force exerted by a seal that usually matters, rather than the amount it would recover if released. The test piece is more or less instantly compressed and held at that compression for a fixed length of time. The test piece is released and its recovered height measured. Set is normally expressed as a percentage of the applied deformation but can be expressed as a percentage of the original thickness. The measurement of set is an effective quality control test: it is a relatively simple test and the results are sensitive to state of cure. However, the usual short-term set measurements do not correlate well with long-term performance. A direct practical test for creep is needed.

RESEARCH APPROACH

Elastomeric bearings placed between the bridge girders and their supports have two main functions: support the gravity loads (dead load and live loads) and accommodate the changes in the length of the bridge resulting from temperature variations and rotations caused by bending. Bearing performance is affected by the following parameters: stiffnesses (i.e., compressive, rotational, and shear), slip, rubber-to-metal reinforcement bond strength, fatigue of the elastomer, creep and stress relaxation, aging, steel reinforcement stresses, and elastomer stresses and strains. Many of these parameters are controlled by the characteristics of the stress-strain curve of the elastomer represented by the shear modulus, so it is important to have an accurate measure of shear modulus in the finished bearing. Some other parameters cannot be checked directly by simple laboratory tests. For example, the stresses in the steel laminates cannot be measured because they are not accessible. Indirectly, a reduction in the compressive stiffness can be associated with yielding in the steel or failure of the bond at the elastomer-steel interface. In a possible performance test, a bearing could be loaded to, for example, 2 times the design load and the stress-strain relationship established. If there is no decrease in stiffness, then indirectly, the reinforcement stresses and the bond have been checked. Geometric factors affect the maximum shear strain, tensile stress, and compressive stiffness. The effect of steel shim misalignments on the state of stress within the bearing cannot be directly measured, but finite element analysis can be used to establish their probable effect on performance. Therefore, to meet the project objectives, an experimental and analytical research plan was developed to determine how the outcome of material tests and fabrication tolerances relate to the performance of full-size elastomeric bearings. For steel-laminated bearings, the same bearing geometry was used in both the experimental and analytical phases to better coordinate the performance evaluation.

Experimental Phase

The experimental phase (discussed in Chapter 2) focused on the following critical bearing parameters: shear modulus, low temperature performance, creep, and aging. A new test method for shear modulus was developed in which only a compression test machine is required to apply compression and shear forces

simultaneously to a pair of bearings. This test method could be a more cost-effective replacement for ASTM D4014-89, Annex A1. Parameters, such as testing speed, test setup details, and size of specimens, were evaluated in order to develop a method suitable for a testing specification. Experiments were also conducted to compare the results from the new method with those from other shear modulus test methods.

The low temperature phase was designed to evaluate all the test methods listed in Figure 1 except brittleness, which is considered a quality control test. The Level I shear test and the instantaneous thermal stiffening test (ASTM D1043-92) were evaluated with respect to their ability to accurately measure the respective parameters. The first part of the low temperature research focused on heat transfer within the bearing itself in order to establish reliable test techniques, such as the conditioning time required for a bearing to reach a specified temperature. The results have a direct effect on the evaluation of the Level I shear test, which is conducted in the open air outside of the freezer with readings taken between 15 and 30 min after the bearings are removed from the freezer. Crystallization stiffening was studied first by determining if crystallization could occur in actual practice. Previous research suggested that the cyclic nature of bridge loads, many cycles of compressive live load from trucks and daily fluctuations of shear strain because of daily temperature changes retard crystallization. Most of the low temperature research in Chapter 2 is related to low temperature performance criteria that required the development of methodology to evaluate the site-specific temperature history and its effect on bearing performance. After performing some tests to determine the actual cold temperature properties of four bearing materials certified as Grade 3, virtual experiments were conducted to establish their performance over a 50-year period in four selected cities. This work was used to develop performance-based criteria for establishing cold temperature test requirements and evaluate the existing criteria (low temperature $G \leq 4 \times$ room temperature G) at specified temperatures and conditioning times.

The compression set test ASTM D395-89 cannot be related to long-term creep behavior, so a new 6-hr test was developed to determine the long-term shear modulus, which the research team hoped was directly related to the long-term compressive and shear deflection. Full-size bearings were tested to obtain creep data that were used in evaluating the new test. The new test method would be expected to replace the compression set test. The same test setup and test specimens were evaluated for determining the shear-bond performance and as a replacement for the bond (peel) test, ASTM D429-82.

The heat resistance (i.e., aging) test ASTM D573 was evaluated by conducting experiments for shear modulus at elevated temperatures for specified periods. The changes in the shear modulus at elevated temperatures over time were used to predict long-term changes in the bearings shear stiffness (i.e., shear modulus). Both large and small test samples were considered.

Analytical Phase

In Chapter 3, the analytical phase of the research program is presented. Two existing finite element computer programs that could handle the nonlinear properties of the elastomeric material were used to evaluate the performance consequences of steel laminate (shim) misalignment and surface cracks. The evaluation of the tolerance limits on shim misalignment given in Figure 1 was accomplished by developing a statistically based research approach to determine the effect of three types of shim movement (i.e., horizontal shift, vertical shift, and rotation) on eight performance parameters (e.g., compressive stiffness, maximum steel stress, and maximum elastomer strain). Four different stress-strain relationships from the experimental phase were used to represent soft (50 durometer) and hard (70 durometer) materials, of both natural rubber and neoprene, so that general conclusions could be reached with respect to fabrication tolerances.

A crack growth study was used to evaluate the significance of ozone-induced surface cracking and its consequences as cycles of live load are applied to the bearing during its service life. A slow crack growth would indicate that the ozone test could be eliminated.

Implementation

The results of the research reported in Chapters 2 and 4 are coordinated into recommended changes to the AASHTO bridge construction specifications and the AASHTO material test specifications as discussed in Chapter 4. The draft changes to these sets of specifications are given in Appendixes D and E. The individual test method specifications that were developed and some of the details from certain phases of the research are reported in the other appendixes.

CHAPTER **2**

EXPERIMENTAL STUDIES

The four experimental phases described in this chapter—shear modulus, low temperature behavior, creep and aging—all used the same bearing material and bearing configuration. So, before presenting the testing details, the test bearings used will be described. The basic rectangular steel-laminated bearing design chosen for testing and analysis was 44.5 × 229 × 356 mm (1.75 in. × 9 in. × 14 in.) with two 3.2-mm (0.125-in.) steel shims. The three elastomer layers all had the same 12.7-mm (0.50-in.) thickness as shown in Figure 4. All laminated pads had an edge cover of 6.4 mm (0.25 in.). The actual manufactured bearing had a length of 711 mm (28 in.), which was typically cut in half, 229 × 356 mm (9 × 14 in.), and tested in pairs in most of the test setups. This ensured that the pair of bearing came from the same material. When cut in half, these bearings have dimensions commonly used in practice; the shape factor (loaded area/area free to bulge) is 5.5. A steel-laminated circular bearing with a 381-mm (15-in.) diameter and same thickness profile as shown in Figure 4 (shape factor = 7.5) and a 24.5 × 229 × 711-mm plain pad (shape factor = 2.7 when the bearing is cut in half) were also manufactured. Some bearings were fabricated with thermocouple wires inserted within the bearing for use in the low temperature phase. All bearings were flat. In general, the supplied bearings had dimensions close to the specified ones. Some minor variations were present, but they did not significantly influence the test results, so the specified dimensions will be used in calculations.

All bearings were ordered from the same manufacturer with a specified shear modulus, not hardness, and Grade 3 low temperature rating. In order to investigate the possible differences between compounds, both natural rubber (NR) and neoprene (NEO) bearings were used, each with three different shear modulus values: 0.69, 1.03, and 1.38 MPa (100, 150, and 200 psi). These modulus values represent typical values that have been used in practice. All bearings with the same specified material came from the one rubber batch to minimize variations among individual bearings. Throughout this report, a bearing is identified by its material and specified shear modulus in psi. Thus, NR150 is a natural rubber bearing with a specified shear modulus of 1.03 MPa (150 psi). Selected results from the certified test reports supplied by the manufacturer are given in Table 3. The certifications indicate that the bearings satisfied the specified AASHTO requirements. In addition, when bearings were cut, it was observed that there was no significant shim misalignment. The tolerance values for shim misalignment in the AASHTO M251-97 were satisfied. A total of 54 bearings were used in the test program, because many of the test phases were conducted simultaneously. The surfaces of the bearings were steam cleaned, prior to testing, to remove surface wax.

INCLINED COMPRESSION TEST FOR SHEAR MODULUS

For a satisfactory design, the shear modulus of the bearing has to be determined reliably. Currently, a cost-effective, easy test method for determining the shear modulus of full-size elastomeric bearings is needed. The focus of this research phase was to develop a new test procedure for determining the shear modulus in a finished bearing. A new test method, called the inclined compression test, is proposed for this purpose. The test setup is described and shear modulus results from the new test are correlated with experimental results from a traditional full-size test setup. In addition, the effects of certain test parameters (e.g., compressive stress, shape factor [sample size], surface conditions, speed of testing, and edge cover) were investigated in order to establish a valid test procedure.

Inclined Compression Test Setup

In the inclined compression test setup, two bearings are sandwiched between three inclined aluminum platens (i.e., top, center, and bottom) in a compression test machine as shown in Figures 5 and 6. When compression is applied to this arrangement of bearings and platens, a simultaneous shear force is applied to the bearings. The magnitude of the shear force, H, on one bearing is given by $H = s \times W$, where s is the slope of the platen and W is the measured compressive force. For a 1:10 slope, the shear force is 10 percent of the compressive force. The shear force causes the center platen to move horizontally a distance Δ_s, which is measured. The secant shear modulus can then be calculated from

$$G = \frac{sWh_{rt}}{A\Delta_s} \tag{2}$$

where

h_{rt} = total elastomer thickness of bearing pad and
A = surface contact area.

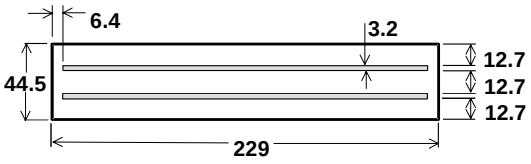

Figure 4. Section of steel-laminated bearing (mm).

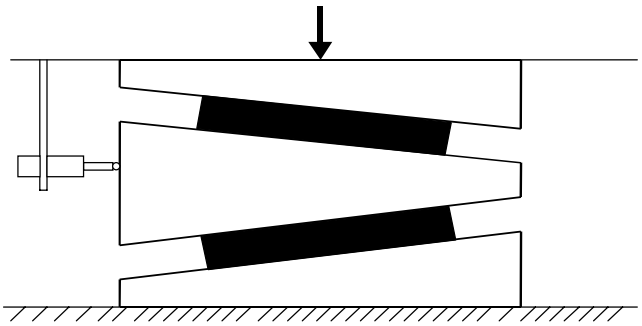

Figure 5. Schematic of the inclined compression test.

Aluminum was chosen for the platen material because of its lighter weight and the lower cost of milling the slope. The platens had 508 × 508 mm (20 × 20 in.) plan dimensions, which were adequate to accommodate most typical sizes of bridge bearings, both circular and rectangular. Top and bottom plates were mounted to a 2700-kN (600-kip) compression machine. The center platen was sloped on both sides. Two sets of inclined platens were used in the research program. One set had a slope of 1:10 and the other set had a 1:20 slope. Platen surfaces were roughened to simulate a concrete surface in order to prevent slipping of the bearings. Several artificial surface conditions were tried (i.e., sandblasted, sand paper, and mechanically roughened), but platen surfaces roughened by an impacting tool used to roughen concrete surfaces (see Figure 7) were the most durable. Details related to different surface conditions will be given later. Compressive load and displacement of the middle platen were recorded during testing using a data acquisition system. Data were recorded every 1 sec so that the complete load-displacement response could be documented. Linear potentiometers accurate to 0.025 mm (0.001 in.) were used to monitor the displacement.

Findings

Independent full-scale shear tests were conducted to evaluate the reliability of the results from the inclined compression test. The full-scale shear test setup (represented schematically in Figure 2a), had independent compression and shear loading systems. The desired compression load was applied first, and then the pair of bearings was displaced to the required shear deformation level using screw jacks. Details of this test setup are provided by Muscarella and Yura (Muscarella and Yura, 1995). The test setup was designed to duplicate the dead weight and the daily thermal deformation response of the bridge girder. In order to simulate the same surface conditions, flat aluminum platens with the same roughness as the inclined compression setup were used. Linear potentiometers were mounted to record the middle platen displacement.

Tests for Shear Modulus Correlation

Rectangular, circular, and plain bearings using all six materials listed in Table 3 were tested in both the full-scale and inclined setups. Roughened aluminum surfaces were used in both test setups. For the full-scale shear tests, a compressive stress of 3.10 MPa (450 psi) was applied to laminated and plain rectangular bearings while a stress of 4.48 MPa (650 psi) was applied to laminated circular pads. The pads were sheared to slightly higher than 50-percent strain in one direction. The direction of the force was then reversed and the pads were sheared to slightly higher than 50-percent strain in the opposite direction. The rate of displacement of the bearings was 2.54 mm (1 in.) in 18 min. The loading and unloading cycles were repeated until the load-displacement curve stabilized. Figure 8 shows a typical shear load-displacement curve obtained from a full-scale shear test after a few cycles. The shear modulus was determined from the slope of the secant line between ±50-percent strain (dashed line) using Equation 2.

TABLE 3 Certified manufacturers' report–selected tests

Specimen Type	Shear Modulus MPa (psi)		Hardness (Durometer)	Normalized Shear Modulus (G_{cold}/G_{room})	
	Specified	Report		Instantaneous	Crystallization
NEO100	0.69 (100)	0.63 (92)	53	1.09	3.33
NEO150	1.03 (150)	1.06 (154)	66	1.23	2.67
NEO200	1.38 (200)	1.25 (182)	70	1.37	2.01
NR100	0.69 (100)	0.78 (114)	52	1.10	2.80
NR150	1.03 (150)	0.97 (141)	59	1.20	2.40
NR200	1.38 (200)	1.34 (194)	66	1.20	2.40

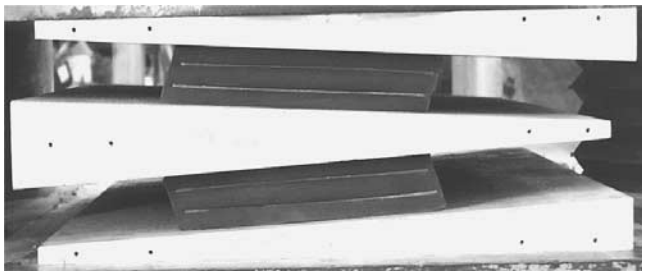

Figure 6. Side view of the inclined compression test setup.

In addition to the two-way test, a one-way test was also performed, but the difference in shear modulus between a one-way and a two-way test was minimal.

Specimens were tested in the inclined compression test setup with both the 1:20 and the 1:10 sloped platens. A compressive force was applied such that the shear strain on the bearings was slightly higher than 50 percent. Then, the specimen was unloaded until the compressive load reached 4.44 kN (1 kip). A similar loading procedure was used for the successive cycles. Testing was continued until the load-displacement curve stabilized—usually about four cycles. In general, the first cycle was significantly different from the others. The rate of displacement of the bearings was similar to that used in the full-scale shear test. Figure 9 shows a typical load-displacement response obtained from an inclined compression test, which includes all five loading-unloading cycles. The shear modulus was determined from the secant line corresponding to a change in strain of 50 percent on the last cycle, using Equation 2. For this test, the shear modulus changed from 0.96 to 0.99 MPa (140 to 144 psi) from the first to the fifth cycle. In Figure 10, the full-size test results, nondimensionalized by the specified shear modulus, are compared with those from the ASTM 4014-89, Annex 1, test, hereinafter called the quad shear test. In Figure 10 and subsequent figures, the letters R, P and C refer to *R*ectangular, *P*lain and *C*ircular full-size bearings. The quad shear test results were taken from the test certification in Table 3. The purpose of the comparison is to evaluate the significance and reliability of the quad shear test to predict the shear behavior of a full-size bearing. These certified results could have come from a similar rubber batch, not necessarily from the rubber batch actually used. The quad shear test results are within the ±15 percent tolerance required by AASHTO. The full-scale shear test gave lower shear modulus values than the quad shear test. Other researchers made the same observation (Arditzoglou et al., 1997). The average difference for all the data in Figure 10 is 21 percent.

There are three principal reasons for the difference between the full-scale shear modulus and the quad shear shear modulus:

1. Different strain levels are used to define the shear modulus. Because of the nonlinear response characteristics of rubber, the amount of strain can significantly affect the differences between these two test methods. In the quad shear test the shear modulus was determined at 25-percent strain, while in the full-scale shear test, the shear modulus was calculated at 50-percent strain. In Table 1 the effect of strain level was 11 percent; examination of many other data shows that the effect is

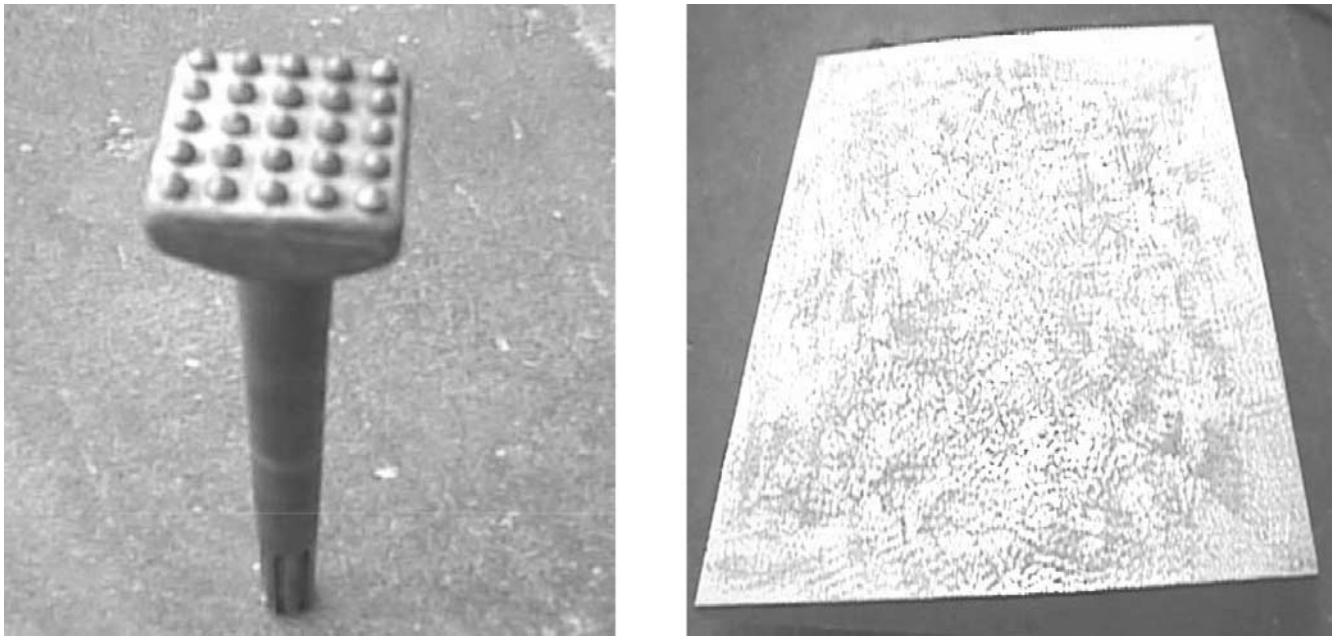

(a) roughening tool

(b) roughened aluminum

Figure 7. Surface preparation of platen surface.

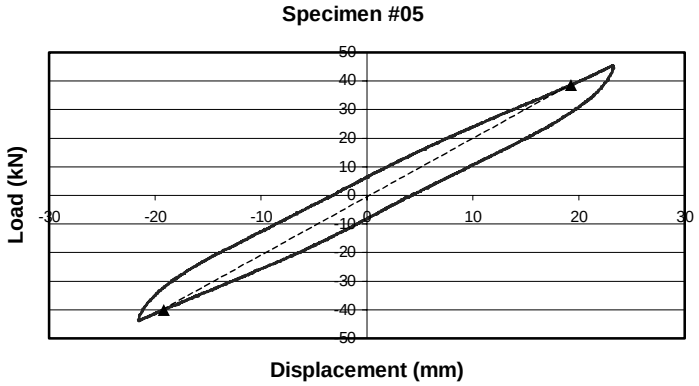

Figure 8. Typical load-displacement curve from a full-scale shear test.

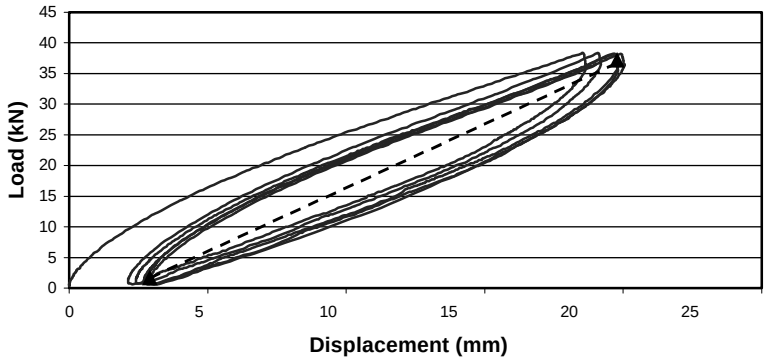

Figure 9. Typical load-displacement curve from an inclined compression test.

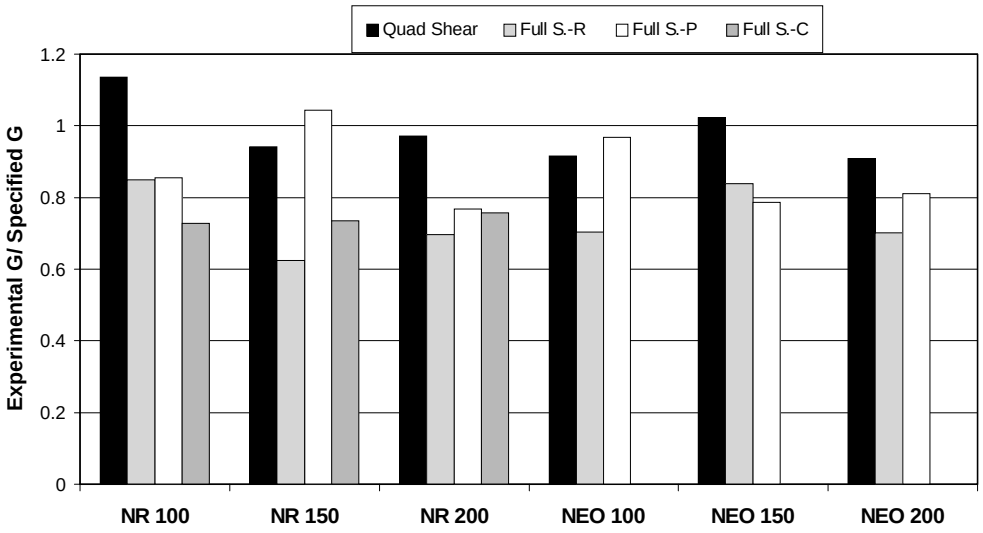

Figure 10. Comparison of quad-shear and full-scale test results.

generally about 10 percent for rubbers within the range of 50 to 60 durometer. Shear modulus decreases as the percent strain increases in the range of shear strain found in bridge bearings (± 50 percent). Given that the manufacturer did not report the quad shear modulus at 50-percent strain, it is not possible to make direct comparisons at the same strain level.

2. Quad shear samples are bonded to the fixtures; full-size specimens were not bonded. Data presented later show that the full-size test with bonded fixtures increases the shear modulus about 10 percent, which is consistent with theoretical analysis on bearings with and without bonded fixtures (Hamzeh et al., 1995).
3. The rubber may not be from the same batch.

For each of the elastomeric compounds there were only small differences in the full-size shear modulus values (usually less than 10 percent) for different types of full-size specimens, except for the NR150-P specimen. The circular bearings used consisted of natural rubber compounds and their results were similar to those from rectangular bearings. The inclined compression test results are compared with the full-size shear modulii in Figure 11. For bearings with steel laminates, the inclined compression test gives good estimations of shear modulus at 50-percent strain. The difference in shear modulus is within the +5 to −12 percent range for tests with 1:10 platen slopes (−4 percent average) and the +2 to +15 percent range for a 1:20 slope (+9 percent average). The variation in test results because of platen slope might be related to the level of compressive stress. A bearing tested with 1:20 slopes is subjected to twice the compressive stress of the case with 1:10 slopes. This will be discussed in more detail later.

On the other hand, for the plain unbonded rectangular pads, there are large differences between the two test methods. For some bearings, the difference exceeds 40 percent. In general, for plain pads the inclined compression test gives a lower shear modulus compared with the full-scale shear test. When compressive load is applied in the inclined compression setup, there is an immediate proportional shear force applied that causes the flexible edges to bulge, roll, and slip. A typical load-shear displacement response for the first two cycles is shown in Figure 12. At low compressive loads, there is insufficient mechanical interlocking between the pad and the platen surface to prevent slip. The rolling action that results is similar to a snake-like movement. With plain pads, the middle platen of the inclined compression setup does not return to its original position after each cycle of loading, indicating slip has occurred. For plain pads not prevented from slipping, the load-displacement curve never stabilizes. The results given in Figure 11 were obtained after two loading cycles. In the full-scale setup the rolling action is prevented by the application of the full compressive load before any shear is applied, thus providing good slip resistance. In steel-laminated bearings the rolling action is prevented even at low compressive loads by their high flexural stiffness. In summary, the inclined compression test is capable of estimating the behavior of full-size laminated pads. However, this test method gives inaccurate values of shear modulus for plain pads. Flexible pads would first have to be cold-bonded to sole plates in order to determine the shear modulus in the inclined compression setup.

Investigation of Testing Parameters

Some potential test parameters were investigated that might affect the performance of the full-size bearing or the results from test methods designed to determine the shear modulus. The parameters investigated were level of compressive stress, speed of testing, platen surfaces, edge cover, and specimen size.

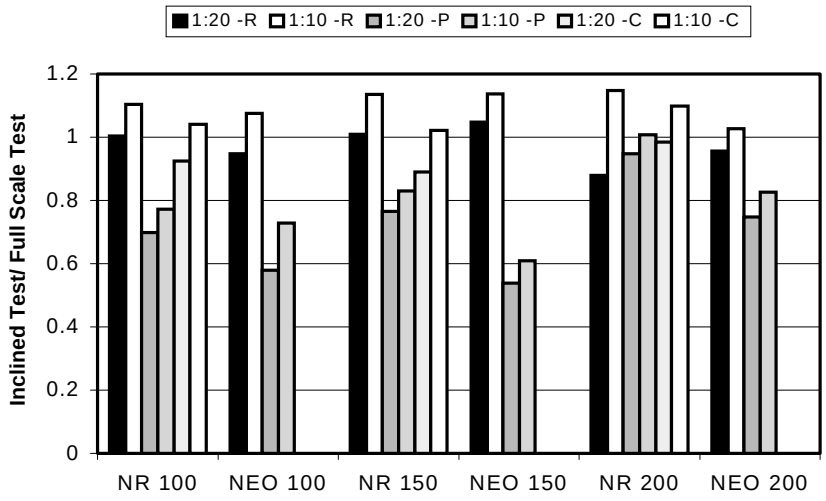

Figure 11. Comparison of inclined and full-scale test results.

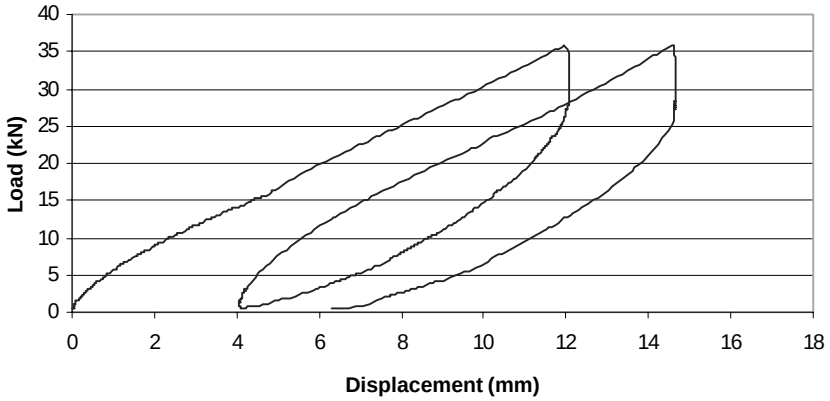

Figure 12. Plain pad tested in inclined compression.

Compressive Stress. As presented in the previous section, there was a difference in the shear modulus from the inclined compression between tests with two different platen slopes. As the slope gets steeper, less compressive force is required to attain a certain level of shear strain. To determine if the difference in test results is related to compressive stress, additional tests were performed with the full-scale shear test setup. Tests were conducted on laminated rectangular bearings and the compressive stress was increased from 3.1 to 6.2 MPa (450 to 900 psi). The same test procedure explained earlier was followed. Table 4 shows the test results for the two different compressive stress values in Columns 5 and 6 together with the inclined compression results, which were presented in Figure 11 in a nondimensional form. The maximum applied compressive stress in the inclined compression tests is shown in parentheses in Columns 2 and 3. According to full-scale shear test results, there is a slight change in shear modulus with the increase in compressive stress as shown by the ratio in Column 7 that could be attributed to test scatter. On the other hand, for the inclined compression test, specimens with low compressive stress (1:10 slopes) gave an average 12-percent higher shear modulus value compared with the ones subjected to high compressive stress (1:20 slopes). The difference in the experimental shear modulus from test setups with two different platen slopes cannot be explained by the level of compressive stress. However, the application of compressive stress might have an effect on the results. In the full-scale shear test setup, compressive stress is kept constant throughout the test period. On the other hand, in the inclined compression test, compressive stress is increased from zero to the maximum value at each cycle. The results in Table 4 indicate that the inclined compression test with 1:20 platens gives a shear modulus that best represents those from the full-scale test setup, except for bearings with high stiffness (NR200 and NEO200) where the 1:10 platens were better.

Loading Rate. In order to establish a test method, the effect of the loading rate was investigated. To accomplish this task,

TABLE 4 Test results for effect of compressive stress

Specimen	INCLINED COMPRESSION TEST			FULL-SCALE TEST		
	Shear Modulus (max applied comp stress) in MPa		Col (2) / Col (3)	Shear Modulus in MPa		Col (5) / Col (6)
(1)	1:10 Slopes (2)	1:20 Slopes (3)	(4)	3.1 MPa (5)	6.2 MPa (6)	(7)
NR100	0.64 (3.23)	0.59 (5.87)	1.10	0.58	0.58	1.00
NEO100	0.52 (2.61)	0.46 (4.60)	1.13	0.48	0.47	1.02
NR150	0.73 (3.67)	0.65 (6.51)	1.12	0.65	0.71	0.91
NEO150	0.98 (4.92)	0.91 (9.07)	1.08	0.87	0.94	0.92
NR200	1.10 (5.51)	0.84 (8.44)	1.30	0.96	1.03	0.93
NEO200	0.99 (4.97)	0.93 (9.25)	1.07	0.97	0.99	0.98

certain bearings were tested in the inclined compression test setup for different durations. Platens with 1:20 slopes were used to perform the tests. NEO100 and NEO200 laminated rectangular bearings were chosen as the test specimens. In the previous tests, specimens were strained to 50 percent in 14 min. In service bearings are strained in one direction over a 12-hr period. For commercial evaluation of material properties, tests with a short loading duration are preferred. Bearings were strained to 50 percent over periods that ranged from 2 min to 7 hr. Bearings were first cycled 3 times not considering the duration. Figure 13 shows the load-displacement response of the NEO200 bearing for different test periods. Test results revealed that testing time has a small influence on the shear modulus. The 2-min loading rate gave a 5-percent higher shear modulus than the 14-min rate for NEO200. For the NEO100 bearing, the difference was only 2 percent. These results are consistent with the creep study presented later in this chapter (a 3- to 10-min time from zero to maximum strain will be the recommended loading rate in the test). There was little difference between the 14-min test and the 7-hr test in Figure 13 because the bearing is being continuously strained during the period, so creep effects are not significant. These findings reveal that the short testing times can be used for a standardized test method and the results will represent actual daily performance.

Testing Surfaces. In the early stages of this research, a significant effort was devoted to find a robust test surface for the inclined compression test that simulates a concrete surface, prevents slipping of bearings, is reproducible, and is not costly. First the surfaces were sandblasted. There was little slipping with the sandblasted aluminum surfaces, but the roughness appeared to deteriorate with use. Then, 40-grit cloth sandpaper was glued to the metal platens. The tests with the glued sandpaper showed no slip. Unfortunately, the cloth deteriorated and tore rather quickly, so such a surface is not practical for a standardized test. Finally, the aluminum surfaces were roughened with the tool shown in Figure 7. This surface solved the slip problem and was used in all of the tests reported for both test setups. There was a surface maintenance problem caused by the wax that many manufacturers add to the bearing for ozone protection. The wax would build up on the roughened aluminum surface and affect the test results. Topkaya gives a detailed evaluation of this problem and recommends that the surfaces of the platens be cleaned after each test (Topkaya, 1999).

The effect of cold-bonding sole plates to the top and bottom bearing surfaces was investigated. Four types of laminated rectangular bearings were bonded to steel plates and tested in the full-scale shear test setup and inclined compression test setup with 1:20 and 1:10 slopes. A compressive stress of 3.10 MPa (450 psi) was applied in the full-scale shear tests. The results are provided in Table 5. In general, the shear modulus values increase when specimens are bonded, because the bearing edges cannot lift. As the contact area increases it is more difficult to deform the material, so the bearing shows a stiffer response. In general, the change in shear modulus is about 10 percent. It is evident from the test data that both 1:20 and 1:10 slopes are capable of estimating the shear modulus of bonded bearings. The 1:10 slopes give closer values to the full-scale shear test results for bearings with sole plates.

Edge Cover. Tests were performed to investigate the effects of edge cover on the shear modulus reported by Topkaya (Topkaya, 1999). The laminated rectangular pads had an edge cover on three sides because a larger bearing had been cut in half to provide the pair of specimens needed in each test. The edge covers of the bearings were trimmed off and retested. As expected, test results showed that edge trimming makes little difference on shear modulus.

Specimen Size. Performing full-size bearing tests requires high-capacity testing machines. For example, in the case of a 381-mm (15-in.)-diameter circular bearing with a modulus of 1.03 MPa (150 psi) tested under an inclined compression setup with 1:20 slopes, 1180 kN (265 kips) of compressive force is required to strain the pad up to 50 percent. Because of limited test machine capacity, full-size bearings may have to

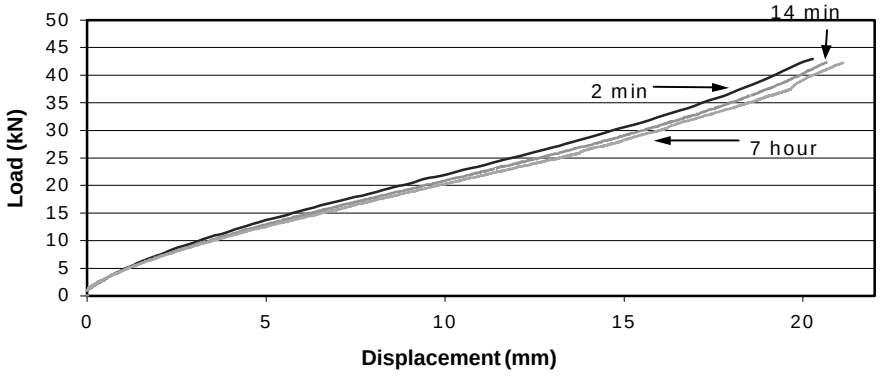

Figure 13. Load-displacement response for different test durations.

TABLE 5 Shear modulus for bearings with and without bonded sole plates (MPa)

Specimen	Without Bonded Sole Plates			With Bonded Sole Plates		
	Full-scale	Inclined 1:10	Inclined 1:20	Full-scale	Inclined 1:10	Inclined 1:20
NR100	0.58	0.64	0.59	0.65	0.64	0.62
NEO100	0.48	0.52	0.46	0.54	0.55	0.50
NR200	0.96	1.10	0.84	1.07	1.07	faulty data
NEO200	0.97	0.99	0.93	1.00	1.00	1.03

be cut into smaller sizes for testing. A change in dimensions changes the shape factor of the bearing and also changes the bearing length-to-thickness ratio, L/h. This section discusses how shape factor and L/h affect shear modulus. First, three types of circular bearings (having a shape factor of 7.5) were cut into squares having an edge length of 254 mm (10 in.) and a shape factor of 5.0. Then these bearings were cut into even smaller dimensions of 171 × 254 mm (6.75 × 10 in.) and 127 × 254 mm (5 × 10 in.) that resulted in shape factors of 4.0 and 3.33, respectively. All these bearings were tested in the inclined compression test setup with 1:20 slopes. The shear modulus of each sample normalized by the shear modulus of the full-size bearing is shown in Figure 14 by the solid data points.

For bearings with shape factors of 4.0 and 3.33, the shear modulus values were found by straining them in the direction of shorter dimension (127 mm [5 in.] and 171 mm [6.75 in.]), respectively. Both shape factor and L/h appear to organize the data in a similar fashion. In order to distinguish the effect of these two variables, bearings having dimensions of 127 × 254 mm (5 × 10 in.) were retested, but this time the bearings were strained in the direction of longer dimension, 254 mm (10 in.). This change in orientation did not alter the shape factor (3.33) but the L/h ratio was doubled, from 2.86 to 5.71. The test results are shown by the three open data points in each graph. Even though the shape factor remained at 3.33, the shear modulus for all three materials increased about 30 percent—to values very close to those for bearings having dimensions of 254 × 254 mm (10 × 10 in.) with a shape factor of 5.0. Thus, the prime variable has been determined to be L/h, not shape factor. When the L/h ratio of the test specimen is less than 4.5, the small sample shear modulus will not directly represent the shear modulus of the full-size bearing. However, the following expression that is a curve fit to the data in Figure 14 can be used to adjust the test results for the effect of specimen size when $L/h < 4.5$:

$$\frac{G}{G_{\text{full}}} = A\left(\frac{L}{h}\right)^{0.7} \tag{3}$$

where

A = 0.35 for $G \le 1.0$ MPa (150 psi) or $A = 0.30$ for $G >$ 1.0 MPa (150 psi),
G = the shear modulus for the small sample, and
G_{full} = the predicted shear modulus for the full-size bearing.

The test results show that decreasing the specimen dimension in the direction of strain causes P-Δ effects in the setup, resulting in a more flexible behavior. The L/h of the test sample should not be less than 3, the AASHTO stability limit.

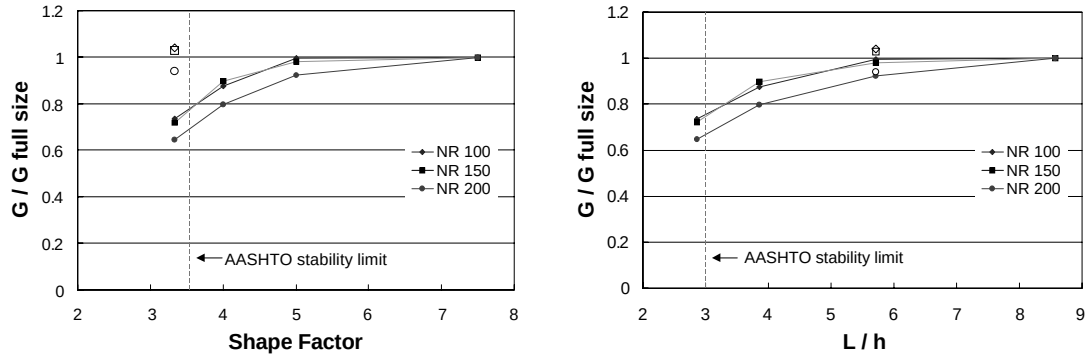

Figure 14. Effect of specimen size on shear modulus.

INTERPRETATION AND APPLICATIONS

The research has shown that the inclined compression test can be used to accurately determine the shear modulus of steel-laminated elastomeric bearings. Plain, flexible elastomeric bearings cannot be tested with this system unless they are cold-bonded to steel sole plates prior to testing. The inclined compression test method that has been developed is reliable when directly compared with more complex and costly full-scale tests. The new method will enable finished bearings to be checked by the use of a compression test machine without additional shear loading devices. The new method relies on geometric principles to produce simultaneous compression and shear on a bearing merely through application of compression load. Most current testing of full-size bearings is limited to compressive loads because of the inherent difficulty and cost of applying compression and shear simultaneously.

For the inclined system to function properly, slip between the bearing and platen contact surfaces must be prevented. The surface used in this research tried to simulate a concrete surface, but that imitation is not necessary when implementing this test method. Smooth, machine surfaces cannot be used, but any type of roughened plates should work. The tapered platens were machined from aluminum plates because aluminum is lightweight and less costly to machine. For commercial testing, probably the use of grit-blasted, steel-covered plates on the sloped platens would be a practical alternative to the surface used in this research. Sandblasted aluminum surfaces work initially, but the surface roughness does not hold up as well as steel surfaces for continuous testing. The use of plates with machined grooves perpendicular to the direction of the shear force, probably no more than 1 mm deep, may be the best solution because regular cleaning of the surface for wax residue would be easier than with blasted or roughened surfaces.

The inclined compression test can be used as a replacement or alternative to (1) the quad shear ASTM D4014-89, Annex A1 shear modulus test and (2) the full-scale shear test. The advantages of the inclined compression test over the quad shear test are that the inclined compression test (1) can handle bearings with and without sole plates, (2) does not required destruction of the bearing, and (3) measures bearing performance directly. The current quad shear test does not give a shear modulus value that is suitable for a performance evaluation because the modulus is calculated at 25-percent strain. If the quad shear test method is retained in the AASHTO specifications, it is recommended that the shear modulus be calculated from the stress at 50-percent strain. The full-scale shear test requires separate compression and shear loading setups, whereas the inclined test only needs a compression machine. All the shear modulus test methods should define shear modulus based on the same maximum strain. The 50-percent strain level is recommended for all of these tests.

The inclined compression test can also be used to test full-thickness samples cut from full-size bearings. Test samples with $L/h \geq 4.5$ will provide a value of shear stiffness that is directly representative of the value in the full-size bearing. For $L/h < 4.5$, Equation 3 must be used to convert the G from the small sample to the equivalent G in the full-size bearing. In AASHTO M251-97, the nondestructive shear stiffness test method on a pair of sampled bearings contains the following statement: “the shear modulus shall be computed from measured shear stiffness of the bearings, taking into account the influence on shear stiffness of bearing geometry and compressive load.” No guidance is given on how to correct for the geometry or level of compressive load. This research has addressed both factors—geometry and level of compressive load—and has found that compressive stress has little influence on the outcome of the shear modulus test. However, geometry is important and Equation 3 was developed to address this issue. Equation 3 should be applicable to the full-scale test, as well as the inclined compression test.

The inclined compression test can also be used to replace the compressive-load proof test at 1.5 times the maximum design load. In this test, the compressive deformation is limited to 10 percent of the original thickness and the two pads are examined for damage or delaminations during the test. The inclined compression test can provide the same function. It is recommended that the slopes of the platens be limited to the values within the range used in the test program, namely 1:10 and 1:20. There is no physical reason why other slopes could not be used, but all the test data have been generated for these values. For bearings with a specified shear modulus between 0.7 and 1.0 MPa (100 and 150 psi), the use of a platen slope 1:20 gives compressive stresses close to the AASHTO design values when the bearing reaches a strain of 50 percent. In general the 1:20 slope is recommended, which in some instances may result in compressive stress levels higher than the design compressive stress. But because the factor of safety is very large in compression, typically six or more, the higher stresses pose no problem during testing. If there is concern about the level of compression, a steeper slope, such as 1:10, can be used. A detailed specification for the inclined compression test, which is intended as an annex for the AASHTO M251-97 specification is provided as Appendix A.

LOW TEMPERATURE BEHAVIOR

Introduction

As discussed in Chapter 1, elastomers stiffen as they are cooled. The four low temperature test methods in AASHTO M251-97 and their associated performance criteria purport to evaluate the stiffening of the bearing as it is cooled to various low temperature levels (i.e., brittleness and instantaneous stiffening) and held at particular temperatures for a specified number of days (i.e., crystallization). In order to evaluate these test methods and performance criteria, an experimental research plan was developed that mainly focused on variables and

procedures that were not adequately addressed in previous low temperature research. Based on a literature search summarized in Appendix B of the research team's final report, the following parameters were selected for study:

1. Temperature response within the bearing,
2. Cyclic stress and cyclic strain,
3. Temperature history,
4. Slip, and
5. Rate of loading and shear strain amplitude.

From the results of these studies, test methods and performance criteria were developed.

Temperature response within the bearing as the ambient temperature varies had not been studied extensively. The response of the bearings affects the minimum time required for a bearing to reach the desired temperature for determining the instantaneous (i.e., initial steady state) stiffness, test procedures, and field performance. Very limited and conflicting data were found on the effect of *cyclic strain*, which has been claimed to retard crystallization, thereby making static tests meaningless (Ritchie, 1989). Research on the effect of *cyclic stress* was initiated but not completed (Du Pont, 1989). Only very limited studies were conducted using realistic *temperature histories* and their associated strain limits. The interaction between minimum low temperature and the expected daily temperature change at that temperature needs to be studied based on some typical temperature histories. *Slip* is an important performance limit for bearings without bonded sole plates. Slip coefficients at low temperature appear to be different than those at room temperature, which can affect the maximum shear forces. For practical laboratory tests, shear *loading rates* should be as fast as possible, but if the test results cannot be related to performance in the bridge, the test may give an erroneous indication.

Findings

Monitoring Bearing Temperature

Before developing a test procedure at low temperatures, the response of the elastomeric material to exterior temperature should be investigated. It is known that elastomers are poor conductors of heat. In order to determine the response of bearings to outside temperatures, the temperature inside the bearings has been monitored using thermocouples for various temperature ranges. Two NR100, two NEO100, two NR150, and two NEO150 bearings were ordered with 24 thermocouples inserted in the top and middle layers of the bearings during their manufacture. The thermocouples were used to monitor the temperature variation within each bearing as the exterior temperature changed with time. Type J thermocouples were installed because they perform better than do other types. Figure 15 depicts the thermocouple layout. A freezer unit that can hold temperatures down to −65°C (−85°F) was selected for this study. Almost 70 percent of thermocouples were observed to perform well. Specimens NR100 and NR150 were conditioned at various temperatures in the freezer, and the temperatures within the bearings were monitored. Full-size bearings (229 × 711 mm [9 × 28 in.]) were studied first. Then smaller 229 × 356 mm (9 × 14 in.) bearings that were cut from the 229 × 711 mm (9 × 28 in.) bearings were monitored. The effect of exposure condition on the bearing temperature response was investigated by monitoring a 229 × 356 mm (9 × 14 in.) NR100 bearing that had been placed between two concrete platens.

Response of Bearings to Temperature Changes. A typical measured temperature-time response is exponential as shown in Figure 16. The freezer reached the desired temperature in 30 to 75 min while being cooled depending on the tem-

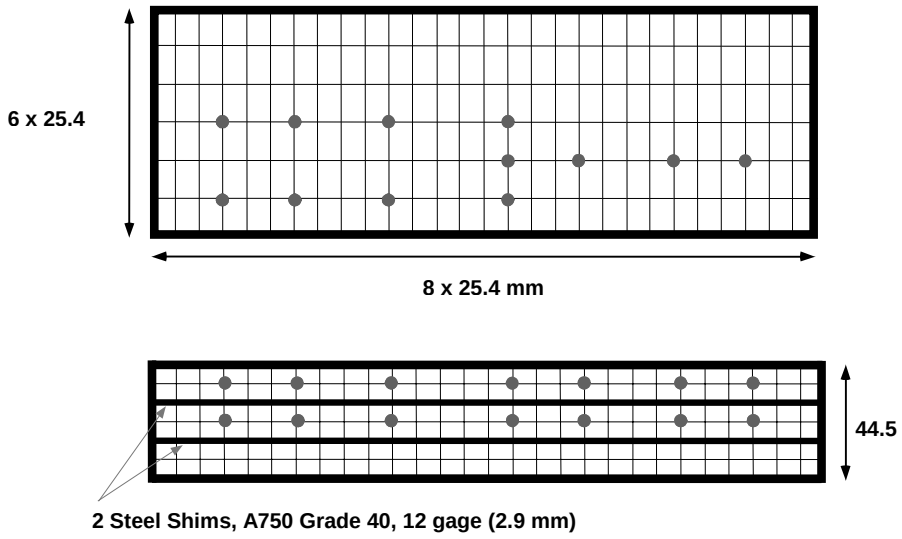

Figure 15. Thermocouple layout.

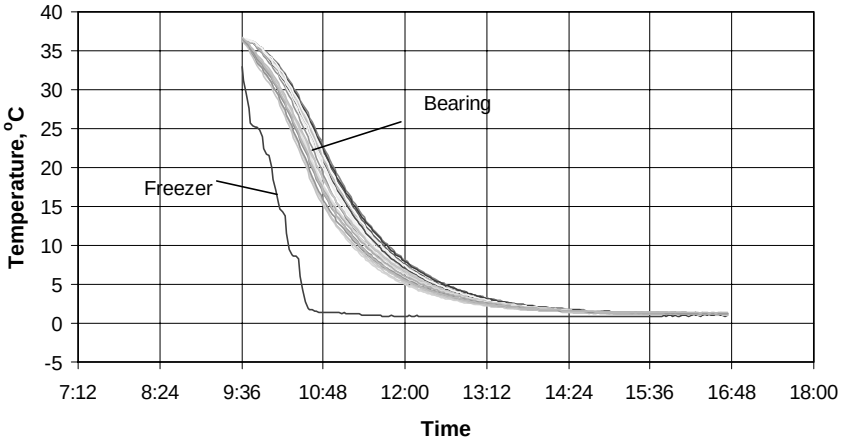

Figure 16. Cooling curves for NR100 (228.6 × 711.2 mm).

perature setting. Heating, on the other hand, was quite fast—the freezer reached the room temperature in 10 to 35 min. Each temperature response was examined for the time required to reach the outside temperature and the maximum difference of measured temperature values between thermocouples. The time to reach the steady-state temperature (SST) was defined as the time elapsed from the beginning of the temperature change to the point when the bearings attained 97 percent of the temperature change. The bearings reached a steady-state condition in 3 to 6.5 hr at low temperatures. However, it took 8 to 11 hr for the bearings to reach the room temperature when heated. The reason for a longer time in case of heating was that, during heating, a film of condensation (resulting from high humidity) covered the bearing surface and retarded the warming of the bearing. The maximum difference in cooling thermocouple readings (i.e., 4°C to 11°C) occurred between the top and middle layers during the first 70 min of cooling. The maximum difference of 8 to 11°C was recorded during the first 30 min of heating. The temperature difference within a layer was observed to be insignificant.

The results of this study (Yakut, 2000) showed that the response of bearings having different hardness/rigidity was very similar. The behavior of the 229 × 356 mm (9 × 14 in.) and 229 × 711 mm (9 × 28 in.) bearings was quite similar. This indicates that heat transfer is mainly through the thickness of the bearings. When only the edges of the bearing were exposed, the rate of cooling/heating was slower. However, the difference between the times to reach SST was insignificant.

The optional low temperature shear test procedure in AASHTO M251-97 requires that the bearing be conditioned at −29°C (−20°F) for 96 hr and then be tested within 30 min after being removed from the freezer. Figure 17 shows that the bearing temperature changes considerably within the first 30 min of heating. For this particular bearing, the average bearing temperature changed from −31°C (−24°F) to −12°C (10°F) within 30 min of heating. When only the edges of the bearing

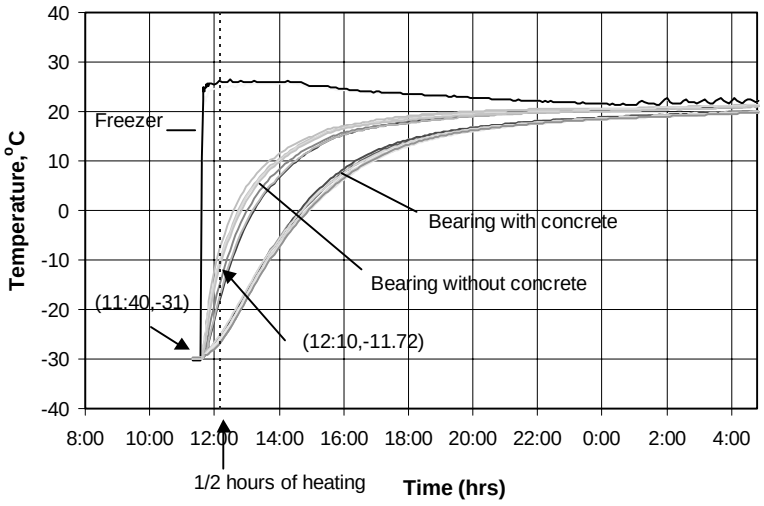

Figure 17. Change of temperature during heating.

were exposed to air because of concrete blocks, the change in bearing temperature was more gradual than that for full exposure, but there was no significant effect on the total time needed to reach steady state.

Theoretical Investigations. Heat flow characteristics of elastomeric bridge bearings are not very well known. During manufacturing and vulcanization, thermal properties are known to change. Experimentally obtained thermal response data were used to estimate the heat transfer properties of the bearings employed for this research. These properties were then used to generate responses for the bearings that have different thickness than the ones monitored. The bearings monitored were modeled, and analytical solutions were obtained. The results of the study herein, as documented in *NCHRP Report 298*, have shown that previous research failed to estimate the response of bearings analytically. For bearings that have a thickness of 51 mm (2 in.) or less, research suggests that the time required to reach thermal equilibrium would be less than 1 hr (Roeder and Stanton, 1987). The details of the theoretical investigations are given elsewhere (Yakut, 2000).

The experimental and analytical responses of the NR100 specimen are compared in Figure 18. Theoretical results indicated that the time to SST does not depend on the temperature range. In all temperature ranges, a period of 275 ± 5 min was required to reach SST when cooling and the time to SST during heating was 256 ± 5 min. In order to obtain a relationship between the time required to reach SST and the thickness of full-size elastomeric bearings, numerical results were obtained for bearings having thicknesses other than 45 mm (1.5 in.). Figure 19 shows the time to reach SST as a function of the thickness. Curves were generated for the conditions where a condensation film is developed on the bearing surface and when condensation was not a problem. These curves can be used to obtain the conditioning time required for a particular bearing to reach SST at which instantaneous stiffness of a bearing needs to be determined. For example, in order to determine the instantaneous stiffness of a 76-mm (3-in.)-thick elastomeric bridge bearing, the shear stiffness test should be conducted 17 hr (Figure 19) after the bearing is conditioned at the desired temperature when condensation is not a problem. Equations representing these curves are given later.

Test Setups

The results presented in the previous section revealed that, to determine low temperature properties, elastomeric bearings need to be tested in an environment where the temperature can be maintained (e.g., a freezer). Elastomeric bridge bearings are generally tested in shear in pairs. Two identical specimens are placed between plates and compression is applied to provide friction when testing bearings without bonded sole plates. The middle plate is sheared and its displacement is measured. Compression need not be applied when testing bearings with bonded sole plates. Bearings without bonded sole plates were used in this research. All the specimens were typical full-size bridge bearings (229×356 mm [9×14 in.]). Test setups were designed for installation inside an environmental chamber ($2.7 \times 2.7 \times 2.4$ m [$9 \times 9 \times 8$ ft]). Shear tests were the primary tests conducted. Compression was applied to provide enough friction for the shear tests. The test setup was designed to apply cyclic compression from traffic loading. The freezer unit had thin, weak walls and floor, so no structural attachment of any kind could be made to them. This limited the options for load application. The ideal solution would be to apply shear using screw jacks (i.e., displacement controlled) to simulate thermal expansion and contraction, and to use hydraulic jacks (i.e., load controlled) for compression to represent the vertical loading from the weight of the bridge and traffic.

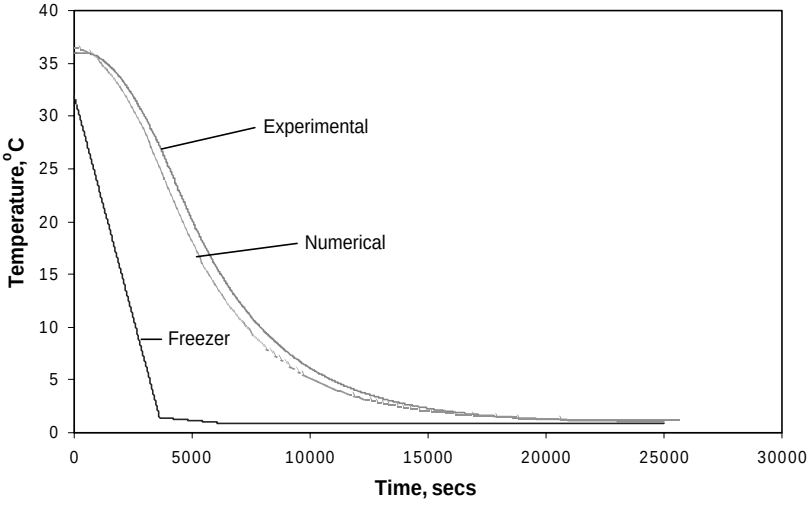

Figure 18. Analytical results.

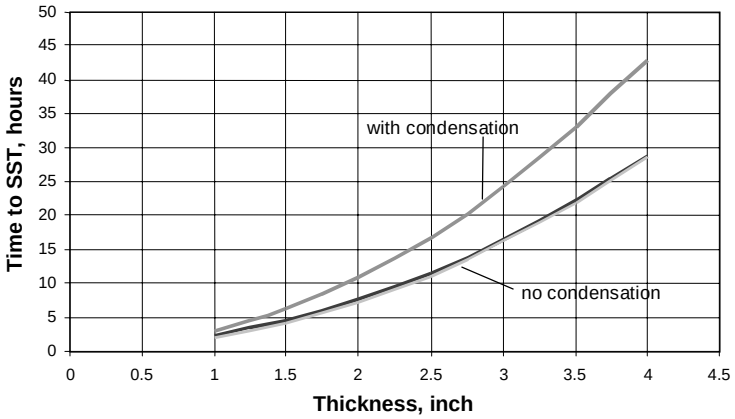

Notes: Chamber must be able to reach desired temperature in 60/30 minutes when cooling/heating
"with condensation" curve must be used when there is condensation

Figure 19. Time to reach SST.

The setups designed for low temperature research consist of the following major components:

1. Cyclic compression setup,
2. Control setup,
3. Shear test setup,
4. Cyclic shear and slow speed shear setup, and
5. A compression setup.

In addition, a load maintainer, a continuous MTS pump capable of providing a maximum pressure of 17.24 MPa (2500 psi) and the data acquisition system were used to conduct tests at cold temperatures. Figure 20 depicts the test setups, which are explained in more detail in Appendix B of the research team's final report; NR100, NR150, NEO100, and NEO150 bearings were used in the test program. Unless otherwise specified, all pairs of bearing specimens were 224 $\times$ 356 $\times$ 45 mm (9 $\times$ 14 $\times$ 1.75 in.) with each of the bearings in the pair cut from the same full-size bearing. All the bearings used for the low temperature study were specified as Grade 3.

Cyclic Stiffness Tests

Cyclic compressive loads to simulate the truck loading were applied to the bearings while they were being conditioned at a certain temperature. This is a more realistic representation of truck loading than the application of compressive strain, which was employed by previous research (DuPont, 1989). Previous limited research had shown that cyclic straining inhibits crystallization of the elastomers. However, the research team found that applying cyclic load, simulating trucks, did not produce the same effect as cyclic straining. As the bearing stiffened under cold temperature, the compressive strain decreased, even though the maximum cyclic load was

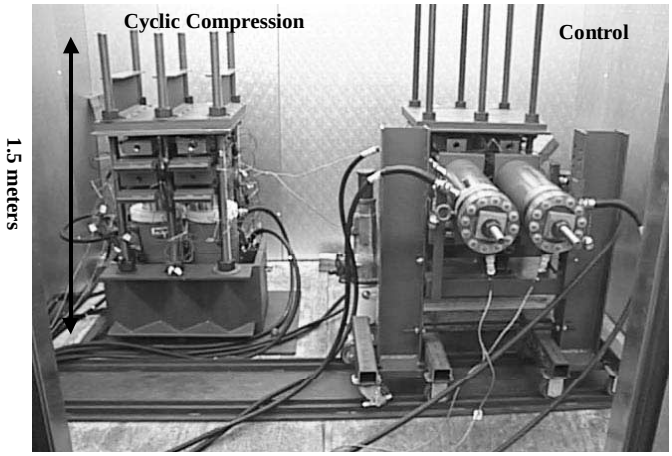

Figure 20. Test setups.

held constant. The cyclic load produced very little compressive strain in the neoprene after a few days of testing. The reason large strain cycles curtail crystallization might be the heat built up inside the bearing, which produced lower stiffness values as reported in earlier research (Suter and Collins, 1964). The research team's tests showed that cyclic loading in compression need not be considered in developing a performance test at low temperatures.

Cyclic shear loads were applied to simulate the daily thermal expansion/contraction cycles of the bridges. An average shear strain of 17 percent was applied over 12 hr while the specimen was being conditioned at a certain temperature. Results indicated that slow application of cyclic shear strain does not curtail or retard crystallization of the bearings. The reduction in the amount of stiffening between the slow-speed cyclic shear strain and the fast loading resulted mainly from the rate of loading effect. The results of this research do not agree with previous research. Ritchie conditioned bearings under the application of 5-percent constant compressive strain while straining the specimen through a ±25-percent daily shear strain cycle for 14 days, which is fairly large for stiff bearings because it results in unrealistic compressive loads. Furthermore, the specimens tested were relatively crystallization-resistant (i.e., shear stiffness increase of 2 times the room temperature value was noted after 2 weeks of conditioning at –10°F [14°F]) (Ritchie, 1989). Dynamic strain in shear was found to have no significant effect on the performance of the bearings, thus it should not be included in a performance test. It is assumed that the shear strain resulting from the acceleration or braking action of vehicles is insignificant.

Low Temperature Stiffness Tests

The purpose of this part of the research was to investigate the behavior of full-size elastomeric bearings at various temperatures. The main focus was devoted to crystallization of elastomers. Although low temperature crystallization has long been recognized as a property of elastomeric bearings, no specific test method was required by AASHTO to determine the effect of crystallization on the stiffness of bearings until 1992. Until 1992, crystallization was not considered a problem for bridge bearings (DuPont, 1959). Whether or not crystallization affects the performance depends on the temperature, rate of loading, type of compound, time, and strain amplitude (i.e., daily temperature fluctuation). Research was required to find out whether crystallization is important in terms of performance under the conditions to which bridge bearings are generally subjected. There have been no reported bearing failures associated with low temperature stiffening.

Common practice in low temperature tests has been to carry out tests at constant temperatures for certain durations. The range of temperatures employed was usually –10°C (14°F) and –25°C (–13°F) which are believed to be the optimum crystallization temperatures for neoprene and natural rubber, respectively. In this study, tests were conducted at constant temperatures, as well as varying temperatures during the conditioning of bearings. Test temperatures of –10°C (14°F), –20°C (–4°F), and –29°C (–20°F) were applied to investigate the effect of crystallization. Tests were performed at variable temperatures to study the effect of temperature history on the performance. A semi-continuous temperature history and two historical temperature profiles obtained from temperature records of Anchorage and Minneapolis were introduced. All specimens were tested under as identical conditions as possible.

Shear Stiffness Tests. Test specimens were conditioned under a compressive stress of 3.45 MPa (500 psi). Periodic shear tests were performed during conditioning. Over 450 shear stiffness tests were performed on the specimens, using the test setups described earlier. The bearings were sheared to a strain of 35 percent and the calculations were performed at three strain levels: 12.5 percent, 25 percent, and 30 percent. Figure 21 shows the load-deflection curves of NEO150 as a function of time at –20°C (–4°F). This figure illustrates how the shear stiffness increases as a function of time. The curves after the 4th day do not extend to 30-percent strain (a displacement of 11 mm [0.45 in.]) because of slip.

Normalized shear modulus curves for all bearings are depicted in Figures 22 through 25. Results revealed a very significant stiffening of NEO150, especially at –29°C (–20°F) (normalized shear modulus was about 9 after 4 days, which resulted in slip). The stiffening of NEO100 was noted at –29°C (–20°F) as well. After 2 weeks, the normalized shear modulus of NEO100 reached the value of 3.9, 3.7, and 3.4 at –29°C (–20°F), –20°C (–4°F), and –10°C (14°F), respectively. Natural rubber compounds exhibited their greatest stiffening at –29°C (–20°F). NR150 stiffened more than NR100: the shear modulus increased by a factor of 3.6 and 2.6 for NR150 and NR100 at –29°C (–20°F), respectively, after 2 weeks. At –29°C (–20°F), the sharp change in the curve after 2 weeks occurred because a freezer problem caused the temperature to increase. After day 16, the problem was fixed and the freezer was cooled to –29°C (–20°F) again. The large stiffening of the

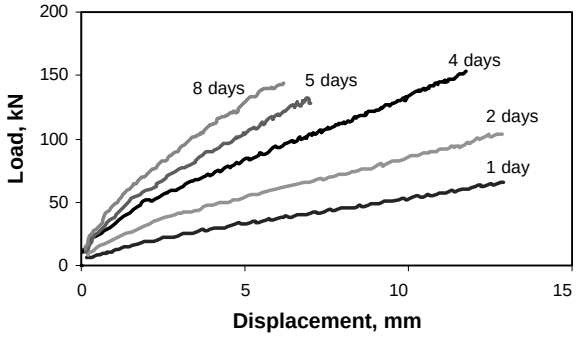

Figure 21. Load-displacement curves for NEO150 at –20°C (–4°F).

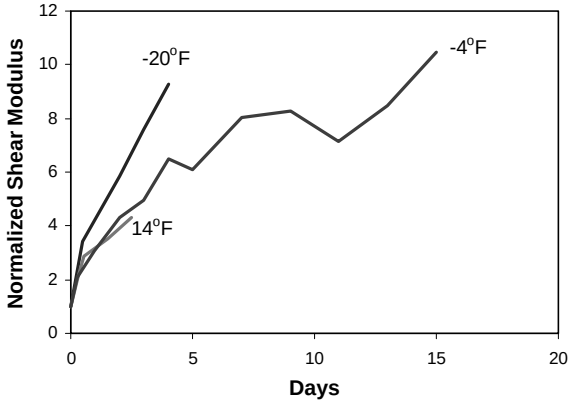

Figure 22. Behavior of NEO150 at 12.5% strain.

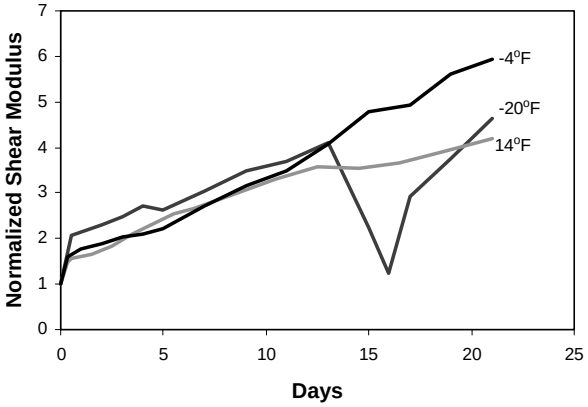

Figure 24. Behavior of NEO100 at 12.5% strain.

NEO150 material was a surprise because a Grade 3 bearing was specified; this requires that the stiffening not exceed 4 times the room temperature value at –26°C (–15°F). The certified report supplied by the manufacturer indicated that the NEO150 passed the current AASHTO test with a value of 2.67 < 4. Another NEO150 bearing was tested and showed similar behavior, so it appears that the certified report is in error. A NEO200 bearing whose certified report also complied with a Grade 3 requirement was tested and the behavior was similar to the NEO100 bearing. In Appendix B of the research team's final report, the behavior of the tested bearings is shown to be similar to the behavior of the bearings reported in *NCHRP Report 325*.

Effect of Temperature History. After completing tests at constant temperatures, additional tests were conducted on all the 0.69 MPa (100 psi) and 1.03 MPa (150 psi) bearings to study the effect of temperature variation on the behavior. Two real temperature records were selected for the tests as follows:

1. A record collected in Anchorage, Alaska, for the period of January 27, 1999, through February 12, 1999, and
2. A history obtained from the Minneapolis, Minnesota, data in January 1969.

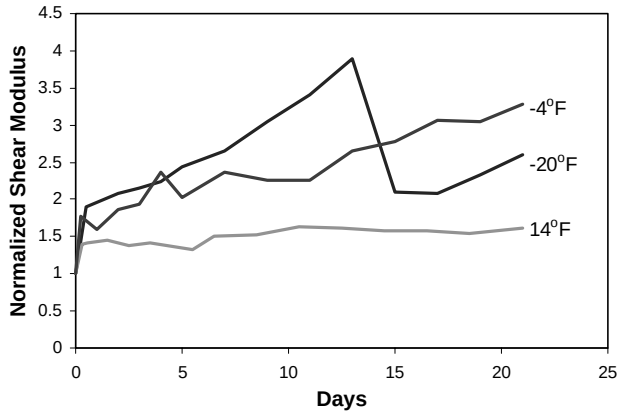

Figure 23. Behavior of NR150 at 12.5% strain.

Both records had average daily temperature values below –10°C (14°F) for the duration selected, representing various ranges of daily temperature fluctuations. The Anchorage record had a small value for the daily temperature fluctuations whereas the Minneapolis record had large differences between daily high and low temperature measurements such that a 30-m (100-ft) bridge girder would reach a strain of 12.5 percent several times during that period. Figures 26 and 27 depict the temperature histories employed in this study. The real data were represented by a stepwise temperature distribution: A constant temperature was used over a period of 12 hr. Each record was approximated for 7 days. The Anchorage history was extended 2 days by applying an assumed temperature increase for the last 2 days. In Figure 27, the hourly temperature measurements and stepwise approximations do not belong to the same date. Given that hourly data were not available for January 1969, January 1998 data were used to determine the trend of daily temperature variation (straight lines represent daily high and low temperature measurements in January 1969 whereas continuous data depict the hourly temperature record in January 1998).

All four specimens were tested at both temperature histories and the measured behavior is shown in Figures 28 and 29. The shear modulus reached a maximum value after 4.5 days at –25°C (–13°F) under the Minneapolis history; the normalized shear modulus were 7.9, 4.17, 1.95, and 1.62 for NEO150, NEO100, NR150, and NR100, respectively. Results obtained from the Anchorage record indicate that maximum stiffening occurred on day 7 (NEO150 had a normalized shear modulus value of 10). A comparison of the low temperature tests for the various temperature histories performed on NEO100 is given in Figure 30. Constant temperature tests yield a continuous stiffening curve with time; temperature histories, however, show a different trend. The Anchorage record has fewer fluctuations because of the small changes in daily temperatures; the Minneapolis history, on the other hand, produced very

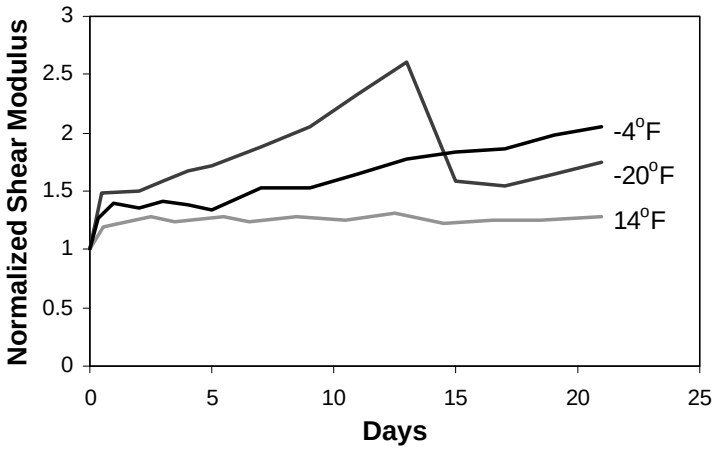

Figure 25. Behavior of NR100 at 12.5% strain.

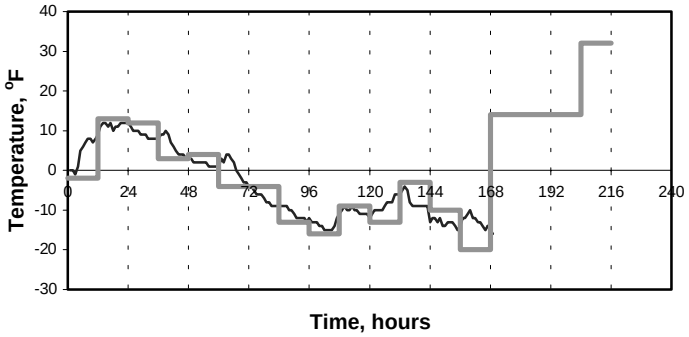

Figure 26. Temperature history from Anchorage, January 1999.

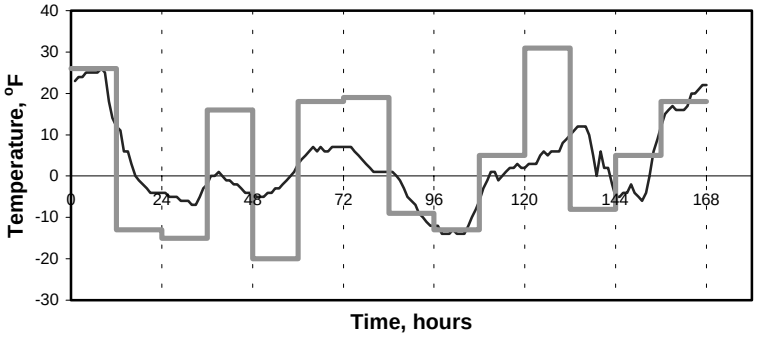

Figure 27. Temperature history from Minneapolis, January 1969.

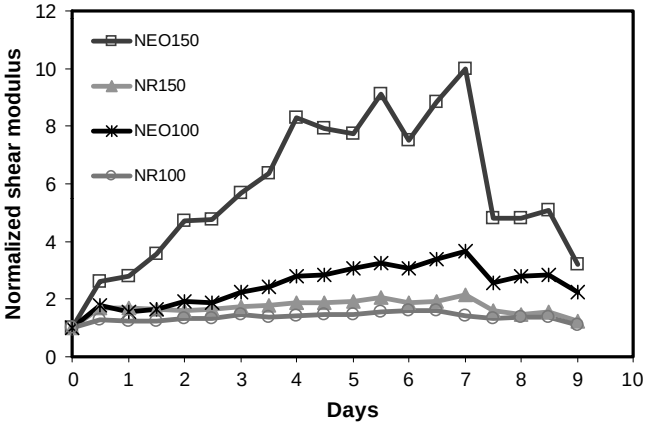

Figure 28. Results for temperature history—Anchorage.

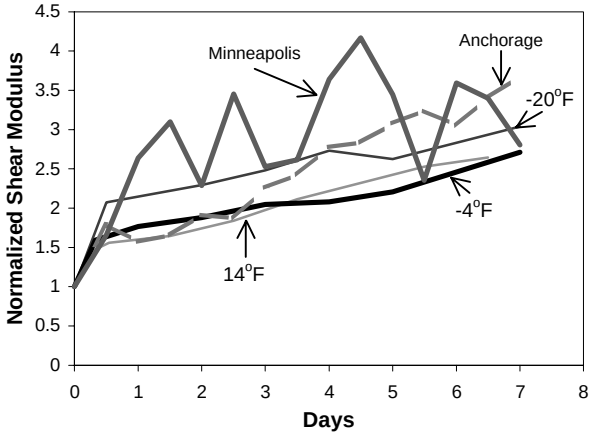

Figure 30. Comparison of results for NEO100.

appreciable changes in shear modulus, depending on the change in the temperature. These results indicate that temperature variation and level of strain directly affect the shear modulus. If fluctuations are small, there is no significant effect on the breakdown of crystallization, but if temperature change is high, a considerable reduction on the rate of crystallization is possible (Figure 31).

Effect of Slip Coefficient on Performance

A drop in temperature results in an increase in stiffness of the bearing, which, in turn, transmits higher forces to the bridge substructure. An increase in shear force increases the possibility of the slip of a bearing without bonded sole plates. The current AASHTO bridge design specifications do not address slip between the bearing and the guides or abutment explicitly. The horizontal force must be less than 20 percent of the compressive force; this implies a coefficient of friction of 0.20. Previous research has revealed that the coefficient of friction depends on the compressive stress, decreasing with an increase of compressive stress at room temperature (Muscarella and Yura, 1995). Because an elastomer goes through a phase change at low temperatures, the coefficient of friction may change. No data have been reported for the coefficient of friction between an elastomeric bearing and concrete at low temperatures. It is important to determine when the bearing will slip because this might supersede the effect of stiffening for bearings without mounting plates.

Four types of load-displacement curves were observed in this research as shown in Figure 32. Slip load is defined as the maximum load for Curves a, b, d and e. For Curve c, slip load is taken as the load at which the rate of displacement increases significantly.

Slip Tests. All plate surfaces were roughened by double O (buckshot) size sandblasting, the coarsest grit size commercially available, to simulate a concrete surface. The slip load and corresponding coefficient of friction were determined from the load-displacement curves obtained from the standard shear tests. Thus, slip data are available only for the compounds that slipped during the shearing of specimens up

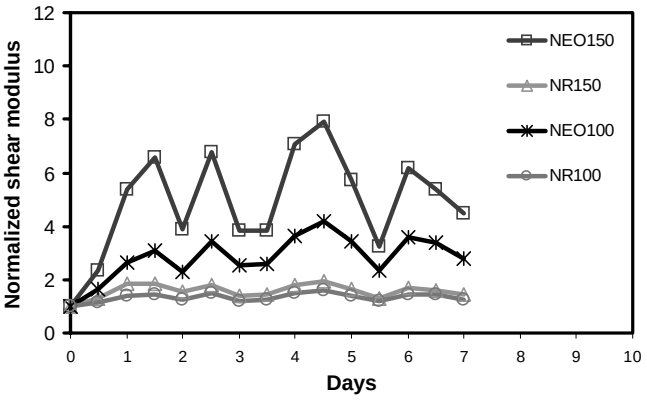

Figure 29. Results for temperature history—Minneapolis.

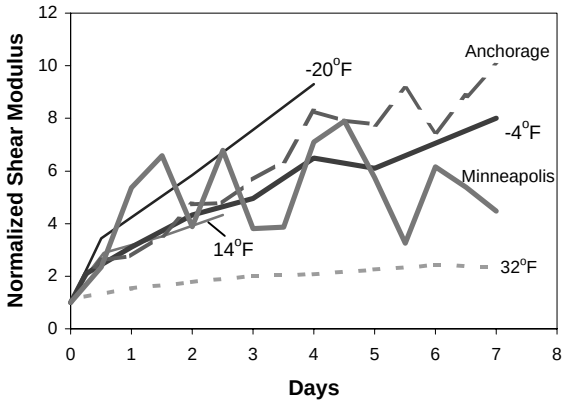

Figure 31. Comparison of results for NEO150.

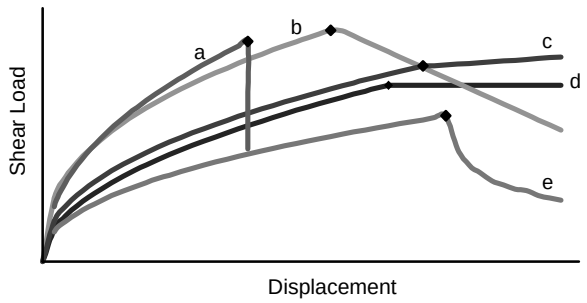

Figure 32. Typical load-displacement curves in slip of elastomeric bearings.

to 30-percent strain level. Only NEO150 and NEO100 were observed to slip. Most slip data pertain to NEO150, which slipped at almost all exposure temperatures because of the large stiffening.

A typical load-deflection curve for NEO150 is shown in Figure 33. A sudden drop in load with no change in displacement was measured when the maximum load was reached. This type of behavior does not resemble the common slip curves shown in Figure 32. A sound was released from the setup at the instant of load drop that was considered to be energy released. To investigate whether this was a slip or a mechanical problem inherent to setup, acoustic emission tests were conducted. Acoustic emission test results indicated that noise released during the tests was a result of slip on the bearing and steel plate interface. Details of the acoustic emission tests are given elsewhere (Yakut, 2000).

Maximum Shear Force. The shear modulus changes as a function of temperature, time, rate of loading, and other parameters as discussed previously. Shear force increases directly with an increase in *G* provided that slip does not occur. Therefore, the change in force is not directly related to a change in *G* for bearings without bonded sole plates. Consequently, the following criteria were used in calculating the maximum shear force experienced by the bearings:

1. At room temperature, a strain of 50 percent was used as recommended by AASHTO.
2. At cold temperatures, a strain of 30 percent was used, if slip did not occur.
3. In case of slip, the maximum load was taken as slip load.
4. Shear tests were stopped after the bearing slipped before reaching 12.5-percent shear strain.

Figure 34 gives the maximum measured shear force on each day for different temperature histories normalized by the room temperature shear force. Because bearings were not tested to the slip limit state in all tests, the shear force curves have fluctuations after the first occasion of slip.

The maximum increase in force because of stiffening at –20°C (–4°F) is 3.5 times the room temperature value. For the variable temperature history, the maximum normalized shear force was 3.2, which occurred at temperatures of –18°C (0°F) and –20°C (–4°F). The maximum normalized shear force was 2.6 and 2.2 at –29°C (–20°F) and –10°C (14°F), respectively. Although the shear modulus increased about 10 times, the shear force increased only 3.5 times because of slip. This indicates that slip controls the design and performance for this particular bearing. The maximum normalized shear force for NEO100 versus time curve is displayed in Figure 35. The force increased with time reaching a value of 3.2 on day 17 when slip occurred, whereas the normalized shear modulus value recorded for NEO100 at –20°C (–4°F) was 6, which indicates that the maximum shear force is the critical parameter in the performance design of this bearing as well.

Coefficients of friction were calculated on the basis of the slip data from the neoprene compounds and the results are shown in Table 6. For NEO100 bearings, data were available only at –20°C (–4°F). The coefficient of friction was approximately 0.45 for both NEO100 and NEO150 at –20°C (–4°F). A smaller value was observed at –10°C (14°F) and –29°C (–20°F), 0.29 and 0.39, respectively. Muscarella reported a value of 0.42 at room temperature for

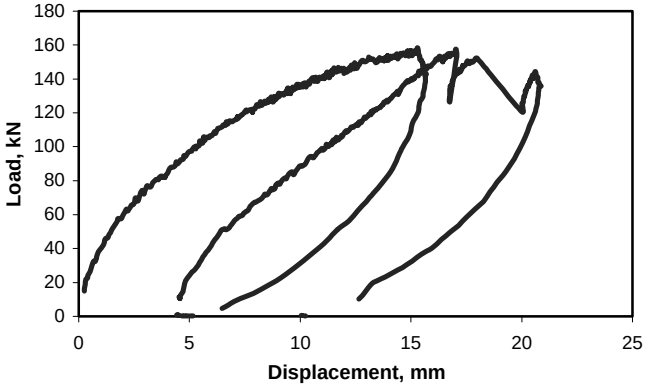

Figure 33. Load-deflection curve of NEO150 at –20°C (–4°F).

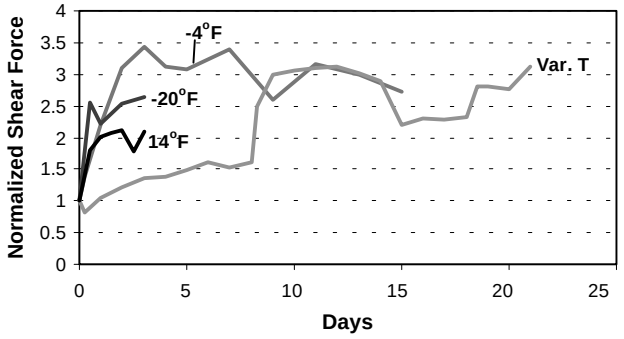

Figure 34. Maximum measured shear force for NEO150.

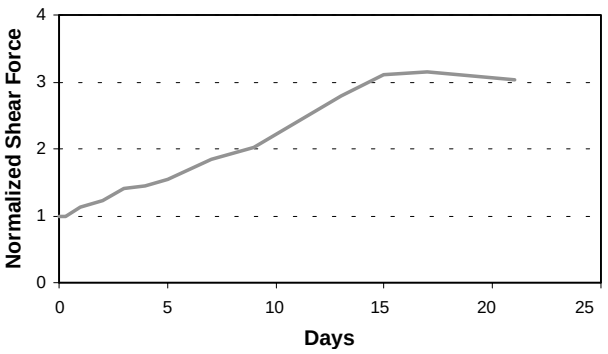

Figure 35. Maximum measured shear force for NEO100 at –20°C (–4°F).

natural rubber compounds. Because tests at –10°C (14°F) and –29°C (–20°F) were conducted much later than tests at other temperatures, the roughness of the sand-blasted plate surfaces decreased over time, resulting in a reduction in the friction. In addition, during heating and cooling cycles of the freezer, moisture accumulated on the bearing-plate interface and, at cold temperatures, frozen moisture might have acted as a bond. At warmer temperatures (–10°C [14°F]), the bonding effect of moisture was less than at colder temperatures. The change of coefficient of friction with temperature is not very clearly understood.

Effect of Loading Rate and Strain Amplitude

Rate of loading is one of the most important parameters that influence the behavior of elastomeric bridge bearings. Laboratory tests generally employ very fast speeds of testing. *NCHRP Report 325* low temperature research was conducted at a rate of 1.0-percent shear strain/sec and the service condition test was conducted at a slow rate, similar to typical daily cycles of a bridge, but the effect of rate of loading was not investigated. The horizontal movements of a bridge occur very slowly, and short-term thermal fluctuations are usually completed in a day. Thus, a very slow cyclic speed in shear will simulate the service condition of the bearings. Creep properties and relaxation properties are affected by the rate of loading. The influence of relaxation was studied in *NCHRP Report 325*. Relaxation tests are conducted to measure the change in the shear load at a fixed shear displacement, which reflects the time-dependent properties of the materials. Rate of loading, however, is a direct measure of such an effect.

Previous research showed that a bridge girder expands/contracts continuously without a period of constant displacement (English et al., 1994). Therefore, relaxation tests do not reflect the true in-service behavior of the bearings. In addition, work done by DuPont, which formed the basis for earlier AASHTO specifications, indicates that the shear modulus is independent of temperature when the rate of strain is very low, such as the strain from a daily temperature cycle (DuPont, 1959). Tests were conducted to determine the effect of loading rate on the performance of bearings. A standard test speed, 0.30-percent shear strain/sec, and a slow speed, 30-percent shear strain/ 10 hr, were used. Bearings were tested at room temperature and at certain low temperatures.

Shear Modulus. Shear modulus depends strongly on the rate of loading and the level of strain. At very small strains, shear modulus is very large, approaching infinity at zero strain. Shear modulus changes rapidly, decreasing with an increase in shear strain between strain levels of 0 percent and 4 percent. The change is more gradual at higher strain levels as depicted in Figure 36. The relationship between shear modulus and shear strain can be represented by a power function obtained by a least-squares fit through the data. Figure 37 shows the shear modulus for NEO150 for the first 4 days of conditioning at –20°C (–4°F) for various strain levels. The shape of the curves is quite similar between strain levels of 4 percent to 30 percent.

The shear modulus Curve 4 is normalized with Curve 2 and the resulting relationship is also shown in Figure 37. At the range of strain levels considered in this study, there is no significant change in the normalized shear modulus with the strain level. Therefore, the shape of the shear modulus curve for a material remains the same during crystallization; the only change is the shift of the curve. The change in shear modulus as a function of shear strain is obvious, especially at small strain levels. Therefore, shear modulus (or shear force) should be compared only at the same strain level. In the current AASHTO test procedures, room temperature shear modulus and low temperature shear modulus are determined differently. Room temperature shear modulus is determined at

TABLE 6 Coefficient of friction for the neoprene compounds

Compound	Temperature							
	14 ˚F		-4 ˚F		-20 ˚F		Var T .	
	No. of Tests	Average Value	No. of Tests	Average Value	No. of Tests	Average Value	No. of Tests	Average Value
NEO150	5	*0.29*	7	*0.46*	4	*0.38*	5	*0.46*
NEO100	-	-	4	*0.45*	-	-	-	-

Numbers in italic are the coefficient of friction values

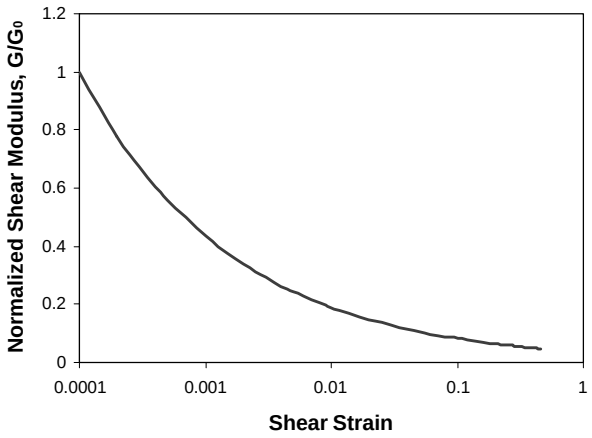

Figure 36. Shear modulus as a function of shear strain.

25-percent strain after the specimen is strained to 50-percent strain, in one direction; whereas low temperature shear modulus is determined at 25-percent strain, but the specimen is strained to 25-percent strain. In addition, room temperature quad shear uses a secant modulus, whereas cold temperature quad shear uses a tangent modulus. Strain level is a result of expansion/contraction of a bridge because of changes in the temperature. Therefore, in a performance test, emphasis should be given to the range of temperature variations.

Loading Rate. A test setup, described in Appendix B of the research team's final report, was designed to study the effect of loading rate on the load-displacement behavior in shear. Tests were performed at −10°C (14°F), −20°C (−4°F), −29°C (−20°F), and room temperature. Tests were conducted at room temperature to investigate the effect of fast loading rates on the behavior of the bearings. Test speeds of 30-percent strain in 30 sec to 5 min were employed. Results indicated that the effect of loading rate is insignificant for the range of 30-percent shear strain in 30 sec to 3 min (Yakut, 2000). In the cold temperature experiments, NEO100 and NR150 compounds were tested extensively, whereas a few tests were conducted on NR100 and NEO150 compounds. Two rates of loading were applied: 30-percent shear strain in 2 to 3 min (fast test) and 30-percent shear strain in 10 hr (realistic performance speed). Figure 38 presents the load-displacement plot in shear for NEO100 for the two test speeds selected. Table 7 includes the results from other tests. Under fast loading, the bearings tend to exhibit stiffer behavior. A slowly loaded specimen creeps more and shows more flexible behavior. The effect of speed is more significant for neoprene compounds. At room temperature, a change of 16 percent (average of five tests) in shear modulus was determined for the two test speeds. At low temperatures, the difference between results from the slow test and the fast test is generally between 20 percent and 45 percent for neoprene compounds and 15 percent and 30 percent for natural rubber bearings.

Compression Tests

One of the primary tasks of the low temperature test phase of this research project is to recommend performance-related test procedures. For the purpose of developing simple test procedures, compression tests were conducted in order to determine if any correlation exists between the stiffening in shear and the stiffening in compression.

Test Procedure. Attempts at determining the compressive stiffness of the full-size bearing at low temperatures were not satisfactory because of the low level of strains introduced. Therefore, a new setup was designed to test small-size bearings under compression. NEO150 and NEO100 bearings were cut into pieces of 102 × 102 mm (4 × 4 in.), keeping the thickness unchanged. Two bearings of the same material were sandwiched between steel plates. The total displacement of the two bearings was measured at four points. The axial displacement of the bearing was computed by averaging the four measurements. These bearings were tested in the cyclic compression test setup, using only one hydraulic ram for the pair of bearings. The NEO100 bearing was placed on one of the rams and

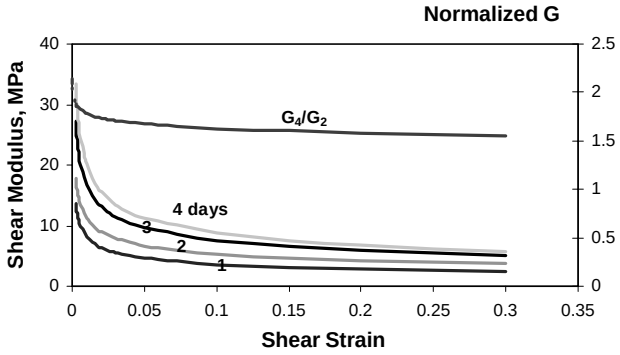

Figure 37. Change of shear modulus with time at −20°C (−4°F).

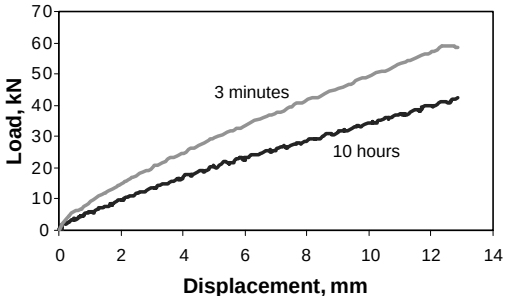

Figure 38. Load-displacement behavior of NEO100 at −20°C (−4°F).

TABLE 7 Results of speed of testing

Compound	Shear Modulus at 30% Strain, MPa (% change)							
	Room Temp.		–10°C		–20°C		–29°C	
	Fast	Slow	Fast	Slow	Fast	Slow	Fast	Slow
NEO150	1.57(16)	1.35(0)	5.47(50)	3.65(0)	-	-	-	-
			6.55(31)	5.01(0)	-	-	-	-
NR150	0.88(13)	0.78(0)	1.23(27)	0.97(0)	-	-	3.64(24)	2.93(0)
			1.34(30)	1.03(0)	-	-	3.74(19)	3.15(0)
			1.34(22)	1.10(0)	-	-	1.90(33)	1.43(0)
NEO100	0.72(16)	0.62(0)	1.54(21)	1.28(0)	1.07(35)	0.79(0)	2.28(46)	1.56(0)
	0.66(23)	0.54(0)	1.85(19)	1.56(0)	3.38(19)	2.83(0)	2.33(36)	1.71(0)
	-	-	2.17(26)	1.72(0)	-	-	-	-
	-	-	2.31(25)	1.84(0)	-	-	-	-
NR100	0.68(15)	0.59(0)	0.85(15)	0.74(0)	0.95(16)	0.82(0)	-	-
	-	-	0.85(15)	0.74(0)	1.00(14)	0.88(0)	-	-

the NEO150 bearing was placed on the other ram; thus, both bearings were tested under identical conditions inside the freezer. A load maintainer, described in Appendix B of the research team's final report, was used to apply compression. Tests were conducted at –20°C (–4°F). Bearings were conditioned for 10 days, and tests were conducted first after thermal equilibrium was reached and every day thereafter. A loading rate of approximately 2 kN (0.4 kips) per second was applied. Typically one loading cycle was completed in 2 min. Bearings were loaded to maximum load for two cycles, and the stiffness was determined from the second loading cycle.

Test Results. Figure 39 depicts the compressive load as a function of displacement for the compounds tested at room temperature. Two different procedures were used to calculate compressive stiffness as illustrated in Figure 39. The compressive behavior is almost linear at small strains. The curves start to become highly nonlinear above 10 percent compressive strain (a displacement of 7.6 mm [0.3 in.]-total elastomer thickness is 76 mm [3.0 in.] for two bearings). The slope of the best-fit line to the data between 1-percent and 10-percent strain, K_1 (or the maximum strain if less than 10 percent), was used as the first approach. The second method, K_2, was based on the slope of the straight line between the origin and a desired strain level.

Figures 40 and Figure 41 compare the normalized stiffness (i.e., stiffness at low temperature divided by the stiffness at room temperature) determined from the shear and the compression tests. As explained earlier, shear stiffness was calculated at three strain levels and it was shown that the normalized shear modulus does not depend on the level of strains at which the calculations were based. In compression, however, strain level had a significant effect on the stiffness because of the nonlinear behavior in compression. Figure 40 presents the normalized stiffness determined at various compressive strain levels. Because of the large stiffening of NEO150, data were not available beyond 4-percent strain from all tests. Also shown in Figure 40 is the comparison based on the slope of the best-fitted line to the load-displacement curve between 1-percent strain and 10-percent strain (or maximum strain if less than 10 percent), K_1. Normalized stiffness based on K_1 appears to be a better representation of the compressive behavior. Large stiffening in compression was observed for NEO150. The effects of instantaneous thermal stiffening and

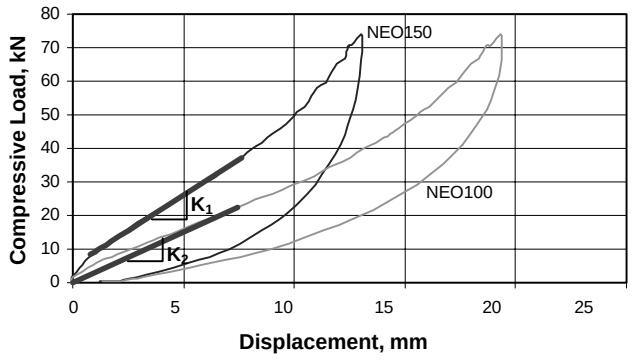

Figure 39. Compressive behavior of neoprene compounds.

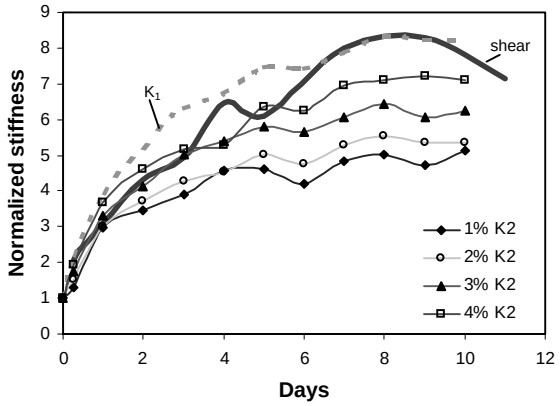

Figure 40. Comparison of results for NEO150.

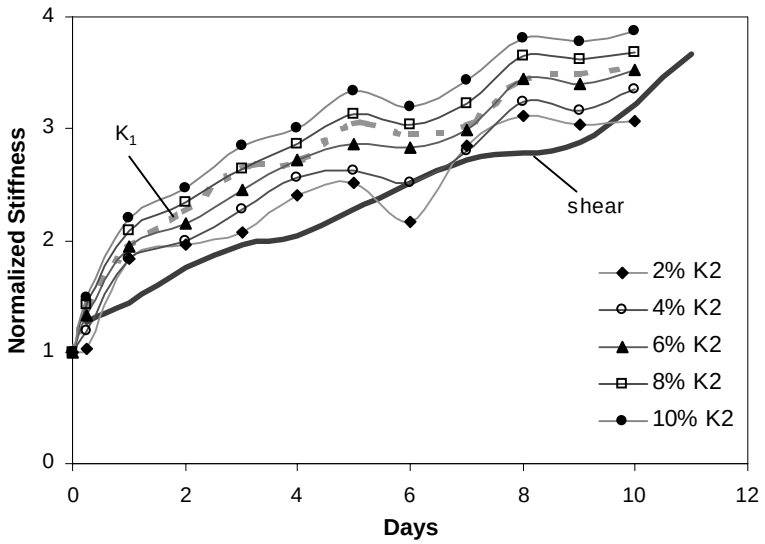

Figure 41. Comparison of results for NEO100.

crystallization are evident for both compounds. The trend of crystallization stiffening in compression and in shear is very similar. Although the size of the specimens tested in compression and in shear was different, the normalized stiffness, a relative measure of stiffness with respect to room temperature value, is considered to be independent of size. The results indicate that there is a reasonable correlation between stiffening in shear and stiffening in compression. Therefore, compression tests can potentially be used to predict the increase in the shear modulus at low temperatures. The behavior under compression, expected to be linear at small strains, is not perfectly linear, hence stiffness needs to be compared based on the slope of straight line between 1 percent and 10 percent (or maximum strain).

Interpretation

Thermal Response of Bearings

Results of this low temperature research revealed that elastomeric bridge bearings are poor conductors of heat and heat transfer occurs mainly through the thickness of typical-size bridge bearings. The time required for a bearing to reach SST is a function of the total elastomer thickness. The effect of exposure condition on the time to reach SST is not very significant. It was shown that thermal response does not depend on the type of compound and the plan area of the bearing. The heat transfer response of the bearings to temperature changes is exponential, leading to significant change in the bearing temperature during the first hour of cooling/heating (Figure 17).

Based on this observed behavior, it can be concluded that the AASHTO M251 Level 1 test procedure discussed earlier (shear strain is held for a required 15-min duration before shear stress is recorded) does not represent actual performance at the conditioning temperature. The period for the test permits significant heating of the bearings. Figure 17 showed that a bearing with an overall thickness of 44.5 mm (1.75 in.) (total elastomer thickness of 38 mm [1.5 in.]) will heat up from −31°C to −12°C in 30 min. This would result in a change of about 50 percent in the shear modulus (in Figure 29, the normalized shear modulus changed from 8.0 to 3.7 for NEO150 and from 4.0 to 2.2 for NEO100 when the bearing temperature increased from −30°C to −8°C [Figure 27]). For thinner bearings, the effect would be even more significant. The M251 Level 1 test does not give a realistic measure of the shear modulus at the conditioned temperature. Also, the test requires the measured G be less than $G = 0.83$ MPa (120 psi) for NR and $G = 1.38$ MPa (200 psi) for NEO for a 50 durometer bearing with no provisions for bearings that have durometer hardness other than 50. Given that the 60 durometer bearings allowed in the specification frequently have room temperature shear modulus values in excess of 0.83 MPa (120 psi), this test with fixed limits is unrealistic for such bearings. Therefore it is recommended that this test be eliminated.

Thickness-time curves presented in Figure 19 can be used to determine the time required for a bearing that has a certain thickness to reach the equilibrium temperature. The curves given in Figure 19 can be approximated by the following equations

$$t_{SST} = 2.0\,h^2 \quad \text{with no condensation} \tag{4a}$$

$$t_{SST} = 2.9\,h^2 \quad \text{with condensation} \tag{4b}$$

where

t_{SST} is the time to reach SST in 1 hr and
h is the total elastomer thickness in inches.

This information can be used to obtain the instantaneous thermal stiffness of full-size bridge bearings. The bearing is conditioned for the duration of time obtained from Figure 19 at a certain temperature, then the shear stiffness tests are conducted to measure the stiffness. Numerical solutions of the heat transfer equation indicated that the time required to reach SST is not a function of the temperature range/temperature difference (i.e., the difference between the initial and the final temperature of exposure does not influence the time to reach SST). Examination of the measured temperature data within the bearing gave a diffusion coefficient of approximately 0.04 mm^2/sec (0.0000602 in^2/sec).

Low Temperature Stiffness Tests

Extensive experimental research was conducted to determine the performance of elastomeric bridge bearings at cold temperatures. Full-size bridge bearings were tested for various parameters, including the type of compound, the temperature history, the rate of loading, the time, and the cyclic loading. All the tests were conducted inside a freezer. The results confirmed that neoprene compounds were more prone to crystallization than their natural rubber counterparts. Because of continuous stiffening of the neoprene compounds with time, some bearings did slip, which limited the amount of maximum shear force that could be experienced by the bearings without bonded sole plates. This research shows that the performance criteria need to be based on the maximum shear force for bearings without bonded sole plates. The value of the maximum shear force depends on the daily temperature fluctuations, the type of the elastomeric compound, the average ambient temperature, and the duration of the average ambient temperature.

Current AASHTO tests require that the shear modulus at cold temperature be compared with the shear modulus determined at room temperature. There is a significant discrepancy between the modulus obtained in this research and the ones provided in the certified reports. The full-scale shear test results are compared with the results from the certified reports in Table 8. The full-scale shear test results indicated that NEO150 fails the AASHTO crystallization test. The NEO100 also did not pass the full-scale crystallization test, but the results are close to the certified results. The full-scale shear and full-scale crystallization tests showed much greater instantaneous stiffening at all test temperatures than given by the ASTM D1043-92 test at –40°C (–40°F).

The temperature-shear modulus response for instantaneous thermal stiffening is shown in Figure 42. Instantaneous stiffness is measured when bearing thermal equilibrium is reached. Least-squares curves through the data points give the shear modulus temperature curves for the materials tested in this research. The certified reports indicate that the bearings pass current AASHTO low temperature tests, whereas the test results showed that NEO150 and NEO100 (Figures 22 and 24) would fail the current AASHTO crystallization test. Performance evaluation of the bearings for cold temperature applications requires the examination of temperature data of the location in which the bearings will be installed. In addition, bearing design should take into account the maximum shear force that is expected by the bearings.

Loading Rate

Tests performed to investigate the effect of the loading rate on the performance of the bearings showed that the speed of testing is an important parameter that influences the behavior of elastomeric bridge bearings. *NCHRP Report 325* included the effect of relaxation to account for the loading rate effect. Relaxation and creep properties of the bearings can be used to estimate the effect of loading rate indirectly (Yakut, 2000). The results indicated that a slow rate of loading (i.e., longer test duration) produced smaller shear modulus values. The significance of the loading rate depends on the type of the compound and the temperature of exposure. The results of fast tests need to be lowered to account for the rate of loading. This reduction should be applied on the basis of crystallization

TABLE 8 Comparison of tests with the certified report

Test	NEO150	NEO100	NR150	NR100
	Crystallization (after 15 days)			
–10˚C (14˚F)	4.32(3^{rd} day)	3.55	1.6	1.23
–20˚C (-4˚F)	10.5	4.8	2.77	1.83
–30˚C (-20˚F)	9.3(4^{th} day)	4.11(13^{th} day)	3.89(13^{th} day)	2.6(13^{th} day)
Certified (-15˚F)	2.67	3.33	2.4	2.8
	Instantaneous Stiffening			
–10˚C (14˚F)	2.88	1.56	1.42	1.2
–20˚C (-4˚F)	2.1	1.6	1.78	1.27
–30˚C (-20˚F)	3.44	2.07	1.9	1.5
Certified (D1043)	1.23	1.09	1.2	1.1

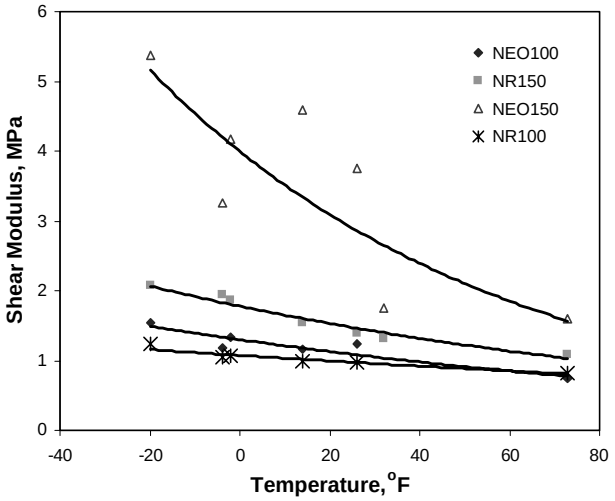

Figure 42. Shear modulus versus temperature (instantaneous stiffening).

resistance and the type of the compound (i.e., a greater reduction should be applied to less crystallization-resistant compounds). The reductions of 30 percent and 20 percent are recommended for neoprene and natural rubber, respectively.

Methods for Determining Stiffness Properties

Current AASHTO low temperature test procedures need modifications and the method of evaluation needs to be altered. Identical test procedures should be used to determine the room temperature and the cold temperature stiffness of the bearings. The quad shear test procedure (one-way) is the most realistic test employed by AASHTO to determine the shear stiffness of the bearings. This test procedure can be used to determine the instantaneous thermal stiffness of the bearings as well as the crystallization temperature. The evaluation procedure described previously can be used in conjunction with the quad shear test or other shear test methods (e.g., the inclined shear test or dual lap test) to check the performance of the bearings for a certain application. Compressive stiffness tests conducted in this research indicated that there is a good correlation between the normalized shear stiffness (i.e., the low temperature stiffness divided by the room temperature value) and the normalized compressive stiffness of elastomeric bridge bearings. A shear stiffness test of full-size elastomeric bearings requires more complicated setups and equipment, especially for the bearings without bonded sole plates. Compressive stiffness tests, however, are simple and can be conducted by using readily available test machines (e.g., hydraulic compression machines). Therefore, compressive stiffness tests can be used to determine the normalized shear stiffness of the elastomeric bridge bearings at cold temperatures. Because of the nonlinear nature of the load-displacement characteristic of the bearings, the K_1 procedure, described earlier, needs to be used to compute the stiffness. If the results of the compressive stiffness test suggest that the bearing should be rejected, then the direct shear stiffness test might be conducted.

The British Standard recommends the following expression to account for the increase in stiffness at cold temperatures (British Standard, 1983):

$$\frac{G_T}{G_0} = 1 - \frac{T}{25} \tag{5}$$

where

T is the temperature in centigrade.

A comparison with the results of this research given in Table 9 shows that Equation 5 is unconservative. Figure 43 shows the comparison of Equation 5 with the results from this research and from *NCHRP Report 325*. Equation 5 is unconservative because it does not take into account the crystallization and type of compound. Given that the behavior of elastomeric bridge bearings depends strongly on the compound, a test is necessary to determine the low temperature behavior. It would be unrealistic to suggest equations to predict the low temperature stiffening.

AASHTO gives three ways to establish the low temperature grades of elastomers for a certain region in the following order of preference:

1. The historic low temperature over a 50-year period,
2. The maximum number of consecutive days the daily high temperature stays below 0°C (32°F), or
3. The zone maps provided.

The grades for Preferences 1 and 2 are given in Table 2. Table 10 shows the statistical summary of the records for the selected regions (Yakut, 2000). The historic low temperature is –37°C (–34°F), –36°C (–32°F), –33°C (–27°F), and –37°C (–34°F) for Anchorage, Billings, Chicago, and Minneapolis, respectively. The grades based on these temperatures would be

TABLE 9 Comparison of the normalized shear modulus

Compound	Crystallization after 10 days					
	-10˚C (14˚F)		-20˚C (-4˚F)		-30˚C (-20˚F)	
	Tests	Eq.5 / Test	Tests	Eq.5 / Test	Tests	Eq.5 / Test
NEO150	10.4	0.13	8.3	0.22	19.0	0.12
NEO100	3.2	0.44	3.3	0.55	3.6	0.61
NR150	1.6	0.88	2.3	0.78	3.2	0.69
NR100	1.3	1.08	1.6	1.13	2.2	1.00
	Instantaneous Thermal Stiffening					
NEO150	2.9	0.48	2.1	0.86	3.4	0.65
NEO100	1.6	0.88	1.6	1.13	2.1	1.05
NR150	1.4	1.00	1.8	1.00	1.9	2.02
NR100	1.2	1.17	1.3	1.38	1.5	1.47

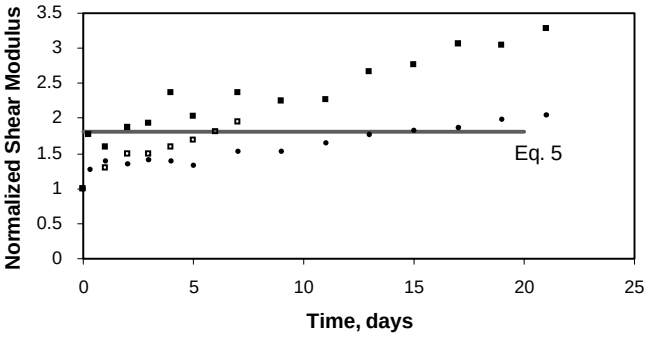

Figure 43. Natural rubber compounds at –20°C.

Grade 3 for Chicago and Grade 4 for the other three cities. On the other hand, the number of consecutive days below 0°C (32°F) is 60, 26, 46, and 66 for Anchorage, Billings, Chicago, and Minneapolis, respectively, suggesting a Grade 4 or 5. The zone maps provided in AASHTO give a Grade 5 for Anchorage and Grade 4 for the other cities.

Performance-Based Testing and Acceptance Criteria

Background

The function of elastomeric bridge bearings is to accommodate displacements resulting from expansion/contraction of the bridge and to transmit forces to the supporting structure. In typical design, the minimum thickness of the bearings is determined on the basis of the longitudinal displacement of the bridge girder using the equation

$$h = \frac{(\Delta T)L_g\alpha + \Delta_{sc}}{\gamma} \quad (6)$$

where

h is the total elastomer thickness,
ΔT is the temperature difference,
α is the coefficient of thermal expansion,
γ is the design shear strain,
L_g is the length of the girder, and
Δ_{sc} is the displacement resulting from creep and shrinkage.

AASHTO specifies ΔT = 27°C (80°F) for concrete bridges in cold climates. Common design practice employs a maximum 50-percent design shear strain limit as specified in the AASHTO specifications. Therefore, the L_g/h ratio of the bearings designed according to AASHTO does not show too much variation. In this research, a value of 800 will be used for L_g/h (e.g., L_g = 30 m [100 ft], h = 38 mm [1.5 in.]) in the evaluation of the bearings. The design shear force based on 50-percent shear strain is

$$H_R = 0.5\, G_R A \quad (7)$$

TABLE 10 Statistics of the temperature records

	Daily Low Temperature(in °F)			
	Anchorage, AL 1953-1993, 1996-1999	Billings, MT 1948-1993, 1996-1999	Chicago, IL 1958-1993, 1996-1999	Minneapolis, MN 1948-1993, 1996-1999
Historic low	-34	-32	-27	-34
Historic high	52	62	71	69
No. of Cons. days below 32°F	60	26	46	66
Average(μ)	14.94	23.06	25.7	18.57
St. Dev.(σ)	14.3	15.01	15	17.11
Prob.(x<-20),%	1.3 (0.27)[a]	0.79 (0.16)	0.14 (0.03)	1.33 (0.3)
Prob.(x<-4),%	12.5 (1.15)	7.23 (0.56)	3.84 (0.42)	12.07 (0.82)
Prob.(x<14),%	44 (2.39)	23.8 (1.4)	20.8 (0.97)	37.45 (1.79)
	Difference Between Daily High and Low			
Minimum	1	1	1	1
Maximum	48	63	49	49
Average(μ)	13.44	19.76	16.68	17.1
St. Dev.(σ)	5.87	7.84	7.74	7.79
Prob.(x>20),%	12.8% (2.88)[a]	41.61 (4.95)	29.75 (4.46)	31.71 (4.04)
Prob.(x>30),%	0.5% (0.24)	9.64 (2.04)	4.88 (1.01)	5.81 (1.28)
Prob.(x>40),%	0.03% (0)	1.16 (0.37)	0.25 (0.12)	0.24 (0.08)

[a] Values in parentheses indicate the probability of occurrence

where

H_R is the design shear force,
A is the plan area of the bearing, and
G_R is the shear modulus at room temperature.

The shear modulus and plan area of the bearing are determined so that the magnitude of the shear force is limited to a maximum value. At low temperatures, the shear modulus increases because of the stiffening of the elastomer, which leads to a concern that excessive shear force may be transmitted to the substructure. The magnitude of the shear force at cold temperatures is

$$H_C = G_C \gamma_C A \tag{8}$$

where

H_C is the cold temperature shear force,
G_C is the shear modulus,
γ_C is the shear strain, and
A is the plan area of the bearing.

The G_C is a function of the level of the strain, the temperature, and the duration of the temperature. Additionally, γ_C is related to the temperature change (the difference between the daily high temperature and the daily low temperature, ΔT_C). Therefore, Equation 8 can be rewritten as

$$H_C = G_C \frac{(\Delta T_C) L_g \alpha}{h} A \tag{9}$$

The G_C should be obtained from tests at cold temperatures. The ΔT_C is determined from an analysis of temperature records at the site. The factor of $\alpha L_g/h$ will be taken as 0.0044 for ΔT_c in °F, and 0.00792 for ΔT_C in °C ($\alpha = 9.9 \times 10^{-6}$ mm/mm/°C [5.5×10^{-6} in./in./°F]).

The concern over low temperature performance of elastomeric bridge bearings can be considered in two ways—the failure of the bearing because of brittle behavior (i.e., glass transition) and excessive shear forces experienced by the bearing. The brittle behavior, which is a material property, is a function of the lowest temperature for a particular elastomer. The excessive shear force may have two undesirable consequences: (1) damage to the guides and/or the supporting structure and (2) slip of the bearings without bonded sole plates. Therefore, a performance evaluation of elastomeric bridge bearings at cold temperatures should determine whether excessive forces or slip would be a problem. An evaluation methodology is described in the following section, with emphasis on the parameters that influence the evaluation.

Objective

AASHTO Specification M251-97 requires that the shear modulus test be performed at specified temperatures after conditioning the bearings for a certain number of days. The shear modulus is required to be less than 4 times the room temperature value in order to limit the magnitude of the shear force. The limit of 4 was developed by Roeder et al. by testing one neoprene compound that stiffened to 11 times the room temperature value in the crystallization test (12 days at –25°C) (Roeder et al., 1989). That compound, then subjected to one arbitrary temperature history (10 days at –13°C, then 5 days at –28°C) and a constant daily 10-percent strain test history, gave a maximum measured shear force that was 4.6 (not 11) times the room temperature design shear force. A permissible cold temperature shear force of 1.5 times the room temperature value was recommended. The 11/4.6 ratio, which was assumed constant for all compounds, was multiplied by 1.5 to give 3.6, which was rounded up to 4. This shear modulus limitation does not adequately consider the level of shear strain resulting from those thermal expansion and contraction cycles of a bridge that can be expected at low temperatures. Bearings that fail the current AASHTO cold temperature tests may perform satisfactorily in service, and this satisfactory performance may be evident given a more realistic evaluation.

The following sections discuss how a performance-based evaluation, which is a more realistic representation of the in-service behavior of the bearings, should be carried out. The expected performance of a bearing is investigated on the basis of experimental data available from the tests conducted and the temperature data of some selected cities.

Parameters Influencing the Evaluation

The performance of the elastomeric bearings at cold temperatures should be evaluated on the basis of the behavior under cold temperatures and the service conditions that the bearings will be subjected to during their lifetimes. In this research, the behavior of the bearings at cold temperatures was investigated experimentally, at –10°C (14°F), –20°C (–4°F), and –30°C (–20°F), and the results were presented in the previous sections. The service conditions, however, depend on the temperature variation, which is a function of the geographic location where the bearing will be installed. In this section, the effect of the temperature variation (i.e., service condition) on the performance-based evaluation of the bearings is investigated. A performance-based evaluation of the bearings at cold temperatures depends on the following parameters pertaining to the temperature record of the selected region:

1. Average daily temperature,
2. Number of consecutive days that the temperature remains below a certain average daily temperature, and
3. Daily shear strain values resulting from the daily temperature changes.

The temperature records included in this study contain daily high and daily low temperatures for each day. (The historic temperature records available from the National Weather Service were archived in °F, so that format will be used in this section.)

1. **Average daily temperature.** Bridge bearings should be checked against two types of stiffening related to cold temperature: (1) instantaneous thermal stiffening resulting from short-term changes in the temperature and (2) crystallization stiffening that occurs after prolonged exposures at a certain temperature. Because instantaneous stiffening can be critical over a short period of cold temperature (3 to 15 hr), the performance-based evaluation should be based on daily low temperatures. Results of this research and previous research indicate that the lowest temperature is the most critical temperature for instantaneous stiffening. Therefore, for instantaneous stiffening, an evaluation temperature should be based on the historic minimum daily temperature (HL) over a 50-year period or a more conservative lower value.

   Crystallization depends on the length of time of exposure, as well as the temperature. The daily low temperature is not appropriate to determine the performance of bearings for crystallization because this temperature is not continuous. The average daily temperature reflects a continuous temperature history better than the daily low temperature. Therefore, a performance-based crystallization test needs to be based on the average daily temperature record. Figure 44 presents the average daily temperature histogram of Anchorage, Alaska, for the period of 1953 through 1999. The minimum average daily temperature is –31°C (–23°F) in Anchorage. The determination of temperatures, at which crystallization tests are to be conducted, requires a thorough analysis of the temperature data, which will be discussed later.
2. **Number of consecutive days.** The number of consecutive days indicates how long the average daily temperature stays below a specified value and is an important parameter that affects crystallization of the bearings. The significance of the number of consecutive days (i.e., duration) depends on the specified temperature. For example, if the average daily temperature stays below 5°C for 30 consecutive days, a significant crystallization (i.e., increase of stiffness with time) will not occur, because crystallization does not take place at such relatively high temperatures. However, if the bearings were conditioned at –20°C for 10 days, a significant crystallization will occur for some elastomers. The significance of the duration depends on the amount of the shear strain produced by the daily temperature changes. Therefore, the number of consecutive days should be considered along with the daily shear strain at a specified temperature.
3. **Daily shear strain.** As shown by Equation 8, the value of shear strain experienced by a bearing and the value of the shear modulus determines the magnitude of the shear force. A bearing in a very cold environment will not have any problems unless it is strained. The level of the expected shear strain is a result of the daily temperature fluctuation, which generally is larger at higher temperatures. Figure 45 presents the maximum daily shear strains computed for average daily temperatures ≤–10°C (14°F) (L_g/h = 800) based on the Anchorage, Alaska, data. An equation of the best fit to the data obtained from a least-squares approximation is also presented in this figure. Similar evaluations for the four locations and three specified temperatures are shown in Figure 46. Generally, the maximum daily shear strain decreases as the number of consecutive days increases. Table 11 gives the maximum and the minimum daily shear strains at –10°C (14°F), –20°C (–4°F) and –30°C (–20°F). In Table 11, a strain value 5 percent less than the maximum daily strain (MS) is also shown, which will be discussed later.

Evaluation of Tested Bearings

The parameters that should be included in a performance-based evaluation of the bearings were explained above. These parameters were used to evaluate the expected performance of bearings tested in this research assuming the bearings were installed in four cities: Anchorage, Alaska; Billings, Montana; Chicago, Illinois; and Minneapolis, Minnesota. The full-size neoprene bearings tested in this research failed the current AASHTO crystallization tests. The NEO150 bearing stiffened by a significant factor of 10 (>4) after 2 weeks at –20°C (–4°F)

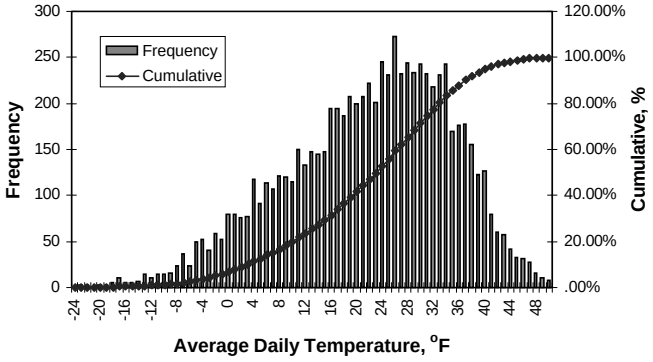

Figure 44. Average daily temperature histogram of Anchorage.

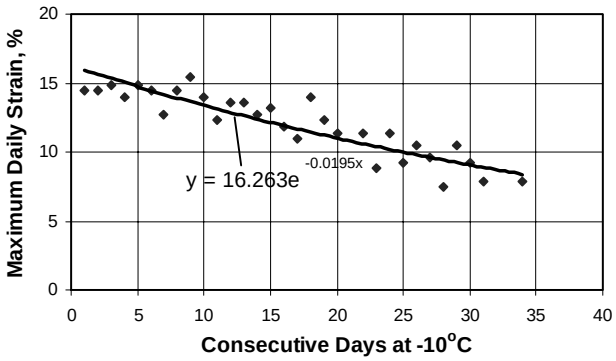

Figure 45. Maximum daily strain for Anchorage.

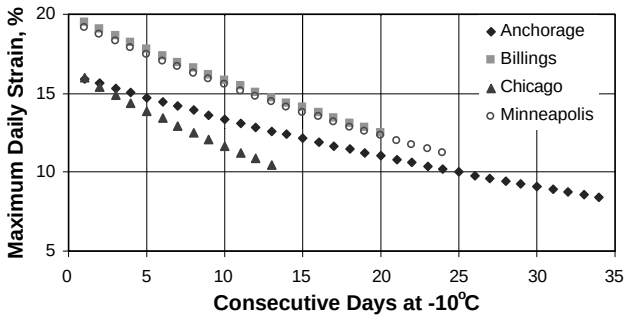

a) At –10°C

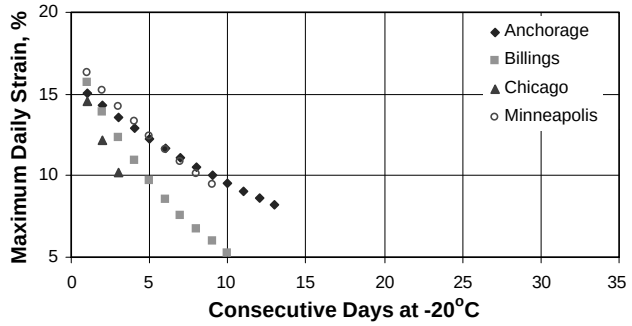

b) At –20°C

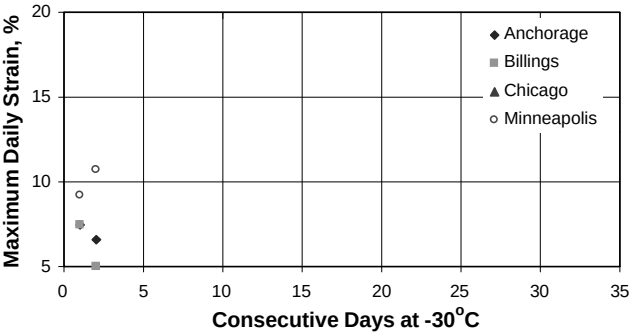

c) At –30°C

Figure 46. Maximum daily strain.

as shown in Figure 22. The normalized shear modulus of the NEO100 bearing was 5 (>4) after 2 weeks at –20°C (–4°F) (Figure 24). The NR100 and NR150 bearings satisfied the current AASHTO test requirements.

The performance-based evaluation of the bearings is given in Appendix B of the research team's final report. Two performance parameters were considered: (1) the maximum shear force and (2) possible slip, which is a potential problem for bearings without bonded sole plates. Steel-laminated bearings of the size used in the experimental research and fabricated from NEO100, NEO150, and NR150 material were assumed. The numerical results from the maximum shear force evaluation are summarized in Tables B3, B4, and B5. The NEO100 bearing, which failed to satisfy the current AASHTO requirements in the full-size tests, would have performed quite well in Anchorage, Billings, Chicago, and Minneapolis. The largest shear force occurred at –10°C (14°F) for the NEO100 bearing because the bearing was exposed to that cold temperature for longer periods and had larger temperature-induced strains. The shear force normalized by the room temperature value was generally less than 1.0 at all temperatures for all specimens, except for the NEO150 bearing (the normalized shear force of the NEO150 was less than 2.0). As shown in the Objective section earlier, the current AASHTO cold-temperature stiffening provision, $(G_C/G_R) \leq 4.0$, is based on an assumed maximum ratio of cold temperature/room temperature shear force of 1.5. On the basis of this current performance requirement and the assumption that only one of the two support bearings must accommodate all of the movement within the span, the NEO150 bearing used in this research would only be satisfactory in Chicago. In the other three cities, the $H_C/H_R > 1.5$. If the two bearings share the bridge movement equally, then even the NEO150 bearing would perform satisfactorily in all four cities. The results also revealed that crystallization was not important for the NR150 material because the normalized shear force was less than 1.0 at all temperatures. The NR100 material was not evaluated, because its performance would be even better than the NR150 material.

The slip evaluation (in Section B7.1 of Appendix B of the research team's final report) for the NEO100 material indicated there would be no slip in any of the four cities (see Figure B29) even though the dead load compressive stress used in the evaluation was only 1.90 MPa (275 psi). An AASHTO Method B bearing design assuming $G = 0.69$ MPa (100 psi) would permit a dead load stress of 3.7 MPa (540 psi). No slip evaluation was made for the NR150 bearing because its stiffening characteristics were less than those of the NEO100 bearing. The slip study of the NEO150 bearing did show that slip would occur only once in the bridge lifetime in each of the four cities. For the NEO150 bearing a higher dead load compressive stress was used, 3.45 MPa (500 psi), to account for the use of a higher shear modulus. The Method B maximum dead load design stress is 5.7 MPa (820 psi) for this bearing, with a shape factor of 5.5. The single slip occurrence is based on the premise that only one of the two end bearings must support all the bridge movement. If the two end bearings were used, then no slip would occur. Given that the slip evaluation for this NEO150 material with a normalized $G_C = 10$ after 4 days conditioning (see Figure 22) indicated only one slip, it appears that slip at cold temperatures is not an important issue and need not influence the development of test standards. The use of bearings with unbonded sole plates provide a means of limiting the maximum shear force to the slip load. There have been no reports of service failures associated with slip at cold temperatures.

TABLE 11 Daily shear strains (%)

Temperature		Location							
		Anchorage		Billings		Chicago		Minneapolis	
		strain	day	strain	day	strain	day	strain	day
-10˚C	Max. strain (MS)	16	1	19.5	1	16	1	19.2	1
	Min. strain	8.4	34	12.5	20	10.5	13	11.2	24
	MS-5	11	20	14.5	14	11	12	14.2	14
-20˚C	Max. strain (MS)	15.1	1	15.7	1	14.6	1	16.3	1
	Min. strain	8.2	13	5.3	10	10.1	3	9.5	9
	MS-5	10.1	9	10.7	4	9.6	-	11.3	6
-30˚C	Max. strain (MS)	7.5	1	7.5	1	-	-	10.7	2
	Min. strain	6.6	2	4.4	2	-	-	9.2	1
	MS-5	2.5	-	2.5	-	-	-	5.7	-

The performance-based evaluation indicated that the bearings would perform adequately, even though the neoprene bearings did not satisfy the current test requirements. Therefore, it appears that the current cold temperature test requirements are too severe, given that bearing materials that will perform well in service are being rejected.

Development of Testing Criteria

Test Parameters. The shear modulus must be determined at the cold temperatures and the conditioning periods that establish the suitability of the bearing material for use at a particular geographic location. The performance test parameters at cold temperatures are test temperature, duration of conditioning, and level of shear strain. The determination of these parameters requires an analysis of the temperature data that contain daily high and low temperatures for a period of at least 50 years. The method of developing these test parameters is discussed in detail in the following section. These test parameters can then be consolidated into a few grade requirements similar to the current system, but it is expected that the testing conditions will be less severe.

Test Temperature. The test temperature is different for the instantaneous stiffness tests and the crystallization tests. For the instantaneous stiffness tests, the test temperature should be taken as the historic daily low temperature (HL) or a more conservative lower value. To include the probability of lower temperatures in future years, a test temperature 5°C lower than the HL is recommended. The crystallization test temperature should be based on the average daily temperature value. Because there is an optimum temperature for the fastest rate of crystallization, performance tests should take into account the possibility of an optimum temperature. In other words, the lowest temperature may not be the most critical temperature for crystallization. Most previous research (Murray and Detender, 1961; Nagdi, 1993; Eyre and Stevenson, 1991) suggests that −10°C and −25°C are the optimum crystallization temperatures for neoprene and natural rubber, respectively. In this research, crystallization of neoprene bearings was significant at −10°C (14°F) and insignificant at 0°C (32°F). The maximum crystallization was observed at −30°C (−20°F) for all bearings. A reasonable minimum crystallization temperature (MCT) can be selected from the average daily temperature histogram. A value corresponding to 1-percent cumulative frequency is recommended as the minimum crystallization temperature (which is MCT) which is −11°F (−24°C) in Figure 44. This value has an occurrence rate of 1.6 per year over a 50-year period (80 total occurrences). The number of consecutive days that the temperature stays below the MCT is generally very small as will be shown in the next section. In addition, a test conducted at a higher temperature for a longer period of conditioning might be more critical than a test at a lower temperature for a shorter duration. The NEO100 bearing stiffened about 3.5 times after 12 days at −10°C (14°F), whereas the normalized stiffness was about 2.5 after 5 days at −30°C (−20°F) as shown in Figure 24. Therefore, the test temperature should be considered in conjunction with the conditioning time. The MCT determined from the histogram will be different for each histogram, so it would be more practical to round off this number to a nearest general category. To accomplish this, four categories were selected for the MCT: 0°C, −10°C, −20°C, and −30°C. The ranges of the MCT that should be rounded off to the nearest category are shown in Table 12. If the selected category of

TABLE 12 Categories of MCT

MCT from histogram	MCT rounded off
MCT 5˚C	No Test
5˚C ≤ MCT > -5˚C	0˚C
-5˚C ≤ MCT > -15˚C	-10˚C
-15˚C ≤ MCT > -25˚C	-20˚C
MCT ≤ -25˚C	-30˚C

MCT is −20°C, then the crystallization temperatures of −10°C and −20°C are recommended. For the MCT = −30°C, the crystallization temperatures should be taken as −10°C, −20°C, and −30°C. If the MCT happens to be larger than −20°C (14°F), then the crystallization temperature can be taken as the MCT only (0°C or −10°C). Because the effect of crystallization is insignificant at high temperatures, tests need not be conducted when MCT > 4.5°C (40°F) (*NCHRP Report 325*).

Duration of Conditioning. To determine the instantaneous stiffening, the bearings should be conditioned until the bearing temperature reaches the test temperature. The thermal response of the bearings indicated that a certain amount of time is required for the bearings to reach the test temperature. For typical full-size bearings, the time to reach the test temperature, which is a function of the bearing thickness, is 5 to 12 hr. Equation 4 can be used to determine the time to reach the test temperature. The duration of the crystallization conditioning is a critical parameter to be determined from an analysis of the temperature data. Regional temperature histograms that contain the frequency of the number of consecutive days at a certain temperature should be developed. Figure 47 illustrates the regional temperature histogram developed for Anchorage at −10°C (14°F). The procedure to develop these histograms is given in Appendix B of the research team's final report. The number of consecutive days (NCD) is obtained from the regional temperature histogram. These histograms also contain information about the number of occurrences of a certain strain level. The determination of a particular strain level is discussed next.

Level of Shear Strain. The amplitude of the shear strain at which performance tests are conducted must be determined such that conservative estimates of the shear force are produced. A test strain value equal to the maximum daily shear strain (MS) is recommended. Figure 48 presents the shear force calculated at −10°C (14°F) for the NEO100 bearing, based on the maximum shear strain values given in Table 11. The solid lines represent the shear force calculated at the MS. The data points represent the actual performance. The shear force calculated on the basis of the maximum daily shear strain (MS) gives conservative results for the four cities. The importance of a certain temperature-induced strain depends on its number of occurrences over a period. If a large strain (greater than the slip strain) occurs only a few times over the lifetime of the bearing, only a few occasions of slip will occur. Consequently, the frequency of large strains determines whether or not the strain should be ignored. A critical strain value of 5 percent less than the maximum historic low temperature strain (MS-5) is recommended. Regional temperature histograms contain information about the occurrence of the critical strain level as a function of the number of consecutive days at each specified crystallization temperature. In Figure 47, the maximum daily strain was computed as 16 percent at −10°C (14°F) leading to the critical strain value of 11 percent. Thus, the histogram of Figure 47 shows the frequency of daily strains larger than 11 percent. The NCD should be determined on the basis of the occurrence of the strain level. In Figure 47, the maximum number of consecutive days that the average temperature remained below −10°C (14°F) is 34 with a frequency of 2. However, an 11-percent strain level had not been reached at the end of this period. Thus, conditioning the bearing for 34 days would not be appropriate. It is recommended that the NCD have at least two occurrences at the strain level selected. The NCD should be selected by taking into account the critical strain level from the regional temperature histograms developed at some specified crystallization temperatures.

Testing. All low temperature testing must be conducted in a closed environment so the temperature can be controlled during the test. It is recommended that the current AASHTO low temperature brittleness test, ASTM D746–95, Method B, be retained as a quality control test for all bearing materials. For low temperature stiffening, the current AASHTO specifications require two different tests: instantaneous stiffening (ASTM D1043-92) and crystallization stiffening (ASTM

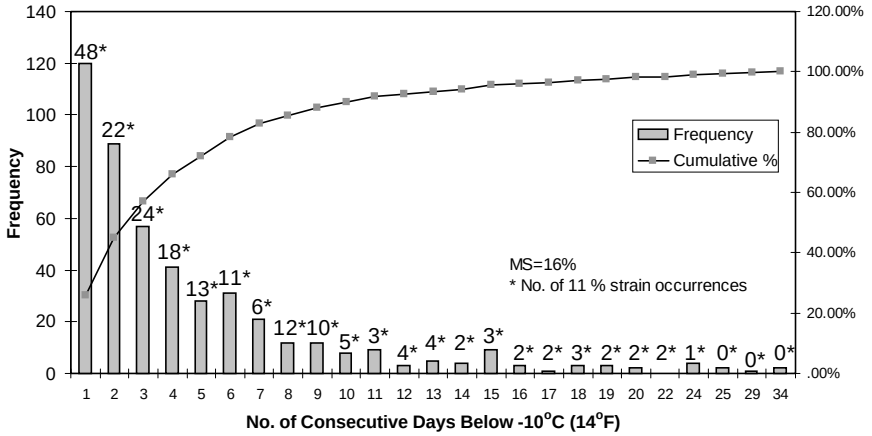

Figure 47. Histogram of Anchorage from 1953 to 1999.

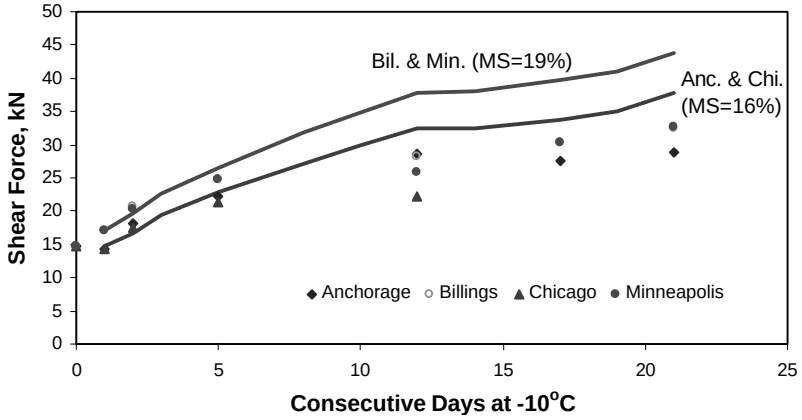

Figure 48. Shear force for NEO100.

D4014-89, modified), a quad shear test. The instantaneous test is supposed to measure the shear modulus as soon as the temperature within the test sample reaches the desired level. The crystallization test merely conditions the bearing at a constant specified low temperature for a specific number of days before testing the bearing stiffness. Given that both of these current tests provide a measure of shear stiffness, they can be replaced by a single test method—any of four shear modulus tests listed in Table 13, which gives the general low temperature test requirements. Because a ratio between the low temperature and the room temperature is specified in the test requirements, a compression test as presented in Appendix B of this report can also be used to determine this ratio. The compression test is more suitable for smaller samples cut from the full-size bearing as discussed earlier.

The secant shear modulus at low temperature G_C should be determined at 15 to 20 percent. This strain level is consistent with the strains expected in a low temperature service environment and will permit more options for adhesives needed for specimen preparation. For full-size elastomeric bridge bearings, the time required to reach SST (t_{SST}) can be computed from Equation 4 or the simplification given in Table 13. For small test samples where the plan area is less than one-fifth of the plan area of the full-size bearing, t_{SST} can be reduced by 20 percent.

The HL (historic low temperature), NCD (number of consecutive days) at CT (crystallization temperature), the test requirements, $\#_1$, $\#_2$, and MS (maximum daily strain) are all derived from the temperature history. The details (i.e., test temperature and conditioning time) depend on the current grading system, which is based on the temperature history at the site under consideration. The basic performance criteria herein, which have the same premise as the current criteria, require that the low temperature shear force (Equation 8) be equal to or less than 1.5 times the acceptable room temperature shear force (Equation 7). Using the adjustment factor 0.7 for neoprene, developed earlier to account for the fast loading rate used in the shear modulus test, the crystallization performance criterion, $\#_2$, can be developed as follows:

$$0.7\ G_C\gamma_C A \le 1.5(0.5)G_R A \text{ or}$$
$$(G_C/G_R) \le (1.07/\gamma_C) = \#_2 \qquad (10)$$

The maximum cold temperature strain γ_C is derived from the maximum daily temperature change at the site for the particular CT. From Table 11, for Anchorage, $\gamma_C = 0.16$, so Equation 10 becomes $(G_C/G_R) \le 6.7$, not 4.0 as currently required. In addition, the test parameters from the temperature record defining the low temperature shear modulus G_C are also significantly reduced: 22 days at –10°C compared with the current Grade 4 (21 days at –37°C) or Grade 5 (28 days at –37°C). It is not clear which of these two current grades should be applied to Anchorage. The $\#_1$ requirement can be derived in a similar manner. To implement the recommended method as illustrated for Anchorage, the temperature histories of numerous locations should be evaluated as presented in this section and Appendix B of the research team's final report in order to produce an accurate Low Temperature Grade Map. The ratio G_C/G_R can be determined from any of the four shear modulus setups or the compressive stiffness test in Appendix B of this report.

TABLE 13 Low temperature stiffening tests

Test Method	Test Parameters	Test Criteria
Quad shear (modified D4014) Dual Lap (Appendix D) Inclined Compression (Appendix A) Full scale shear test Compression (Appendix C)	t_{SST} hours @ historic low (HL) ˚C where $t_{SST} = 3\ h^2$ - see Equation 4	$G_C/G_R \le \#_1$
	NCD (days)@ CT ˚C from temperature records	$G_C/G_R \le \#_2$

CREEP OF ELASTOMERIC BEARINGS

Introduction

All elastomers exhibit the undesirable behavior of creep (or continuing time-dependent deformation under constant load) and stress relaxation (or time-dependent decay in stress at constant deformation). The processes contributing to creep and relaxation behavior of rubber are both physical and chemical in nature (Derham, 1973; Curro and Salazar, 1977). Under ambient temperature, physical processes dominate the relaxation of rubber; at elevated temperatures, chemical processes dominate. Derham (1973) and Freakley and Payne (1978) have noted that physical relaxation usually decreases linearly with the logarithm of time, while chemical relaxation is approximately linear with time. The physical relaxation rates depend on the difference between the service temperature and the glass transition temperature under static conditions. The creep and relaxation rates are high near the glass transition temperature and decrease as the temperature rises. The rate of creep and relaxation depends on the mode of deformation. For the same stress, creep is highest in tension and lowest in compression. Reinforcing fillers (e.g., carbon black) in rubber increases the relaxation rate. The relaxation rate of rubber swollen with appropriate solvent is higher as compared with dry rubber.

The creep of elastomers has generally been studied by applying a constant load for a long period and measuring the deflection at specified intervals. There is some controversy on the definition of creep. In the rubber industry, creep is defined as the increase in deformation after a specified time interval expressed as a percentage of test piece deformation at the start of that time interval. In other industries, creep is defined as the increase in deformation expressed as a percentage of original unstressed thickness of the test piece. ISO 8013 has both definitions, called creep increment and creep index, respectively. AASHTO (1998) uses the first definition and estimates the creep to 45 percent and 25 percent of the instantaneous deformation for 70 and 50 durometer hardness, respectively. Based on the results of a 2-year ongoing creep study conducted on full-scale laminated elastomeric bearings, Takayama et al. (1998) reported that, under axial stresses of 10.8, 14.8, and 19.7 MPa, the maximum creep deformation was about 0.15 percent to 0.6 percent of the total rubber thickness.

Creep can be measured under compression load or shear load. In the international standard, the test pieces for measurements in compression are discs either 29 mm (1.1 in.) in diameter and 12.5 mm (0.50 in.) thick or 13 mm (0.5 in.) in diameter and 6.3 mm (0.25 in.) thick, the same as used for compression set. It is optional whether the test pieces are bonded to end plates (i.e., the measurements can be made with no slippage at the compressed surfaces or with some slip, lubrication being recommended). The essential requirements for the apparatus in compression tests are that one compression plate is fixed and the other is free to move without friction. The force must be applied smoothly and without overshoot and the mechanism must be such that the line of action of the applied force remains coincident with the axis of the test piece as it creeps. The compression of the test piece should be measured to ±0.1 percent of the test piece thickness. For measurements in shear, a double sandwich test piece is used, preferred dimensions being 25-mm diameter and 5-mm thickness. The apparatus for measurements in shear is essentially the same as for compression, except for the differences in geometry of the test piece and its mounting. The international standard recommends that the test piece be mechanically conditioned by straining five times to a higher strain than used in the test between 16 and 48 hr before the test, which will remove any irreversible behavior. A force is applied within 6 sec such that an initial strain of 20 ± 2 percent is realized. The deformation of the test piece is measured after 10 min with further measurements after 10, 100, 1000 min, and so forth. There are no particular load fixtures, and there is no method suggested for estimating the long-term deflection.

The standard creep test is basically a quality control test and cannot be used to predict the behavior of full-size bearings because the shape factor, boundary conditions, loading conditions, and exposure conditions (e.g., temperature) of the full-size bearings can vary considerably as compared with the test specimen. The objective of the present study is to investigate the creep behavior of bridge bearings and propose a method to predict creep of such bearings based on small-scale testing. To understand the long-term behavior of bridge bearings under sustained axial loads, full-scale testing of selected bridge bearings was performed. The methodology and results of this study are summarized herein. Full-scale creep tests are time consuming, uneconomical, and specific to the bearings tested. Given that creep of elastomers is a material property, creep must be controlled by imposing limitations on the time-dependent shear modulus. A short-term method to predict long-term creep of elastomeric bearings based on the time-dependent shear modulus is suggested.

Full-Scale Creep Tests

Test Setup and Procedure

The full-scale creep tests were performed on bearings with smooth unbonded top and bottom surfaces and fully bonded top and bottom surfaces. Thus two extreme boundary conditions were considered. Bearings made from NEO100 (53), NEO200 (70), NR100 (52), and NR200 (66) were tested (please note that the Shore A durometer hardness is given in parentheses). The plan dimensions of the test specimens were 213×340 mm with no cover at the edges so that the shims were clearly visible on all four sides. Figures 49, 50, and 51 show the test setup. Bearings were stacked between a hydraulic ram with an 8900 kN (2000 kip) capacity and a support frame. The ram was pressurized by a constant weight hanging as shown schematically in Figure 49. The bearings were separated by means of smooth 12.7-mm (0.5-in.)-thick aluminum plates. The axial deflection of each bearing was recorded with respect to time. The deflection at the center of the bearing was

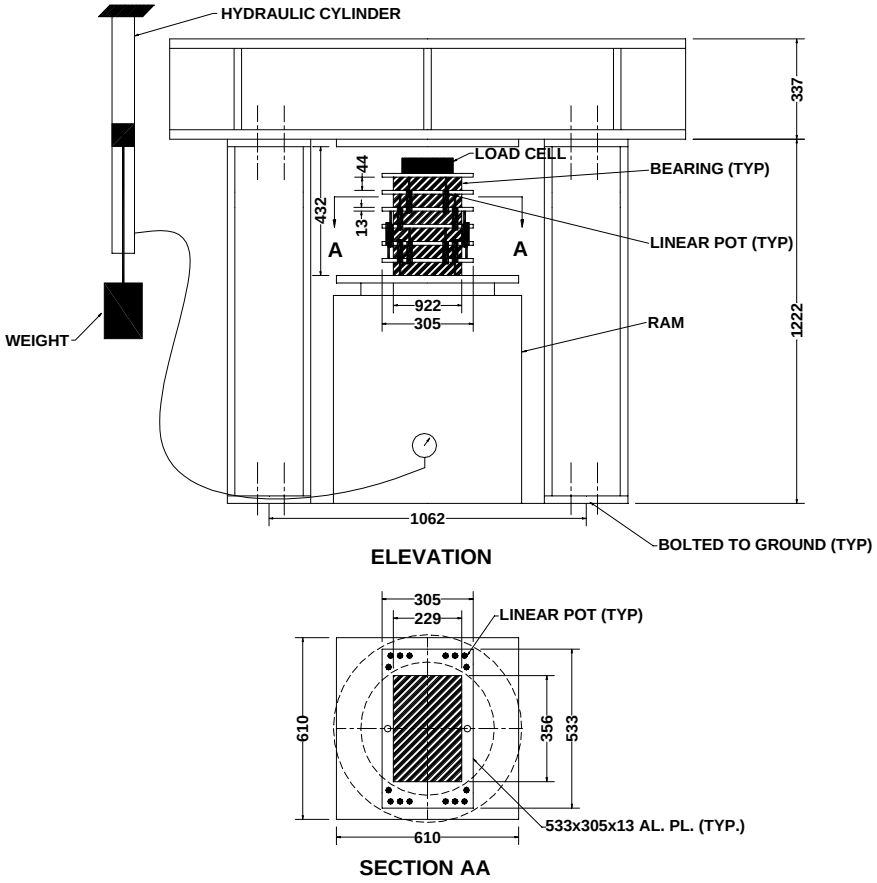

Figure 49. Schematic of test setup (mm).

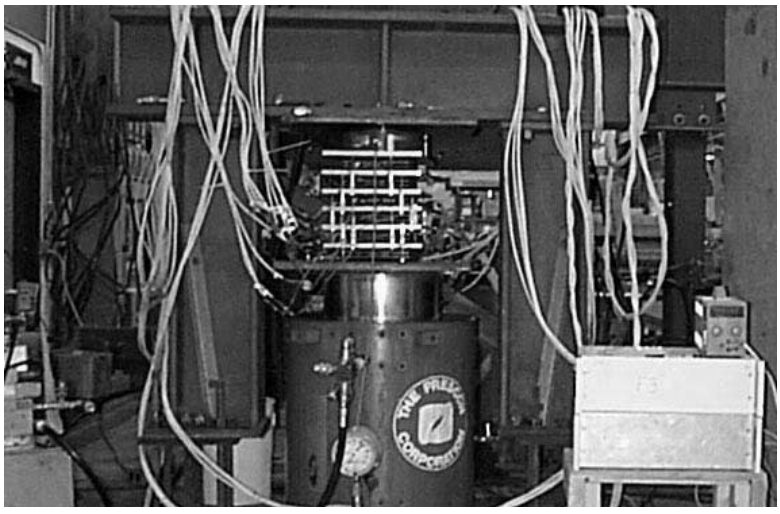

Figure 50. Creep test setup.

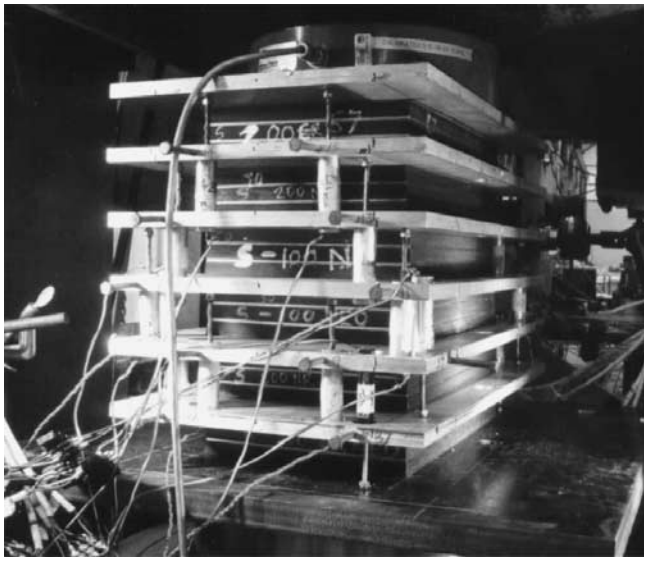

Figure 51. Creep test setup—close-up.

calculated from the relative displacement between the top and bottom plate surfaces by four calibrated linear pots and the load was measured by a load cell. The data were acquired by a data acquisition system that simultaneously scanned the data channels at predetermined time intervals.

A buckling analysis was performed to estimate the maximum number of bearings that could be tested at a time. This calculation predicted a maximum number of six bearings in a stack. About 6 months of pilot testing was performed wherein six bearings, with and without top and bottom surfaces bonded, were tested at a time. The results of pilot testing indicated that there was a significant amount of friction in the loading system and the load increased with time (10–15 percent in 1 month of testing period). Also there were some minor leaks in the hanging weight system that caused the weight to slide down gradually with time and eventually hit the bottom of the cylinder. The total time for the weight to translate its full stroke was about 1 month. Also bearings at the top and bottom of the stack showed considerable end effects.

To account for these deficiencies in the test setup, the variation of load was included in the creep calculations. In order to ensure monotonically increasing load and eliminate cyclic effects, the duration of testing was limited to 1 month each for bonded and unbonded bearings. The initial intent of placing six bearings was to have two replicates; however, because of end effects, this idea was dropped. The two stiffer replicate bearings were placed at the ends of the stack for stability reasons and to mitigate end effects for the four test bearings: NR200, NEO100, NR100, and NEO200. A weight was hung and maintained for 30 days to produce the intended maximum axial load. The measured load varied from 310 to 370 kN (69.7 to 83.1 kips) as shown in Figure 52 for NR100 because of friction in the loading system. The corresponding average bearing stresses were 4.29 to 5.12 MPa (0.622 to 0.743 ksi), which is roughly the maximum design compressive stress (shape factor = 5.15) for the NEO100 or NR100 unbonded bearings.

Results of Full-Scale Creep Tests

The results of the creep tests for NR100 with bonded top and bottom surfaces are shown in Figures 52 through 54. Figure 53 shows a plot of axial deflection versus time, while Figure 52 shows a plot of axial load versus time. These two figures are combined in Figure 54, which also shows the results

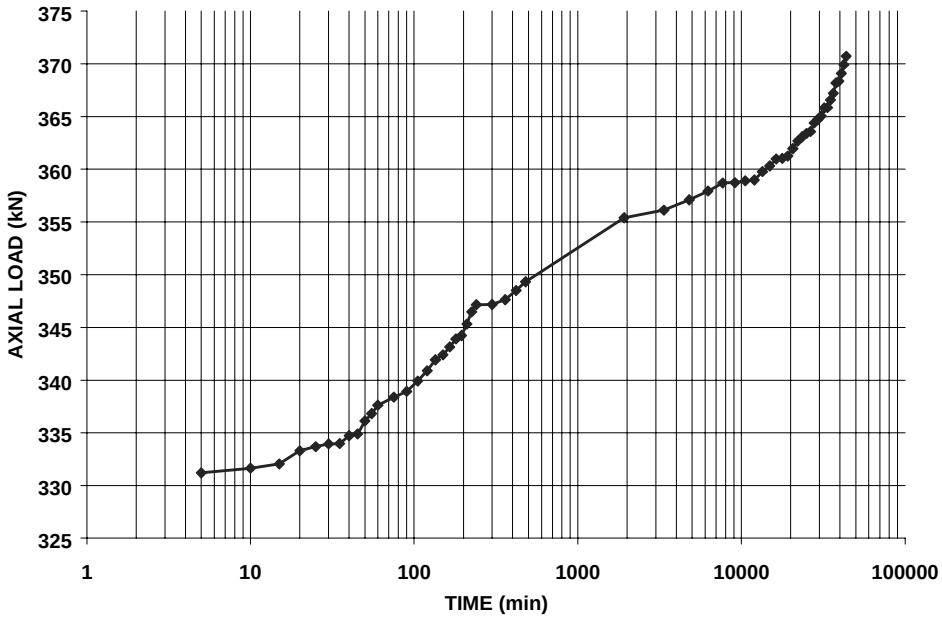

Figure 52. NR100 with bonded sole plates—axial load vs. time.

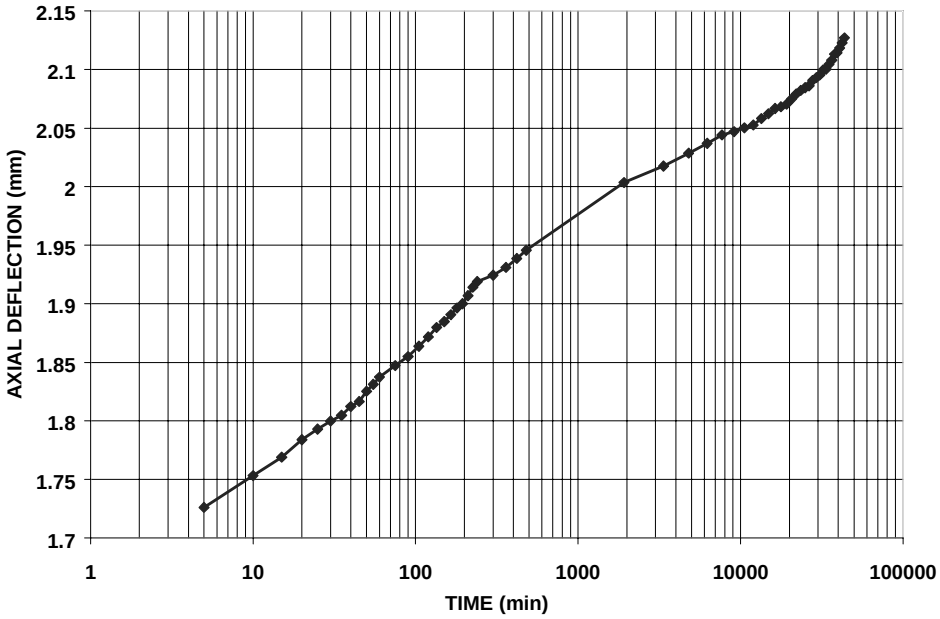

Figure 53. NR100 with bonded sole plates—axial deflection vs. time.

of a regression analysis and the regression equations that relate the total deflection to time and load variation in the region of the measurements. Other plots, similar to Figure 54, for NR100, NEO100, NR200, and NEO200 are included in Appendix E of the research team's final report. The form of the regression equation is the same for all bearings as follows:

$$\ln(z) = a + b\ln(x) + c\ln(y) \tag{11}$$

where

z = total axial deflection (mm),
x = time (min),
y = axial load (kN), and
a, b, and c = the regression coefficients tabulated in Table 14.

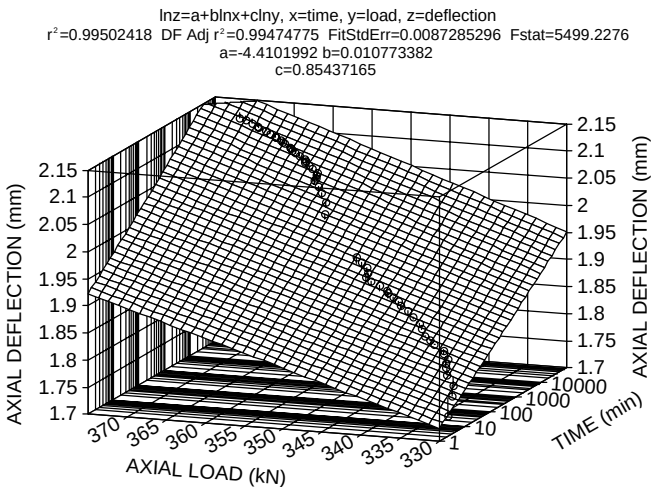

Figure 54. NR100 with bonded sole plates—creep tests data and regression results.

The coefficients of correlation, R, shown in Table 14 substantiate the validity of this equation in the range of loading under consideration.

The predicted instantaneous deflections and creep deflections after 1 hr, 30 days, and 25 years using the regression equations for the test bearings under a constant 350 kN axial load are tabulated in Table 15. Creep deflection expressed as a percent of instantaneous deflection (deflection at 1 min) for various bearings and end conditions is tabulated in Table 16. Creep deflection expressed as a percent of total deflection after 1 hr for various bearings and end conditions is tabulated in Table 17. Creep deflection expressed as a percentage of original unstressed rubber thickness for various bearings and end conditions is tabulated in Table 18.

Findings of Full-Scale Creep Tests

The results of the full-scale creep tests show that time-dependent deformation of elastomeric bearings is significant. Both natural rubber and neoprene bearings fabricated from low or high durometer rubber deform significantly because of elastomer creep as shown in Table 16. Bearings with bonded top and bottom surfaces exhibited considerably less creep deformation compared with bearings placed on smooth unbonded top and bottom surfaces. The axial deflection of unbonded bearings was about twice as much as the axial deflection of bearings with bonded sole plates. Without creep, the unbonded bearings would be expected to have about 30 percent more axial displacement than the same

TABLE 14 Regression coefficients in Equation 15 for various bearings

Bearing Type	Regression Coefficients							
	Bonded Top and Bottom Surfaces				Smooth Unbonded Top and Bottom Surfaces			
	a	b	c	R^2	a	b	c	R^2
NR100	-4.4102	0.010773	0.854372	0.995	-2.63104	0.018138	0.634728	0.996
NEO100	-4.0886	0.009053	0.802724	0.987	-2.0482	0.016151	0.537228	0.986
NR200	-5.49775	0.012885	0.955414	0.99	-3.65523	0.023189	0.727482	0.993
NEO200	-5.05718	0.01178	0.874482	0.991	-3.05407	0.02152	0.618314	0.993

TABLE 15 Deflections from Equation 15 for 350 kN load

Bearing Type	Axial Deflection (mm) at Various Times for 350 kN Axial Load							
	Bonded Top and Bottom Surfaces				Smooth Unbonded Top and Bottom Surfaces			
	1 min	1 hour	30 days	25 years	1 min	1 hour	30 days	25 years
NR100	1.812	1.894	2.033	2.162	2.966	3.194	3.599	3.993
NEO100	1.847	1.917	2.035	2.143	3.001	3.206	3.565	3.910
NR200	1.104	1.164	1.267	1.364	1.834	2.016	2.349	2.682
NEO200	1.068	1.120	1.211	1.295	1.765	1.927	2.220	2.511

TABLE 16 Creep deflection expressed as percent of instantaneous deflection

Bearing Type	Percent Creep Deflection at 350 kN Axial Load					
	Bonded Top and Bottom Surfaces			Unbonded Top and Bottom Surfaces		
	1 hour	30 days	25 years	1 hour	30 days	25 years
NR100	4.51	12.19	19.31	7.71	21.36	34.62
NEO100	3.78	10.15	16.00	6.84	18.81	30.31
NR200	5.42	14.74	23.52	9.96	28.08	46.24
NEO200	4.94	13.40	21.30	9.21	25.82	42.30

TABLE 17 Creep deflection expressed as percent of 1-hr deflection

Bearing Type	Percent Creep Deflection at 350 kN Axial Load			
	Bonded Top and Bottom Surfaces		Unbonded Top and Bottom Surfaces	
	30 days	25 years	30 days	25 years
NR100	7.35	14.17	12.67	24.99
NEO100	6.14	11.78	11.21	21.97
NR200	8.85	17.17	16.48	33.00
NEO200	8.06	15.59	15.21	30.29

TABLE 18 Creep deflection expressed as percent of original unstressed rubber thickness

Bearing Type	Percent Creep Deflection at 350 kN Axial Load					
	Bonded Top and Bottom Surfaces			Unbonded Top and Bottom Surfaces		
	1 hour	30 days	25 years	1 hour	30 days	25 years
NR100	0.21	0.58	0.92	0.60	1.66	2.70
NEO100	0.18	0.49	0.78	0.54	1.48	2.39
NR200	0.16	0.43	0.68	0.48	1.35	2.23
NEO200	0.14	0.38	0.60	0.43	1.20	1.96

bearings with bonded sole plates. In bonded bearings the time-dependent deformation results mainly from material creep whereas not only material creep but also gradual slip at the top and bottom surfaces with time significantly contributes to the time-dependent deformation of unbonded bearings. The rubber is almost incompressible, so the axial deformation of bearings results from bulging of the rubber that is controlled by the constraints imposed by top and bottom contacting surfaces. The slip of the top and bottom bearing surfaces with respect to the contacting surfaces gives rise to additional bulge as shown in Figure 55. In the unbonded specimens, the bearings have two layers with unbonded surfaces (exterior layers) and one interior layer. The external metal contact surfaces are very smooth. All rubber layers have the same thickness, so the two external layers would be expected to contribute at least 75 percent of the initial deflection. As the number of internal rubber layers increase, the influence of the creep in the external layers on the overall creep deflection will diminish.

As expected, high modulus bearings show higher percent creep than do low modulus bearings because of a higher carbon black (filler) content (refer to Tables 16 and 17). For example the 30-day creep of NR200 is 15 percent as compared with 12 percent for NR100, while 30-day creep of NEO200 is 13 percent as compared with 10 percent for NEO100. These numbers refer to bearings with bonded top and bottom surfaces based on instantaneous deflection. The absolute creep deformation of high modulus bearings is lower than that of the low modulus bearings as shown in Table 15. So, if the designer is interested in small absolute creep deformation, high modulus bearings can be used. Neoprene bearings show slightly less creep as compared with natural rubber bearings, however the difference is not significant (see Tables 16 and 17). The percent creep deflection is insensitive to small fluctuations of loads; however, for large load variations, the creep deformation at higher loads will be higher as compared with the lower loads. For example, bearings subjected to a compressive stress of 7.6 MPa (1.1 ksi) will exhibit slightly more creep deformation (1 to 3 percent higher) as compared with bearings subjected to a compressive stress of 6.9 MPa (1.0 ksi).

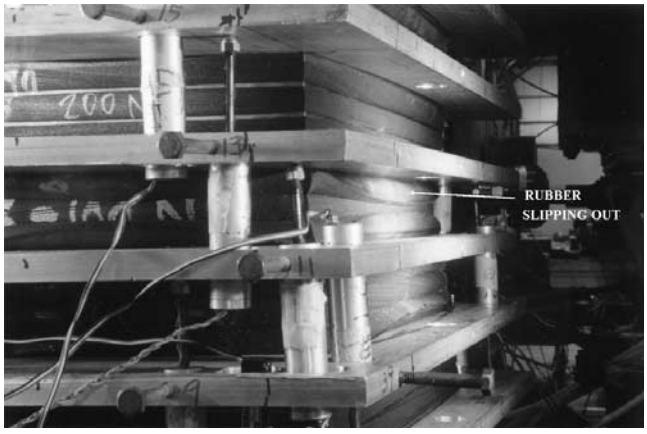

Figure 55. Bearings with unbonded top and bottom surfaces after 1 month of sustained loading.

Table 14.7.5.2-1 in the AASHTO LRFD Bridge Design Specifications (1998) provides criteria to evaluate creep deflection at 25 years expressed as percent of instantaneous deflection when test data are not available, 25 and 45 percent for 50 and 70 durometer bearings, respectively. The bearings with bonded top and bottom surfaces meet these criteria, while bearings placed on smooth top and bottom surfaces marginally fail to meet these criteria (except NEO200). The smooth surface, as in the case of smooth aluminum plates, is an extreme situation. In reality, the surfaces will not be that smooth and the bearings will probably meet the creep criteria. However, it must be emphasized that the unbonded end surfaces result in highly uncertain boundary conditions.

The effects of creep and relaxation on overall bearing performance are (a) an increase in axial displacement, (b) a reduction in shear force, and (c) an increase in indirect shear strains and reinforcement stresses. From a performance point of view, an increase in axial displacement is more important as long as internal stresses and strains are within allowable limits. For single-span, simply supported girders, excessive creep can cause misalignment in adjacent spans; for multispan continuous girders, excessive creep affects the moment distribution in the girder. Reduction in shear force is generally beneficial; however, it can affect the performance of a bearing seated on a sloping abutment. The true instantaneous deformation of an elastomeric bearing is very difficult to measure because a considerable amount of creep occurs within the first few minutes of loading. AASHTO specifications compare the creep deformation with the instantaneous total deformation of the bearing. A better criteria for creep is to compare the creep deformation with the total deformation after 1 hr of loading as shown in Table 17, because the full dead load on the bearings is associated with the deck pour that is applied in a matter of hours not minutes.

Small-Scale Relaxation Tests

Creep is a material property, so it must be considered during the design phase of the bearings. Given that time-dependent behavior of an elastomeric bearing is governed by time-dependent shear modulus, limitations must be imposed on the variation of shear modulus over time, rather than on axial deflection. This way not only will the axial deflection be controlled but the shear stiffness will also be controlled. This section describes a test method to calculate time-dependent shear modulus and suggests a simple method to estimate long-term creep deformation using the time-dependent shear modulus. This method is applicable for bearings where the creep deformation results mainly from material creep as in the case of bearings with bonded top and bottom surfaces. The time-dependent shear modulus, also known as relaxation shear modulus, was determined by means of a stress relaxation test

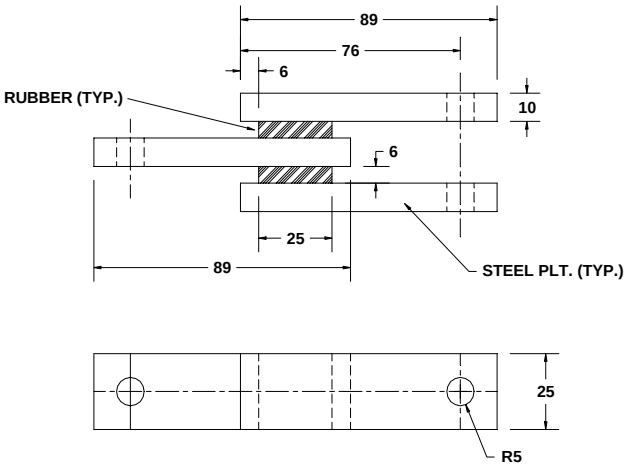

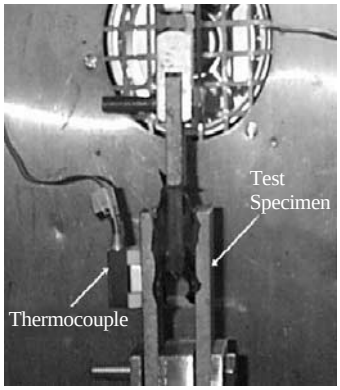

Figure 56. 1 × 1 shear specimen (mm).

in simple shear wherein the strain was kept constant while the stress was measured over time. A 6-hr stress relaxation test was found adequate to predict the long-term shear modulus.

Test Setup and Procedure

The shear specimen shown in Figure 56, hereafter referred to as 1 × 1, was used for the stress relaxation tests. Specimens using NR100, NEO100, NR200, and NEO200 unvulcanized rubbers were molded and cured at 127°C for 3 hr. Lords Corporation's Chemlok 205/220 rubber-to-metal bonding agents were used to bond the rubber to the metal plates during the vulcanization process. A compression molding process was used to fabricate the specimen. Prior to molding, the three metal bars were sand-blasted and thoroughly cleaned using vapor degreasing and a chemical rinsing system. The primer 205 and adhesive 220 were applied per Chemlok specifications. These surface preparation and bonding agents were the same as those used in the fabrication of the full-size bearings. The specimens were tested in a closed-loop system. Figure 57 shows the test setup. An environmental chamber was used to control the testing temperature precisely. In order to find the strain dependence of the relaxation modulus, the relaxation shear modulus was measured at three shear strain levels: 50 percent, 100 percent, and 150 percent, respectively.

The same test procedure was used for all four types of rubbers. The test specimen was attached to the displacement-controlled test machine fixtures within an environmental chamber and an SST temperature of 32°C was maintained during the test to be consistent with the temperature for the full-size tests. The specimen was loaded to 150-percent shear strain 10 times at 10 percent strain/sec to eliminate the Mullins effect (Mullins, 1987). This was done only once for each specimen tested. The specimen was loaded to 50-percent strain level in 1 sec and the stress relaxation test was started. The strain level was maintained at 50 percent while the stress and elapsed time was recorded for 6 hr using an automated data acquisition system. The relaxation modulus was calculated as the ratio of stress/strain at pre-determined times. The strain was constant, while the stress was varying with time. The relaxation test was repeated at 100-percent and 150-percent strain levels.

Test Results

Plots of shear modulus versus time at the three different strain levels were prepared, and a sample plot is shown in Figure 58. The shear modulus changes from about 0.63 MPa to 0.55 MPa in the first 5 min and then to 0.51 MPa in the next 355 min. The experimentally determined values of relaxation modulii at 1, 60, and 360 min at various strain levels for NR100, NEO100, NR200, and NEO200 are tabulated in Table 19. This table also shows the values of relaxation modulii experimentally deter-

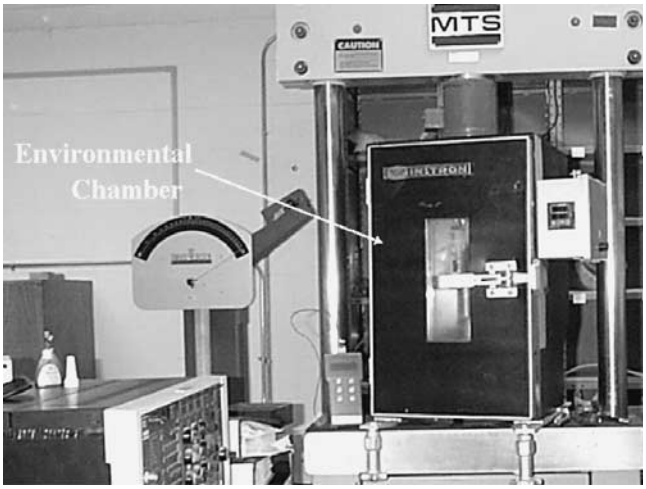

Figure 57. Test setup for stress relaxation test.

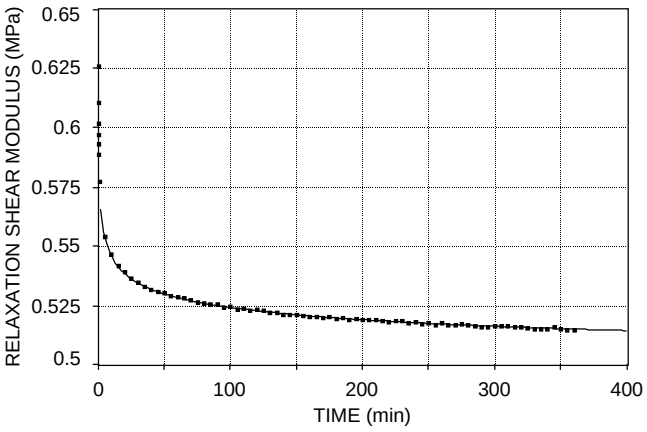

Figure 58. Relaxation test data for NR100 at 50-percent shear strain and 32°C.

mined for two other sizes of specimens (2×2 and 3×3) that were cut from the full-size bearings and cold-bonded to the pull plates. Details of these specimens are given in the section on Aging.

If the first 30 min of relaxation modulus versus time data are excluded, a simplified power law of the following form can be conservatively used to predict the relaxation modulus at times greater than 30 min.

$$G(t) = at^b \tag{12}$$

where a and b are coefficients determined from the experimental data. Equation 12 is very attractive for practical purposes because it represents a straight line on log paper as follows:

$$\log(G(t)) = \log(a) + b \log(t) \tag{13}$$

Figure 59 shows a plot of log ($G(t)$) versus log(t) using the test data for the 1×1 NR100 at 50-percent strain level and a straight line fit using the method of least squares. The regression coefficients in Equation 12 for various rubbers and strain levels for the 1×1 specimen are tabulated in Table 20. Figure 60 shows the curve fitting of Equation 12 for NR100 at 50-percent strain.

Table 21 shows the shear modulii after 1 hr, 30 days, and 25 years for NR100, NEO100, NR200, and NEO200 rubbers at 50-percent shear strain levels as predicted using Equation 12 based on the 1×1, 2×2, and 3×3 specimen 6-hr stress relaxation data. The values for the 2×2 are shown as a ratio of 1×1 to 2×2 modulus, while the values for 3×3 are shown as a ratio of 2×2 to 3×3 modulus. The shear modulii determined for the 2×2 and 3×3 specimens cut from the full-size bearing are very similar (ratio is close to 1.0). The 1×1 modulii are about 10 percent lower than the larger specimens for NR100, NEO100, and NR200 and 15 percent lower for the NEO200 specimens. The difference between the 1×1 and the larger specimen can be attributed to the fact that 1×1 specimens were vulcanized as part of this research and the 2×2 and 3×3 specimens were cut from manufactured bearings. All specimens within each rubber type presumably came from the same rubber batch.

Prediction of Creep Deformation

The instantaneous axial deformation (i.e., deformation at 1 hr) of an elastomeric bearing is generally known either by a physical test or design calculations. The average shear modulus is also known at the time of initial design. If the deformation at time $t1$ (1 hr) is known, an estimate of the long-term axial deformation at any time t can be approximated as follows:

$$d_t = d_{t1} \frac{G_{t1}}{G_t} \tag{14}$$

where d_{t1} and d_t are the axial deformation at time $t1$ and t, respectively, while G_{t1} and G_t are the shear modulus at times $t1$ and t, respectively, calculated using Equation 12. Assum-

TABLE 19 Experimentally determined values of relaxation shear modulus

Specimen	Time (min)	Shear Modulus (MPa)				
		1x1 Shear Specimen			2x2 Shear Specimen (50 % Strain)	3x3 Shear Specimen (50 % Strain)
		50 % Strain	100 % Strain	150 % Strain		
NR100	1	0.5768	0.5583	0.5464	0.6164	0.6338
	60	0.5284	0.5077	0.4915	0.5654	0.5793
	360	0.5144	0.4932	0.4760	0.5532	0.5656
NEO100	1	0.6799	0.6717	0.7322	0.6911	0.7086
	60	0.6129	0.6019	0.6531	0.6516	0.6593
	360	0.5989	0.5860	0.6330	0.6385	0.6447
NR200	1	1.1415	1.0371	1.2189	1.2500	1.1717
	60	1.0069	0.9088	1.0695	1.1012	1.0328
	360	0.9753	0.8776	1.0305	1.0691	1.0023
NEO200	1	1.1173	1.1383	1.8304	1.3222	1.2836
	60	0.9998	1.0057	1.6145	1.1720	1.1451
	360	0.9712	0.9739	1.5584	1.1378	1.1163

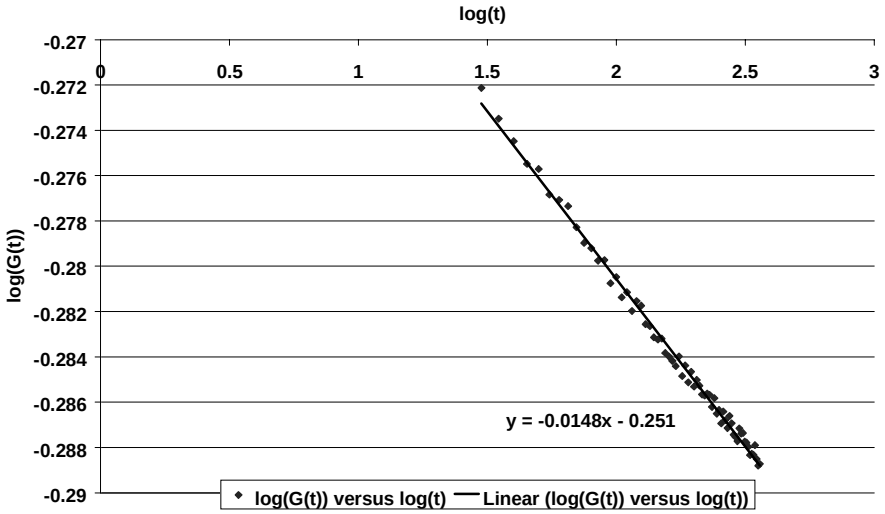

Figure 59. Least-squares fit of Equation 17 for NR100 at 50-percent strain and 32°C.

ing that the instantaneous axial deflection is the 1-hr value given in Table 15 for full-size bearings, Figure 13 shows the predicted axial deformation after 30 days for the NR100, NEO100, NR200, and NEO200 bearings, with bonded top and bottom surfaces, at 50-percent strain using Equations 12 and 14. Table 22 shows the predicted axial deformation expressed as percent of the 1-hr deflection for various bearings with bonded top and bottom surfaces using Equation 14. The 30-day deflection can be predicted conservatively within 3 to 4 percent based on Equations 12 and 14 and the 6-hr relaxation test. The 25-year estimate is 5 to 7 percent conservative. Figure 61 shows that the size of the specimen used for the stress relaxation test has an insignificant effect on the predicted deflection. Also, the test temperature was 32°C, but additional tests at other temperatures (Kumar, 2000) show that room temperature tests would give about the same result.

A 6-hr test method has been developed, using Equations 12 and 14, that gives a fairly accurate estimate of axial creep deformation for bearings with bonded top and bottom surfaces. The long-term deflection is directly related to the long-term shear modulus determined from the 6-hr relaxation test. A draft test method for predicting creep deflection is given in Appendix C of this report. If the instantaneous deflection in the AASHTO bridge specifications is defined as a 1-hr deflection, then Table 23 shows the limitation on the 6-hr time-dependent shear modulus corresponding to the AASHTO creep recommendations. The test method can also be used to determine the basic shear modulus and the adequacy of the shear bond between the elastomer and the steel laminates. For bearings with unbonded top and bottom surfaces, the friction at the contact surface plays an important role and the long-term axial deformation is highly unpredictable. More research is needed to predict the long-term behavior of such bearings.

EFFECTS OF AGING ON ELASTOMERIC BEARINGS

Introduction

All elastomers are attacked by oxygen, even at room temperature, and heat, light, and the presence of certain metallic impurities accelerate the reaction. This process is called aging. Degradation of physical properties is observed in elastomers even at quite low levels of oxidation. The changes observed vary considerably depending on the specific elastomer and the aging conditions to which it is subjected. Most elastomers harden and eventually embrittle as a result of aging (Hamed, 1992; Shelton, 1972). Since aging is related to the oxidation

TABLE 20 Regression coefficients for Equation 16

Specimen	Regression Coefficients					
	50% Shear Strain		100% Shear Strain		150% Shear Strain	
	a	b	a	b	a	b
NR100	0.561126	-0.01481	0.543704	-0.01652	0.530035	-0.01848
NEO100	0.648426	-0.01374	0.641033	-0.0155	0.70225	-0.01774
NR200	1.086329	-0.01856	0.987704	-0.02019	1.166732	-0.02129
NEO200	1.070865	-0.01673	1.083917	-0.01836	1.755371	-0.02036

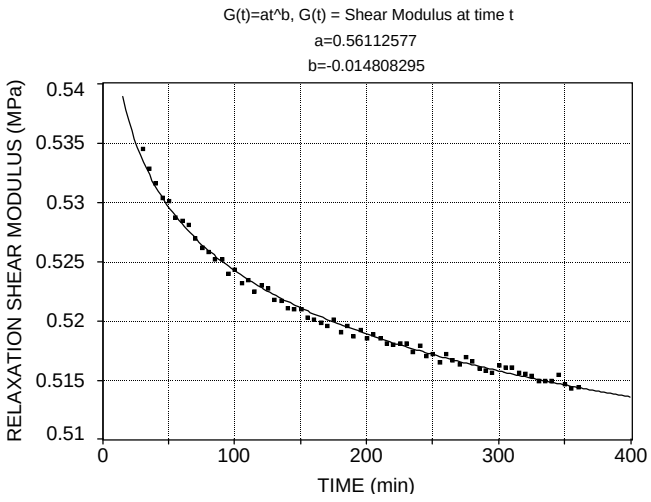

Figure 60. Regression analysis using Equation 16 for NR100 at 50-percent strain.

process, the rate and extent of diffusion of oxygen through the elastomer governs the change in properties due to aging. The rate of diffusion depends on temperature, pressure, exposed surface area, and permeability of the elastomer. In the case of elastomeric bearings, oxygen ingress is generally limited to a thin layer of exterior edge surface only because of the small exposed surface area (relative to loaded area) and low permeability of the elastomer. Given that heat accelerates the oxidation process, heat aging (also known as accelerated aging) has been used to predict the long-term elastomer properties at ambient temperatures.

There are several standardized tests available for quality control and for determining heat resistance or aging. ASTM D573, which is specified by AASHTO M251-97, describes a test procedure to determine the influence of elevated temperature on the physical properties (i.e., hardness, elongation at break, and tensile strength) of vulcanized rubber. Specimens of vulcanized rubber are exposed to the deteriorating influence of air at specified temperatures for known periods of time, after which their physical properties are determined. These are compared with the properties measured on unaged specimens and changes are noted. The changes should be below the specified requirements. ASTM D573 itself neither specifies the value of the exposure temperature nor the aging time. AASHTO M251-97 specifies the different periods of exposure time and temperature as well as the different tolerances for the changes in the physical properties for neoprene and natural rubber as summarized in Table 24. The specified aging time, temperature, and tolerances are different for natural rubber and neoprene. The international standard for heat aging is ISO 188 (1982), which specifies an air oven and an oxygen bomb method. The equivalent British standard, BS 903: Part A19 (1986) is identical.

Moakes (1975) reported changes in tensile modulus, observed over a 15-year period, of small specimens of different elastomers in temperate, tropical, and desert conditions. He reported that the aged tensile modulus increased between 60 percent and 100 percent compared with unaged values for nitrile and between 20 percent and 110 percent compared with unaged values for natural rubber. Accelerated aging tests were performed on each elastomer at 70° and 82°C (158° and 180°F). For nitrile, he found that 14 days at 82°C (180°F) appeared to be equivalent to 10 years of aging in tropical temperatures and that use of aging temperatures above 100°C (212°F) would give misleading results. Barker (1988) aged four natural rubber compounds at 23°C (73°F) over 5 years and reported increases in tensile modulus in the range of 10 to 75 percent. The results were compared with Arrenhius-based predictions (such predictions will be discussed later) from measurements taken at an accelerated aging temperature of 40°C (104°F). He observed that the lower aging temperature of 40°C (104°F) compared with the usual 70°C (158°F) or higher temperature provided a better basis for predicting changes in modulus. Hogan et al. (1997) performed a more direct study on the effects of aging on elastomeric bearings used in oil field applications. They predicted the 30-year changes in the shear modulus of nitrile and natural rubber elastomer compounds using the time-temperature reaction rate transformation applied to controlled-aging experiments. Several different experimental techniques for obtaining the necessary measurements of accelerated material behavior were employed and compared. Different analytical techniques for characterizing rate changes over time and temperatures were applied to the measured data and significantly different results were obtained, depending on the assumptions. Changes in the accelerated aging temperatures, the relative availability of oxygen to the test specimen during aging, and the size of the test specimen had a significant effect on the results.

TABLE 21 Predicted shear modulus at 50% strain using Equation 16

Specimen	Shear Modulus (MPa)			Shear Modulus Ratio					
	1x1 Specimen			Ratio of 1x1 to 2x2			Ratio of 2x2 to 3x3		
	1 hour	30 days	25 years	1 hour	30 days	25 years	1 hour	30 days	25 years
NR100	0.528	0.479	0.440	0.934	0.917	0.903	0.975	0.988	0.998
NEO100	0.613	0.560	0.518	0.940	0.927	0.915	0.989	0.998	1.009
NR200	1.007	0.891	0.801	0.914	0.902	0.891	0.970	1.067	1.067
NEO200	1.000	0.896	0.814	0.853	0.851	0.850	1.02	1.010	0.998

TABLE 22 Predicted axial deformation as % of 1-hr deflection for bearings with sole plates

Rubber Type	Creep Deflection Expressed as Percent of Instantaneous Deflection (1 hour)							
	Full Size Bearing (from Table 17)		1x1 Specimen at 50% Shear Strain using Equation 14		2x2 Specimen at 50% Shear Strain using Equation 14		3x3 Specimen at 50% Shear Strain using Equation 14	
	30 Days	25 Years	30 Days	25 Years	30 Days	25 Years	30 Days	25 Years
NR100	7.35	14.17	10.23	19.97	8.28	16.03	9.68	18.84
NEO100	6.14	11.78	9.46	18.41	7.87	15.21	8.97	17.41
NR200	8.85	17.17	12.99	25.64	11.48	22.53	11.55	22.66
NEO200	8.06	15.59	11.64	22.84	11.35	22.26	9.88	19.25

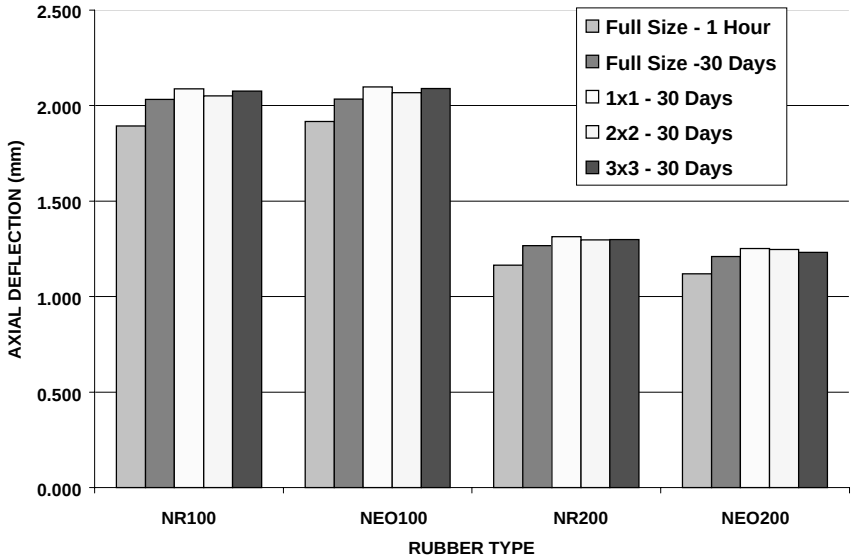

Figure 61. Axial deflection after 30 days of loading—predicted and measured.

TABLE 23 Performance criteria for 6-hr creep test

Specified Shear Modulus, MPa (Hardness)	Percent Change in 25 years	
	Creep Deformation	6-hour Shear Modulus
0.65(50 Durometer)	25	<25
0.90(60 Durometer)	35	<35
1.15(70 Durometer)	45	<45

TABLE 24 AASHTO M251-97 heat resistance requirements for ASTM D573

Test Requirements	Polyisoprene (Natural Rubber)	Polychloroprene (Neoprene)	Units
Specified Temperature of the Test	70	100	˚C
Aging Time	168	70	Hours
Max Change in Durometer Hardness	+10	+15	Shore A
Max Change in Tensile Strength	-25	-15	Percent
Max Change in Ultimate Elongation	-25	-40	Percent

Several case studies have shown that there has been no evidence of any significant deterioration of elastomeric bearing physical properties over the period that the bearing had been in service. Nakauchi et al. (1992) analyzed and characterized small samples of a 100-year-old bridge bearing from a viaduct in Australia by means of microanalytical methods. The test results convincingly showed the longevity of rubber pads for civil engineering applications. The aging of natural rubber was limited to the outside surfaces and the ingress of oxygen to rubber deep within the bearing was inhibited by the oxidized rubber formed. Doody and Noonan (1998) compared the results of accelerated aging tests, per AASHTO specifications, versus as-received recovered properties of steel-laminated elastomeric bearings that had been in service. They found insignificant differences in mean tensile strength and elongation between the accelerated tests and bearings in service after 22 years. The mean surface hardness, however, differed significantly. They concluded that the bearings performed very well in service and were relatively insensitive to the deficiencies in design, construction, and material properties.

Almost all accelerated aging tests mentioned in various specifications are performed on very thin specimens loaded in tension wherein the oxidation affects the whole specimen. Any change in the overall shear stiffness of elastomeric bearings because of aging is more relevant than the change in localized tensile properties represented by the accelerated aging tests. The objective of the present study is to investigate the effect of specimen size on the shear stiffness characteristics resulting from accelerated aging and extrapolate the results to ambient temperatures for full-size bearings. Four different sizes of specimens were subjected to shear deformation. The specimens were made from NR100, NEO100, NR200, and NEO200 types of elastomers: polychloroprene rubber (neoprene) and natural rubber, at two hardness levels (i.e., Shore A Durometer 50 and 70 were tested). Hereafter the 50 and 70 durometer neoprene bearings will be referred to as NEO100 and NEO200, respectively, while the 50 and 70 durometer natural rubber bearings will be referred to as NR100 and NR200, respectively. In the following sections, the specimen geometries, test methodology, and results of accelerated aging tests are followed by the interpretations and predictions of aging at ambient temperature.

Test Specimens, Methodology, and Results

The effect of accelerated aging on the shear characteristics of four sizes of specimens was studied. The four sizes of specimens were as follows: (a) rheometer specimens, (b) 1×1 shear specimen (25×25 mm), (c) 2×2 shear specimens (51×51 mm), and (d) 3×3 shear specimens (76×76 mm). The accelerated aging was done at two temperatures, 82° and 100°C (180° and 212°F), in order to extrapolate the aging results to service temperatures using the theoretical Arrenhius relation presented later. The sizes and aging temperatures were selected on the basis of the results of a pilot study so that a significant spread in the post-aging shear characteristics could be observed without damaging the specimens because of overheat. All the specimens were aged in an air oven wherein the airflow and temperature were precisely controlled.

Moving Die Rheometer (MDR) Specimens

The rheometer (also known as curemeter) shown in Figure 62 is generally used by rubber manufacturers to study the vulcanization characteristics of elastomers. A schematic of the rheometer is shown in Figure 63. A 5-gm sample of raw elastomer is placed in a die cavity (formed by two similar dies) that is sealed and maintained at a constant temperature and pressure. The lower die is shown in Figure 64 along with a schematic of the lower die and specimen cross-section and a typical MDR after it is fully cured. The average thickness is 2 mm (0.08 in.), while the outer diameter is 40 mm (1.6 in.). The size is small enough for the oxygen to affect the whole specimen. One of the dies is oscillated through a rotary amplitude of ±0.5° at 1.66 Hz while the other is kept stationary. This produces a sinusoidal alternating torsional shear strain of 14 percent in the test piece and a sinusoidal reaction torque, measured at the stationary die, that is directly proportional to the shear modulus of the rubber compound. The reaction torque is continuously recorded during the vulcanization process. Figure 65 shows the reaction torque versus time relationship for NR200 cured at 182°C (360°F), which is a typical curing temperature used in the manufacture of the bearings. As the rubber vulcanizes, cross-linking is dominant and the torque increases during this process until it reaches a maximum value M_H, after which reversion is dominant. The time to reach 90 percent of M_H is called t_{90} and is generally used as a measure of the cure rate. As demonstrated herein, a rheometer can be effectively used to study the aging response in shear, since the weight, geometry, and testing environment

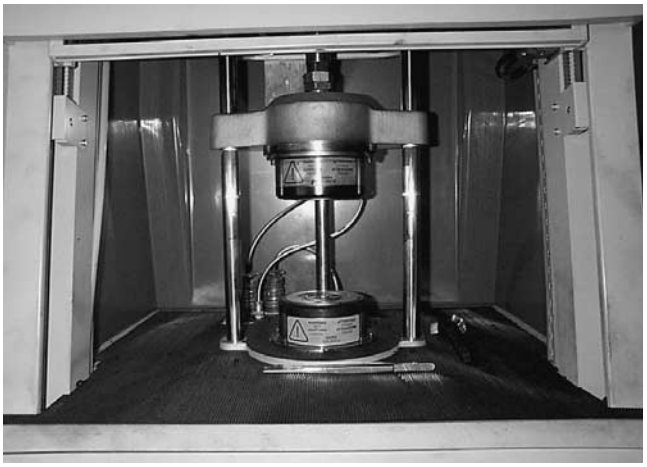

Figure 62. Moving die rheometer.

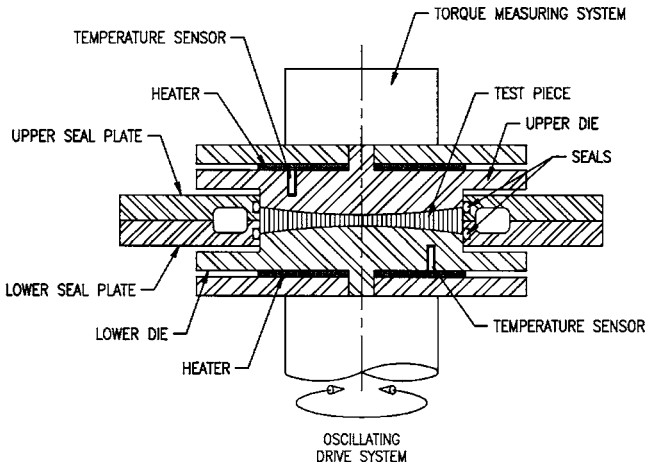

Figure 63. Schematic of moving die rheometer operation.

(i.e., temperature and pressure) of the specimen can be precisely controlled and the torque, which is related to the shear stiffness, can be precisely measured.

The MDR specimens were cured at a temperature of 127°C (261°F) until the reaction torque was almost constant (SST with little reversion). The specimens were cured at a lower temperature for a longer period than normally used in manufacturing in order to minimize reversion, thus ensuring reasonable similarity among specimens (Kumar, 2000). Specimens from four rubbers (NR100, NEO100, NR200, and NEO200) were prepared and, after removal from the rheometer, stored at room temperature for 3 days. The specimens were then aged for 3, 10, 17, 24, 31, 38, 45, and 52 days and tested in the rheometer where the reaction torque was again measured. All the post-vulcanization and post-aging tests were performed at 32°C (90°F). Given that the specimens

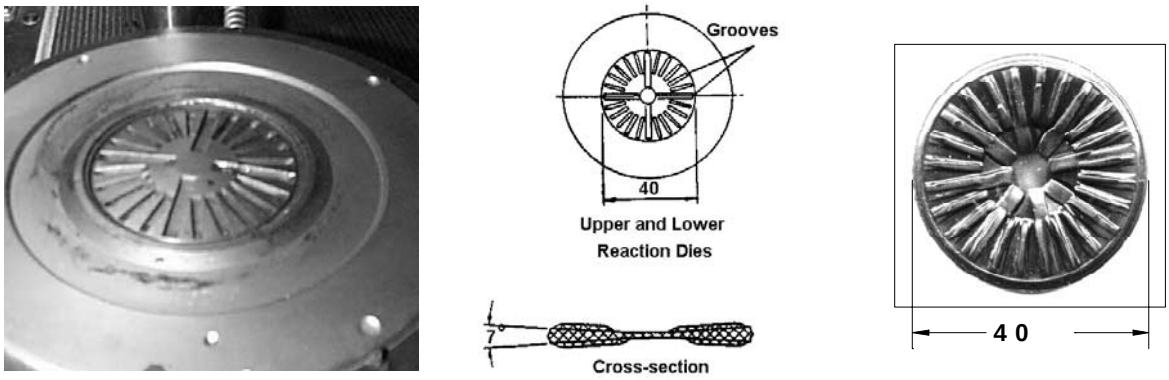

Figure 64. Rheometer die and specimen.

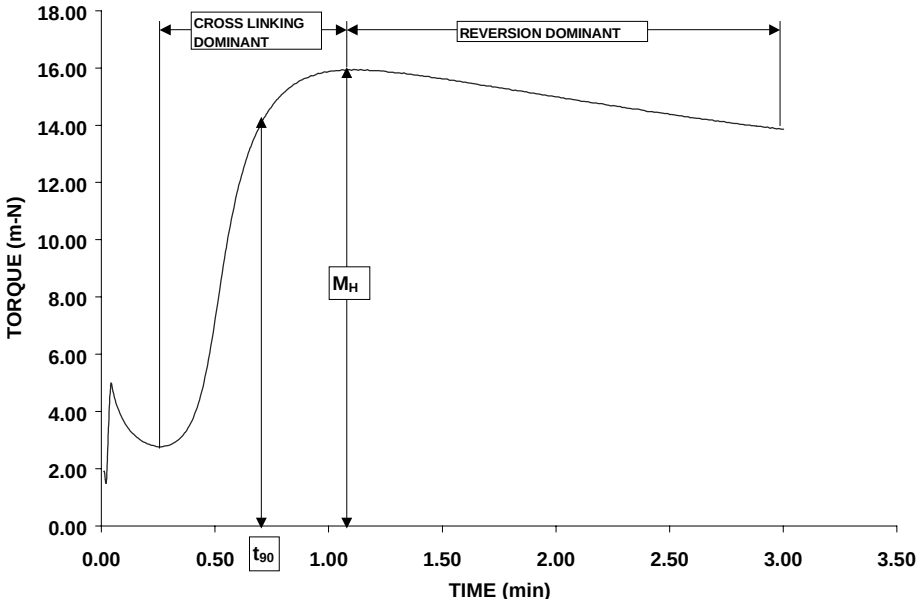

Figure 65. Vulcanization curve for NR200 at 182°C.

were already cured, a steady-state torque (oscillating maximum torque remained constant) was achieved in only a few seconds after the start of the test. The torque was recorded after 2 min to ensure an SST. Some results from the rheometer specimen aging tests are shown in Figure 66 on a log-log scale; the 82 and 100 in the legend are the two aging temperatures in degrees centigrade. The percent change in shear stiffness is relative to the torque or shear stiffness at 0 days of aging (i.e., before the specimens were placed in the air ovens).

1 × 1 Dual-Lap Shear Specimens

The aging specimens and test setup were the same as used previously for the creep experiments (see Figure 56). NR100, NEO100, NR200, and NEO200 unvulcanized rubbers were molded into specimens and cured at 127°C (261°F) for 3 hr. The shear stiffness was measured after aging in the air oven for 0, 1, 2, 3, 4, 5, 6, and 7 weeks. The specimens were tested at 32°C (90°F) using the MTS system with an attached environmental chamber. In order to find the strain dependence of the aging effects, the shear stiffness was measured at three shear strain levels: 50 percent, 100 percent, and 150 percent, respectively. The specimen was loaded to 150-percent shear strain 5 times at 1-percent strain per sec to eliminate the Mullins effect. This was done every time after the specimens were removed from the air oven. Each specimen was loaded to the 50-percent, 100-percent, and 150-percent strain at 1 percent per second, and the load was recorded at each of the three strain intervals. The secant shear modulus was calculated at each strain level. The results of accelerated aging of 1 × 1 specimens are shown in Figures 67 through 70 for NR100, NEO100, NR200, and NEO200 elastomers, respectively. In the legends of these plots, the strain level refers to the shear strain at which shear stiffness (or shear modulus) was calculated and the temperature refers to the temperature of the air oven at which the specimens were aged. The percent change in stiffness (secant shear modulus) is relative to the stiffness at 0 time of aging.

2 × 2 and 3 × 3 Shear Specimens

Figure 71 shows the test fixtures for the 2 × 2 (51 × 51 mm) and the 3 × 3 (76 × 76 mm) shear specimens while Figure 72 shows the test setup. The specimens were cut from the actual NEO100, NEO200, NR100, and NR200 bearings and cold-bonded to the metal plates. Elmer's™ industrial-grade crazy glue was used for rubber-to-metal cold bonding. Prior to the adhesive application and assembly, the three metal plates were sandblasted and cleaned using vapor degreasing and a chemical rinsing system. The rubber surfaces were cleaned and the primer and adhesive were applied per manufacturer's specifications.

To avoid debonding at the cold bond surface at the test fixture, the shear stiffness was measured only at 50-percent strain for these specimens. The same test procedure was used for all the specimens. The test specimen was mounted on the displacement-controlled MTS fixtures in an environmental chamber, and a test temperature of 32°C (90°F) was maintained during the test. The specimen was loaded to 50-percent shear strain 5 times at 1-percent strain per sec to eliminate the

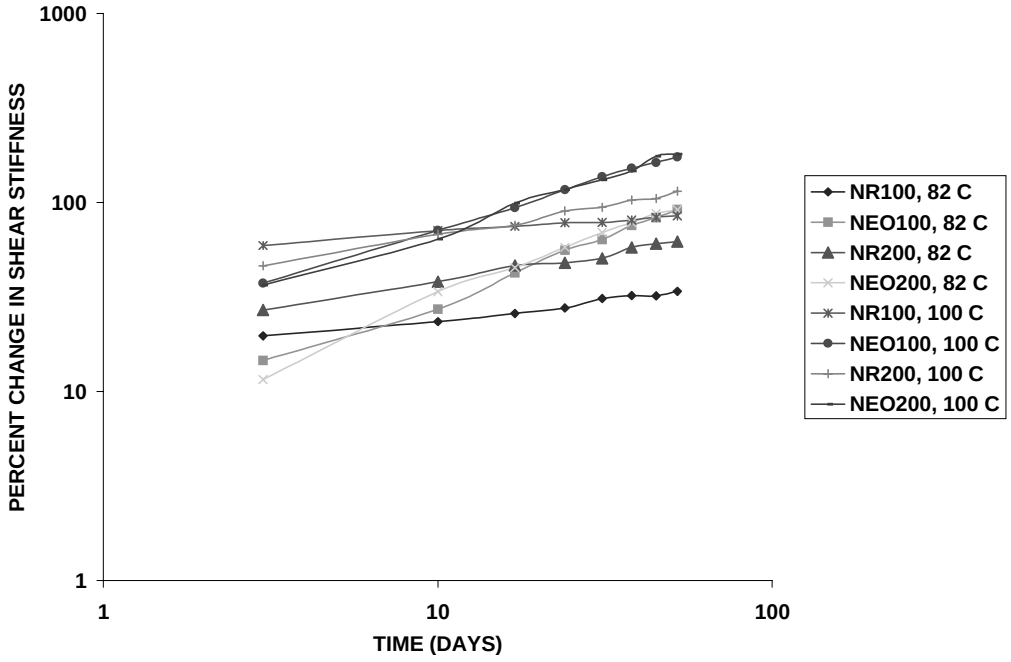

Figure 66. Aging tests on rheometer specimens.

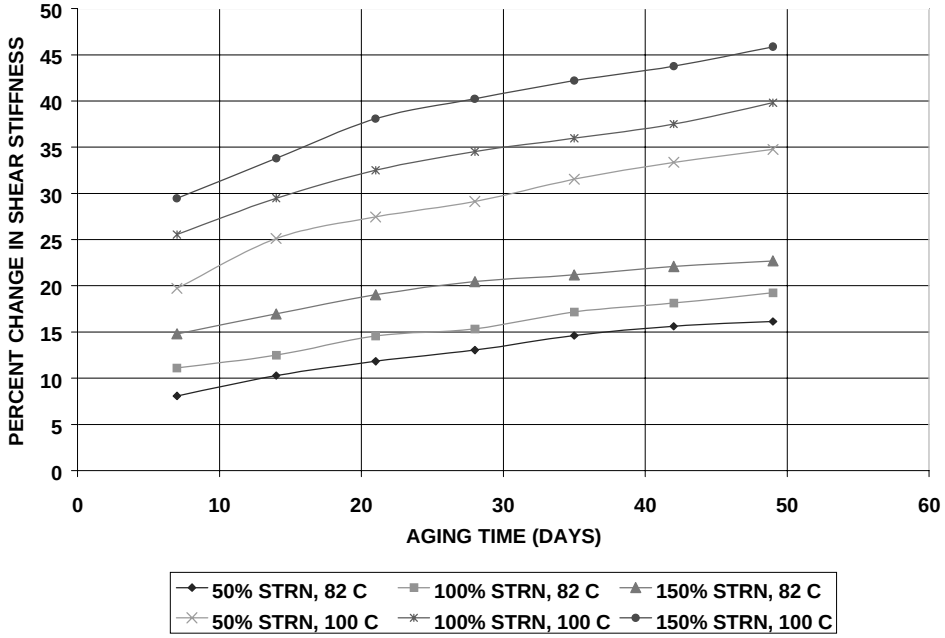

Figure 67. Accelerated aging of 1 × 1 NR100 specimens.

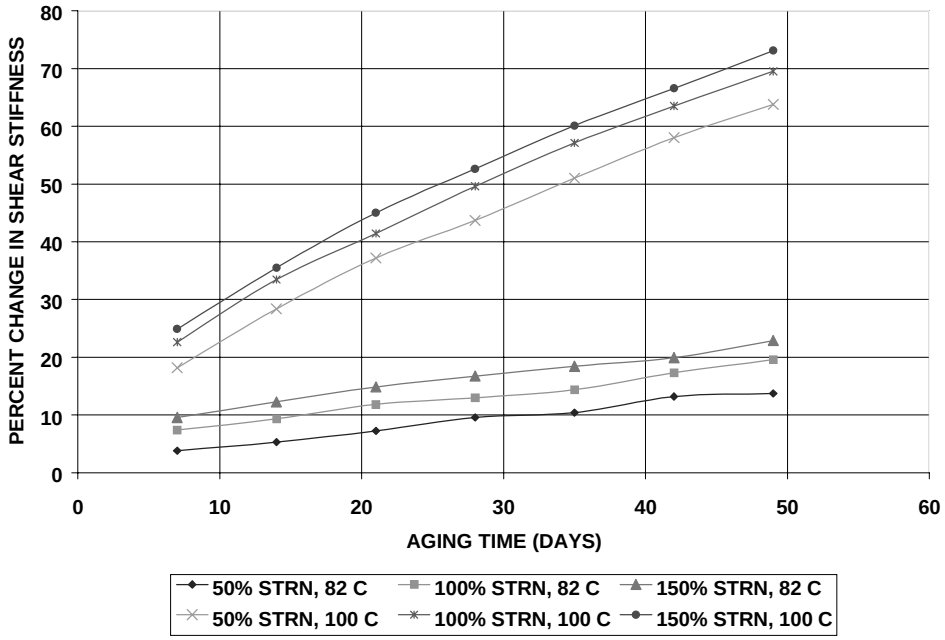

Figure 68. Accelerated aging of 1 × 1 NEO100 specimens.

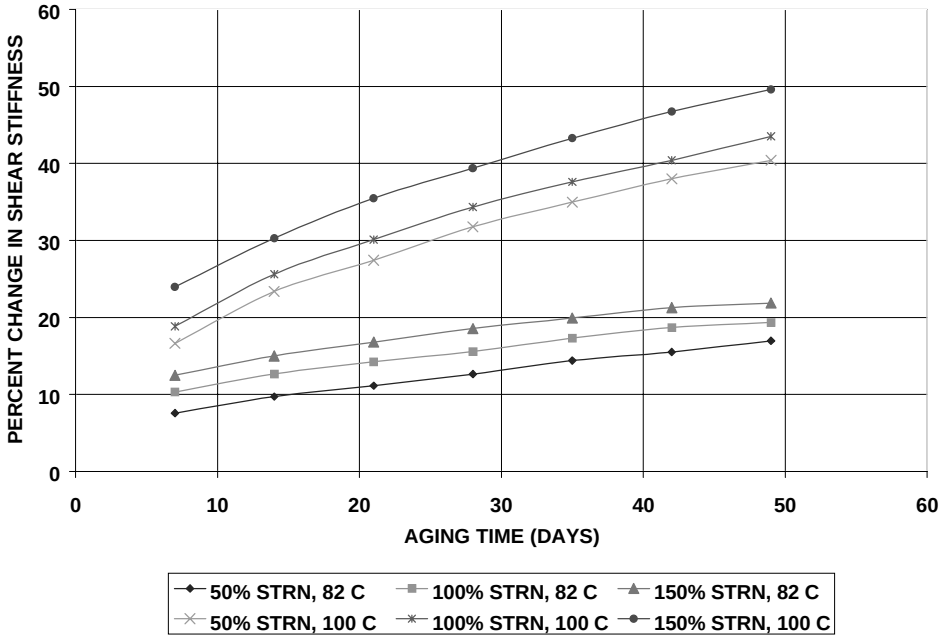

Figure 69. Accelerated aging of 1 × 1 NR200 specimens.

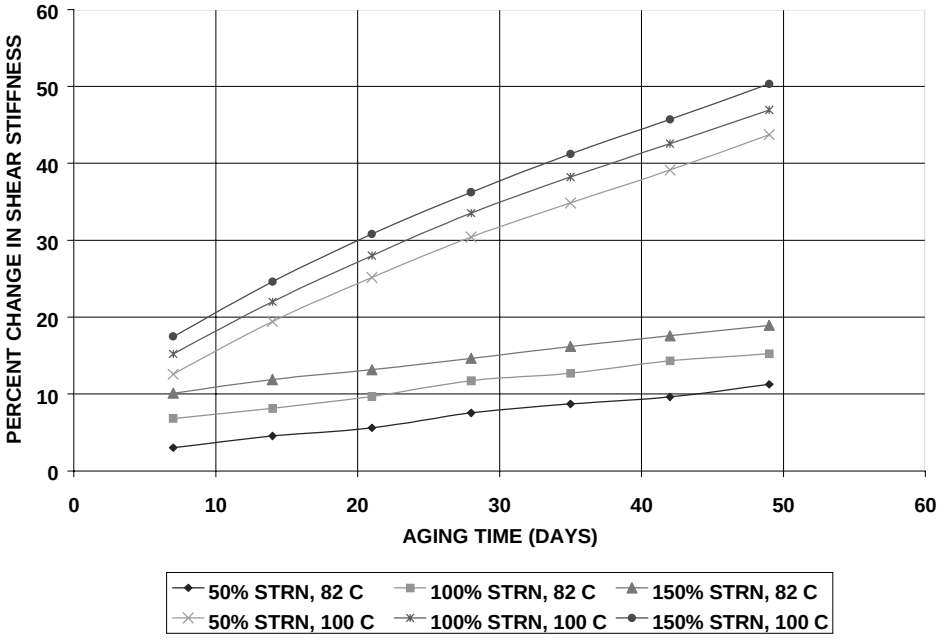

Figure 70. Accelerated aging of 1 × 1 NEO200 specimens.

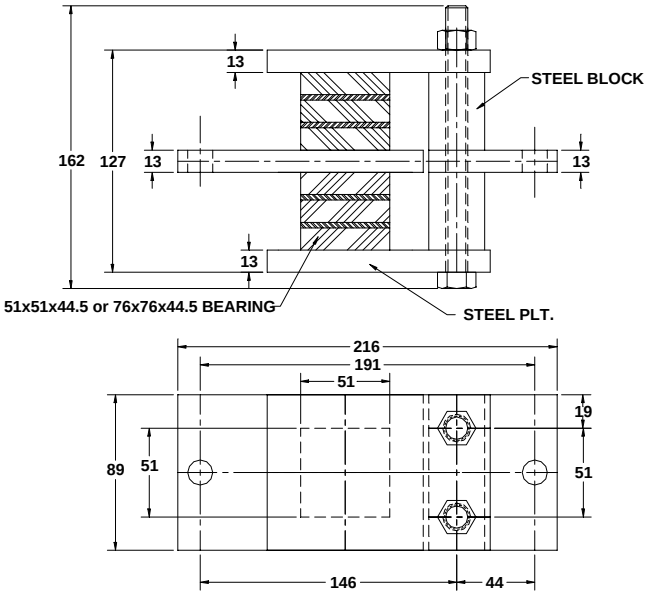

Figure 71. Structural configuration of 2 × 2 and 3 × 3 shear specimens.

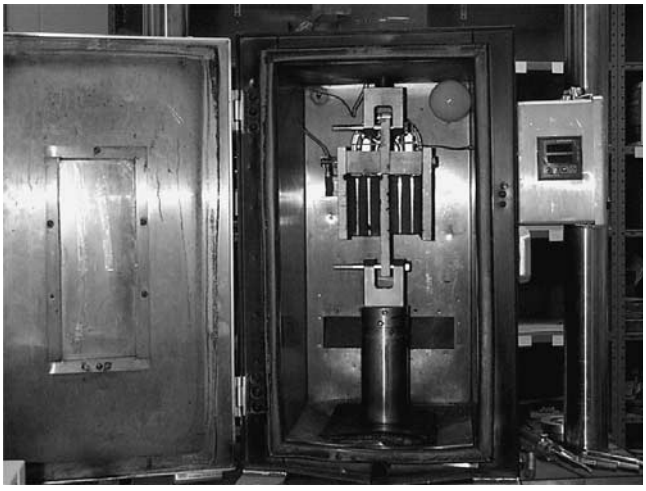

Figure 72. Test Setup for 2 × 2 and 3 × 3 shear specimens.

Mullins effect, and the load was recorded during the 6th cycle. This was done every time the specimens were removed from the air oven. The secant shear modulus was calculated at 50-percent shear strain. The results of accelerated aging of the 2 × 2 and 3 × 3 specimens are shown in Figures 73 through 76 for NR100, NEO100, NR200, and NEO200, respectively. The results of the 1 × 1 specimen aging tests at 50-percent shear strain are also included for comparison. The plot legends refer to the specimen sizes and the aging temperature. The percent change in stiffness is relative to the stiffness (secant shear modulus) at 0 time of aging (i.e., before the specimens were placed in the air oven).

Interpretation and Evaluation of Results

Interpretation of Results

Figures 66 through 76 show that the effects of aging are more dominant at higher shear strains. Figures 77 and 78 show

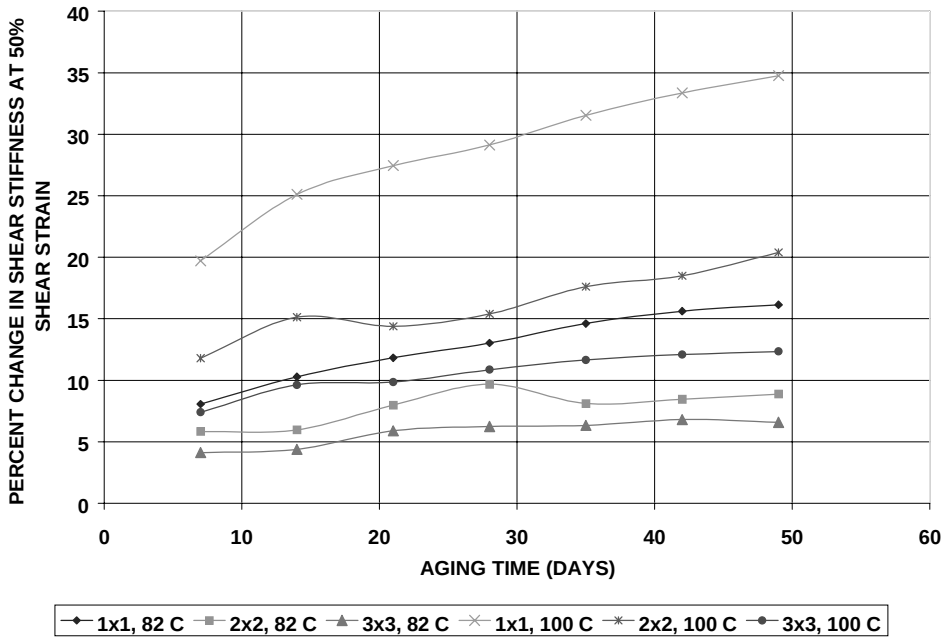

Figure 73. Aging tests for 1 × 1, 2 × 2, and 3 × 3 NR100 shear specimens.

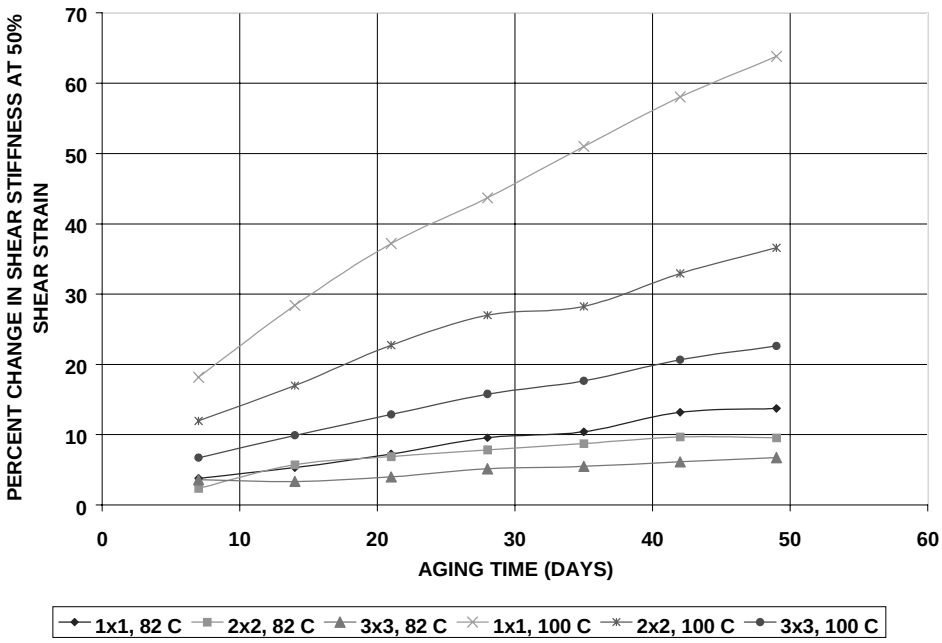

Figure 74. Aging tests for 1 × 1, 2 × 2, and 3 × 3 NEO100 shear specimens.

the change in shear stiffness for the four sizes of specimens after 7 weeks of accelerated aging at 82° and 100°C (180° and 212°F). These last two figures have different vertical scales. The change in shear stiffness because of aging definitely depends on the size of the specimen. As the size increases, the percent change in shear stiffness decreases drastically. This can be attributed to the amount of rubber affected by the oxidation process. For the rheometer specimens, the stiffness change is very significant because the entire specimen is affected by aging. As the size increases, the ratio of the surface area to the total rubber volume decreases and, therefore, the effect of aging on the overall shear stiffness decreases. At higher aging temperatures, the stiffness change is higher. This is because of a higher oxygen diffusion rate at higher temperatures.

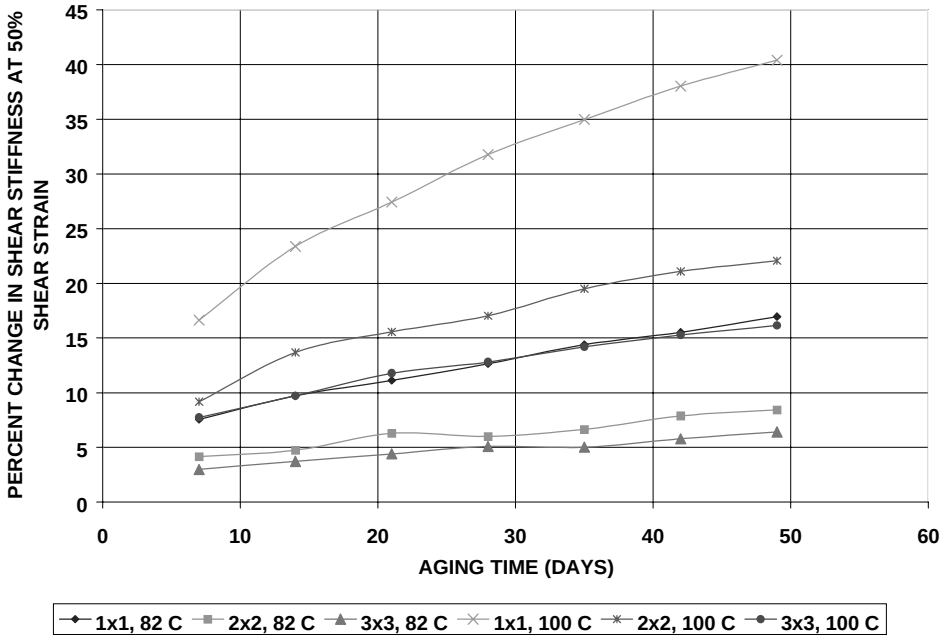

Figure 75. Aging tests for 1 × 1, 2 × 2, and 3 × 3 NR200 shear specimens.

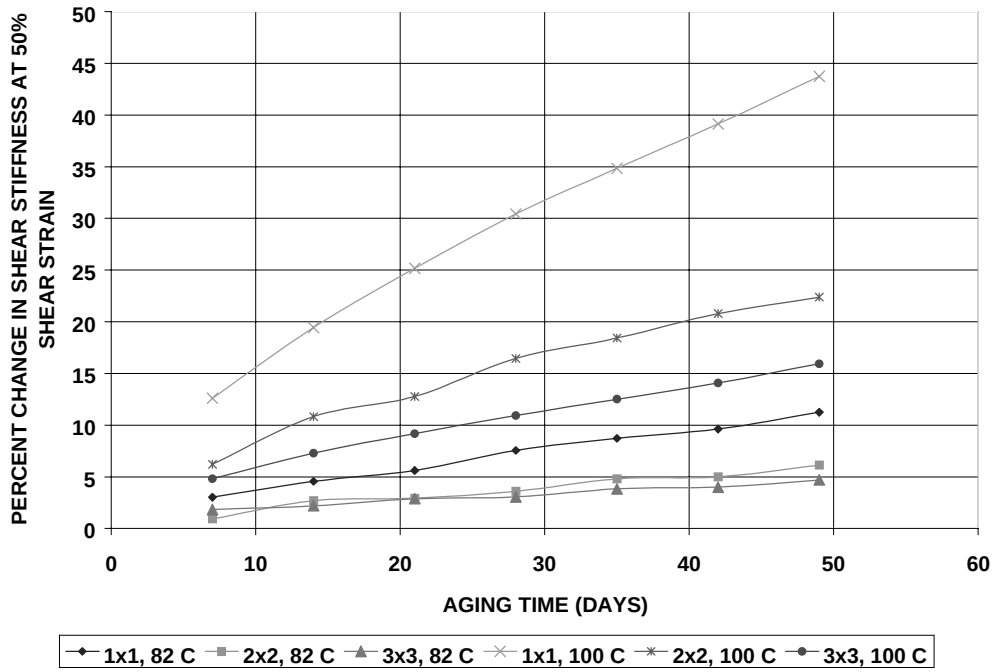

Figure 76. Aging tests for 1×1, 2×2, and 3×3 NEO200 shear specimens.

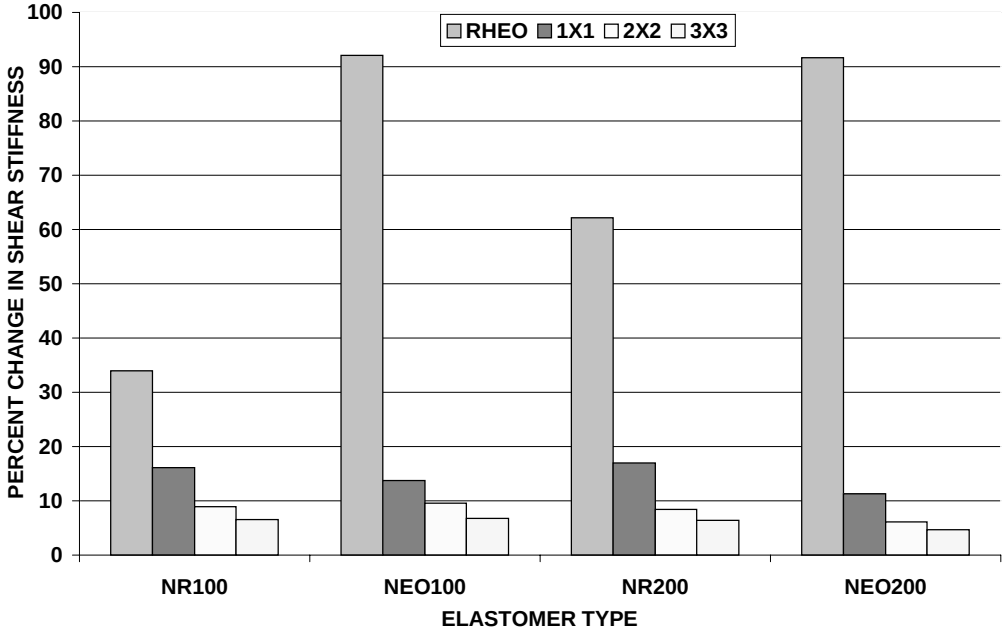

Figure 77. Aging results after 7 weeks of aging at 82°C.

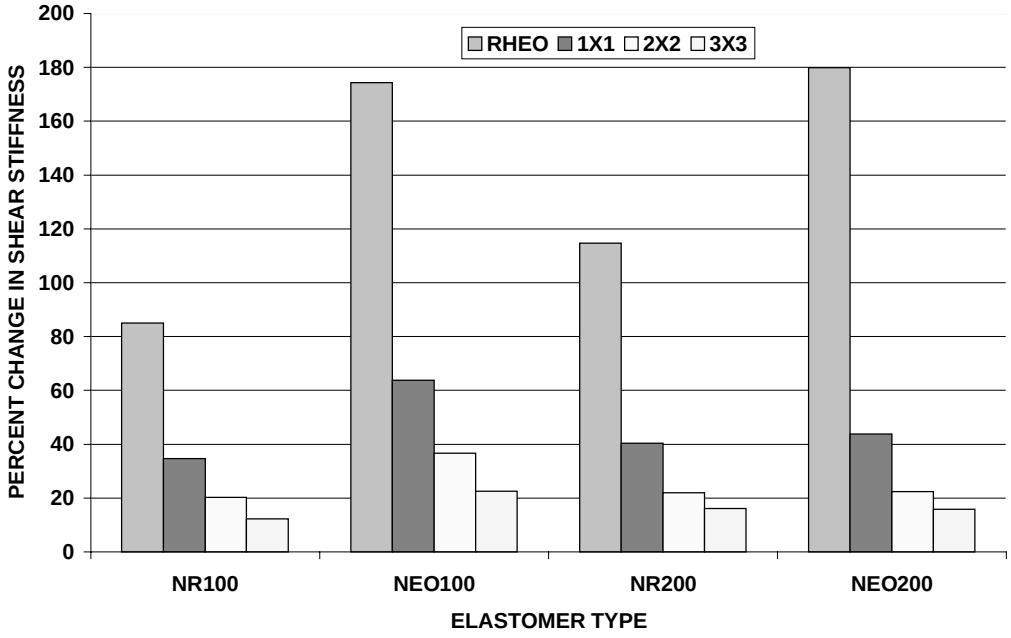

Figure 78. Aging results after 7 weeks of aging at 100°C.

Aging at Ambient Temperature

The change in shear stiffness due to aging is the consequence of chemical reactions and the diffusion rate of oxygen. Given that both chemical reaction and diffusion rate depend on temperature, the Arrenhius relation that gives the chemical reaction rate as a function of absolute temperature can be used to predict the effect of aging at various temperatures. The Arrenhius relation is given by

$$k = Ae^{\left(-\frac{Ea}{RT}\right)} \tag{15}$$

where

k is the general rate of reaction (changes/unit time),
A is the rate of reaction constant (changes /unit time),
Ea is the activation energy (J/mol),
R is the molar gas constant (J/mol-*K*) and
T the is absolute (Kelvin) temperature (K = C° + 273°).

Equation 15 can be rearranged to obtain an expression for equivalent times for the same property change with exposures at different temperatures as follows:

$$\Delta t_2 = \Delta t_1 e^{\left(\frac{Ea}{R}\right)\left(\frac{1}{T_2}-\frac{1}{T_1}\right)} \tag{16}$$

where Δt_1 is the aging time at test temperature T_1 while Δt_2 is the aging time at test temperature T_2. Since the 3×3 specimen was the largest tested, it was used to predict the percent change in stiffness at 32°C or 305°K (90°F) using the Arrenhius relationship. The procedure is summarized as follows. From the results of the aging studies, a relationship between time and percent change in shear stiffness was developed using regression analysis. A power law of the following form worked fairly well:

$$Y = aX^b \tag{17}$$

where

Y is the time in days,
X is the percent change in shear stiffness, and
a and *b* are regression coefficients.

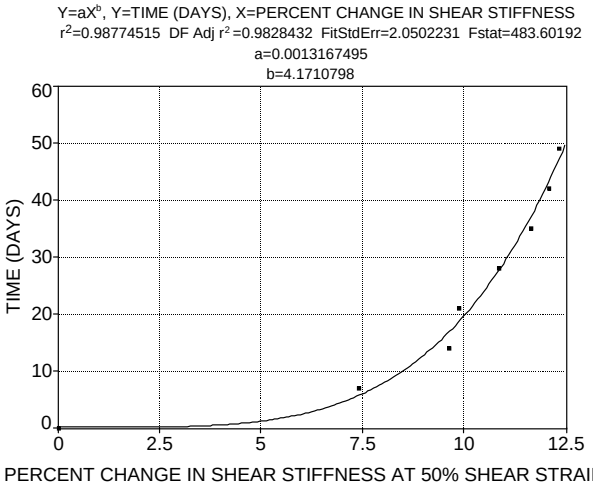

Figure 79. Aging time and percent change in stiffness for 3×3 NR100 at 100°C.

TABLE 25 Prediction of time required to age 3 × 3 specimen at 32°C

Specimen	Percent Change in Shear Stiffness	Test Temperature 355 K			Test Temperature 373 K			Ea/R	Time Required at 32°C
		Regression Coef. *a*	Regression Coef. *b*	Time Required DAYS	Regression Coeff. *a*	Regression Coeff *b*	Time Required DAYS		YEARS
NR100	5	0.03568	3.72354	14.29	0.00132	4.17108	1.08	18973	250.00
	10	0.03568	3.72354	188.79	0.00132	4.17108	19.52	16691	1151.25
NEO100	5	1.02883	2.03685	27.29	0.42804	1.52020	4.94	12568	24.79
	10	1.02883	2.03685	111.99	0.42804	1.52020	14.18	15203	343.43
NR200	5	0.78208	2.24931	29.20	0.04170	2.53935	2.48	18130	346.14
	10	0.78208	2.24931	138.86	0.04170	2.53935	14.44	16652	831.30
NEO200	5	3.72233	1.69332	56.81	0.64802	1.57021	8.11	14318	115.76
	10	3.72233	1.69332	183.71	0.64802	1.57021	24.09	14946	500.25

As an example, the results of regression analysis for aging of NR100 at 373°K are shown in Figure 79. The results for other conditions are tabulated in Table 25. Because testing was performed at two temperatures, the values of (Ea/R) for various compounds corresponding to a particular change in shear stiffness were calculated using the test results in Equation 16. Once (Ea/R) is known, Equation 16, in conjunction with one of the test temperatures, is used to predict the percent change in shear stiffness at ambient temperature. Based on this method, the times required to change the shear stiffness by 5 percent and 10 percent at 32°C (90°F) are tabulated in Table 25 for the four rubber compounds tested. These times are for 76 × 76 mm (3 × 3 in.) specimens and that the actual size of bridge bearings is much larger than the test specimen. The results of this study show that the aging effects reduce exponentially as the specimen size increases, so the effect of aging on full-size bearings will be insignificant.

As shown in Table 25, it will take hundreds of years to change the shear stiffness of a 3 × 3 specimen by 10 percent. For full-size bearings, it will take several hundred years to change the shear stiffness by 10 percent. Other researchers have drawn this conclusion based on microanalytical methods. Based on the results of this study, it can be concluded that full-size bearings will experience insignificant aging over their lifetime. Therefore, ASTM D573 (heat resistance) can be eliminated from AASHTO M251-97 for elastomeric bridge bearings.

CHAPTER **3**

ANALYTICAL STUDIES

Analytical studies were undertaken for two principal purposes: (1) to evaluate the effect of steel laminate misalignment on the performance of the bearing under compression, shear, and rotation, and (2) to determine the growth of edge surface cracks resulting from manufacturing defects or ozone cracking. The behavior of rubber was modeled in terms of the strain energy function proposed by Yeoh (1993) to fit the measured nonlinear stress-strain response of some typical rubbers used in bridge bearings. Both analytical phases conducted research on the same model bearing with three 12.7-mm (0.5-in.)-thick elastomer layers, two 3.2-mm (0.125-in.)-thick steel laminates and 6 mm (0.25 in.) of edge cover as was shown in Figure 4. The plan dimensions of the model bearing were 229×356 mm (9×14 in.) and the overall thickness was 44.5 mm (1.75 in.). This configuration was selected because it was used in the physical testing phase of the project and its shape factor is at the lower end of the range found in practice. Therefore, this configuration will conservatively represent the overall structural behavior of most bearings.

STATIC BEHAVIOR

Introduction

Most of the steel-laminated elastomeric bearings are manufactured using compression molding wherein the outside dimensions can be precisely controlled by the mold dimensions. However, the internal steel laminates (also called shims or reinforcements), if not properly constrained, can shift horizontally or vertically or rotate because of the flow of rubber under pressure inside the mold. The most common external defects (e.g., variation in overall horizontal and vertical dimension, overall horizontal and vertical slopes of surfaces, and size and position of holes, slots, or inserts) can be easily inspected using the tolerances given in AASHTO M251-97. The effects of marginal laminate movement are more difficult to assess by merely external visual examination. The objective of this study was to assess the effects of marginal laminate misalignments on the structural behavior of steel-laminated elastomeric bearings.

Assuming that the outside dimensions are precisely controlled during molding, the three most probable laminate misalignments are as follows:

- **Vertical shift** causing variations in rubber layer thickness,
- **Horizontal shift** causing variations in external cover, and
- **Rotation** resulting in non-uniform rubber layer thickness.

Given that the effects of laminate misalignments are difficult to measure directly, finite element computer simulation was used to study the combined effect of the above three probable misalignments on the overall structural behavior of the bearing. The range of each misalignment was selected on the basis of tolerances of equipment used in the molding process as follows: vertical shift ±3 mm, horizontal shift 6 mm, and angular rotation ±1.5 deg.

NR100, NR200, NEO100, and NEO200 bearings as used in the experimental phase were chosen for theoretical evaluation because they represent the extremes in material stiffness usually found in practice. Because of the many uncertainties involved in modeling the friction between rubber and contacting surface, the top and bottom surfaces were assumed fully bonded for the major sensitivity study. For the purpose of comparison with unbonded end conditions, a few critical cases with a constant coefficient of friction between the rubber and contacting surface were also analyzed. The effects of misalignments were investigated under a combined axial load, shear deformation, and rotation of the bearing. For NR100 and NEO100 bearings, an axial load corresponding to 3.8 MPa (550 psi) axial stress in conjunction with a shear deformation corresponding to 50-percent direct shear strain and 1-deg rotation was used. For NR200 and NEO200 bearings, an axial load corresponding to 7.6 MPa (1100 psi) axial stress in conjunction with a shear deformation corresponding to 50-percent direct shear strain and 1-deg rotation was used.

Essentially this study consisted of a set of computer-simulated experiments using the finite element method in which the effect of three independent variables (i.e., horizontal shift, vertical shift, and rotation of laminates) on eight performance (dependent) variables as follows:

1. Axial stiffness,
2. Shear stiffness,
3. Rotation stiffness,
4. Maximum shear strain in elastomer,
5. Maximum principal strain in elastomer,
6. Maximum triaxial tension in elastomer,

7. Maximum bond stress at the interface of elastomer and steel laminate, and
8. Maximum von Mises stress in steel laminates.

(These eight performance variables govern the structural behavior of the bearings.)

In the following sections, the design of the virtual experiments is presented first, followed by the evaluation criteria and constraints used on the performance parameters. After a synopsis of the finite element analysis, the results of the statistical analysis and the interpretation of results are given.

Design of Virtual Experiments

Given that there are unlimited combinations of the three misalignments considered, a response surface methodology, generally used in statistical design and analysis of experiments (John, 1971), was used to find an approximating function relating the various structural responses (dependent variables) to the combined effect of the misalignments (independent variables). A Center Composite Design (CCD) was employed in selecting various runs and values of the three independent variables. Details of the CCD are given in Appendix E of the research team's final report. For the number of variables considered, 16 computer runs are needed for each of the four materials in order to establish a statistically reliable evaluation of the misalignments. The derived values of the misalignments used in each of the runs are given in Table 26. Runs 15 and 16 are identical and represent the bearing with all shims perfectly aligned.

Performance Parameters and Criteria

The structural behavior of a bearing depends on the axial, shear, and rotation stiffnesses; the structural integrity is controlled by limits on the internal stresses and strains. From the point of view of performance, the stiffnesses are more important as long as the internal stresses and strains remain within the allowable limits generally imposed by the strength of materials (i.e., elastomer and steel). Therefore, to assess both the structural behavior and structural integrity of the subject bearing configuration, the effects of three independent variables, described in Section 2, were studied on the eight performance parameters. The performance (dependent) variables and their evaluation criteria are described as follows:

TABLE 26 Design matrix for independent variables

RUN	Actual Values		
	X_1 (mm)	X_2 (mm)	X_3 (Degrees)
1	-1.7321	2.5358	-0.86605
2	1.7321	2.5358	-0.86605
3	-1.7321	9.4642	-0.86605
4	1.7321	9.4642	-0.86605
5	-1.7321	2.5358	0.86605
6	1.7321	2.5358	0.86605
7	-1.7321	9.4642	0.86605
8	1.7321	9.4642	0.86605
9	3	6	0
10	-3	6	0
11	0	12	0
12	0	0	0
13	0	6	1.5
14	0	6	-1.5
15,16	0	6	0

- **Axial Stiffness (AXSTIF).** This represents the ratio of axial load to axial deflection at 3.8 MPa (550 psi) and 7.6 MPa (1100 psi) average axial stress for 50 (NR100 and NEO100) and 70 (NR200 and NEO200) durometer bearings, respectively. Vertical deflection of the bearing is controlled by axial stiffness, which is important for both single-span and multi-span bridges. For single-span bridges, excessive axial deflection at supports results in an uneven road surface at the supports. Excessive vertical deflection at supports of multi-span bridges can result in excessive stress in girders. The variation of axial stiffness with respect to the axial stiffness of a perfect configuration was limited to ±10 percent for evaluation purposes.
- **Shear Stiffness (SHRSTIF).** This represents the ratio of shear load to shear deflection corresponding to 0.5 (50-percent) direct shear strain. Given that the thermal movement of the bridge girder causes the shear deflection, the force transferred from the bridge girder to its support is controlled by the shear stiffness of the bearing. Therefore, shear stiffness is very important. The variation of shear stiffness with respect to the shear stiffness of a perfect shim configuration was limited to ±10 percent for evaluation purposes.
- **Rotation Stiffness (ROTSTIF).** This represents the ratio of cocking moment to cocking rotation corresponding to 1-deg rotation of the bearing. Given that rotation stiffness of flat pads is not very important, no limit on its variation is imposed. For applications where rotational stiffness is important, a cylindrical or spherical bearing is usually used.
- **Maximum Shear Strain (SHSTRN).** This represents the total of direct and indirect shear strain. There are two types of shear strains that a rubber layer experiences under combined axial load and shear deformation: (1) direct shear strain resulting from shearing action and (2) indirect or bulge shear strain resulting from bulging action. As per good engineering practice used in the rubber bearing industry, the direct shear strain is limited to 1.75 (175 percent) while the indirect shear strain is limited to 6 (600 percent). The direct and indirect shear strains are combined to give total shear strain. In the present study, given that the direct shear strain is just 0.5 (50 percent), the total shear strain is limited to 6 (600 percent).
- **Maximum Principal Strain (PRNSTN).** This represents the maximum uniaxial strain in the elastomer. The

TABLE 27 Constraints on dependent variables

Dependent Variables	Constraints			
	NR100	**NEO100**	**NR200**	**NEO200**
AXSTIF (kN/mm)	186-227	190-232	342-418	395-483
SHRSTIF (kN/mm)	0.86-1.05	0.86-1.05	1.64-2.0	1.87-2.28
ROTSTIF (kN-m/deg)	No constraint	No constraint	No constraint	No constraint
SHSTRN	< 6	< 6	< 6	< 6
PRNSTN	< 2	< 2	< 2	< 2
TENS (MPa)	< 3.5	< 3.53	< 7.2	< 7.5
BOND (MPa)	< 1.31	< 1.81	< 3.4	< 7.4
MISES (MPa)	< 345	< 345	< 345	< 345

maximum allowable uniaxial tensile strain in elastomer layers is limited to 2 (200 percent).

- **Triaxial Tension (TENS).** The maximum triaxial tension in rubber is limited to 6 times the design shear modulus as per good engineering practice used in the rubber industry. Rubber is commonly found to undergo internal cavitation at triaxial tension equivalent to 6*G*, where *G* is the linear shear modulus. This phenomenon is a consequence of an elastic instability known as "an unbounded elastic expansion of preexisting cavities, too small to be readily detected" (Gent and Tompkins, 1969). The critical stress does not depend on the strength of the rubber, but only on its elastic modulus.
- **Maximum Bond Stress (BOND).** This represents the resultant of the nominal tensile stress and the nominal resultant shear stress carried at the interface nodes of the elastomer and the steel. This stress is limited to the average shear stress corresponding to 2 (200 percent) shear strain as determined from a dual-lap shear test.
- **Maximum von Mises Stress (MISES).** This represents the stress in the laminates corresponding to von Mises failure (yield) theory. In this theory, yielding occurs for a complex stress state when the von Mises stress, defined by Equation 18, at any point in the laminate becomes equal to the yield stress from a simple tension test.

$$\sigma = \sqrt{\frac{(\sigma_1 - \sigma_2)^2 + (\sigma_2 - \sigma_3)^2 + (\sigma_3 - \sigma_1)^2}{2}} \qquad (18)$$

where σ_1, σ_2, and σ_3 are the maximum, intermediate, and minimum principal stresses, respectively.

The constraints imposed on the performance variables based on the evaluation criteria for the model bearings are summarized in Table 27.

Finite Element Analysis

Given that rubber is an almost incompressible material, the finite element model of the rubber portion was prepared using three-dimensional, 27-node, second-order, solid, hybrid-finite elements. The steel parts were modeled using three-dimensional, 27-node, second-order, solid, finite elements. The commercial finite element program, ABACUS©, was used to perform the analysis. The finite element model for the perfect configuration is shown in Figure 80 and the models for the 16 shim configurations tabulated in Table 26 are shown in Figure 81. Only one-half of the bearing was modeled because of the symmetry of geometry and loading. Symmetric boundary conditions were applied at the plane of symmetry.

Four shear stress-strain responses from NR100, NR200, NEO100, and NEO200 bearings were used to represent the extreme range of the material behavior found in elastomeric bearings. The measured stress-strain relationships for low-hardness and high-hardness natural rubber and neoprene samples are shown in Figure 82. The stress-strain curves in simple shear were experimentally obtained using a molded dual-lap

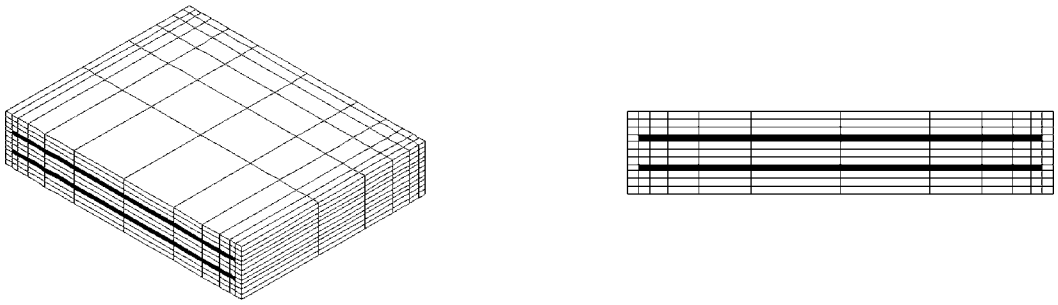

(a) (b)

Figure 80. Finite element model of perfect configuration (a) isometric view, (b) cross section.

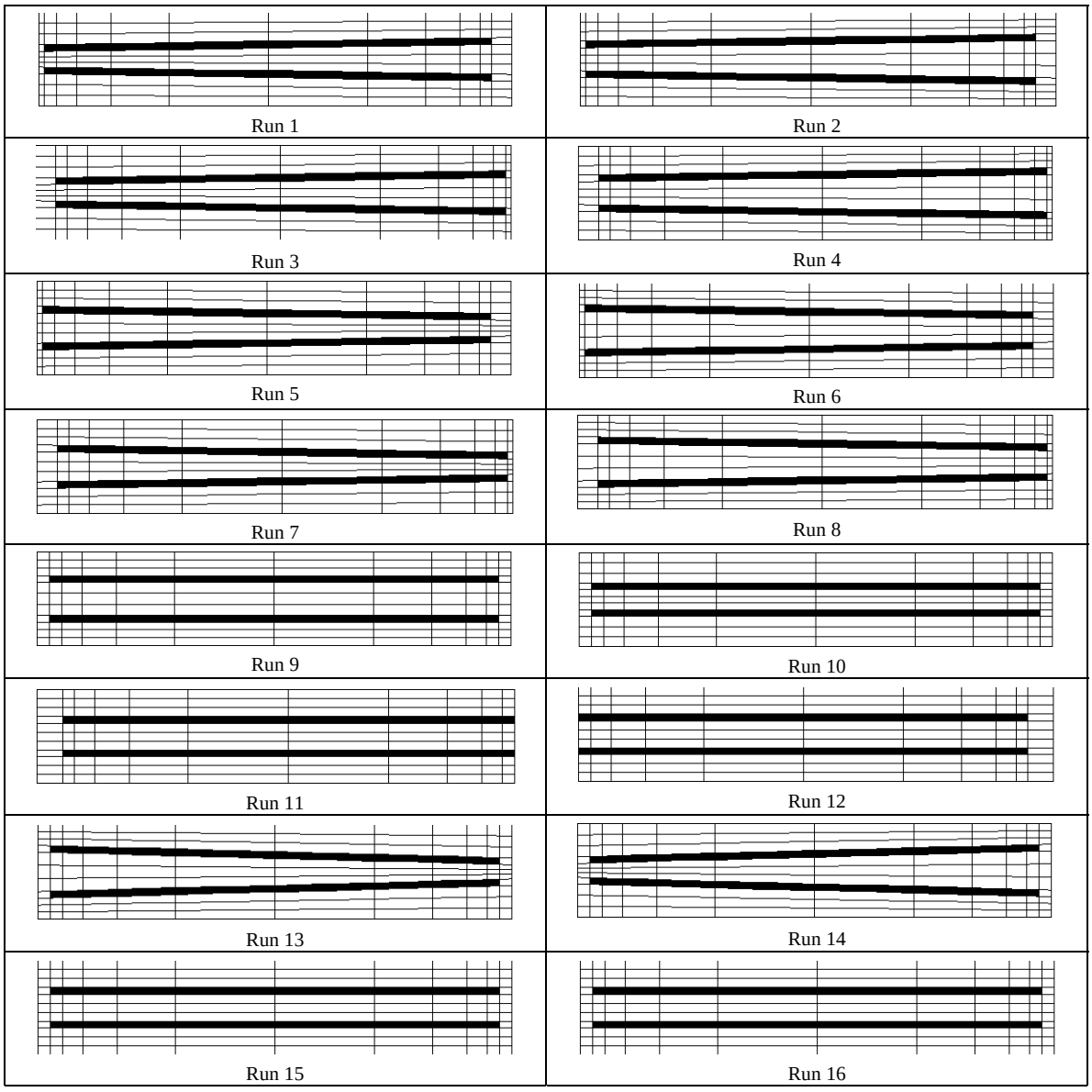

Figure 81. Cross section of finite element models for various runs.

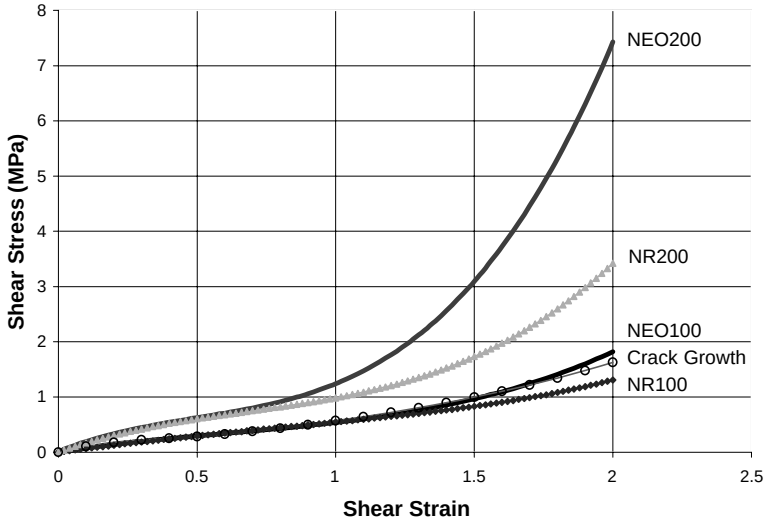

Figure 82. Shear stress-strain response for various elastomers.

shear specimen described in the Creep Section of Chapter 2. A nonlinear regression analysis was used to determine the material constants in Yeoh's formulation for incorporation into the finite element analysis. Details of this process are given in Kumar (2000). The steel components were modeled using isotropic material with Young's Modulus equal to 200,000 MPa and a Poison's ratio equal to 0.3. A bilinear, stress-strain curve (first line connecting 0 and yield point [345 MPa] and the second line connecting yield point to ultimate [490 MPa] at 30-percent elongation) was used to define the plastic behavior of steel.

Structural analyses consisted of nonlinear quasi-static analysis with geometric and material nonlinearities to incorporate the effects of large deformation and large strains. A solution was obtained as a series of increments, with iterations within each increment to obtain equilibrium. Given that several nonlinearities were acting simultaneously, the loads were applied in small increments to ensure correct modeling of history-dependent effects and to increase the computational efficiency.

Finite Element Analysis Results

The values of the eight performance variables mentioned earlier extracted from finite element analyses of bearings with bonded top and bottom surfaces for the 16 runs are tabulated in Tables 28 through 31 for NR100, NEO100, NR200, and NEO200, respectively. A comparison between the perfect bearing configurations with bonded and unbonded top and bottom surfaces in terms of the eight dependent variables is shown in Table 32. The displacement plots and key contour plots for a perfect shim configuration with bonded top and

TABLE 28 Values of performance variables for NR100

Run	Axial Stiffness kN/mm	Shear Stiffness kN/mm	Rotation Stiffness kNm/deg	Max. Shear Strain in Rubber	Max. Principal Strain in Rubber	Max. Triaxial Tension Stress in Rubber MPa	Max. Bond Stress at Steel Shims MPa	Max. von Mises Stress in Shims MPa
1	193	0.988	2.06	1.74	1.81	1.72	1.023	114
2	188	0.982	1.25	1.72	1.74	1.63	1.005	149
3	203	0.973	3.14	1.72	1.84	1.45	1.005	159
4	197	0.974	2.40	1.68	1.73	1.32	0.970	206
5	187	0.978	1.15	1.73	1.75	1.76	1.014	178
6	189	0.973	1.79	1.69	1.73	2.26	0.978	155
7	194	0.966	2.10	1.60	1.81	1.25	0.904	188
8	199	0.962	2.88	1.61	1.80	1.31	0.912	171
9	194	0.956	2.14	1.74	1.73	2.07	0.996	157
10	196	0.960	2.22	1.80	1.85	1.93	1.081	162
11	211	0.956	3.22	1.66	1.84	1.33	0.953	155
12	193	0.972	1.13	1.64	1.71	1.56	0.936	130
13	184	0.997	1.85	1.73	1.78	2.01	1.014	187
14	189	1.010	2.28	1.75	1.79	1.62	1.033	176
15,16	206	0.959	2.42	1.77	1.79	2.03	1.052	132

TABLE 29 Values of performance variables for NEO100

Run	Axial Stiffness kN/mm	Shear Stiffness kN/mm	Rotation Stiffness kNm/deg	Max. Shear Strain in Rubber	Max. Principal Strain in Rubber	Max. Triaxial Tension Stress in Rubber MPa	Max. Bond Stress at Steel Shims MPa	Max. von Mises Stress in Shims MPa
1	198	0.989	2.34	1.66	1.64	1.61	1.151	117
2	193	0.982	1.54	1.64	1.58	1.51	1.068	150
3	209	0.972	3.44	1.65	1.66	1.53	1.181	166
4	202	0.972	2.70	1.61	1.56	1.41	1.041	210
5	191	0.980	1.43	1.64	1.58	1.70	1.068	182
6	195	0.976	2.08	1.61	1.56	2.14	1.041	160
7	199	0.966	2.42	1.63	1.63	1.33	1.137	194
8	204	0.963	3.19	1.56	1.63	1.39	1.137	177
9	200	0.956	2.43	1.64	1.58	2.00	1.068	158
10	201	0.960	2.51	1.72	1.67	1.88	1.196	167
11	217	0.955	3.53	1.61	1.68	1.39	1.211	162
12	198	0.974	1.41	1.57	1.55	1.47	1.028	134
13	189	1.000	2.16	1.65	1.60	1.97	1.095	193
14	194	1.009	2.57	1.68	1.63	1.54	1.137	180
15,16	211	0.958	2.70	1.69	1.62	1.97	1.123	137

TABLE 30 Values of performance variables for NR200

Run	Axial Stiffness kN/mm	Shear Stiffness kN/mm	Rotation Stiffness kNm/deg	Max. Shear Strain in Rubber	Max. Principal Strain in Rubber	Max. Triaxial Tension Stress in Rubber MPa	Max. Bond Stress at Steel Shims MPa	Max. von Mises Stress in Shims MPa
1	351	1.88	3.95	1.69	1.68	3.21	2.20	177
2	349	1.87	2.36	1.68	1.62	3.03	2.03	232
3	375	1.84	6.12	1.67	1.69	3.16	2.23	256
4	364	1.85	4.65	1.64	1.75	2.97	2.42	316
5	346	1.86	2.09	1.67	1.62	3.40	2.03	270
6	351	1.85	3.37	1.64	1.60	4.27	1.97	244
7	360	1.83	4.06	1.75	1.66	2.64	2.14	292
8	367	1.82	5.59	1.61	1.66	2.80	2.14	272
9	360	1.82	4.12	1.71	1.62	3.93	2.03	239
10	363	1.82	4.27	1.75	1.71	3.69	2.29	252
11	389	1.81	6.29	1.64	1.70	2.91	2.26	249
12	358	1.85	2.07	1.60	1.58	2.90	1.92	204
13	341	1.89	3.52	1.68	1.65	3.90	2.11	286
14	350	1.91	4.41	1.72	1.68	3.03	2.20	279
15,16	380	1.82	4.61	1.73	1.66	3.84	2.14	211

TABLE 31 Values of performance variables for NEO200

Run	Axial Stiffness kN/mm	Shear Stiffness kN/mm	Rotation Stiffness kNm/deg	Max. Shear Strain in Rubber	Max. Principal Strain in Rubber	Max. Triaxial Tension Stress in Rubber MPa	Max. Bond Stress at Steel Shims MPa	Max. von Mises Stress in Shims MPa
1	414	2.16	6.12	1.53	1.39	2.90	2.52	195
2	402	2.13	4.49	1.48	1.35	2.63	2.33	240
3	436	2.11	8.31	1.51	1.37	3.43	2.42	280
4	423	2.10	6.82	1.46	1.31	3.28	2.17	335
5	400	2.13	4.32	1.50	1.33	3.29	2.25	289
6	407	2.13	5.60	1.47	1.32	3.96	2.21	261
7	417	2.09	6.29	1.49	1.68	3.03	4.30	312
8	428	2.09	7.85	1.46	1.35	3.12	2.33	292
9	417	2.08	6.29	1.51	1.34	3.93	2.29	253
10	421	2.08	6.46	1.57	1.39	3.76	2.52	270
11	453	2.06	8.51	1.50	1.42	2.93	2.66	280
12	412	2.12	4.29	1.43	1.31	2.66	2.17	220
13	396	2.18	5.78	1.52	1.34	3.95	2.29	305
14	405	2.20	6.51	1.56	1.39	2.83	2.52	295
15,16	439	2.08	6.88	1.54	1.36	3.92	2.38	232

TABLE 32 Comparison between bonded and unbonded perfect bearing configuration

Performance Variable	NR100		NEO100		NR200		NEO200	
	Bonded	Unbonded	Bonded	Unbonded	Bonded	Unbonded	Bonded	Unbonded
AXSTIF (kN/mm)	206	172	211	179	380	313	439	334
SHRSTIF (kN/mm)	0.96	0.78	0.96	0.79	1.82	1.52	2.08	1.72
ROTSTIF (kN-m/deg)	2.42	2.06	2.7	2.37	4.61	4.01	6.88	6.02
SHSTRN	1.77	1.27	1.69	1.17	1.73	1.32	1.54	1.31
PRNSTN	1.79	1.48	1.62	1.29	1.66	1.46	1.36	1.31
TENS (MPa)	2.03	1.60	1.97	1.54	3.84	3.14	3.92	3.54
BOND (MPa)	1.05	0.89	1.12	0.87	2.14	2.05	2.38	2.31
MISES (MPa)	132	145	137	147	211	233	232	274

bottom surfaces are shown in Figures 83, 84, 85, and 86 for NR100, NEO100, NR200, and NEO200 respectively. Similar plots for unbonded surface conditions with a constant coefficient of friction equal to 0.3 between the rubber and the contacting top and bottom surfaces are shown in Figures 87, 88, 89, and 90 for NR100, NEO100, NR200, and NEO200, respectively. For all 16 configurations, the deformed shapes and stress contours for NR100 are given in Appendix F of the research team's final report.

Evaluation and Interpretation

A summary of the analysis results for bearings with bonded top and bottom surfaces is given in Table 33. The minimum and maximum values of each performance parameter from all 16 runs, the percent variation of these extreme limits relative to the case of no shim misalignment (Run 15, 16), and the recommended performance constraints from Table 27 are given. The axial stiffness and the shear stiffness are proportional to the shear modulus and are not significantly affected by the shim misalignments. The maximum shear strain and principal strain in the elastomer are not significantly affected by the bearing material specified or the misalignments. The remaining four performance parameters (i.e., rotational stiffness, triaxial tensile and bond stresses in the elastomer, and the maximum von Mises stress in the steel reinforcements) are affected by the steel shim misalignments, the shear modulus of the elastomer, or both. The following observations are based on the results

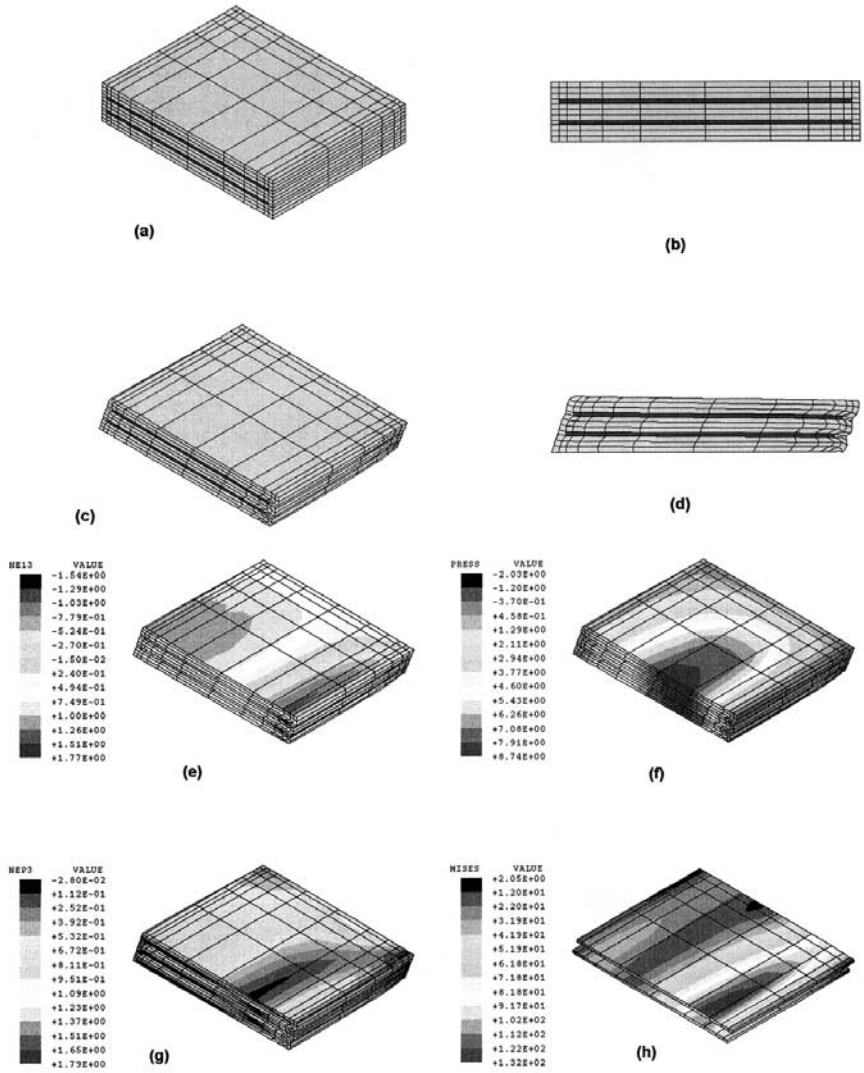

Figure 83. Deformed shapes and Stress Contour Plots—NR100 Perfect Configuration-Bonded Top and Bottom: (a) and (b) undeformed shape; (c) and (d) deformed shapes; (e) elastomer shear strain; (f) elastomer triaxial stress (MPa); (g) elastomer principal strain; (h) steel von Mises Stress (MPa).

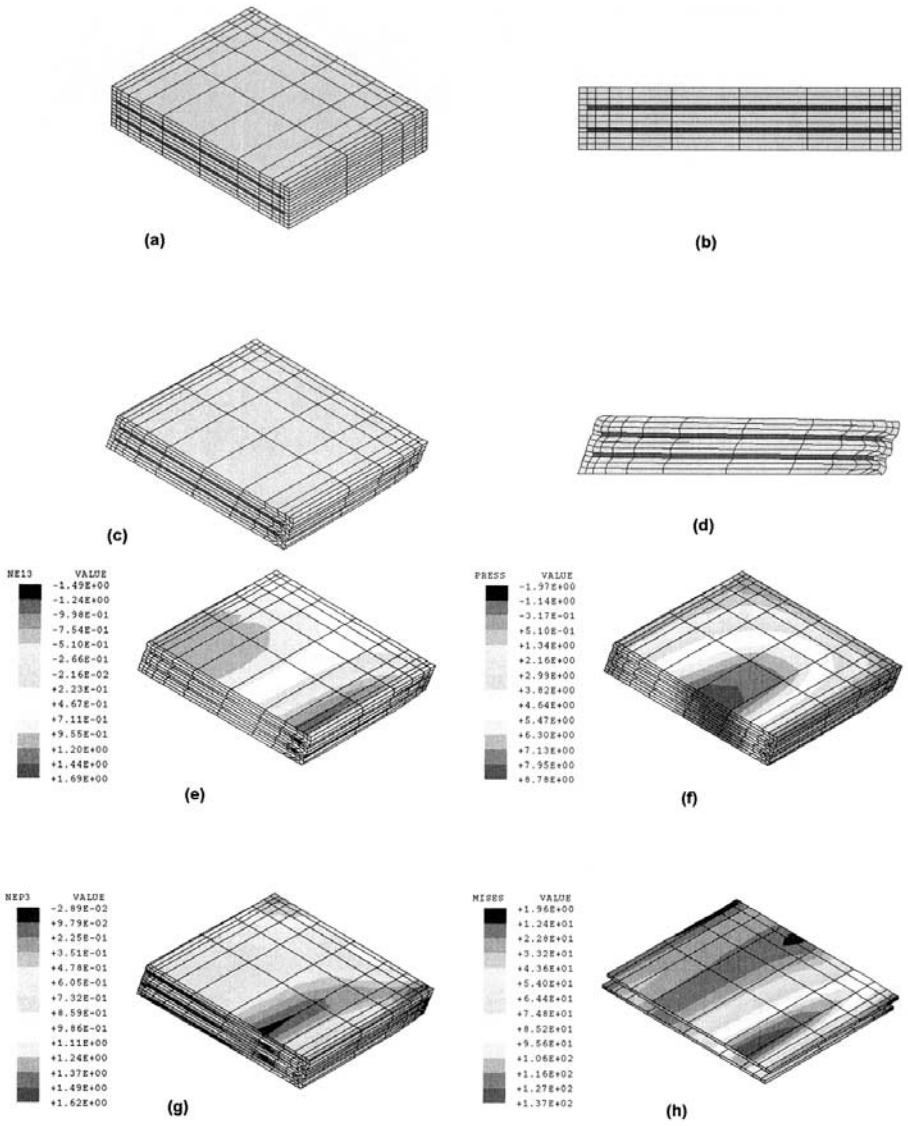

Figure 84. Deformed shapes and Key Stress Contours—NEO100 Perfect Configuration-Bonded Top and Bottom: (a) and (b) undeformed shape; (c) and (d) deformed shapes; (e) elastomer shear strain; (f) elastomer triaxial stress (MPa); (g) elastomer principal strain; (h) steel von Mises Stress (MPa).

in Tables 28 through 32 and the stress and strain data from all the runs.

Rotational Stiffness

Ideally, the rotational stiffness should be zero so that the bridge girder could rotate freely without developing restraining moments. The rotational stiffness varied as much as 50 percent from the perfect case. The maximum and minimum values were always associated with Cases 11 and 12, respectively, for each of the four materials. These two cases only involve edge cover, no other misalignment, so the magnitude of the rotational stiffness is very sensitive to the edge cover. The bearing rotational stiffness is 2 to 3 times greater when the edge with no cover is compressed during rotation compared with the case when the edge with large cover is compressed. The rotational stiffness is also directly affected by the shear modulus of the material; the NR200 bearing is about twice as stiff as the NR100 bearing for the perfect configuration. The NEO200 bearing is stiffer than the NR200 bearing because of the shape of the stress-strain curve as shown in Figure 82. At 50-percent strain, these two materials have about the same shear modulus, but at 150-percent strain, the NEO200 is about twice as stiff as the NR200. Despite the variations noted, the rotational stiffness has lit-

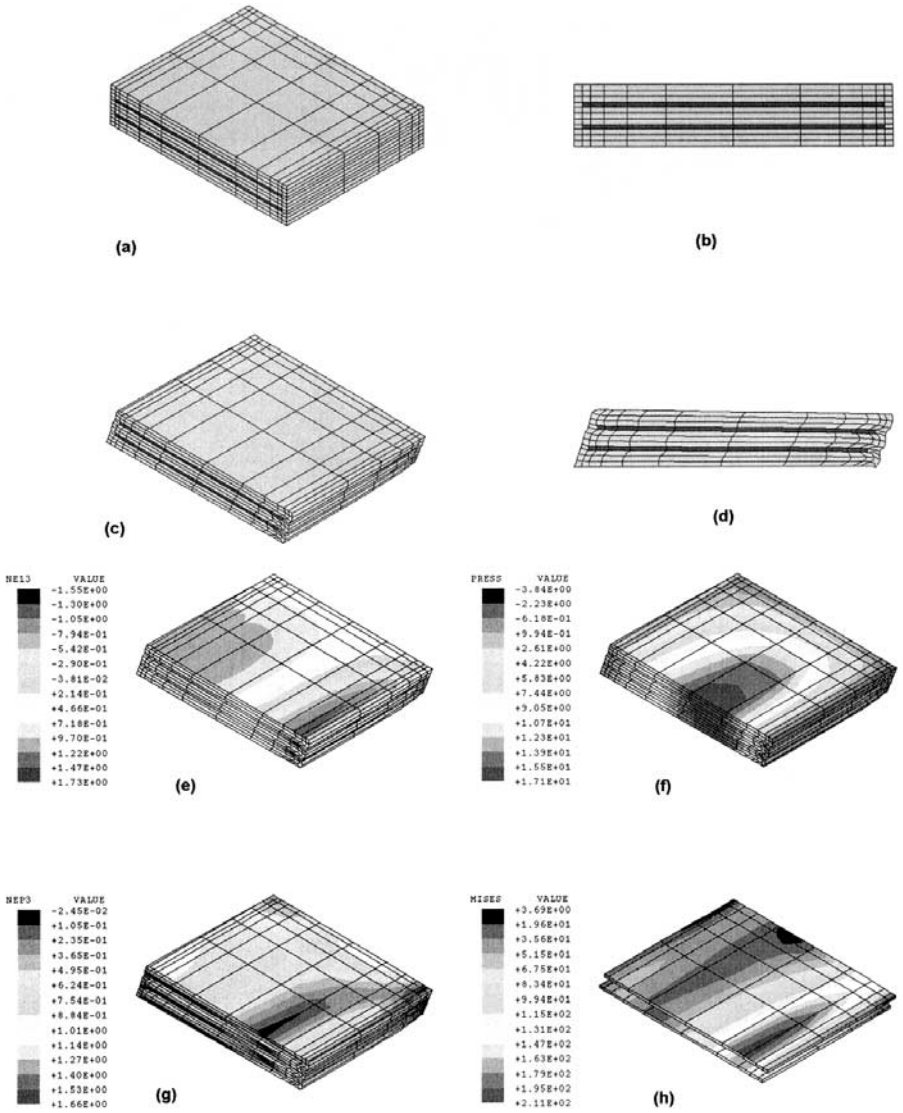

Figure 85. Deformed shapes and Key Stress Contours—NR200 Perfect Configuration-Bonded Top and Bottom: (a) and (b) undeformed shape; (c) and (d) deformed shapes; (e) elastomer shear strain; (f) elastomer triaxial stress (MPa); (g) elastomer principal strain; (h) steel von Mises Stress (MPa).

tle to do with the performance of the bridge because the rotational stiffness of the bearings is so much smaller than the rotational end stiffness of a typical bridge girder. The maximum rotational stiffness determined in the research (Run 11 for NEO200) was 8.51 kN-m/deg (6.27 kip-ft/deg), which is about 1/300th of the stiffness of a typical steel girder for a 30-m bridge span and span/depth ratio of 20. No rotational stiffness constraints have been imposed because of the low relative rotational stiffness of an elastomeric bearing and the fact that the maximum end rotation is controlled by the end rotation of the girder, not the characteristics of the bearing. Good design practice, such as avoiding bearing designs with high shape factors (>12), coupled with a small overall bearing thickness, will provide bearings with low rotation stiffness.

Triaxial Tension

The maximum triaxial tension stress in the elastomer occurs at the edge of the shim for all four materials and all 16 runs and its value is proportional to the shear modulus—the 200 grade material has about twice the stress of the 100 grade material. Edge cover dominates this performance parameter. The smallest edge cover and largest edge cover on the right edge (Runs 11 and 12, respectively, as shown in

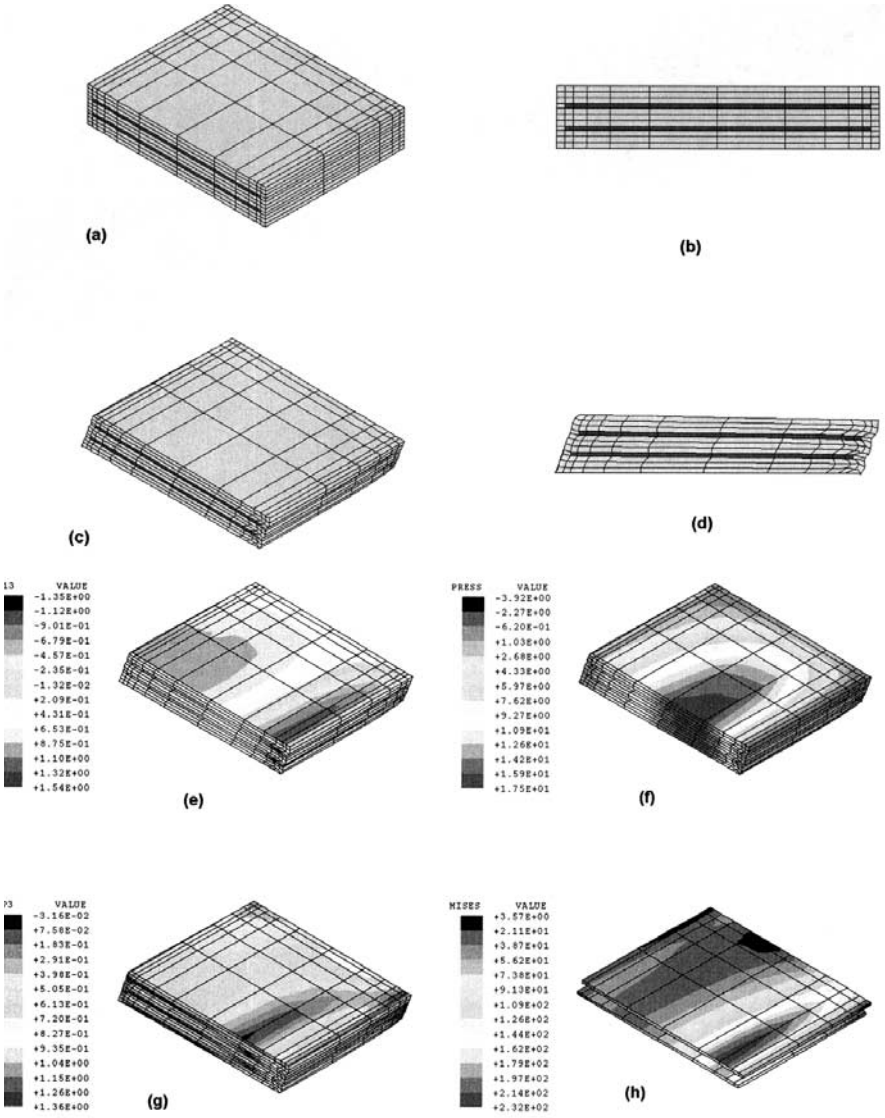

Figure 86. Deformed shapes and Key Stress Contours—NEO200 Perfect Configuration-Bonded Top and Bottom: (a) and (b) undeformed shape; (c) and (d) deformed shapes; (e) elastomer shear strain; (f) elastomer triaxial stress (MPa); (g) elastomer principal strain; (h) steel von Mises Stress (MPa).

Figure 81) gave about the same level of triaxial tension stress. For covers between these extremes, the relationship between the stress and the edge cover on the right side is nonlinear. The average of the four cases with a 2.5 mm (0.10 in.) cover is almost the same as the two extreme covers. Edge covers of 6 and 9.5 mm (0.24 and 0.37 in.) give triaxial tension stresses that are about 40 percent higher than the minimum values shown in Table 33. The highest stress always occurs with Run 6, with a right edge cover of 9.5 mm (0.37 in.). This maximum, however, is still only about 60 percent of the stress limit specified. AASHTO M251-97 requires a minimum cover of 3 mm (0.12 in.) and a tolerance of −0, +3 mm (−0, +0.12 in.) on the cover specified by the designer. It appears that cover that is smaller or larger than the specified value will not adversely affect the performance.

Bond Stress

In all cases, the maximum bond stress occurs near the edge of the steel shim and it reasonably follows the principal strain distribution shown in Contour (g) of Figures 83 through 90. The bond stress for the perfect shim alignment is directly proportional to the shear modulus. Bearings with a higher shear

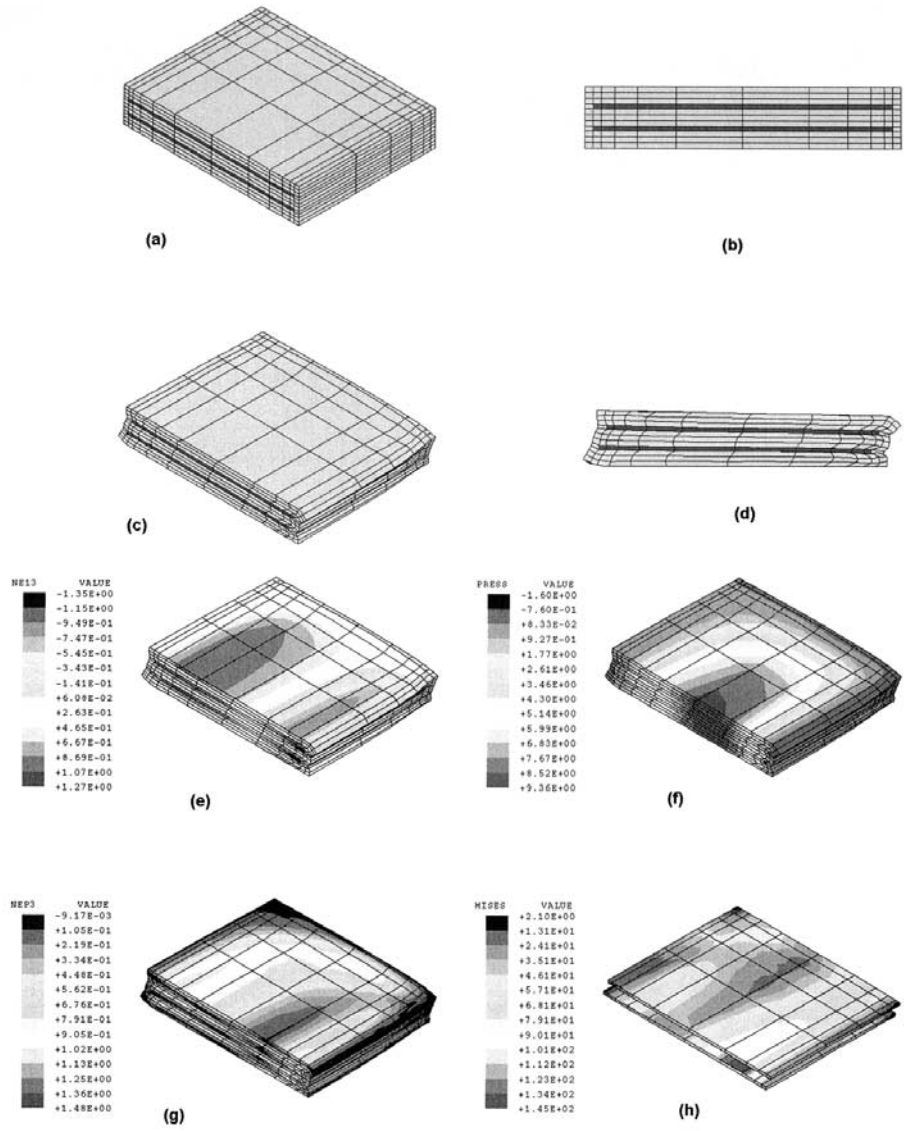

Figure 87. Deformed shapes and Key Stress Contours—NR100 Perfect Configuration-Unbonded Top and Bottom: (a) and (b) undeformed shape; (c) and (d) deformed shapes; (e) elastomer shear strain; (f) elastomer triaxial stress (MPa); (g) elastomer principal strain; (h) steel von Mises Stress (MPa).

modulus have higher bond stresses. Except for NEO200, Run 7, the maximum bond stress is insensitive to shim misalignment. For NR100, NEO100, NR200, and NEO200, the maximum increase in bond stress compared with the perfect arrangement is 3, 8, 13, and 11 percent, respectively. The maximum increase for NEO200 is 81 percent (Run 7) because there is a steep increase in the slope of the stress-strain curve at strains greater than 100 percent as noted earlier. The maximum bond stress is 82, 67, 71, and 58 percent of the specified limit for NR100, NEO100, NR200, and NEO200, respectively. This maximum stress is confined to a very small region of the bearing; the bond stress over a more major portion of the bearing is approximately 50 percent of the maximum value.

Steel Stress

The maximum steel stresses mainly result from bending of the plate near the edge of the bearing as shown in Contour (h) of Figures 83 through 90. For the perfect configuration, the maximum steel stress appears to be related to the shear modulus—the higher the shear modulus, the higher the steel stress. However, additional analyses by Kumar (2000)

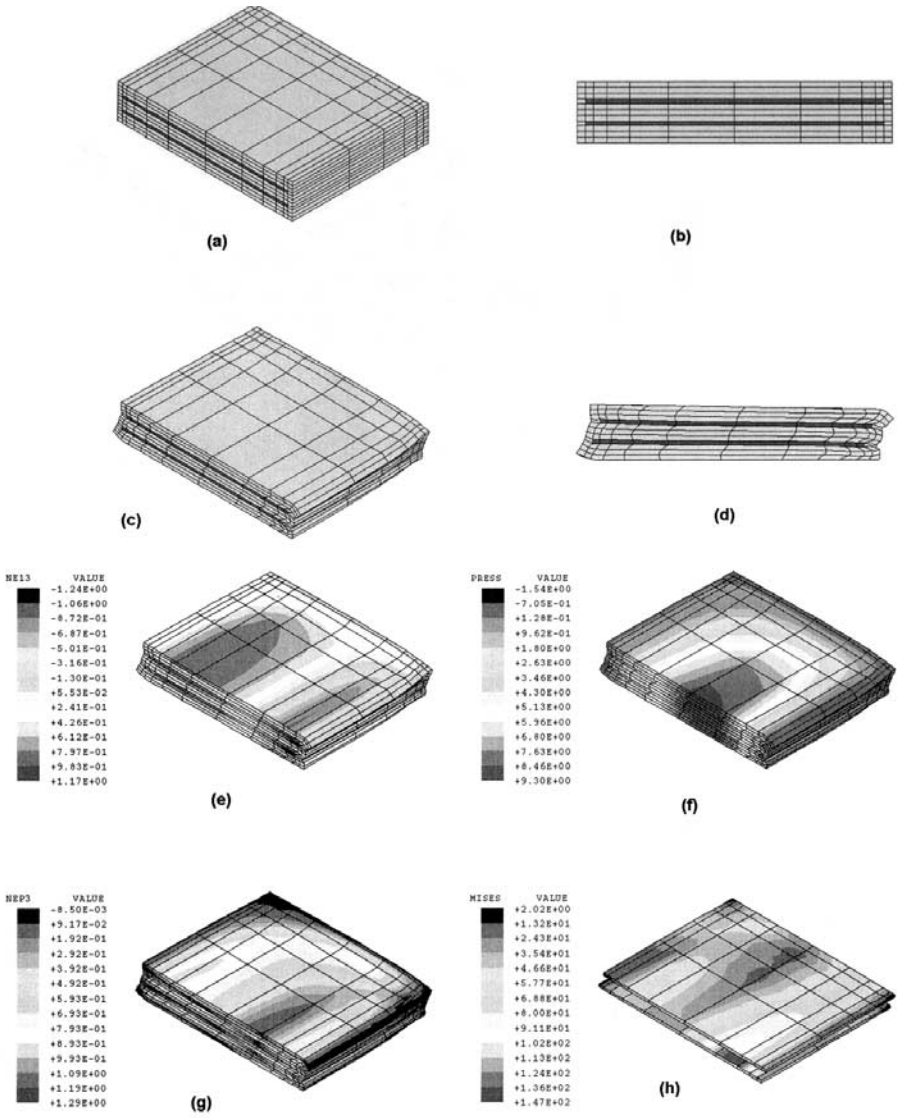

Figure 88. Deformed shapes and Key Stress Contours—NEO100 Perfect Configuration-Unbonded Top and Bottom: (a) and (b) undeformed shape; (c) and (d) deformed shapes; (e) elastomer shear strain; (f) elastomer triaxial stress (MPa); (g) elastomer principal strain; (h) steel von Mises Stress (MPa).

show that the increased steel stresses result from the fact that the compressive force applied to the higher modulus was double that for the lower modulus bearings. The average maximum stress for NR100/NEO100 is 134 MPa (19.5 ksi) and for NR200/NEO200 is 221 MPa (32.1 ksi) for the perfect configuration (see Run 15/16 of Tables 28 through 31). The AASHTO LRFD (1988) formula for minimum thickness of steel reinforcement (Formula 14.7.5.3.7-1) can be rearranged to determine the steel axial (membrane) stress (σ_r, with the factor of safety of 2 removed as follows:

$$\sigma_r = 1.5\sigma_s \frac{h_{r\max}}{h_s} \tag{19}$$

where

σ_s = compressive stress,
$h_{r\max}$ = elastomer layer thickness, and
h_s = shim thickness.

Equation 19 gives 23 and 46 MPa (3.3 and 6.6 ksi) steel stress for the NR100/NEO100 and NR200/NEO200 bearings, respectively. The maximum steel stresses are about 5 times greater than the AASHTO theoretical axial stress, but these maximum stresses are confined to small areas less than 1 percent of the plan area near the edge of the bearing. For the NEO200 bearing, the steel stress for the perfect configuration is at two-thirds of the assumed yield strength, 345 MPa (50 ksi).

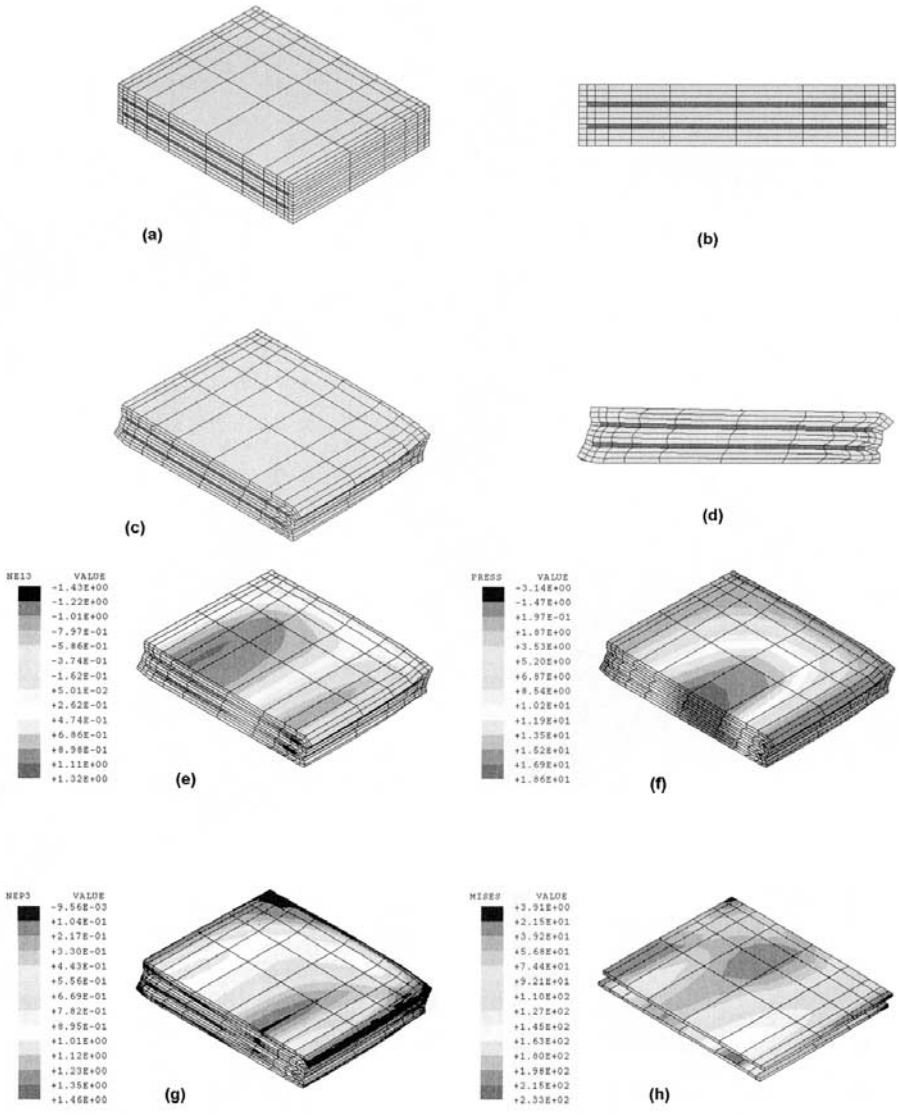

Figure 89. Deformed shapes and Key Stress Contours—NR200 Perfect Configuration-Unbonded Top and Bottom: (a) and (b) undeformed shape; (c) and (d) deformed shapes; (e) elastomer shear strain; (f) elastomer triaxial stress (MPa); (g) elastomer principal strain; (h) steel von Mises Stress (MPa).

The analysis implies that, for bearings subjected to shear and rotation, there should be a minimum shim thickness limit associated with plate bending. If the shim is too thin, the reinforcement will yield in bending and the bearing will have a permanent kink near the edge as observed in some tests (Crozier et al., 1974). A minimum 3-mm (⅛-in. or 12-gauge)-shim thickness as used in this research will usually limit the maximum steel bending stresses to prevent permanent plate deformations. The plate bending will have little effect on the function of the bearing, but it may be visually objectionable.

The shim misalignments cause significant increases of up to 50 percent of the perfect alignment stresses. The data indicate that the misalignments associated with Run 4 always give the highest steel stresses for all four materials, and for Run 1 always give the lowest steel stresses. The perfect alignment gives the second lowest stress level. A reduction in the edge cover increases the steel stresses up to 20 percent (compare Runs 11 and 15/16); an increase in edge cover has little effect. The percent change in the elastomer layer thickness at the edge of the bearing because of shim misalignment from the perfect configuration is directly related to the increase in the maximum steel stresses. For example, the 1.5-deg rotation of Run 14 changes the edge thickness of the interior layer on the compressed side from 12.7 to 18.7 mm (0.50 to 0.74 in.), a 47-percent change in the edge thickness. A similar percent change in edge thickness occurs for Run 13. The

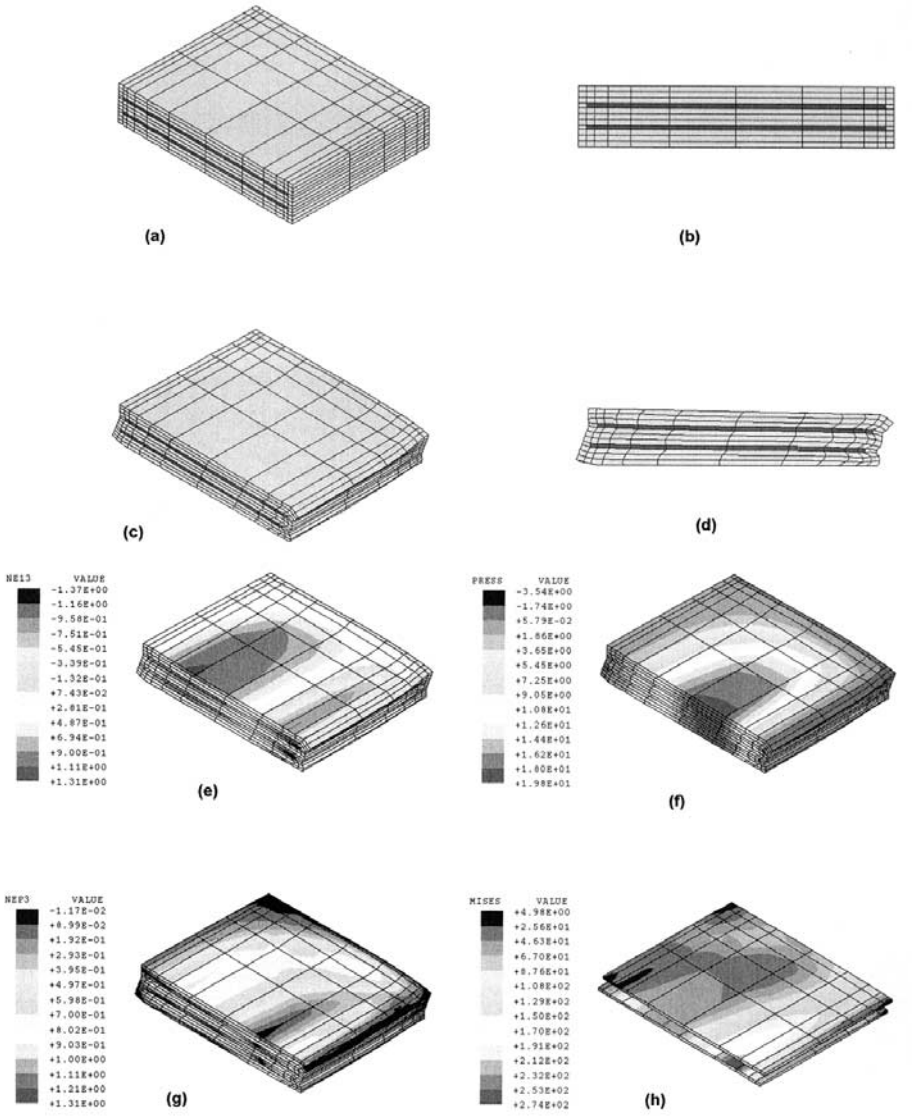

Figure 90. Deformed shapes and Key Stress Contours—NEO200 Perfect Configuration-Unbonded Top and Bottom: (a) and (b) undeformed shape; (c) and (d) deformed shapes; (e) elastomer shear strain; (f) elastomer triaxial stress (MPa); (g) elastomer principal strain; (h) steel von Mises Stress (MPa).

change in the steel stress was about 32 percent for Run 14 and 41 percent for Run 13. A vertical shift of 3 mm (0.12 in.) in Runs 9 and 10, a 24-percent change in thickness, results in a 17- and 22-percent increase in steel stress for NR100 and NEO100 bearings, respectively. Other combinations give similar results because the perfect alignment case of three equal elastomer layers is close to ideal (i.e., lowest steel stresses). Any change in thickness generally increases the steel stresses.

Unbonded Top and Bottom Bearing Surfaces

Because of slip at the contact surface, especially near the edges, an elastomer layer with one of its bearing surfaces unbonded to a steel plate will bulge more than a bearing with bonded sole plates. This additional bulging increases the vertical displacement within a layer by a factor of 1.4, based on the $\beta = 1.4$ factor for cover layers in AASHTO Design (1996). Thus, the axial stiffness of the unbonded bearing should be $3/(1.4 + 1 + 1.4) = 0.79$ times as stiff as the same bearing with sole plates (there should be 21 percent more vertical displacement in the unbonded bearing with two shims). The ratio of the average axial stiffness of the bearings with and without bonded sole plates is 0.82 for the four elastomer materials, which is close to the predicted value of 0.79. The average shear stiffness of the unbonded bearings is 0.82 that of the bonded bearings. The stiffness ratio is consistent with the reduction factor of 0.8 to 0.9 for a three-shim bearing reported

TABLE 33 Summary of static analysis results

Bearing Material (G)	Performance Variable	Minimum Value	Maximum Value	Variation From Perfect Alignment (Percent of Run 16)		Maximum Specified Limits
NR100 (0.585 MPa) (84.9 psi)	Axial Stiffness (kN/mm)	184	211	-11	+2	186-227
	Shear Stiffness (kN/mm)	0.96	1.01	-0	+5	0.86-1.05
	Rotational Stiff. (kN-m/deg)	1.13	3.22	-53	+33	No constraint
	Shear Strain	1.60	1.80	-9	+2	< 6
	Principal Strain	1.71	1.85	-4	+3	< 2
	Tensile Stress (MPa)	1.25	2.26	-38	+11	< 3.5
	Bond Stress (MPa)	0.90	1.08	-14	+3	< 1.31
	von Mises Stress (MPa)	114	206	-14	+56	< 345
NEO100 (0.590 MPa) (85.7 psi)	Axial Stiffness (kN/mm)	187	217	-11	+4	190-232
	Shear Stiffness (kN/mm)	0.95	1.01	-1	+5	0.86-1.05
	Rotational Stiff. (kN-m/deg)	1.41	3.53	-52	+31	No constraint
	Shear Strain	1.56	1.72	-8	+2	< 6
	Principal Strain	1.55	1.68	-4	+4	< 2
	Tensile Stress (MPa)	1.33	2.14	-32	+9	< 3.53
	Bond Stress (MPa)	1.03	1.21	-8	+8	< 1.81
	von Mises Stress (MPa)	117	210	-15	+53	< 345
NR200 (1.21 MPa) (175 psi)	Axial Stiffness (kN/mm)	341	389	-10	+2	342-418
	Shear Stiffness (kN/mm)	1.81	1.91	-0	+5	1.64-2.0
	Rotational Stiff. (kN-m/deg)	2.07	6.29	-55	+36	No constraint
	Shear Strain	1.60	1.75	-8	+1	< 6
	Principal Strain	1.58	1.75	-5	+5	< 2
	Tensile Stress (MPa)	2.64	4.27	-31	+11	< 7.2
	Bond Stress (MPa)	1.92	2.42	-10	+13	< 3.4
	von Mises Stress (MPa)	177	316	-16	+50	< 345
NEO200 (1.25 MPa) (182psi)	Axial Stiffness (kN/mm)	396	453	-10	+3	395-483
	Shear Stiffness (kN/mm)	2.06	2.20	-1	+6	1.87-2.28
	Rotational Stiff. (kN-m/deg)	4.29	8.51	-38	+24	No constraint
	Shear Strain	1.43	1.57	-7	+2	< 6
	Principal Strain	1.31	1.68	-4	+23	< 2
	Tensile Stress (MPa)	2.63	3.96	-33	+1	< 7.5
	Bond Stress (MPa)	2.17	4.30	-9	+81	< 7.4
	von Mises Stress (MPa)	195	335	-16	+44	< 345

1 MPa = 145 psi, 1kN = 0.224 kips, 1 mm = 0.039 in., 1m = 3.28 ft

by Hamzeh et al. (1995). The reduced stiffness is caused by the roll at the edge for unbonded bearings—compare deformed shapes (d) of Figures 83 and 87. The rotational stiffness and the internal stresses and strains in the rubber are all smaller in an unbonded bearing. The stresses in steel laminates are approximately 10 percent higher in the NR100, NEO100, and NR200 unbonded bearings and 18 percent higher in the NEO200 bearing. However, the zone of high steel stress is much smaller in the unbonded bearings shown in Contour (h) of Figures 87 through 90 than in the bonded bearings of Figures 83 through 86. Overall, an unbonded elastomeric bearing is a better design choice because of its lower stresses and lower shear and rotational stiffnesses.

Development of Shim Misalignment Limits

Based on the interaction of Equation F1 with appropriate coefficients in Table F2 of Appendix F of the research team's final report, the combined limits on vertical misalignment (X1), edge cover misalignment (X2), and shim inclination (X3) were determined so that the resulting performance parameter just meets the constraints tabulated in Table 27. The minimum value of each misalignment from all eight performance parameters for all four materials was determined and plotted. Usually the axial stiffness constraint ±10 percent, the shear stiffness constraint ±10 percent, or the steel stress limit F_y = 345 MPa (50 ksi) controlled the minimum misalignment limit. Figure 91 shows the allowable shim misalignments applicable to satisfy all the performance constraints for all four types of bearings (i.e., NR100, NEO100, NR200, and NEO200) studied.

The limiting surface equation defining the interaction among the three misalignment variables is shown in Figure 91 where v, y, and θ are the absolute values of vertical misalignment (mm), horizontal misalignment (mm), and rotation of the shim, respectively. If two misalignments are known, their absolute values can be used in this equation to get the maximum allowable value (±) of the third misalignment. Note that these misalignments are measured from the perfect configuration. For example, if the perfect cover is 6 mm (0.24 in.), a horizontal misalignment of 3 mm (0.12 in.) means that

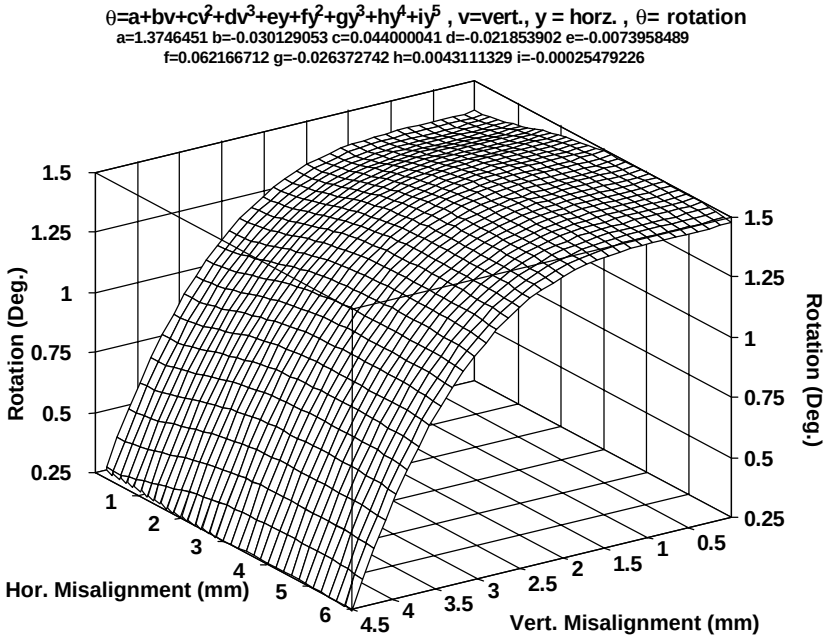

Figure 91. Allowable misalignments of laminate in elastomeric bearings.

the cover on one side is 3 mm (0.12 in.) while on the other side the cover is 9 mm (0.35 in.). If the perfect layer thickness is 12.7 mm (0.50 in.), a vertical misalignment of 3 mm (0.12 in.) means that the layer thickness can be 9.7 or 15.7 mm (0.38 or 0.62 in.). Similarly, a rotation misalignment of 1 deg means that shims can have an angle of ±1 deg from the horizontal during the molding process. Figure 91 shows that the effect of horizontal misalignment on the performance is small. By eliminating the horizontal misalignment variable and converting the shim inclination from degrees to radians, the following conservative equation can be used to define shim-tolerance limits in AASHTO:

$$\theta \le 0.024 - 0.001\left(0.55v - 0.77v^2 + 0.38v^3\right) \qquad (20)$$

where θ (radians) and v (mm) are absolute values. If the specified elastomeric layer thickness is h_r, the bearing length is L, and H_1 and H_2 are the measured thicknesses at the two ends of the layer, then $v = |h_r - 0.5(H_1 + H_2)|$ and $\theta = |(H_1 - H_2)/2L|$ for interior layers and $\theta = |(H_1 - H_2)/L|$ for top and bottom layers. From Equation 20, the maximum inclination of a shim would be 0.024 (2.4 percent). Figure 91 and Equation 20 can be used for other bearing geometries (Kumar, 2000) provided that the minimum elastomer layer thickness $H_2 \ge 5$ mm (3/16 in.). A simpler but more conservative expression

$$7.5\theta + \frac{v}{h_r} \le 0.35 \quad \text{provided } \theta \le 0.02 \qquad (21)$$

could also be used to define shim tolerance limits.

In general, the tolerances given in Table 2 of AASHTO M251-97 are well below the laminate misalignments that affect the performance of the bearings. Equation 24 indicates that greater tolerances can be permitted without affecting performance. The existing AASHTO layer thickness tolerance (Figure 1), ±20 percent of the design value but no more than ±3 mm (1/8 in.) should be replaced by Equation 21. The current 20 percent of design limit controls the tolerance for specified layer thicknesses of 15 mm (0.59 in.) or less. Given that elastomeric layer thicknesses less than 6 mm (1/4 in.) are not very practical the 20-percent limit varies the tolerance between 1 and 3 mm (0.05 to 0.12 in.). Because of the cover, it is difficult to measure and locate the edge of each shim precisely, so it is doubtful that any measurement of layer thickness could be accurate to better than ±1.5 mm (1/16 in.). Therefore it is recommended that the same tolerances be applied to all bearings. The minimum layer dimension of 5 mm (3/16 in.) will control the permitted shim misalignment for bearings with small specified layer thicknesses. It is recommended that the current tolerance for edge cover be maintained at –0, +3mm (+1/8 in.).

Evaluation of the Peel Test

As shown in Figure 92, the bond integrity at the interface of the rubber layer and the steel laminate is governed by a tangential stress, t, and a normal stress, n. A tensile normal stress is detrimental to the metal-to-rubber bond, while a compressive normal stress strengthens it. For the elastomeric bearings analyzed in the present study, the normal stresses at all loca-

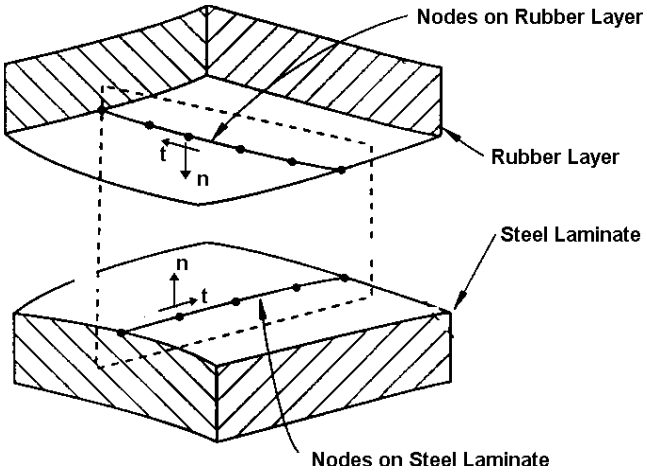

Figure 92. Bond stress at the interface of rubber layer and steel laminate.

tions at the bond line were always compressive. The maximum tangential stresses, tabulated in Table 33 as Bond stress, were well below the failure limit for the respective bearing.

AASHTO specifications require a peel test, ASTM D429-82 Method B modified, shown in Figure 93(a), to assess the integrity of the metal-to-rubber bonds. Note that this test is a measure of bond failure in tension and, therefore, is not representative of the loading mode experienced by elastomeric bearings as shown in Figure 92. The shear test shown in Figure 93(b) is more applicable for the elastomeric bearings. The experimental data shown in Figure 82 were obtained using a similar test shown in Figure 93(b). In these figures, average shear stress, which can also be interpreted as average bond stress, is plotted against average shear strain. Note that the experimental data extend above the maximum allowable bond stress tabulated in Table 33. No bond failure was observed during these tests, implying that the allowable bond stresses tabulated in Table 33 are adequate to address failure due to delamination at the bond line. Based on these analytical and experimental results, a dual-lap shear bond test method is presented in Appendix C of this report that is more appropriate than the peel test currently stipulated. The recommended test is conservative because no helpful compression force is applied for simplicity.

CRACK GROWTH

The study of fatigue crack growth had two objectives. The principal objective was to determine the rate of growth of pre-existing surface cracks under repeated mechanical loadings and, thereby, to ascertain the significance of ozone-induced surface cracking. The secondary goal of the analytical study was to evaluate the likely behavior of debonds, whose origins would lie in the manufacturing process. Some investigators (Stevenson and Lindley, 1982; Stevenson, 1983) have questioned the importance of ozone in the fatigue of elastomers when compared with physical tearing at the crack tip. Others (Lee and Moet, 1993; Selden, 1998; Young, 1986) have reported a significant increase in crack growth rate resulting from ozone. Although the conclusions made from these investigations are useful in understanding the fatigue behavior of elastomers in general, they are probably insufficient in indicating the behavior of an ozone-induced surface crack in an elastomeric bridge bearing. All of these investigations involved bonded rubber blocks, test coupons, or other configurations that differ considerably from a laminated bridge bearing. In addition, these investigations did not consider loading conditions similar to those of a bridge bearing. Therefore, because of these differences in specimen design and loading conditions, a crack growth study was undertaken to evaluate the fatigue behavior of a real bridge bearing with ozone-induced surface cracks.

The exact quantification of fatigue life cannot be made without the experimental determination of material parameters, the cost of which is well beyond the scope of the present project. Nor was it possible to analyze all classes of bearings. However, by making, at every point, conservative assumptions and obtaining predictions for the fatigue life of a typical bearing design that are orders of magnitude in excess of any realistic requirements, the research team concluded that a more detailed effort in this matter is not warranted.

Method of Analysis

The analytical studies used a single bearing design that is referred to as the model bearing. The model bearing design is

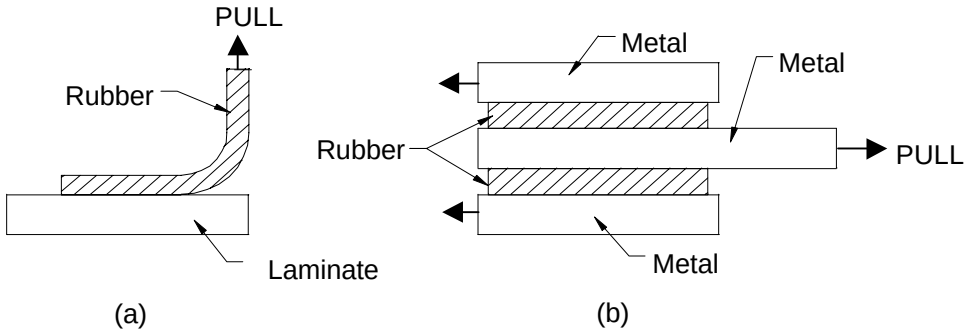

Figure 93. Peel test and shear test to measure bond strength.

one of the designs used in the experimental phases of the project and is typical of reinforced bearings. All analyses were done on the model bearing, which is shown in Figure 4. The edge cover was 6.4 mm (0.25 in.). The model bearing contains two steel reinforcing plates and does not have sole plates. The rubber is a medium-filled (50phr carbon black) natural rubber compound with a nominal shear modulus of 6.9 MPa (1000 psi). The stress-strain response of the model in shear is shown in Figure 82 by the open circles. The material response is very similar to the measured shear stress-strain behavior of NEO100.

In order to represent the true behavior of the bearing and thus obtain accurate values of crack growth, the application of proper loading conditions was necessary. All bridges experience a constant compressive load (dead load) resulting from the weight of the bridge structure. Also, the bridge experiences a cyclic compressive load (live load) resulting from traffic. A 107 kN (24 kips) live load and a 200 kN (45 kip) dead load was calculated (Collingwood, 1999) based on a simple static analysis using only large trucks with a typical axle weight of 142 kN (32 kips). These two compressive loads account for the compressive loading on the bearing. In addition to compression, the bridge undergoes two types of shear loading resulting from thermal expansion of the girders. The first involves a yearly maximum shear deformation resulting from seasonal changes and the second involves a daily maximum deformation resulting from daily temperature changes. The AASHTO specifications specify that the maximum shear strain in a bearing be no greater than 50 percent, which is assumed to occur once a year. The maximum daily shear strain was determined from a calculation of thermal expansion and contraction of the girders of a typical bridge due to daily temperature changes. The calculation was made using a worst-case scenario for girder length and change in temperature. The value of shear strain obtained was 20 percent. The final loading condition that the bearing undergoes is a rotation resulting from bending in the girders. This rotation is usually on the order of a few degrees. Rotation was not considered in this research. A typical highway bridge has on the order of 2 million heavy trucks pass over each year; thus, a frequency of 2 million was assigned to the live load on the bridge. The maximum yearly shear (50 percent) obviously occurs once each year and the daily shear (20 percent) occurs 365 times per year. The yearly loading spectrum used in the crack growth analysis is summarized in Table 34.

A two-dimensional, finite element model was used to model a typical bearing based on plane strain assumptions and stress distribution results of a preliminary three-dimensional analysis. Submodeling was used to capture the behavior of the bearing in critical areas (i.e., crack regions). Crack trajectories were predicted and used in subsequent crack growth models to determine tearing energies. The tearing energies calculated for each crack length were then used to predict the time necessary for a surface crack to grow 40 percent through the depth of the cover (rubber beside shims). The analytical study consisted of a sequence of finite element analyses of the typical model bearing design. Ten crack locations along the edge were initially investigated. The critical crack location, Crack 2, as shown in Figure 94, was identified by analyzing surface cracks at the various locations. The model bearing, including the critical surface crack, was analyzed subject to the loading patterns given in Table 34. Compressive loading was most significant for Crack 2. It was determined that the shear loading caused more tearing as the crack approached the bottom corner of the bearing. Based on these results, the bottom crack was chosen as the second critical location. These cracks were used in the fatigue analysis and were identified as Crack 1 (bottom crack) and Crack 2 (middle crack). Figure 94 shows the two surface crack locations chosen for the fatigue analysis.

TABLE 34 Fatigue loading spectrum

Mean Compression (kN)	Cyclic Compression (kN)	Mean Shear Strain (%)	Cyclic Shear Strain (%)	Frequency (cycles/year)
200	107			2×10^6
200		0	50	1
200		0	20	365

Crack Growth Analysis

The method of predicting fatigue crack growth utilizes fracture mechanics principles for which the key parameter (i.e., the tearing energy available to drive the crack growth) is calculated using finite element analyses. This scheme has been developed and validated through the research effort "International Fatigue Life Project" (IFLP). The IFLP was a joint industry-funded project of the Materials Engineering Research Laboratory (MERL) of Hertford, England. The IFLP included the development of finite element software, materials testing, and component fatigue testing (including several model elastomeric bearings). The fracture mechanics basis for the research team's method is that described by Stevenson (1983). For the finite element analyses, the research team used the software package, FLEXPAC, developed as part of the IFLP, and the commercially available package, ABAQUS®. A detailed description of the finite element analyses procedures is given in Collingwood (1999).

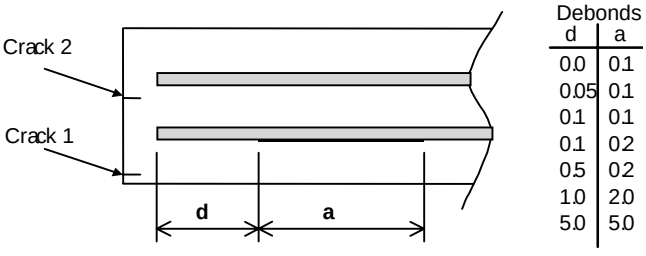

Figure 94. Critical crack locations.

The relevant results of the finite element analyses are the values of *T*, the tearing energy for a given crack geometry subject to a particular pattern of loading. A fatigue crack growth model relates the tearing energy to the rate of crack growth. The calibration of such a model for a given rubber compound requires extensive testing of repeated loadings. Many tests are needed—the magnitude of mean stress as well as stress amplitude must be varied. Individual tests may take weeks to perform. A fatigue model determined in the IFLP for a compound similar to one of the present study's test bearings is shown in Figure 95. The rate of crack growth, *dc/dN*, in millimeters of crack length extension per cycle of loading, is shown as a function of the tearing energy, *T*, in kilojoules per square meter. The odd axes values result from the conversion from the original U.S. units. Curves are given for several values of *R*, the ratio of maximum-to-minimum tearing energy in a cycle of loading. It can be seen that the rate of crack growth is very much smaller when the crack is not completely unloaded between maximum loadings (i.e., when *R* is greater than zero). This behavior is characteristic of strain-crystallizing rubbers (e.g., natural rubber). This aspect of the fatigue behavior of natural rubber is important in bridge bearings. Clearly, the dead load, which is responsible for a large part of the tearing energy seen by a surface crack, is not cyclic in nature. Thus the value of *R* is considerably greater than zero, typically 0.3 to 0.4 in the present study. Fatigue data for large *R* values are scarce because of the long times necessary for such tests. The research team used $R = 0.20$, the largest value for which data are available. Extrapolation of the material data to larger values is not usually reliable and the research team chose not to do so. The use of the smaller value of *R* adds to the conservativeness of the calculations.

Fatigue crack growth calculations were made by integrating the rate of crack growth as determined by the crack growth model and the calculated values of tearing energy at various crack lengths as the crack extends. The path along which the crack growth is modeled is selected by the analyst. In this study, perturbations in the selected path were examined and the path increment having the largest value of tearing energy was used.

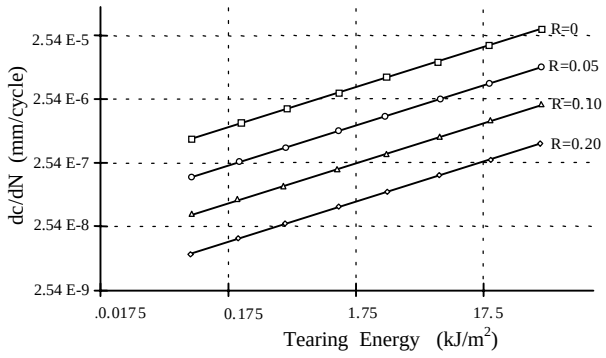

Figure 95. Fatigue model for the elastomer.

Fatigue Crack Growth

The finite element modeling of this phenomenon was achieved by first modeling the global model with a sufficiently fine mesh to capture the general behavior of the bearing. Then, a much more detailed mesh of the critical regions was created in order to study those regions using submodeling techniques. To analyze the critical crack regions, a submodel was created with an initial crack length of 0.51mm (0.02 in.). The incremental value of crack growth for each crack studied was also chosen as 0.51mm (0.02 in.). Once the analysis of the initial crack increment was finished, the strains in the elements at the crack tip were examined to determine the new direction for crack growth. This analysis continued until a crack depth of approximately 3 mm (0.12 in.) was reached.

Two fatigue calculations were made for each crack—one with a stress-softening model included in the fatigue calculation and the other without. Softening is a phenomenon occurring in elastomers that causes the material to relax after the first few cycles of loading. The predicted crack growth history is shown in Figure 96. It is seen that the critical surface crack grows slowly, reaching a depth of 2.5 mm (0.1 in.) in approximately 1200 years for the more conservative, unsoftened model. This is less than 40 percent of the depth of cover. If the softening of the material because of load cycling is included in the model, then the crack growth is slowed and even longer life is predicted. It is concluded that the growth of surface cracks because of fatigue loading is not a realistic concern. In addition, several crack growth scenarios were considered to supplement the primary study relating to surface cracks. Given that AASHTO specifications allow cracks larger than the initial cracks that were considered in the surface crack study, cracks with greater depth were analyzed. The results showed that the rate of crack growth decreases as the crack grows through the cover. The time necessary for an initial crack with a depth of 3 mm (0.12 in.) to grow to 4 mm (0.16 in.) is approximately 800 years. This seems to indicate that the high level of compression in the region bounded by the shims impedes crack growth originating from the bearing surface. Based on these results, further studies of the growth of surface cracks are not warranted.

Delamination Study

Delamination is a separation of the elastomer from the metal shim. The propagation of delamination typically occurs as a cohesive failure in the elastomer adjacent to the bond rather than a failure of the bond itself. It is reasonable, therefore, to utilize the same method of analysis and the material data that are used to predict fatigue growth of cracks in the bulk elastomer. The origin of delamination is a region of weak or totally absent bond over some portion of the interface. In this study, calculations of crack growth rates were made for several hypothetical debonds such as might result from manufacturing defects. The debonds studied were located along the lower sur-

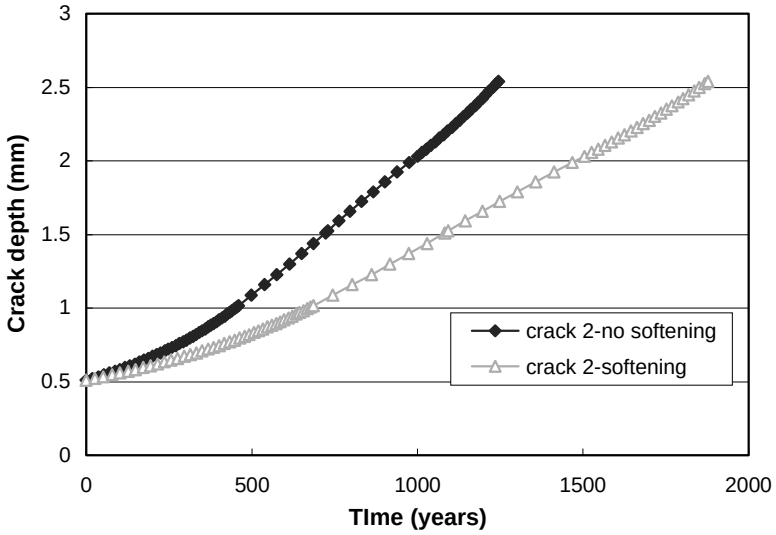

Figure 96. Fatigue life for Crack 2.

face of the lower shim in the two-shim design as shown in Figure 94. This position was selected because it is the location of the maximum tensile strain in the finite element model without debonds. The rate of growth for debonds near the end of the shim is greater than that for debonds near the middle of the bearing. The debonds used in this study are defined by their length, *a* in millimeters, located a distance, *d* millimeters, from the end of the shim in Figure 94. The elastic material model used in this study is that given for NR200 in Figure 82.

The cyclic loading patterns given in Table 35 were applied to the finite element model. The pairs of loads in each pattern were chosen to produce large values of tearing energy along with a small *R* ratio. Because the frequency of load pattern 3 is orders of magnitude greater than any other loading, the growth resulting from this pattern will overwhelm all other loadings unless the tearing energy for the other loadings is orders of magnitude larger than that for pattern 3. Two-dimensional (plane strain) finite element analyses of various crack configurations were performed. In addition to the debond configurations, an edge crack of depth 5 mm, labeled Crack 2 in Figure 94, was also subject to the alternating loads of Table 35. The resulting values of tearing energy for the edge crack and for a typical debond of the same dimension (d = 5 mm and a = 5 mm) are shown in Table 36. Qualitatively similar results were obtained for all debond analyses.

From Table 36, three significant observations can be made. First, the tearing energy for loading pattern 3 compares with that for all other loadings. The implication is that only this dom-

TABLE 35 Cyclic loading spectrum

Pattern No.	Minimum		Maximum		Frequency (cycles/yr)
	Comp. Load (kN)	Shear Strain (%)	Comp. Load (kN)	Shear Strain %	
1	200	0	307	50	1
2	200	0	307	20	365
3	200	0	307	0	2×10^6
4	307	50	200	-50	1
5	307	20	200	-20	365

TABLE 36 Tearing energy values

Pattern No.	Edge Crack T (kJ/m^2)	Edge Crack R	Unbond T (kJ/m^2)	Unbond R
1	0.278	0.26	0.211	0.14
2	0.212	0.31	0.187	0.16
3	0.149	0.40	0.391	0.15
4	0.109	0.71	0.192	0.21
5	0.021	0.85	0.086	0.60

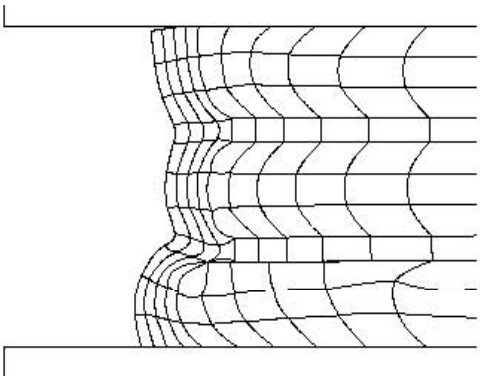

Figure 97. Crack growth initiating at a delamination.

inant mode need be considered in prediction of crack growth. The second observation is that for this dominant loading pattern, the debond has more than twice the tearing energy of the edge crack. Doubling the value of the cyclic tearing energy value increases the rate of crack growth by a factor of approximately 1.5. The third observation is that the *R* ratio for the debond is, for every load combination, significantly less than that of the edge crack. Using the data represented in Figure 95, the research team conservatively estimates that an *R* ratio of 0.15 will produce a crack that grows 10 times faster than a similarly loaded (equal tearing energy values) one with *R* equal to 0.4. Therefore, it is recommended that delamination flaws be strictly avoided. The configuration of a delamination that has grown to the edge of the shim is shown in Figure 97.

CHAPTER **4**

APPLICATIONS

RECOMMENDED REORGANIZATION OF AASHTO SPECIFICATIONS

Test methods and tolerances for elastomeric bearings appear in the two AASHTO bridge construction specifications (Standard and LRFD versions) and the AASHTO M251-97 Materials & Testing Specification. Although all three of these documents have essentially the same requirements, the few differences among them make it difficult for some manufacturers and testing agencies to comply with them. It is not clear which of the documents (construction or testing) take precedent. The following are the substantial differences among the documents for Construction-Standard, Construction-LRFD, and Materials & Testing, identified as CS, CL, and M, respectively:

1. Every bearing is subjected to the short-term compression test in CS and CL at 1.5 times its rated service load; every fifth bearing is subjected to the same test in M but at 1.5 times its maximum design load.
2. A compressive strain test at maximum design load (strain must be less than 0.10) is required by M, no such test is required in CS or CL.
3. In CS and CL, the peel test is ASTM D429-82, Method B; in M, the ASTM D429-82, Method B test is modified.
4. An additional low-temperature, full-size shear test is required in M that is not required in CS and CL.
5. The duration requirements in the heat resistance test are different for natural rubber compounds in M and in CS and CL.
6. The 15-hr compression test is only required for bearing lots that have been designed by Method B in CS and M; the test is not required if Method A is used; in CL, there is no mention of design methodology, so the test is required for all lots.

There are two principal reasons for the differences among the various documents: (1) two different AASHTO subcommittees are responsible for the construction specification and the material specification and (2) the two design specifications (Standard and LRFD) issue almost yearly interims that result in oversights and printing errors.

It is recommended that all requirements related to the manufacturing and testing of elastomeric bearings and their materials be under the purview of the AASHTO materials committee and contained in AASHTO M251-(year). Requirements in the construction specification should be related to the installation of the bearing after it is delivered (e.g., the condition of the bearing contact surfaces). This approach will eliminate all the inconsistencies among the three documents. Draft changes to the sections related to elastomeric bearings in the LRFD Construction Specification (Standard would be similar) are given in Appendix D of this report. A revised AASHTO M251 document is given in Appendix E of this report and incorporates the testing changes recommended above.

RECOMMENDED CHANGES TO AASHTO SPECIFICATIONS

Design Specification

The current AASHTO test matrix shown in Figure 1, in which there are two levels of tests, has evolved because the *AASHTO Bridge Design Specifications* have permitted two different design levels, Method A and Method B, since 1992. Bearings designed by Method A have lower permitted compressive stresses and Level I tests apply; the higher compressive stresses permitted by Method B require compliance with both Level I and Level II test criteria. The method used in design must be shown on the plans so that the proper test level can be established. Given that the bearing manufacture is not altered by the design method, the degree of sophistication implied by the dual test levels appears unwarranted in lieu of the relative low cost of the bearings coupled with their excellent performance record prior to 1992. Therefore, the following general changes to the *AASHTO Bridge Design Specifications* are recommended in order to streamline the testing requirements and remove potential conflicts:

1. **Specify only one design method (e.g., Method B).** Engineers can always use lower compression values if desired, but extensive experimental research has shown that elastomeric bearings with steel laminates can support loads 6 or more times the current design values.
2. **Specify the bearing material by shear modulus only and eliminate hardness requirements.** The requirement that shear modulus and hardness values fall within certain specified limits would reject half the bearings used in this project (NEO150, NEO200, and NR200) for a reason that has nothing to do with bearing performance.

3. **Eliminate the restriction on the use of higher stiffness materials for steel-laminated bearings.** The range of stiffnesses should not be different for plain and steel-laminated bearings.

The shear modulus is determined from the stress-strain response of the elastomer, which basically controls all stiffnesses and internal stresses within the elastomer. All theoretical analyses use the stress-strain curve, not hardness, to represent the material. Except for creep, the AASHTO bridge design formulations for bearings require the use of shear modulus. Therefore, in a performance-based specification, the shear modulus must be specified and then monitored for compliance. Currently, the durometer is required to fall within the range of 50 to –60 for steel-laminated bearings, so instead, a range of shear moduli could be given. However, the approach adopted by Eurocode is suggested wherein one of three grades (shear moduli) of material is specified for use in bridge bearings. The three durometers in Table 14.7.5.2-1 of AASHTO LRFD would be replaced by the three recommended shear modulus grades as shown in Table 37 for steel-laminated elastomeric bearings. Tests results (secant shear modulus at 50-percent strain) would have to fall within 15 percent of the specified shear modulus. The engineer of record can specify higher shear moduli for plain pads. The three recommended shear moduli in Table 37 based on 50-percent strain correspond to 0.70, 1.0, and 1.4 MPa (100, 150, and 200 psi) shear modulus based on the 25-percent strain used in the ASTM 4014-89-Annex A quad shear test. The ratio of the shear modulus at 25-percent and 50-percent strain from full-size bearings with bonded sole plates and from the stress-strain curves in Figure 82 from the creep shear specimens is approximately 20 percent, which accounts for the difference. For bearings without bonded sole plates, 0.9*G* should be used in all formulations and calculations that contain *G* to account for the reduced stiffness noted in Chapter 2 and resulting from the effect of edge roll and edge slip in such bearings.

TABLE 37 Specified shear modulus, *G*, and maximum creep

	Specified shear modulus @ 23°C in MPa (psi)		
	0.55 (80)	0.80 (120)	1.10 (160)
Maximum Creep deflection @ 25 years divided by instantaneous deflection	0.25	0.35	0.45

M251 Materials and Testing Specification

Based on the research presented in Chapters 1, 2, and 3, the tests listed in Table 38 are recommended for the elastomeric material and the finished bearing in a lot.

The following current tests have been eliminated:

1. Hardness (ASTM 2240-91),
2. Heat resistance–aging (ASTM D573),
3. Compression set (ASTM D395-89),
4. Ozone resistance (ASTM D1149),
5. Low-temperature full-scale shear test,
6. ASTM D1043-92 for instantaneous stiffening,
7. Bond strength–peel test (ASTM D429-82, Method B), and
8. Long term compression–15 hr.

TABLE 38 Recommended test matrix

Elastomer or Bearing Property	Test Method
Tensile Strength	ASTM D 412
% Elongation	ASTM D 412
Creep (Stress Relaxation)	New Test –Appendix D
Shear Bond	New Test – Dual Lap Shear Test - Appendix D or Appendix A modified or Full Scale
Shear Modulus @ 23°C	ASTM D 4014-Annex A modified (quad shear test), or New Test - Inclined Compression Test (Appendix A) or New Test - Dual Lap Shear Test Apparatus (Appendix D)
Short Term Compressive Load Test @ 1.5 times the maximum design load	
Compressive Strain (optional)	New Test – Appendix C
Low Temperature Brittleness	ASTM 746 – Procedure B
Low Temperature Stiffening at Temperatures and Strains Specified by Low Temperature Grade 0,2,3,4,5.	ASTM D 4014-Annex A modified (quad shear test), or New Test - Inclined Compression Test (Appendix A) or New Test - Dual Lap Shear Test Apparatus (Appendix D)

These changes are reflected in a revised draft of the *AASHTO M251 Specification* given in Appendix E of this report. In the following sections, the reasons for eliminating or retaining each of these tests will be reviewed.

Tests To Be Eliminated from AASHTO M251

Hardness. In previous sections of this report, two main reasons have been expressed for eliminating hardness: (1) hardness cannot be directly tied to bearing performance and (2) its continued use, within a design specification now based on shear modulus, only causes confusion. In the past, a single allowable maximum compressive stress was used for all bearings, so requiring the elastomer hardness to fall within a particular range was a simple way of maintaining consistency in performance. The current design specifications (AASHTO Bridge, Eurocode) are now more sophisticated with the allowable compressive stress related to the magnitude of the shear modulus. Because it is doubtful that AASHTO will go back to a single stress approach, hardness should be eliminated.

Heat Resistance. In Chapter 2, Aging, the experimental evidence presented shows that the change in shear modulus over time would be insignificant for typical bridge bearings, which are very bulky products loaded mainly in shear, compared with the ASTM D573 very thin specimen loaded in tension. Field studies have also noted that the important bridge bearing elastomer properties do not change significantly, even after decades of use. The result of this ASTM test has no effect on the performance of the bearing in service and more legitimate test methods for predicting aging presented in Chapter 2 show that a 10-percent change in the shear modulus would generally take hundreds of years for even a small bearing. Therefore, heat resistance (aging) tests are unnecessary.

Compression Set. The compression set is essentially a measurement of recovery after the removal of an applied stress or strain, so it cannot be used to address creep or relaxation. The ASTM D395-89 set test is more suitable for applications such as seals where recovery of deformation may be important, rather than bridge bearings were creep is more important. So, for bridge bearings, the test is more of a quality control test because the results are sensitive to cure. A stress relaxation test developed in Chapter 2, which is also sensitive to cure, can give a direct measure of long-term creep deformation. Given that this new creep test (Appendix C of this report) gives a direct measure of one of the important performance parameters, the set test is no longer needed.

Ozone Resistance. The crack growth studies show that any edge surface cracks will not grow significantly during the service life of the bridge. This new information, coupled with the previous work of other researchers discussed in Chapter 1, warrants removal of the ASTM D1149 test requirement. This action will have an important side effect. Rubber suppliers will no longer have to add excessive antiozanant wax fillers to the compound in order to pass the ozone test. These waxes bloom to the surface forming a viscous layer that has caused serious slip problems.

Low Temperature Full-Scale Shear Test. The performance criterion for this test, as discussed in Chapter 1, does not have a rational basis. There is a different criterion for natural rubber and for neoprene. AASHTO M251-97 states that the test is applicable to 50 durometer material, yet is required for elastomers with 50 to 70 hardness with no change in the criterion. The maximum permissible 0.83 MPa (120 psi) shear modulus after 4 days of conditioning at −29°C is less than the room temperature G of many elastomers. In addition, the test, which is conducted in an open environment and not a freezer, requires a 15-min wait after reaching the required strain level—this will significantly change the bearing temperature as illustrated in Figure 17. The bearing can be exposed to room temperature for up to 30 min according to the test requirements. This test must be removed and replaced with a more rational shear modulus test.

ASTM D1043-92 for Instantaneous Stiffening. The test procedure as outlined in Chapter 1 assumes a linear relationship between applied torque and the measured angle of twist as represented by Equation 1. This may be true for plastics, but is not valid for rubber, especially at room temperature. In this test procedure, no specified values of the applied torque or measured angle of twist are indicated. The only requirement is that the measured ϕ should fall between 10 and 100 deg. This limit will ensure that a relatively stiff material remains in the elastic range (small strains). For nonlinear materials such as elastomers, the value of ϕ has a significant effect on the calculated G, because G is a function of strain level for elastomers as explained in Chapter 2. The modulus is higher at low strains than at high strains. Therefore, comparison of the stiffness measured at two different angular deflections is not realistic for nonlinear materials.

Table 39 presents some typical ASTM D1043-92 test results from Grade 3 neoprene and natural rubber bearings tested by a commercial laboratory. Note that the low temperature stiffness of specimens 3, 4, and 5 is less than the room temperature stiffness. This occurs because the stiffness was determined at different strain levels. As a result, the current ASTM D1043 test procedure is invalid and inappropriate to determine instantaneous stiffening of elastomeric bearings at low temperatures. The room temperature G derived from Equation 1 is more than 10 times higher than the G from the certified report (ASTM D4014-89). A rational way of implementing this test is to obtain G versus ϕ curves for a specified range of ϕ (e.g., from 20 deg to 200 deg) at all test temperatures. Then, the room temperature stiffness and the cold temperature stiffness should be calculated at the same ϕ from the curves generated. However, the control of angular deflection is very difficult in this test. In addition, the maximum strain that can be achieved with this test is limited to a value when angular deflection is 360 deg. For a specimen of 1.75 + 0.25 + 0.073 in., the corresponding shear strain is 26 percent,

TABLE 39 Typical results for elastomeric bearings

Spec	Dimensions (in.)	Temp (°F)	Load, F (gr)	Rotation,θ (deg)	Stiffness (F/θ)	G from Eq (1) (psi)	Certified G (psi)
1	1.75x0.25x0.073	73	5.5	32	0.172	1600	123.0
		-40	22	88	0.250	2350	
2	1.75x0.25x0.077	73	5.5	19	0.289	2315	174.8
		-40	22	34	0.647	5176	
3	1.75x0.25x0.073	73	5	12	0.417	3912	118.5
		-40	20	128	0.156	1467	
4	1.75x0.25x0.073	73	5.5	19	0.289	2717	123.0
		-40	22	125	0.176	1652	
5	1.75x0.25x0.073	73	6	12	0.500	4694	118.5
		-40	24	205	0.117	1099	

which explains why the values of *G* in Table 39 are so high. Low shear strains produce high shear moduli. The modification of this test procedure is not very feasible because the shear modulus test procedure used for crystallization can also be used for instantaneous stiffness. Therefore, it is recommended that this test be eliminated.

Bond Strength–Peel Test. The ASTM D429-82, Method B, peel test was evaluated in Chapter 3 and shown to represent the stress conditions at the elastomer-steel interface in a bridge bearing poorly. A new shear-bond test is recommended in Appendix C of this report.

15-hr Compression Test. This test is basically a 15-hr creep test. In Figure 52, the deformation of the NR100 bearing increased 14 percent from 5 min to 900 min (15 hr). There is little gained by this costly test when compared with the short-term compression test, so its elimination is recommended.

Test Methods

Tensile strength and percent elongation (ASTM D412-98a) are quality control tests and no changes are recommended, except the criterion for elongation will be established by the shear modulus of the elastomer, not hardness. Three new test methods have been developed for creep and shear bond, shear modulus, and low temperature compressive stiffness. The creep (stress relaxation) test results are to be compared with the values recommended in the AASHTO bridge design specifications reproduced in Table 37 and the shear modulus test results must be within ±15 percent of the specified shear modulus.

Shear Modulus. Four different test methods are recognized for determining shear modulus. All the methods define the secant shear modulus at 50-percent strain, unless otherwise specified. The four methods are as follows:

1. Quad shear–ASTM D4014-89–Annex A Modified. The modification requires that the secant modulus be determined at 50-percent strain instead of 25-percent strain.
2. Dual-lap shear method. The specimen and test setup are given in Appendix C of this report.
3. Inclined compression test. The test method is given in Appendix A of this report. The platen surfaces must be conditioned to control slip.
4. Full-scale shear test. This method is already cited in AASHTO M251 and no changes are recommended. In this test, the axial force and shear force are applied independently to a pair of bearings. There are no test setup details given for this method, but some sample setups are given in Muscarella and Yura (1996) and Crozier et al. (1974).

When Methods 3 and 4 are used, the experimental shear modulus should be corrected when small specimens are used as per Equation 3. The inclined compression method will be included in AASHTO M251 as Annex A, and the dual-lap method as Annex B. All these methods will give similar results as long as the secant modulus is defined at the same strain level. In all these test methods, the initial strain on the first loading cycle should be taken to 65 percent because the strain does not return to zero upon unloading.

Creep (Stress Relaxation). Currently, there is no AASHTO M251 test for creep, even though the AASHTO bridge design specification contains creep limitations as presented in Table 37. The suggested test procedures for the 6-hr stress relaxation are given in Appendix C of this report. The results of the stress relaxation test are used to calculate the estimated creep as a percentage of the instantaneous (defined as 1 hr) deflection. Given that the creep specimen is loaded to 50-percent shear strain, the shear modulus can be determined from this test also.

Shear Bond. The shear bond test can be a continuation of the creep test using the same specimen for both creep and shear bond. The tests can also be performed independently. The specimen is loaded in shear to 150-percent strain and then examined. Any rubber or bond failure observed constitutes a no-pass rating.

The shear bond test can also be performed using the inclined compression test setup. A pair of bearings in this case would be compressed until 150-percent shear strain is reached. If slip occurs during this test, the test must be repeated using platens with a smaller slope so that a higher compressive force is applied or by attaching restraining devices.

Short-Term Compressive Load Test. This test has been used for many years as a proof test for checking compressive capacity and for establishing the alignment of the laminates and any debonds by examining the elastomer bulge pattern around the perimeter of the bearing. It is a good quality control check of the bearing manufacture process. Testing every one in five bearings as currently stipulated in AASHTO M251-97 appears reasonable and is recommended. The contract documents can always specify a more rigorous proof-testing program, if desired. Bearings that have been tested for shear modulus or bond using the inclined compression or full-scale tests where the compressive force equaled or exceeded 1.5 times the maximum design load need not be subjected to the short-term compressive load test.

Compressive Strain. Prior to 1989, bearing design procedures limited the compressive strain to 0.07. This current test where the strain is limited to 0.10 is a carryover from that time. Given that compressive stress, not strain, is now controlled in the AASHTO design specifications for elastomeric bearings, this test no longer checks a performance requirement. Because there may be instances when compressive deformation is an important design limit (perhaps other types of bearings should be considered in such cases), the test is included as an option (the engineer of record must specify the test strain limit). However, research (Muscarella and Yura, 1995) has shown that compressive deformation is difficult to predict accurately, even when the properties of the material are known. The compressive load-deformation responses for the bearings used in this research were measured and compared with the stress-strain curves for 50 and 60 durometer given in AASHTO LRFD Commentary. Interpolating for the actual hardness of each of the six materials gave ratios of measured/predicted deformation that ranged from 1.21 to 1.47. The formula for calculating compressive deformation in Eurocode with a stated "accuracy in the order of ±25 percent" gave almost the same results as the AASHTO graphs. Given that current methods of calculating deflections are so inaccurate, even with known material properties, it is unlikely that a performance test for compressive deformation will provide meaningful results. In Eurocode, compressive stiffness is used for quality control, when specified, by eliminating bearings whose compressive stiffness is outside the range of ±20 percent of the mean value for the production lot.

Low Temperature Tests. Both brittleness and stiffening are checked in low temperature regions. The details (i.e., test temperature and conditioning time) depend on the current grading system, which is based on the temperature history at the site under consideration. The current performance criteria are the same for instantaneous and crystallization stiffening: $(G_C/G_R) \leq 4$. The research presented in Chapter 2 has shown that the current system is overly conservative in both the testing details and the performance criteria. In order to implement the recommended method accurately, the temperature histories of numerous locations should be evaluated as outlined in Chapter 2 and Appendix B of the research team's final report to produce an accurate Low Temperature Grade Map. It is anticipated that the form of the requirements would be similar to the current system as shown earlier for Anchorage in Chapter 2. After examining the data for all the cities, a suitable number of general categories would be chosen (e.g., six grades) and each city would be rounded into its nearest grade. Based on the four cities investigated, it appears that Anchorage would be in one grade and the other three cities would be in a second grade. The ratio G_C/G_R can be determined from any of the four shear modulus setups or the compressive stiffness test in Appendix B of this report. The question marks shown in Appendix E of this report indicate that further work is necessary (develop the Low Temperature Grade Map) before a rational recommendation can be made.

Outside of Tolerance Test. In Chapter 3, the current tolerances associated with shim misalignment were shown to be conservative. Equations 20 and 21 were developed that define the limits of vertical and rotational misalignments that would result in only minor changes in eight stress, strain, and stiffness parameters of the bearing. Equation 21 is recommended for AASHTO M251. More simply, the layer thickness tolerance could be increased from 3 mm (⅛ in.) to 4.5 mm (3⁄16 in.). However, simply increasing the current tolerances to either Equation 21or 4.5 mm (3⁄16 in.) might encourage sloppy fabrication, so a penalty test is recommended when the current limits, modified by eliminating the ±20 percent of specified thickness limit, are exceeded. Whenever the misalignments in a bearing exceed the modified current limits, but are less than the limiting values of vertical movement and rotation from Equation 21, that bearing must be subjected to the short-term compression test or the inclined compression test.

CHAPTER 5

CONCLUSIONS AND FUTURE RESEARCH

It was established through experimental and theoretical studies that ozone attack, hardness, heat resistance (aging), and compression set do not affect the performance of an elastomeric bridge bearing significantly, so tests measuring the effects of these parameters in AASHTO M251 could be eliminated. The low temperature instantaneous stiffening test and peel test for bond were found to be ineffective in measuring their respective parameters, which were found to be important performance parameters. A new inclined compression test was developed that can more readily determine the shear modulus of a full-size bearing. Surface cracks will take hundreds of years to grow through one-half of the edge cover based on crack growth.

An elastomeric bearing can tolerate considerable vertical, horizontal, and rotation misalignments of laminates without deterioration in performance. The horizontal misalignment (cover) is less influential on the performance of the bearing as compared with the variation of rubber layer thickness and the rotation misalignment. There is a significant interaction between the vertical and rotation misalignments. In general, the tolerances given in Table 2 of AASHTO M251-97 are well below the laminate misalignments that affect the performance of the bearings.

Creep deformation can significantly affect the performance of an elastomeric bearing and must be considered during the design phase of such bearings. The boundary condition at the top and bottom surfaces plays an important role in controlling the long-term deformation. The creep of bearings with unbonded top and bottom surfaces is highly unpredictable because of a gradual decay in friction forces at the interface of the bearing and the contacting surfaces. High modulus bearings show higher percent creep as compared with low modulus bearings. However, the absolute creep deformation of high modulus bearings is lower than that of the low modulus bearings, so when the magnitude creep deformation must be reduced, high stiffness bearings can be used. A time-dependent shear modulus obtained from a short-term stress relaxation test can be conservatively used to predict the long-term axial deflection.

The change in shear stiffness as a result of aging depends on the size of the specimen. As the size increases, the percent change in shear stiffness decreases drastically. In general, the effects of aging are higher in neoprene than in natural rubber. Arrenhius-based predictions show that full-size bearings at ambient temperatures will experience insignificant change in stiffness as a result of aging over their lifetimes, so the aging tests given in various specifications are irrelevant for the elastomeric bearings of the moderate-to-high shape factor rubber layers used in civil engineering applications.

Low temperature stiffening is significant, but its effect on bearing performance must be established. Temperature history has a significant effect on low temperature performance, along with speed of testing and slip. A performance-based evaluation established that the current test requirements are very conservative and that bearing materials are being rejected that would perform satisfactorily in service. The maximum expected daily bridge strain because of the difference between the daily high and low temperature is smaller as the temperature gets lower. So, although the lower temperature increases the shear stiffness, the maximum shear force may actually be higher at warmer temperatures because of higher strains. There is a need to develop a national low temperature performance criteria map following the suggested methodology presented herein.

Although elastomeric bearings with fabric laminates were not specifically addressed in this research, the various test methods described herein should be applicable if they are treated like plain bearings. Given that the laminates are exposed along the edges in such bearings, environmental issues may be more important, especially for delamination. Although AASHTO M251 currently uses the same peel test method for steel and fabric laminates, California DOT requires that samples with fabric laminates be immersed in water for 10 days to represent exposure conditions prior to testing. The shear-bond test described in Appendix C of this report could adopt this same conditioning procedure. Research should be conducted to verify that the procedures presented herein are applicable to elastomeric bearings with fabric laminates.

REFERENCES

1. AASHTO (1973) *Standard Specifications for Highway Bridges*, 11th Edition.
2. AASHTO (1977) *Standard Specifications for Highway Bridges*, 12th Edition.
3. AASHTO (1985) *Standard Specifications for Highway Bridges*, Interim Revisions.
4. AASHTO (1989) *Standard Specifications for Highway Bridges*, 14th Edition.
5. AASHTO (1992) *Standard Specifications for Highway Bridges*, 15th Edition.
6. AASHTO (1996) *Standard Specifications for Highway Bridges*, 16th Edition.
7. AASHTO (1997) *Standard Specifications for Highway Bridges*, 16th Edition, Interim Revisions.
8. AASHTO LRFD (1998) *Bridge Design Specifications*, Interim Revisions.
9. AASHTO LRFD (1998*) Bridge Design Specifications*, 1st Edition.
10. AASHTO LRFD (1998) *Bridge Construction Specifications*, 1st Edition.
11. AASHTO M251-97 (1997) *Standard Specifications for Plain and Laminated Elastomeric Bridge Bearings*.
12. Arditzoglou, Y., J. A. Yura, and A. H. Haines (1997) "An Evaluation of the ASTM Shear Modulus Test for Elastomeric Bridge Bearings," Fourth World Congress on Joint Sealants and Bearing Systems in Concrete Structures–Volume 2, American Concrete Institute, Farmington Hills, Mich., SP-164V2, pp. 903–936.
13. ASTM D1043-92 (1992) "Standard Test Method for Stiffness Properties of Plastics as a Function of Temperature by Means of a Torsion Test."
14. ASTM D2240-91 (1991) "Durometer Hardness."
15. ASTM D395-89 (1989) "Rubber Property – Compression Set."
16. ASTM D4014-89 (1989) "Standard Specification for Plain and Steel-Laminated Elastomeric Bearings for Bridges."
17. ASTM D412-98a (2001) "Standard Test Methods for Vulcanized Rubber and Thermoplastic Rubbers and Thermoplastic Elastomers-Tension."
18. ASTM D429-82 (1982) "Adhesion to Rigid Substrates."
19. ASTM D573 " Standard Test Method for Rubber-Deterioration in an Air Oven," Vol. 9.01.
20. ASTM D746-95 (1995) "Standard Test Method for Brittleness Temperature of Plastics and Elastomers by Impact."
21. Barker, L. R. (1988) "Accelerated and Long-Term Ageing of Natural Rubber Vulcanizates," *NR Technology*, Vol. 19, No. 2, pp. 28–39.
22. Braden, M., and A. N. Gent (1960) "The Attack of Ozone on Stretched Rubber Vulcanizates: I. The Rate of Cut Growth," *Journal of Applied Polymer Science*, Vol. III, No. 7, pp. 90–99.
23. British Standard (1983) "Steel, Concrete and Composite Bridges, Part 9: Bridge Bearings," *BS5400.*
24. Chen, R., and J. A. Yura (1995) "Wax Build-Up on the Surfaces of Natural Rubber Bridge Bearings," *Report No. 1304-4*, Center for Transportation Research, University of Texas, Austin, August, 59 pp.
25. Collingwood, G. P. (1999) "Fatigue Crack Growth in Elastomeric Bridge Bearings," M.S. thesis, University of Texas, Austin.
26. Crozier, W., J. Stoker, V. Martin, and E. Nordlin (1974) "A Laboratory Evaluation of Full Size Elastomeric Bridge Bearing Pads," California Department of Transportation, *Report CA-DOT-TL-6574-1-74-26*, Sacramento, June, 60 pp.
27. Curro, J. G., and E. A. Salazar (1977) "Physical And Chemical Stress Relaxation Of Elastomers," *Rubber Chemistry and Technology*, Vol. 50, No. 5, Nov.–Dec., pp. 895–905.
28. Derham, C. J. (1973) "Creep and Stress Relaxation of Rubbers," *Journal of Materials Science*, Vol. 8, No. 7, July, pp. 1023–1029.
29. Doody, M. E., and J. E. Noonan (1998) "Long-Term Performance of Elastomeric Bridge Bearings," *Special Report FHWA/NY/SR-98/129*, Transportation Research and Development Bureau, New York State Board of Transportation, Albany.
30. E.I. Du Pont de Nemours & Co. (1959) "Design of Neoprene Bridge Bearing Pads."
31. E.I. Du Pont de Nemours & Co. (1989) "Dynamic Compressive Loading Experiments."
32. English, B. A., R. E. Klingner, and J. A. Yura (1994) "Elastomeric Bearings: Background Information and Field Study," *Research Report CTR 1304-1*, Center for Transportation Research, University of Texas, Austin, June, 59 pp.
33. Eurocode prEN 1337-3 (1996) *Structural Bearings: Part 3; Elastomeric Bearings*, Draft Document.
34. Eyre, R., and A. Stevenson (1991) "Performance of Elastomeric Bridge Bearings at Low Temperatures," Third World Congress on Joint Sealing and Bearing Systems for Concrete Structures, Oct. 27–31, Ontario, Canada.
35. Freakley, P. K., and A. R. Payne (1978) *Theory and Practice of Engineering with Rubber*, London: Applied Science Publishers.
36. Gent, A. N., and D. A. Tompkins (1969) "Nucleation and Growth of Gas Bubbles In Elastomers," *Journal of Applied Physics*, Vol. 40, No. 6, May, pp. 2520–2525.
37. Gent, A. N., Editor (1992) *Engineering with Rubber: How to Design Rubber Components*, New York, N.Y.: Hanser Publishers.
38. Hamed, G. R. (1992) "Materials and Compounds," *Engineering with Rubber*, Munich: Hanser Publishers.
39. Hamzeh, O., J. L. Tassoulas, and E. B. Becker (1995) "Analysis of Elastomeric Bridge Bearings," *Report No. 1304-5*, Center for Transportation Research, University of Texas, Austin, August, 139 pp.
40. Hogan, M., R. H. Gunderson, and A. Stevenson (1997) "Predicted Change in Shear Modulus of Semi-EV NBR and NR Elastomer Compounds Over Thirty Years," *Corrosion 97*, Paper 79, NACE International Conference, Houston.
41. ISO 188 (1982) "Accelerated Ageing or Heat Resistance Tests," International Standards Organization, Geneva.
42. ISO 8013 (1988) "Determination of Creep in Compression or Shear," International Standards Organization, Geneva.

43. John, P. W. M. (1971) *Statistical Design and Analysis of Experiments*, New York: Macmillan.
44. Kumar, A. (2000) "Performance Related Parameters of Elastomeric Bearings," Ph.D. dissertation, University of Texas, Austin.
45. Lake, G. J. (1970) "Ozone Cracking and Protection of Rubber," *Rubber Chemistry and Technology*, Vol. 43, p. 1230.
46. Lee, M.-P., and A. Moet (1993) "Analysis of Fatigue Crack Propagation in NR/BR Rubber Blend," *Rubber Chemistry and Technology*, Vol. 66, No. 2, pp. 304–316.
47. Lewis, P. M. (1986) "Effect of Ozone on Rubbers: Countermeasures and Unsolved Problems," *Polymer Degradation and Stability*, Vol. 15, No. 1, pp. 33–66.
48. Long, J. E. (1974) *Bearings in Structural Engineering*, London.
49. Mathew, N. M. (1991) "Ozone Damage of Rubber and Its Prevention." In *Fractography of Rubbery Materials.* (A. K. Bhowmick and S. K. De, Eds.), New York, N. Y.: Elsevier Science Publishing Co.
50. McDonald, J. (1999) "Slippage of Neoprene Bridge Bearings," Master's thesis, Louisiana State University.
51. Moakes, R. C. (1975) "Long Term Natural Ageing," *RAPRA Members Journal*, Parts 1 and 2, July/August, pp. 53–63.
52. Mullins, L. (1987) "Engineering with Rubber," *CHEMTECH*, Vol. 17, No. 12, pp. 720–727.
53. Murray, R. M. and J. D. Detender (1961) "First and Second Order Transitions in Neoprene," *Chemistry and Technology*, Vol. 34.
54. Muscarella, J. V. and J. A. Yura (1995) "An Experimental Study of Elastomeric Bridge Bearings with Design Recommendations," *Research Report No. 1304-3*, Center for Transportation Research, University of Texas, Austin, October, 180 pp.
55. Muscarella, J. V. and J. A. Yura (1996) "An Experimental Study of Flat and Tapered Elastomeric Bridge Bearings," Fourth World Congress on Joint Sealants and Bearing Systems for Concrete Structures, American Concrete Institute, Farmington Hills, Mich., SP-164, pp. 143–164.
56. Nagdi, K. (1993) *Rubber as an Engineering Material: Guideline for Users*, Hanser Gardner Publishers.
57. Nakauchi, H., K. Tanaka, C. Yokoyama, M. Miyazaki, and N. Yamazaki (1992) "Characterization of a 100-Year-Old Rubber Bearing by Microanalytical Methods," *Journal of Applied Polymer Science*, Applied Polymer Symposium 50, pp. 369–375.
58. Ritchie, D. F. (1989) "Neoprene Bridge Bearing Pads, Gaskets and Seals," *Rubber World*, p. 27–31.
59. Roberts, A. D., Editor (1988) *Natural Rubber Science and Technology*. New York: Oxford University Press.
60. Roeder, C. W., and J. F. Stanton (1987) "Performance of Elastomeric Bearings," *NCHRP Report 298*, Transportation Research Board, National Research Council, Washington, D.C., 100 pp.
61. Roeder, C. W., J. F. Stanton, and T. Feller (1989) "Low Temperature Behavior and Acceptance Criteria for Elastomeric Bridge Bearings." *NCHRP Report 325*, Transportation Research Board, National Research Council, Washington, D.C., 69 pp.
62. Selden, R. (1998) "The Effect of Water Immersion on Fatigue Crack Growth of Two Engineering Rubbers," *Journal of Applied Polymer Science*, Vol. 69, No. 5, pp. 941–946.
63. Shelton, J. R. (1972) "Review of Basic Oxidation Processes in Elastomers," *Rubber Chemistry and Technology*, Vol. 45, p. 359.
64. Stanton, J. F. and C. W. Roeder (1982) "Elastomeric Bearings Design, Construction, and Materials." *NCHRP Report 248*, Transportation Research Board, National Research Council, Washington, D.C., 82 pp.
65. Stevenson, A. (1983) "A Fracture Mechanics Study of the Fatigue of Rubber in Compression," *International Journal of Fracture*, Vol. 23, No. 1, pp. 47–59.
66. Stevenson, A. (1985) "Longevity of Natural Rubber in Structural Bearings." *Plastics and Rubber Processing and Applications*, Vol. 5.
67. Stevenson, A., and P. B. Lindley (1982) "Fatigue Resistance of Natural Rubber in Compression," *Rubber Chemistry and Technology*, Vol. 55, No. 2, pp. 337–351.
68. Suter, G. T., and R. A. Collins (1964) "Static and Dynamic Elastomeric Bridge Bearing Tests at Normal and Low Temperatures," *O.J.H.R.P. Report No. 24*, University of Toronto, September.
69. Takayama, M., and K. Morita (1998). "Creep Tests of Full-Scaled Laminated Rubber Bearings," *American Society of Mechanical Engineers, Pressure Vessels and Piping Division (Publication) PVP Seismic, Shock, and Vibration Isolation Proceedings of the 1998 ASME/JSME Joint Pressure Vessels and Piping Conference* (Jul. 26–30 1998), Vol. 379, San Diego, Calif., Sponsored by: ASME Fairfield, N.J., pp. 95–102.
70. Topkaya, C. (1999) "A New Test Method for Determining the Shear Modulus of Elastomeric Bridge Bearings," Master's thesis, University of Texas,Austin.
71. UIC Code 772 (1973) "Code for the Use of Rubber Bearings for Rail Bridges," International Union of Railways (Union Internationale des Chemins de Fer), Brussels.
72. Yakut, A. (2000) "Performance of Elastomeric Bridge Bearings at Low Temperatures," Ph.D. dissertation, University of Texas, Austin.
73. Yeoh, O. H. (1993) "Some Forms of the Strain Energy Function for Rubber." *Rubber Chemistry and Technology*, Vol. 66, No. 5, Nov.–Dec., p. 754.
74. Young, D. G. (1986) "Fatigue Crack Propagation in Elastomer Compounds: Effects of Strain Rate, Temperature, Strain Level, and Oxidation," *Rubber Chemistry and Technology*, Vol. 59, No. 5, pp. 809–825.

APPENDIX A

AASHTO M251-ANNEX A

INCLINED COMPRESSION TEST FOR SHEAR MODULUS

A1. SCOPE

A1.1. This method determines the shear modulus of fullsize elastomeric bearings from the compressive force-displacement curve after three conditioning cycles to 65% strain.

A2. APPARATUS

A2.1 A compression test machine shall be used to apply the load to a pair of test bearings between three inclined platens as shown in Figure A1.

A2.2 The inclined platens shall be made out of steel or aluminum. The surface inclination can vary between 1:10 to 1:20. All platens shall have the same surface inclination. The platen dimensions shall be greater than the dimensions of the bearings tested. The minimum thickness of the aluminum platens shall be 12 mm. The top and bottom platens shall be attached to the testing machine.

A2.3 The platen surfaces, or facing plates attached to the platens, that are in contact with the bearings shall be roughened to prevent bearing slip during the test. The roughening can be performed by impacting with a tool that is used to roughen concrete surfaces, blasting with grit, or other equivalent means. Milled grooves no deeper than 1 mm can also be used to provide a no-slip surface.

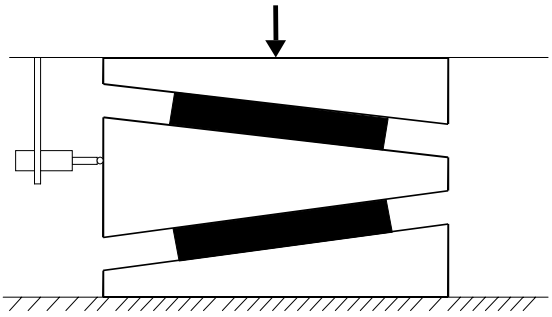

Figure A1. Inclined compression test setup.

A3. TEST SPECIMEN

A3.1 The elastomeric bearings shall be of uniform thickness and of rectangular or circular in cross-section. The thickness shall not be less than 6 mm or ¼ in. The length and width of each bearing shall not be less than four times the thickness.

A3.2 Plain elastomeric pads must be bonded to rigid plates on both the top and bottom surfaces. The bonding system must not require a curing temperature greater than 40°C. The plates shall be of rectangular section and may be of mild steel. Plate dimensions shall be slightly larger than bearing dimensions. A thickness ≥ 5 mm can be used for the plates.

A3.3 Measure the length, width and total elastomer thickness of the bearings to determine the average cross-sectional area (A) and average elastomer thickness (T) of a bearing.

A3.4 Laminated pads shall be tested with or without any sole plates attached.

A3.5 The contact surfaces of bearings that are not bonded to steel plates shall be cleaned to remove any kind of residue.

A4. TEST PROCEDURE

A4.1 Allow time for any bonds to achieve adequate strength and condition the specimen at a test temperature of 23°C ± 2°C at least 8 hours prior to testing unless another test temperature is specified.

A4.2 Bearings shall be sandwiched between the platens until the surfaces are in contact with each other.

A4.3 Two deflectometers shall be attached to monitor the horizontal displacement of the middle platen. The deflectometers shall be accurate to at least 0.025 mm.

A4.4 Carry out four successive loading and unloading cycles to a deformation equal to 65 percent of the average bearing thickness, and at such a loading rate that the time per cycle is within a range of 4–6 minutes. In all the unloading cycles, the minimum load shall be 5 kN or 2 percent of the maximum load, whichever is less.

A4.5 If there is any indication of slip of the bearings relative to the rigid plates or of bond failure during the test, prepare new specimens and repeat the test.

A4.6 If the middle platen does not come back to the same approximate position after the last two successive unloading cycles, a slip may have occurred between the bearing and the platens. This condition must be remedied for a valid test.

A5. DETERMINATION OF SHEAR MODULUS

A5.1 The shear modulus shall be determined from the fourth cycle of compressive load versus average displacement curve as shown in Figure A2.

A5.2 Take an effective origin at force F1, extension X1 where F1 is 5 kN or 2 percent of the maximum force on the fourth cycle, whichever is smaller. Determine the force F2 at an extension X2 given by X1 + 0.5T, where T is the average total elastomer thickness of the pad (overall pad thickness minus the thicknesses of all the laminates within the bearing.

A5.3 The shear modulus is calculated as follows:

$$\text{Shear Modulus} = \frac{2(F2 - F1)}{A \times n}$$

for 1:n sloped platens. The factor n converts the vertical compressive force to a horizontal shear force.

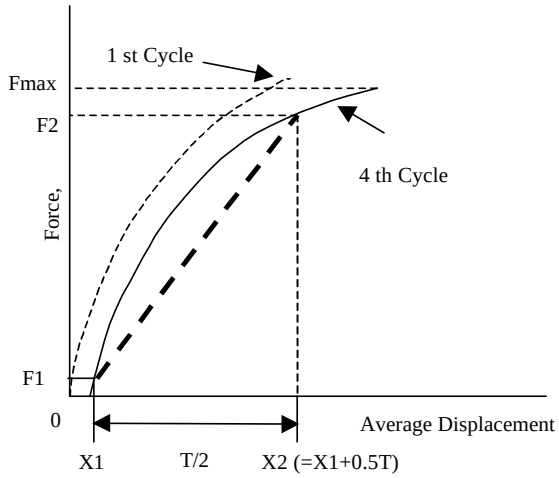

Figure A2. Compression force vs. shear displacement.

APPENDIX B

AASHTO M251—ANNEX C

COMPRESSION STIFFNESS TEST METHOD

C1. COMPRESSION STIFFNESS TEST METHOD

This test determines the compressive stiffness of elastomeric bridge bearings over a wide temperature range by direct measurements of compressive loads and displacements. The test method is useful for determining the relative changes in stiffness over a wide range of temperatures as well as determining the compressive stiffness over a wide range of temperatures.

C2. TEST SETUP

C2.1. A compression testing machine shall be used that is capable of exerting a compressive load of 500 kN to a pair of bearing specimens as shown in Figure C1.

C2.2. Four displacement transducers or other devices with an accuracy of 0.005 mm shall be used to record the displacements. Load shall be monitored with a load cell or other equivalent devices with an accuracy of 1 percent of the test load.

C2.3. The specimens and loading plates shall be conditioned and tested in an enclosed unit capable of controlling temperatures down to −30°C. Depending on the temperature ranges and the conditioning time involved, mechanical refrigeration or a dry-ice chest, or both will be advantageous.

C3. TEST SPECIMEN

C3.1. The test specimen in Figure C1 shall consist of two identical blocks of elastomer sandwiched between rigid plates. The elastomer blocks shall be of uniform thickness, preferably equal to the original thickness of the full-size bearing and of square or rectangular cross-section, the length and width each being not less than four times the thickness.

C3.2. The steel rigid plates shall be of square or rectangular section, a larger width and length than the elastomer block. Suitable plate dimensions for use with 40-mm thick elastomeric pads are a thickness of 25 mm and a plan dimension at least 25 mm larger than each block dimension.

C4. TEST PROCEDURE

C4.1. Measure the length, width and thickness of the blocks and determine the average cross-sectional area, plan area, (A), and the average total elastomer thickness, (T), of the specimen.

C4.2. Attach four displacement transducers to the bottom plate such that the relative displacement between the top and bottom plate can be measured at four points as shown in Figure C2. The center points of each side of the bottom plate are appropriate locations for the transducers.

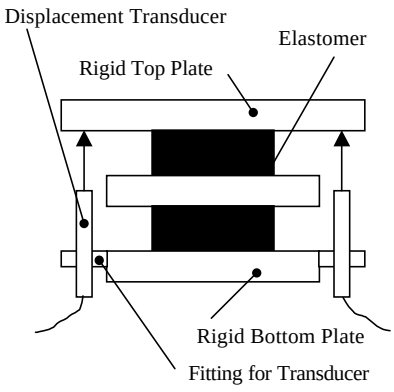

Figure C1. Test setup.

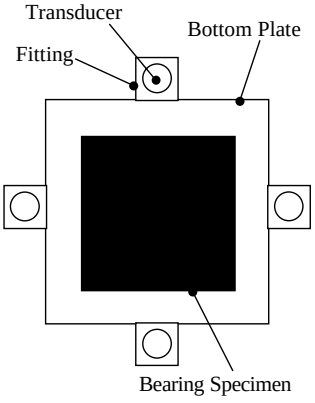

Figure C2. Location of transducers.

C4.3. Place the specimens inside the environmental chamber (or freezer), and bring the freezer to the desired test temperature. Condition the specimens at the specified test temperature for the specified period of time.

C4.4. Attach the specimens to the compression machine. Carry out three successive loading and release cycles to a deformation equal to 10% of the total elastomer thickness of the two blocks, $2T$ at a rate such that the time per cycle is within the range of 30 to 120 seconds.

C4.5. Measure both the load and the displacement at $0.02T$ increments only for the third cycle.

C5. DETERMINATION OF STIFFNESS

C5.1. The compressive modulus E_S shall be determined from the load-displacement curve on the third cycle as shown in Figure C3.

C5.2. Draw a best-fit straight line using the least-squares method through the data points between displacements $0.02T$ and $0.2T$. The line must pass through the $0.02T$ data point. Determine the slope, K_1, of the best-fit straight line.

C5.3. Determine E_S from Equation C1.

$$E_S = K_1 \frac{2T}{A} \qquad \text{(C1)}$$

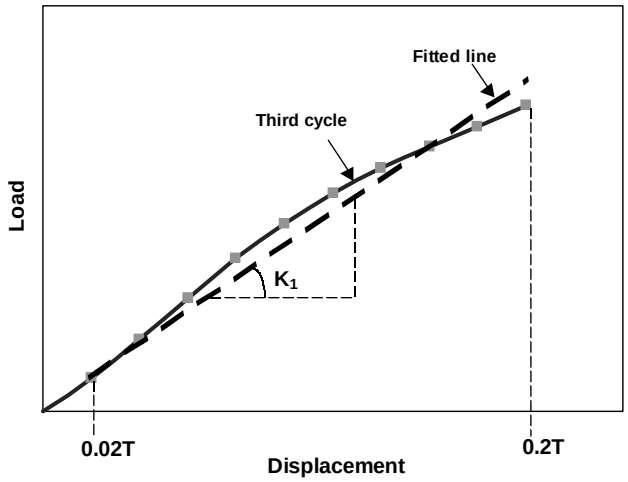

Figure C3. Load-displacement curve.

APPENDIX C

AASHTO M251-ANNEX B

A TEST METHOD FOR CREEP AND SHEAR BOND IN ELASTOMERIC BEARINGS

B1. SCOPE

B1.1 This document describes a procedure to estimate creep of elastomeric bridge bearings.

B1.2 The values stated in SI units are to be regarded as the standard.

B1.3 This document does not purport to address the details of the test setup or safety concerns, if any, associated with its use. It is the responsibility of the user to establish appropriate safety and health practices and determine the applicability of regulatory limitations prior to using the tests summarized in this document.

B2. REFERENCED DOCUMENTS

ASTM D 3183 Practice for Rubber–Preparation of Pieces for Test Purposes from Products.

B3. TEST SPECIMEN

B3.1 The standard test specimen shall consist of two 51×51 mm square pieces of rubber bonded to steel plates as shown in Figure B1.

B3.2 The rubber pieces can be cut from one of the subject bearings per ASTM D 3183 or molded from unvulcanized rubber used in the subject bearings.

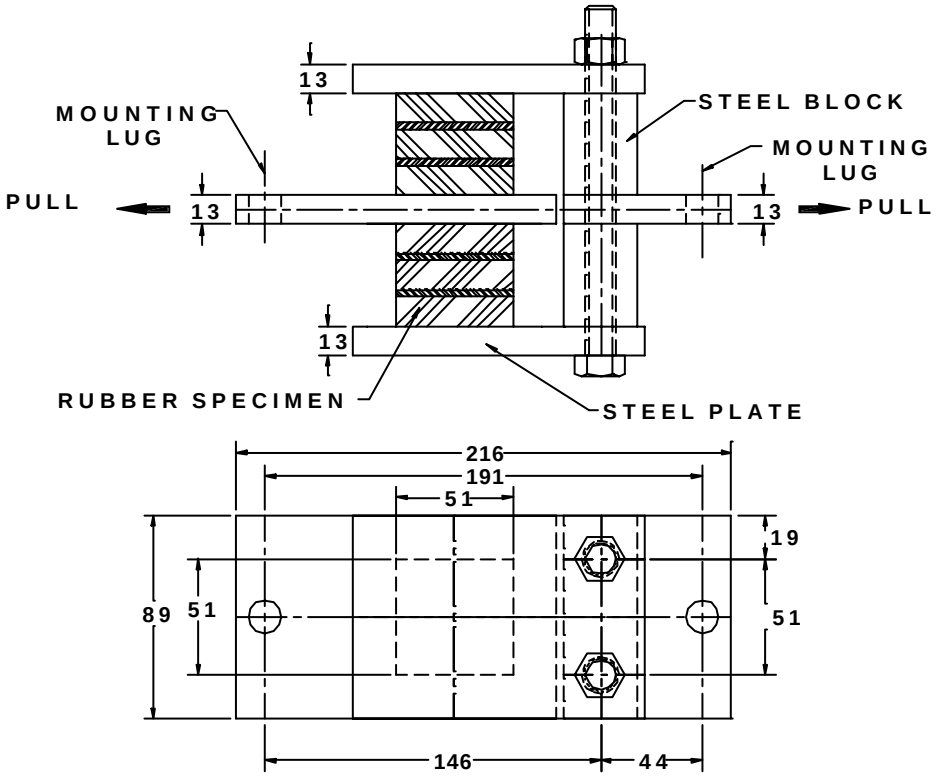

Figure B1. Test setup (mm).

B3.3 The rubber to metal bond can be cold or hot using an appropriate adhesive system and surface preparations adequate to keep the bond fully intact for 8 hours while the test specimen is subjected to a sustained shear strain of 50% at room temperature.

B3.4 The total height of the rubber piece shall be greater than 12 mm and less than 45 mm. If the rubber piece consists of alternate layers of rubber and metal reinforcements cut from actual bearing as shown in Figure B1, the total height of each rubber piece shall be limited to 51 mm.

B4. TEST PROCEDURE

B4.1 Mount the test specimen in a displacement controlled loading system (MTS or equivalent) with appropriate load cell connected to a data acquisition system (automatic or manual).

B4.2 Load the specimen to 50% shear strain 10 times at 1% strain per second. Shear strain is defined as the ratio of shearing displacement to the total thickness of rubber in the test piece. If the rubber thickness in one piece is R_{thk} then for 50% strain, the specimen needs to be displaced $0.5R_{thk}$.

B4.3 Load the specimen to 50% shear strain in 1 second and keep the strain constant for a minimum of six hours.

B4.4 Record the load after 30 minutes of initial loading with further measurements after every 5 minutes for 360 minutes minimum.

B4.5 For each time measurement use Equation B1 to convert the load to shear modulus

$$G(t) = \frac{Load(t)}{51 \times 51 \times 2 \times 0.5} \qquad \text{(B1)}$$

where $Load(t)$ is the load at time t (minutes) and $G(t)$ is the shear modulus (MPa) at time t. Note that (51×51) is the area of test piece and 0.5 is the shear strain. Since there are two test pieces in the test specimen, the load is divided by 2.

B4.6 A power law of the form shown in Equation B2 can be conservatively used to predict $G(t)$ at times greater than thirty minutes.

$$G(t) = at^b \qquad \text{(B2)}$$

where a and b are constants that are calculated by regression analysis of the data obtained in Section B4.5 as described in Section B4.7.

B4.7 Plot $\log(G(t))$ versus $\log(t)$ and fit a straight line using the least-squares method. The constant b is the slope of this line and $\log(a)$ is the intercept of the straight line on the $\log(G(t))$ axis.

B5. CREEP ESTIMATE FOR FULL SIZE BEARING

B5.1 Let T be the time at which creep deflection need to be estimated (e.g., 25 years). Calculate $G(t)$ at $t = 60$ minutes and at $t = T$ using Equation B2.

B5.2 Calculate percent creep using Equation B3.

$$Creep(\%) = \left(\frac{G(60)}{G(\mathrm{T})} - 1\right) \times 100 \qquad \text{(B3)}$$

B6. SHEAR BOND

B6.1 After completion of the six-hour stress relaxation test, load the specimen to 150% shear strain at 1% strain per second. Hold the specimen at 150% strain for 5 minutes and observe any failure in the rubber or debonding at the interface of the rubber layers and laminates. Report the type of failure. Failures in the cold bond (when used) are not important unless they affect the ability to reach 150% strain in which case a new specimen must be fabricated.

APPENDIX D

RECOMMENDED CHANGES TO AASHTO LRFD CONSTRUCTION SPECIFICATION FOR ELASTOMERIC BEARINGS

SPECIFICATIONS	COMMENTARY

18.1.3 Packaging, Handling, and Storage

Prior to shipment from the point of manufacture, bearings shall be packaged in such a manner to ensure that during shipment and storage, the bearings will be protected against damage from handling, weather, or any normal hazard. Each completed bearing shall have its components clearly identified, be securely bolted, strapped, or otherwise fastened to prevent any relative movement, and marked on its top as to location and orientation in each structure in the project in conformity with the contract documents.

All bearing devices and components shall be stored at the work site in an area that provides protection from environmental and physical damage. When installed, bearings shall be clean and free of all foreign substances.

Dismantling of bearings at the site shall not be done unless absolutely necessary for inspection or installation. Bearings shall not be opened or dismantled at the site, except under the direct supervision of, or with the approval of, the Manufacturer.

C18.1.3

Small amounts of grit, dirt, or other contamination can seriously detract from the good performance that could otherwise be obtained from a bearing. It is therefore very important that the bearing not be opened up on site, except under the supervision of the Manufacturer or his agent.

18.1.4 Manufacture or Fabrication

18.1.4.1 GENERAL

The Manufacturer shall certify that each bearing satisfies the requirements of the contract documents and these specifications, and shall supply the Engineer with a certified copy of material test results. Each reinforced bearing shall be marked in indelible ink or flexible paint. The marking shall consist of the orientation, the order number, lot number, bearing identification number, and elastomer type and grade number. Unless otherwise specified in the contract documents, the marking shall be on the face that is visible after erection of the bridge.

Unless otherwise specified in the contract documents, the surface finish of bearing components that come into contact with each other or with concrete, but are not embedded in concrete, shall conform to the requirements of Section 11, "Steel Structures."

Bearing assemblies shall be pre-assembled in the shop by the supplier and checked for proper completeness and geometry before shipping to the site.

Unless otherwise specified in the contract documents, steel bearing components, other than stainless steel, including anchor bolts, shall be galvanized in accordance with Article 11.3.7, "Galvanizing."

C18.1.4.1

In the short term, marking simplifies the identification of the correct bearings and helps in establishing which way up they should be placed at the job site. In the long term, it may permit the removal of bearings after a number of years of service to check the change in material properties over time. It also helps in settling disputes.

SPECIFICATIONS **COMMENTARY**

Bearings except

18.1.4.2 FABRICATION TOLERANCES

Plain elastomeric pads and laminated bearings shall be built as specified in the contract documents within the tolerances of Table 18.1.4.2–1. The classes of tolerances shall be as follows:

- Class A = 0.001 × nominal dimensions
- Class B = 0.002 × nominal dimensions
- Class C = 0.005 × nominal dimensions

Load plate overall dimensions for flatness tolerance and surface finish shall apply only to surfaces in contact with the bearing.

Tolerances for plain and laminated bearings are given AASHTO M 251

C18.1.4.2

Some of the tolerances have been changed to relative values, because an absolute tolerance, such as 1.5 mm, may be overly large for a small bearing and unrealistically small for a large bearing. Parallelism of the two faces of a single layer is controlled by the limitation of the thickness at any point.

Each bearing type has one or more tolerances that are particularly important. In bearings that depend on rocking or rolling surfaces, it is most important to ensure that the curvature of the curved surface is constant to within a fine tolerance. This is more important than the actual value of the radius of curvature. In nested roller bearings, it is also important that all the rollers have exactly the same radius of curvature to ensure that the load will be equally shared between them. In flat PTFE sliding surfaces, the surface finish of the mating surface, usually stainless steel, is particularly important. A 50-μm finish or better is recommended in all cases.

In bearings that depend on the sliding of one curved surface over another, such as curved PTFE sliding bearings, curved bronze sliding bearings, or pins and bushings that allow rotation, the difference in diameter of the two curved surfaces is the most important tolerance. The out-of-round or the variation in curvature of the curved surface is also important, and again, the actual value of the radius of curvature is less important. If two parts of the bearing are made by different fabricators, machining by fitting the two parts is not possible and it is necessary to machine each part to a specific radius within a very high accuracy. In the past, bearings made of components fabricated by different manufacturers have given problems because of lack of a good fit. In pot bearings, the most important tolerances are those on the clearance between the pot and the piston and on the vertical clearance between the upper and lower parts of the bearing.

18.1.5 Testing and Acceptance

18.1.5.1 GENERAL

18.1.5.1.1 Scope

Testing and acceptance criteria for bearings shall conform to the minimum requirements specified in Article 18.1.5.1.2, "Tapered Sole Plates." The Engineer may require more stringent standards.

C18.1.5.1.1

The purpose of testing is to ensure a good-quality finished bearing. The obvious way to achieve this is to conduct rigorous tests on every bearing. However, this is economically infeasible, and resorting to other methods is necessary.

Table 18.1.4.2–1 Fabrication Tolerances

Item	Thickness tolerance (mm)	Dimension tolerance (mm)	Flatness or out-of-round tolerance (mm)	Surface finish (μm) (rms.)
Metal Rocker and Roller Bearings:	—			
Single Roller: diameter	—	−1.600,+1.600	−0.025,+0.025	1.6
Nested Roller: diameter	—	−0.050,+0.050	−0.025,+0.025	1.6
Rockers: diameter	—	−3.170,+3.170	−0.025,+0.025	3.2
Pins: diameter	—	−0.120,+0.000	−0.050,+0.050	0.8
Bushings: diameter	—	−0.000,+0.120	−0.050,+0.050	0.8
Pot Bearings:				
Overall dimensions	−0.000,+6.350	−0.000,+3.170	—	—
Pot depth (inside)	—	−0.000,+0.635	—	—
Pot wall: thickness and ave. I.D.	−0.000,+3.170	−0.075,+0.075	−0.025,+0.025	0.8
Pot base: top and bottom surfaces	−0.000,+0.635	—	Class C	1.6
Piston: rim	−0.000,+1.600	−0.075,+0.075	−0.025,+0.025	0.8
Piston: top and bottom surfaces	−0.000,+0.635	—	Class C	1.6
Elastomeric disc (unstressed)	−0.000,+3.170	−1.600,+0.000	—	—
Disc Bearings:				
Overall dimensions	−0.000,+6.350	−0.000,+3.170	—	—
Shear-restricting element	—	−0.000,+0.120	Class A	0.8
Other machined parts	−0.000,+1.600	−0.000,+1.600	Class B	1.6
Urethane disc	−0.000,+1.600	−0.000,+3.170	Class B	1.6
Flat PTFE Sliding Bearings:				
PTFE	−0.000,+1.600	−0.000,+0.750	Class A	—
Stainless steel	−0.000,+1.600	−0.000,+3.170	Class A	0.2
Flat Bronze and Copper Alloy Sliding Bearings:				
Sliding surfaces	−0.000,+3.170	−0.000,+3.170	Class A	0.8
Curved PTFE Sliding Bearings:				
Convex radius	—	−0.254,+0.000	−0.050,+0.050	0.2
Concave radius	—	−0.000,+0.254	−0.050,+0.050	3.2
Curved Bronze and Copper Alloy Sliding Bearings:				
Convex radius	—	−0.254,+0.000	−0.050,+0.050	0.8
Concave radius	—	−0.000,+0.254	−0.050,+0.050	0.8
~~Steel-reinforced Elastomeric Bearings:~~				
~~Overall dimensions~~	~~−0.000,+6.350~~	~~−0.000,+6.350~~	~~—~~	~~—~~
~~Internal rubber layers~~	~~−3.170,+3.170 & ±0.20 design~~	~~—~~	~~—~~	~~—~~
~~Cover~~	~~−0.000,+3.170~~	~~—~~	~~—~~	~~—~~
~~Parallelism: top and bottom surfaces~~	~~±0.005 radians~~	~~—~~	~~—~~	~~—~~
~~Parallelism: sides~~	~~—~~	~~±0.020 radians~~	~~—~~	~~—~~
Elastomeric Pads:			—	—
Overall dimensions	−0.000,+3.170	−0.000,+6.350		
Guides:				
Contact surface	—	−0.000,+3.170	Class A	0.8
Distance between guides	—	−0.000,+0.750	—	—
Parallelism of guides	—	±0.005 radians	—	—
Load Plates:				
Overall dimensions	−1.600,+1.600	−6.350,+6.350	Class A	3.2
Bevel slope	±0.002 radians	—	—	—

SPECIFICATIONS **COMMENTARY**

corrected by means of a tapered plate or by other means approved by the Engineer. If shim stacks are needed to level the bearing, they shall be removed after grouting and before the weight of the superstructure acts on the bearing.

Metallic bearing assemblies not embedded in the concrete shall be bedded on the concrete with a filler or fabric material conforming to Article 18.10, "Bedding of Masonry Plates."

Where bearings are seated directly on steel work, the supporting surface shall be machined so as to provide a level and planar surface upon which the bearing is placed.

Bearings or masonry plates that rest on steel supports may be directly installed on the supports, provided the support is flat within a tolerance of 0.002 times the nominal dimension, and is sufficiently rigid so as not to deform under specified loads.

18.2 ELASTOMERIC BEARINGS

18.2.1 Scope

Elastomeric bearings as herein defined shall include unreinforced pads (consisting of elastomer only) and reinforced bearings with steel or fabric laminates.

18.2.2 General Requirements

Bearings shall be furnished with the dimensions, material properties, elastomer grade, and type of laminates specified in the contract documents. The design load shall be shown in the contract documents and testing shall be performed accordingly. Unless otherwise specified in the contract documents, bearings shall be Grade 3, 60-durometer elastomer, and steel reinforced, and shall be subjected to the load testing requirements specified herein.

as specified by the minimum grade requirements in Table 14.7.5.2-2 of the *AASHTO LRFD Bridge Design Specification.*

18.2.3 Materials

18.2.3.1 PROPERTIES OF THE ELASTOMER

The raw elastomer shall be either virgin neoprene (polychloroprene) or virgin natural rubber (polyisoprene). The elastomer compound shall be classified as being of low-temperature Grade 0, 2, 3, 4, or 5. The grades are defined by the testing requirements in Tables 18.2.3.1–1 and 18.2.3.1–2. A higher grade of elastomer may be substituted for a lower one.

C18.2.3.1

At present, only natural rubber (polyisoprene) and neoprene (polychloroprene) are permitted because both have an extensive history of satisfactory use. In addition, much more field experience exists with these two materials than with any other, and almost all of it is satisfactory.

For bearings without bonded sole plates the elastomer material shall contain no wax fillers that are designed to bloom to the surface.

Problems with bearings slipping excessively and even walking out (Chen and Yura 1995, McDonald 1999) has been traced to excessive wax fillers in the rubbers used by some manufacturers mainly to satisfy ozone test requirements. The ozone test is no longer required so wax fillers designed to bloom are unnecessary.

SPECIFICATIONS

The elastomer compound shall meet the minimum requirements of Tables 18.2.3.1–1 and 18.2.3.1–2, except otherwise specified by the Engineer. Test requirements may be interpolated for intermediate hardness. If the material is specified by its shear modulus, its measured shear modulus shall lie within 15 percent of the specified value. A consistent value of hardness shall also be supplied for the purpose of defining limits for the tests in Tables 18.2.3.1–1 and 18.2.3.1–2. If the hardness is specified, the measured shear modulus must fall within the range of Table 14.7.5.2–1 of the *AASHTO LRFD Bridge Design Specifications*. When test specimens are cut from the finished product, the physical properties shall be permitted to vary by 10 percent from those specified in Tables 18.2.3.1–1 and 18.2.3.1–2. All material tests shall be carried out at 23°C ± 2°C, unless otherwise noted. Shear modulus tests shall be carried out using the apparatus and procedure described in Annex A.

COMMENTARY

The low-temperature grading system addresses the problem of stiffening of the elastomer at low temperatures. Special compounding and curing are needed to avoid the problem, but they increase cost and, in extreme cases, may adversely affect some other properties. These adverse effects can be minimized by choosing a grade of elastomer appropriate for the conditions prevailing at the site. The grades follow the approach of AASHTO M 251 or ASTM D 4014 with some stringent low-temperature test criteria for higher grades.

Tables 18.2.3.1–1 and 18.2.3.1–2 outline the required properties of the elastomer. The standards are sometimes different for neoprene and natural rubber, which appear inconsistent because in some ways the requirements resemble a performance specification. However, the present state of knowledge is inadequate to precisely quantify those material properties needed to ensure good bearing behavior, so the tests are intended to ensure good-quality material. Natural rubber and neoprene have different strengths and weaknesses, so different tests are indeed appropriate. Generally, natural rubber creeps less, suffers less low-temperature stiffening, and has a better elongation at break, but neoprene has better chemical, ozone, and aging resistance.

The previous low-temperature brittleness test has been augmented by two other tests: the Clash-Berg test for low-temperature stiffness (ASTM D 1043) and a test for low-temperature crystallization stiffening (the quad shear test conducted at low temperature). All three tests are required for elastomers of Grade 3 and above. Previously, the brittleness test at −40°C was required for all elastomers, including those to be used in the southern-tier states; yet no test was required for thermal or crystallization stiffening, even in the northern-tier states or Alaska.

The brittleness test essentially detects glass transition, but gives no indication of stiffening. The Clash-Berg test is introduced to detect instantaneous low-temperature stiffening. It is quick to perform and requires only a modest investment in special equipment. Crystallization stiffening is both time- and temperature-dependent, but constitutes a significant portion of the total low-temperature stiffening of many elastomers. Detecting it is therefore important and is done by the long-duration shear stiffness test. In addition to the quad shear apparatus, this test requires a freezer that surrounds the apparatus. Because of the nature of the crystallization, the test may take up to 28 days; therefore, it is not required for every lot of bearings.

SPECIFICATIONS **COMMENTARY**

Hardness is maintained as a material property because it is widely used in rubber technology and is easy to measure. However, measurements are sensitive to the method used, and hardness generally gives only rough indication of the mechanical properties, particularly at low temperatures. The shear modulus is a much more useful property, but is more time-consuming to measure.

Harder elastomers have a greater shear stiffness and thus exert larger pier forces due to thermal expansion than materials of low hardness, unless the plan area of the bearing is reduced proportionately. This could cause the bearing to be rather slender, possibly leading to instability problems. Further, 70 durometer material generally creeps more than its softer counterparts. Thus, when larger compressive stiffness is required, it is recommended that reinforced bearings of softer elastomer with thinner layers and higher shape factor be used.

Table 14.7.5.2–1, Shear Modulus, is located in "Material Properties" in the *AASHTO LRFD Bridge Design Specifications*, 1994.

In Tables 14.7.5.2–1 and 14.7.5.2–2, ASTM D 1043 refers to the "modulus of rigidity," while AASHTO M 251 or ASTM D 4014 refers to "shear modulus stiffness." The word "stiffness" is used herein to cover both terms.

SPECIFICATIONS **COMMENTARY**

Table 18.2.3.1–1 Polychloroprene (Neoprene) Quality Control Tests

PHYSICAL PROPERTIES				
D 2240	Hardness (Shore A Durometer)	50 ± 5	60 ± 5	70 ± 5
D 412	Tensile Strength, Minimum MPa	15.5	15.5	15.5
	Ultimate Elongation, Minimum %	400	350	300
HEAT RESISTANCE				
D 573, 70 Hours @ 100°C	Change in Durometer Hardness, Maximum Points	15	15	15
	Change in Tensile Strength, Maximum %	−15	−15	−15
	Change in Ultimate Elongation, Maximum %	−40	−40	−40
COMPRESSION SET				
D 395, Method B	22 Hours @ 100°C, Maximum %	35	35	35
OZONE				
D 1149	100 pphm ozone in air by volume, 20% strain 38°C ±1°C 100 hours mounting procedure D 518, Procedure A	No Cracks	No Cracks	No Cracks
LOW TEMPERATURE BRITTLENESS				
D 746, Procedure B	Grades 0 & 2 – No Test Required			
	Grade 3 – Brittleness @ −40°C	No Failure	No Failure	No Failure
	Grade 4 – Brittleness @ −48°C	No Failure	No Failure	No Failure
	Grade 5 – Brittleness @ −57°C	No Failure	No Failure	No Failure
INSTANTANEOUS THERMAL STIFFENING				
D 1043	Grades 0 & 2 – Tested @ −32°C	Stiffness at test temperature shall not exceed 4 times the stiffness measured at 23°C.		
	Grade 3 – Tested @ −40°C			
	Grade 4 – Tested @ −46°C			
	Grade 5 – Tested @ −54°C			
LOW TEMPERATURE CRYSTALLIZATION				
Quad Shear Test as Described	Grade 0 – No Test Required	Stiffness at test time and temperature shall not exceed 4 times the stiffness measured at 23°C with no time delay. The stiffness shall be measured with a quad shear test rig in an enclosed freezer unit. The test specimens shall be taken from a randomly selected bearing. A ± 25% strain cycle shall be used, and a complete cycle of strain shall be applied with a period of 100 seconds. The first 0.75 cycle of strain shall be discarded and the stiffness shall be determined by the slope of the force deflection curve for the next 0.50 cycle of loading.		
	Grade 2 – 7 Days @ −18°C			
	Grade 3 – 14 Days @ −26°C			
	Grade 4 – 21 Days @ −37°C			
	Grade 5 – 28 Days @ −37°C			

SPECIFICATIONS		COMMENTARY		

Table 18.2.3.1–2 Polyisoprene (Neoprene Rubber) Quality Control Tests

	PHYSICAL PROPERTIES			
D 2240	Hardness (Shore A Durometer)	50 ± 5	60 ± 5	70 ± 5
D 412	Tensile Strength, Minimum MPa	15.5	15.5	15.5
	Ultimate Elongation, Minimum %	450	400	300
	HEAT RESISTANCE			
D 573 70 Hours @ −70°C	Change in Durometer Hardness, Maximum Points	10	10	10
	Change in Tensile Strength, Maximum %	−25	−25	−25
	Change in Ultimate Elongation, Maximum %	−25	−25	−25
	COMPRESSION SET			
D 395 Method B	22 Hours @ 70°C, Maximum %	25	25	25
	OZONE			
D 1149	25 pphm ozone in air by volume, 20% strain 38°C ± 1°C 48 hours mounting procedure D 518, Procedure A	No Cracks	No Cracks	No Cracks
	LOW TEMPERATURE BRITTLENESS			
D 746 Procedure B	Grades 0 & 2 – No Test Required			
	Grade 3 – Brittleness @ −40°C	No Failure	No Failure	No Failure
	Grade 4 – Brittleness @ −48°C	No Failure	No Failure	No Failure
	Grade 5 – Brittleness @ −57°C	No Failure	No Failure	No Failure
	INSTANTANEOUS THERMAL STIFFENING			
D 1043	Grades 0 & 2 – Tested @ −32°C	Stiffness at test temperature shall not exceed 4 times the stiffness measured at 23°C.		
	Grade 3 – Tested @ −40°C			
	Grade 4 – Tested @ −46°C			
	Grade 5 – Tested @ −54°C			
	LOW TEMPERATURE CRYSTALLIZATION			
Quad Shear Test as described in Annex A	Grade 0 – No Test Required	Stiffness at test time and temperature shall not exceed 4 times the stiffness measured at 23°C with no time delay. The stiffness shall be measured with a quad shear test rig in an enclosed freezer unit. The test specimens shall be taken from a randomly selected bearing. A ± 25% strain cycle shall be used, and a complete cycle of strain shall be applied with a period of 100 seconds. The first 0.75 cycle of strain shall be discarded and the stiffness shall be determined by the slope of the force deflection curve for the next 0.25 cycle of loading.		
	Grade 2 – 7 Days @ −18°C			
	Grade 3 – 14 Days @ −26°C			
	Grade 4 – 21 Days @ −37°C			
	Grade 5 – 28 Days @ −37°C			

SPECIFICATIONS	COMMENTARY
18.2.3.2 FABRIC REINFORCEMENT	C18.2.3.2
Fabric reinforcement shall be woven from 100 percent continuous glass fibers of "E" type yarn. The minimum thread count in either direction shall be one thread per mm. The fabric shall have either a crowfoot or an 8 Hardness Satin weave. Each ply of fabric shall have a minimum breaking strength of 140 N/mm of width in each thread direction. Unless otherwise specified in the contract documents, holes shall not be permitted in the fabric.	Fiberglass is the only fabric proven to perform adequately as reinforcement, and only one grade is currently permitted. Polyester has proved too flexible, and both it and cotton are not strong enough. The strength of the reinforcement governs the compressive strength of the bearing when minimum amounts are used; therefore, if stronger fabric with acceptable bond properties is developed, the stress limits of Article 14.7.5, "Steel Reinforced Elastomeric Bearings," of the *AASHTO LRFD Bridge Design Specifications*, 1994, may be reconsidered. However, thorough testing over a wide range of loading conditions, including fatigue, will be needed prior to acceptance.
18.2.3.3 BOND	C18.2.3.3
The vulcanized bond between fabric and reinforcement shall have a minimum peel strength of 5.2 N/mm. Steel laminated bearings shall develop a minimum peel strength of 6.9 N/mm. Peel strength tests shall be performed by ASTM D 429, Method B.	Adequate bond is essential if the installation is to be effective. It is particularly important at the edges of the bearing.
18.2.4 Fabrication	
18.2.4.1 REQUIREMENTS FOR ALL ELASTOMERIC BEARINGS	C18.2.4.1
Bearings that are designed as a single unit must be built as a single unit. Steel laminates must first be thoroughly sandblasted and cleaned and then protected against contamination until fabrication is complete. Flash tolerance, finish, and appearance shall meet the requirements of the latest edition of the *Rubber Handbook*, published by the Rubber Manufacturers Association, Inc., RMA F3 and RMA T.063 for molded bearings and RMA F2 for extruded bearings.	The shape factor, bearing stiffness and strength, and general behavior under load will be different if a bearing is built in sections. The provisions for cleaning and protecting laminates are needed in order to achieve good bond. Edge cover is primarily needed to prevent corrosion of the reinforcement and ozone attack of the bond. However, it also decreases the probability of delamination by reducing the stress concentrations at the exposed outer surface. In the past, bonding during vulcanization has been the most successful method of attaching the laminates and is required for bonding of internal laminates. Practical difficulties, however, may arise in hot bonding of external plates; thus, hot bonding is strongly recommended for them, but not required.

SPECIFICATIONS **COMMENTARY**

18.2.4.2 STEEL LAMINATED ELASTOMERIC BEARINGS

Bearings with steel laminates shall be cast as a unit in a mold and shall be bonded and vulcanized under heat and pressure. The mold finish shall conform to standard shop practice. The internal steel laminates shall be sand-blasted and cleaned of all surface coatings, rust, mill scale, and dirt before bonding, and shall be free of sharp edges and burrs. External load plates shall be protected from rusting by the Manufacturer, and should be hot bonded to the bearing during vulcanization.

C18.2.4.2

External load plates are often referred to as sole plates.

In the past, bonding during vulcanizing has been the most successful method of attaching the laminates, and is required for bonding of internal laminates. However, practical difficulties may arise in hot bonding of external load plates; thus, hot bonding is strongly recommended for them, but not required.

18.2.4.3 FABRIC-REINFORCED ELASTOMERIC BEARINGS

Fabric-reinforced bearings shall be vulcanized in large sheets and cut to size. Cutting shall be performed in such a way as to avoid heating the materials and shall produce a smooth finish with no separation of the fabric from the elastomer. Fabric reinforcement shall be at least single ply for the top and bottom reinforcement layers and double ply for internal reinforcement layers. Fabric shall be free of folds and ripples and shall be parallel to the top and bottom surfaces.

18.2.4.4 PLAIN ELASTOMERIC PADS

Plain pads may be molded, extruded, or vulcanized in large sheets and cut to size. Cutting shall not heat the material, and shall produce a smooth finish.

18.2.5 Testing

18.2.5.1 SCOPE

Materials for elastomeric bearings and the finished bearings themselves shall be subjected to the tests described ~~herein. Material tests shall be in accordance with the appropriate Table 18.2.3.1-1 or Table 18.2.3.1-2.~~ in *AASHTO M 251*

C18.2.5.1

Testing requirements fall into two main categories: material quality control tests and load tests on the finished bearings to detect poor fabrication.

Complete bearings may be tested, and this is most easily done using two identical bearings on top of one another with a shear load plate between them. However, in bearings with more than two or three layers, bending and buckling effects may reduce the shear stiffness of the complete bearing below the value

$$\frac{GA}{h_{rt}} \qquad \text{(C18.2.5.1-1)}$$

SPECIFICATIONS **COMMENTARY**

where:

G = the shear modulus of the elastomer (MPa),

A = the plan area of the elastomeric element or bearing (mm^2), and

h_{rt} = total depth of the elastomer (mm),

given by the simple shear model. It is important to distinguish between unacceptable material and failure to analyze the rather complicated behavior with sufficient accuracy.

18.2.5.2 FREQUENCY OF TESTING

The ambient temperature tests on the elastomer specified in Article 18.2.5.3, "Ambient Temperature Tests on the Elastomer," shall be conducted for the materials used in each lot of bearings. In lieu of performing a shear modulus test for each batch of material, the Manufacturer may elect to provide certificates from tests performed on identical formulations within the preceding year, unless otherwise specified by the Engineer. Test certificates from the supplier shall be provided for each lot of reinforcement.

The three low-temperature tests on the elastomer specified in Article 18.2.5.4, "Low-Temperature Tests on the Elastomer," shall be conducted on the material used in each lot of bearings for Grades 3, 4, and 5 material, and the instantaneous thermal stiffening test shall be conducted on material of Grades 0 and 2. For Grade 3 material, in lieu of the low-temperature crystallization test, the manufacturer may choose to provide certificates from low-temperature crystallization tests performed on identical material within the last year, unless otherwise specified by the Engineer. Low-temperature brittleness and crystallization tests shall not be required for Grades 0 and 2 materials, unless especially requested by the Engineer.

Every finished bearing shall be visually inspected in accordance with the provisions of Article 18.2.5.5, "Visual Inspection of the Finished Bearing."

Every steel-reinforced bearing shall be subjected to the short-term load test specified in Article 18.2.5.6, "Short-Duration Compression Tests on Bearings."

From each lot of bearings designed under the *AASHTO LRFD Bridge Design Specifications*, 1994, a random sample shall be subjected to the long-term load test specified in Article 18.2.5.7, "Long-Duration Compression Tests on Bearings." The sample shall consist of at least one bearing chosen randomly from each size and material batch and shall comprise at least 10 percent of the lot. If one bearing of the sample fails, all the bearings

SPECIFICATIONS	COMMENTARY
18.2.5.6 SHORT-DURATION COMPRESSION TESTS ON BEARINGS	C18.2.5.6
The bearing shall be loaded in compression to 150 percent of its rated service load. If a rotational element exists, a tapered plate shall be introduced in the load train so that the bearing sustains the load at the maximum simultaneous design rotation. The load shall be held for five minutes, removed, then reapplied for a second period of five minutes. The bearing shall be examined visually while under the second loading. If the load drops below the required value during either application, the test shall be restarted from the beginning. The bearing shall be rejected if: • the bulging pattern suggests laminate parallelism, • a layer thickness is outside the specified tolerances, • a poor laminate bond exists, or • three or more separate surface cracks greater than 2 mm wide and 2 mm deep exist.	The bulging pattern provides a means of checking gross defects in fabrication. This proof-load test is only an approximate indicator of bearing quality, and it may both allow a few low-quality bearings into service, as well as cause the rejection of a small number of bearings that would have performed adequately. However, the latter is a small price to pay for detecting most major fabrication defects. It is important because only surface hardness and external dimensions can be checked with any ease once the bearing has been delivered.
18.2.5.7 LONG-DURATION COMPRESSION TESTS ON BEARINGS	C18.2.5.7
The long-term compression test shall be conducted as specified in Article 18.2.5.6, "Short-Duration Compression Tests on Bearings," except that the second load shall be maintained for 15 hours. The bearing shall be visually examined at the end of the test while still under load. If any patterns or cracks specified in Article 18.2.5.6, "Short-Duration Compression Tests on Bearings," occur, the bearing shall be rejected.	Delamination is the most common defect, and the 15-hour compression test is more likely to show it than is the 5-minute test. Because the 15-hour test is more time-consuming, it may be done on a random sample of the bearing lot, but the press production time that it uses may be minimized if it is conducted overnight. Bearings made from Grade 4 or Grade 5 elastomers are to be subjected to the same test because achieving the necessary low-temperature properties requires special compounding that could place other properties such as bond at risk if it is not done properly. The 15-hour load test may also be used to resolve differences arising from the failure of a bearing to pass a lower level test.
18.2.5.8 SHEAR MODULUS TESTS ON MATERIAL FROM BEARINGS	C18.2.5.8
The shear modulus of a material in the finished bearing shall be evaluated by testing a specimen cut from it using the apparatus and procedure described in Annex A, amended where necessary in Tables 18.2.3.1–1 or 18.2.3.1–2 or, at the discretion of the Engineer, a comparable nondestructive stiffness test may be conducted on a pair of finished bearings. The shear modulus shall fall within 15 percent of the specified value. If no shear modulus is specified in the contract documents, the range for	The shear test provides a check on the material properties from the body of the bearing. Specially molded samples, such as those used in the material quality control tests, are much smaller than the finished bearing and so may require different curing times and temperatures. Specimens cut from the finished bearing provide a comparison with the material quality control samples. Article 14.7.5.2 is located in "Material Properties" in the *AASHTO LRFD Bridge Design Specifications*, 1994.

SPECIFICATIONS **COMMENTARY**

hardness shall conform to the *AASHTO LRFD Bridge Design Specifications*, Article 14.7.5.2. If the test is conducted on finished bearings, the material shear modulus shall be computed from the measured shear stiffness of the bearings, taking due account of the influence on shear stiffness of bearing geometry and compressive load.

18.2.6 Installation

Elastomeric bearings without external load plates may be placed directly on a concrete or steel surface provided that it is flat to within a tolerance of 0.005 of the nominal dimension for steel-reinforced bearings and 0.01 of the nominal dimension for others. Bearings shall be placed on surfaces that are horizontal to within 0.01 radians. Any lack of parallelism between the top of the bearing and the underside of the girder that exceeds 0.01 radians shall be corrected by grouting or as otherwise directed by the Engineer.

Exterior plates of the bearing shall not be welded unless at least 40 mm of the steel exists between the weld and the elastomer. In no case shall the elastomer or the bond be subjected to temperature higher than 200°C.

C18.2.6

If the bearing seat is not horizontal, gravity loads will cause shear in the elastomer. The underside of the girder and the top surface of the bearing must also be parallel to avoid imposing excessive rotation and the stresses it causes in the bearing.

Welding to load plates should be avoided if possible. If it must be done, proper precautions should be taken to avoid damaging the bond by heat.

Very smooth slick surfaces should be avoided when friction is expected to keep the bearing in position. Roughened concrete and sandblasted steel provide good contact surfaces for bearings without bonded sole plates (mounting plates).

The concrete surface at the abutment should have a roughened surface typical of a wood-trowel finish for bearings without sole plates

18.3 POT AND DISC BEARINGS

18.3.1 General

Pot and disc bearings:

- shall be adequate for the design loads and movements shown in the contract documents or specified, and
- shall be tested at the appropriate level.

18.3.2 Materials

18.3.2.1 GENERAL

All materials shall be new and unused, with no reclaimed material incorporated in the finished bearing.

18.3.2.2 STEEL

All steel except stainless steel components of the pot and disc bearing shall conform to the requirements of Article 11.3, "Materials," for carbon steel or high-strength low-alloy structural steel for welding.

APPENDIX E

AASHTO M251 REVISED—STANDARD SPECIFICATION FOR PLAIN AND LAMINATED ELASTOMERIC BRIDGE BEARINGS

Note: A ? (question mark) means that further work is needed to change the provision noted.

Standard Specification
for

Plain and Laminated Elastomeric Bridge Bearings

AASHTO DESIGNATION: M 251-~~97~~ -00(DRAFT)

1. SCOPE

1.1 This specification covers the material requirements for plain and laminated elastomeric bridge bearings. Elastomeric bearings furnished under this specification shall adequately provide for thermal expansion and contraction, rotation, camber changes, and creep and shrinkage, where applicable, of structural members. Elastomeric bearings as herein defined shall include plain pads (consisting of elastomer only) and laminated bearings with steel or fabric laminates.

2. REFERENCED DOCUMENTS

2.1 *AASHTO Standards:*

2.1.1 M 183M/M 183 Structural Steel
R 11 Indicating Which Places of Figures are to Be Considered Significant in Specified Limiting Values
T 67 Standard Practices for Force Verification of Testing Machines

2.1.2 *Standard Specifications for Highway Bridges*

2.2 *ANSI Standards:*

ANSI B46.1 Surfaces and Surfacing

2.3 *ASTM Standards:*

A 570M Hot-Rolled Carbon Steel Sheet and Strip, Structural Quality
~~D 395 Rubber Property—Compression Set~~
D 412 Rubber Properties in Tension
D 429 Rubber Property—Adhesion to Rigid Substrates
~~D 573 Rubber—Deterioration in Air Oven~~
~~D 1043 Stiffness Properties of Plastics as a Function of Temperature Torsion Test~~
~~D 1149 Rubber Deterioration—Surface Ozone Cracking in a Chamber (Flat Specimens)~~
~~D 2137 Rubber Property—Brittleness Point of Flexible Polymers and Coated Fabrics, Test for~~
D 2240 Rubber Property—Durometer Hardness
D 4014 Specification for Plain and Steel-Laminated Elastomeric Bearings for Bridges

2.4 *Rubber Manufacturer's Association, Inc.:*

RMA F 3
RMA T.063
RMA F 2

2.5 *Steel Structures Painting Council Specifications:*

SSPC, Vis 1-89, Visual Standard for Abrasive Blast Cleaned Steel

3. GENERAL REQUIREMENTS

3.1 All bearings shall be designed in accordance with specifications contained in the latest edition of the AASHTO *Standard Specifications for Highway Bridges.*

3.2 The dimensions of the furnished bearings shall be the dimensions required by the design documents within the tolerances shown in Section 6 of this specification. The bearings shall be composed of the specified materials; shall be tested at the appropriate level; and shall satisfy any special requirements of the purchaser.

3.3 The contractor shall provide the purchaser with written notification 30 days prior to the start of bearing production. This notification shall include the contract number, quantity, and size bearings being produced, manufacturer's name, location, and the representative who will coordinate production, inspection, sampling, and testing with the purchaser.

3.4 Testing for the physical properties of the elastomer may require the destruction of one or more bearings from a lot. In these instances, provisions should be made to provide additional bearings for testing purposes.

3.5 In addition to material requirements for the bearings individual components, this specification provides ~~for two levels of~~ acceptance criteria for finished bearings. ~~Level I acceptance criteria is~~ applied to all bearings without exception. Level II acceptance criteria involves additional testing and, unless otherwise specified by the purchaser, shall be applied to the following:

3.5.1 All bearings designed to accommodate compressive loads in excess of 6900 kPa and be subjected to shear deformation.

3.5.2 All other bearings designed to accommodate compressive loads in excess of 7600 kPa.

3.5.3 In addition, the purchaser may require Level II testing for bearings considered to be more critical or bearings for which Level I testing was inconclusive.

3.6 For bearings that will be expected to perform at lower temperatures, an optional low temperature shear test requirement is included ~~in the Level I testing.~~

DRAFT REVISION

4. MATERIALS

4.1 *Properties of the Elastomer*—The elastomer compound used in the construction of these bearings shall contain only virgin crystallization resistant polychloroprene (neoprene) or virgin natural polyisoprene (natural rubber) as the raw polymer. All materials shall be new with no reclaimed material incorporated in the finished bearing.

4.2 The cured elastomer shall meet the minimum requirements of Table 1. The properties of the cured elastomeric compound material listed in Table 1 shall be determined using samples taken from actual bearings.

4.3 All material tests shall be carried out at 23 ± 2°C unless otherwise noted.

4.4 For the purpose of determining conformance with this specification, an observed or calculated value shall be rounded off to the nearest 100 kPa for tensile strength, to the nearest 10 percent of elongation, and to the nearest 1 percent for change in aged tensile and aged elongation. Hardness and aged hardness shall be rounded off to nearest point in accordance with AASHTO R 11.

4.5 *Steel Laminates*—Steel laminates used for reinforcement shall be made from rolled mild steel conforming to AASHTO M 183M/M 183, ASTM A 570M, or equivalent, unless otherwise specified by the purchaser. The laminates shall be of the thickness specified by the purchaser or, if left unspecified, have a minimum nominal thickness of 1.52 mm. Holes in plates for manufacturing purposes shall not be permitted unless considered in the design of the bearing.

4.6 External load bearing plates shall conform to the requirements of AASHTO M 183M/M 183, unless otherwise specified in the contract documents. Except as noted, all bearings surfaces of external load plates shall be finished or machined flat within 0.25 mm. The bottom surfaces of external load plates (masonry plates) designed to rest on bearing pads shall not exceed an out-of-flatness value of 1.59 mm. The external load bearing plates shall be protected from rust until all exposed surfaces can be field painted. Any rust inhibitor utilized must be removed from all surfaces to be welded prior to welding.

4.7 *Fabric Laminates*—Fabric laminates shall be woven from 100 percent glass fibers of "E" type yarn with continuous fibers. The minimum thread count in either direction shall be 10 threads per cm. The fabric shall have either a crowfoot or an 8-harness satin weave. Each ply of fabric shall have a minimum breaking strength of 140 kN/m of width in each thread direction.

5. FABRICATION

5.1 Bearings with steel laminates shall be cast as a unit in a mold and bonded and vulcanized under heat and pressure. The molds shall have standard shop practice mold finish. The internal steel laminates shall be blast cleaned to

0.01 MPa for shear modulus

0.55 0.80 1.10 0.55 0.80 1.10 MPa

See Sect 8.9.2

TABLE 1 Elastomer Properties

Material Property	ASTM Standard	Test Requirements	Polyisoprene (Natural Rubber) 50 Duro	60 Duro	70 Duro	Polychloroprene (Neoprene) 50 Duro	60 Duro	70 Duro	Units
Physical properties	D 2240	Hardness	50 ± 5	60 ± 5	70 ± 5	50 ± 5	60 ± 5	70 ± 5	Shore "A" points
	D 412	Min tensile strength	15.5	15.5	15.5	15.5	15.5	15.5	MPa
		Min ultimate elongation	450	400	300	400	350	300	Percent
Heat resistance	D 573 at specified temp.	Specified temperature of the test	70	70	70	100	100	100	°C
		Aging time	168	168	168	70	70	70	Hours
		Max change in durometer hardness	+ 10	+ 10	+ 10	+ 15	+ 15	+ 15	Shore "A" points
		Max change in tensile strength	− 25	− 25	− 25	− 15	− 15	− 15	Percent
		Max change in ultimate elongation	− 25	− 25	− 25	− 40	− 40	− 40	Percent
Compression set	D 395 Method B at specified temp.	Specified temperature of test	70	70	70	100	100	100	°C
		Max permissible change (after 22 hrs.)	25	25	25	35	35	35	Percent
Low temperature brittleness	D 746 Procedure B	Grades 0 & 2 - No test required							
		Grade 3 Test @ −40°C	Passes	Passes	Passes	Passes	Passes	Passes	
		Grade 4 Test @ −48°C	Passes	Passes	Passes	Passes	Passes	Passes	
		Grade 5 Test @ −57°C	Passes	Passes	Passes	Passes	Passes	Passes	
Ozone Resistance	D 1149	Concentration of ozone during test	25	25	25	100	100	100	MPa
		Duration of test	48	48	48	100	100	100	Hours
		Tested at 20-percent strain 37.7°C ± 1°C, mounting procedure D 518, procedure A	No Cracks	No Cracks	No Cracks	No Cracks	No Cracks	No Cracks	

Shear modulus

Must be established

DRAFT REVISION

and a recommended edge cover of 6 mm.

a condition matching that of SSPC-Vis 1-89, Pictorial Standard BSP6 or CSP6 and additionally cleaned of any oil or grease before bonding. Plates shall be free of sharp edges and burrs, and shall have a minimum edge cover of 3 mm. External load plates (sole plates) shall be protected from rusting by the manufacturer, and shall be hot bonded to the bearing during vulcanization. Bearings with steel laminates which are designed to act as a single unit with a given shape factor must be manufactured as a single unit.

5.2 Fabric-laminated bearings may

The following equation may be used to define shim-tolerance limits when tolerance 3.(±3mm) is exceeded:

$$7.5\theta + \frac{v}{h_r} \le 0.35 \qquad \text{provided} \quad \theta \le 0.02$$

where θ (radians) and v (mm) are absolute values of shim rotation and vertical displacement. If the specified layer elastomeric layer thickness is h_r, the bearing length is L, and H_1 and H_2 are the measured maximum and minimum thicknesses at the edges of the layer, then $v = |h_r - 0.5(H_1+H_2)$ and $\theta = |(H_1-H_2)/2L|$ for interior layers and $\theta = |(H_1-H_2)/L|$ for top and bottom layers.provided that the minimum elastomer layer thickness $H_2 \ge 5$ mm. Bearings with tolerances that satisfy this equation must also satisfy the compression test in Sect. 8.8.2 or the inclined compression test in Annex A.

the materials, and shall produce a smooth finish to ANSI B46.1, 6.3 μm. Plain pads shall be molded or extruded to the finished thickness. Fabricators will not be allowed to make pads of finished thickness by plying pads of lesser thickness together. External load plates, when used, shall be protected from rusting by the manufacturer, and shall be hot bonded by vulcanization during the primary molding process.

5.4 Flash tolerance, finish, and appearance of bearings shall meet the requirements of the latest edition of the *Rubber Handbook* as published by the Rubber Manufacturers Association, Inc., RMA F 3 and T.063 for molded bearings and RMA F 2 for extruded bearings.

6. TOLERANCES

6.1 Plain pads and laminated bearings shall be manufactured to the design dimensions tolerances listed in Table 2, unless other tolerances are shown on the design drawings.

7. MARKING

7.1 Each elastomeric bearing shall be marked in indelible ink or flexible paint. The marking shall consist of the order number, lot number, bearing identification number, and elastomer type and grade. Unless otherwise specified in the contract documents, the marking shall be on a face which is visible after erection of the bridge.

8. BEARING TESTING AND ACCEPTANCE CRITERIA

or less fabric-laminated bearings of different plan size if cut from a large sheet or sheets meeting these requirements.

8.3 The manufacturer shall designate the bearings in each lot and certify that each of the bearings in the lot were manufactured in a reasonably continuous manner from the same batch of elastomer, and cured under the same conditions. In addition, the manufacturer shall certify that each bearing in the lot satisfies the requirements of the design specification and meets the dimensional tolerances of Section 6 of this specification.

8.4 The dimensions of each bearing shall be checked. If any dimensions are outside the limits listed in Section 6 of this specification, the lot shall be rejected.

8.5 The purchaser shall select sam- lot for testing in ecification. Sam- ollows: ee full size bear-

—One full size r lot, a minimum

n from the sam- sted for conform- nents of Section ation. If the sam- neet any of these hall be rejected. ng shall be conducted on the sampled bearings. ~~The acceptance criteria shall be at two levels. Level I acceptance shall be applied to all bearings. Level II acceptance criteria,~~

TABLE 2 Tolerances

	mm
1. Overall vertical dimensions:	
Design thickness 32 mm or less	−0, +3
Design thickness over 32 mm	−0, +6
2. Overall horizontal dimensions:	
For measurements 914 mm and less	−0, +6
For measurements Over 914 mm	−0, +12
3. Thickness of individual layers of elastomer (laminated bearings only) at any point within the bearing	~~±20 percent of design value but no more than~~ ±3 mm
4. Variation from a plane parallel to the theoretical surface: (as determined by measurements at the edge of the bearings):	
Top	Slope relative to the bottom of no more than 0.005 radians
Sides	6
5. Position of exposed connection members	±3
6. Edge cover of embedded laminates of connection members	−0, +3
7. Size of holes, slots, or inserts	±3
8. Position of holes, slots, or inserts	±3

DRAFT REVISION

unless otherwise specified by the purchaser, shall be applied to the following:

8.7.1 All bearings designed to accommodate compressive loads in excess of 6900 kPa and be subjected to shear deformation.

8.7.2 All other bearings designed to accommodate compressive loads in excess of 7600 kPa.

8.7.3 In addition, the purchaser may require Level II testing for bearings considered to be more critical or bearings for which Level I testing was inconclusive. Level I and Level II tests may be performed by the manufacturer, by the purchasing agency or by an outside independent laboratory subject to the approval of the purchaser. If testing is performed by the manufacturer or an independent laboratory, certified test results shall be provided. Regardless of the agency designated to test the pads, the purchaser reserves the right to obtain test samples from the bearings for confirming test results.

8.8 Level I criteria shall include the following requirements:

8.8.1 Each sampled bearing shall be tested to determine compressive strain at the maximum design compressive load in accordance with Section 9.1 of this specification. If the resultant compressive strain exceeds 0.10, the lot shall be rejected.

8.8.2 Each sampled bearing shall be subjected to a compressive load equal to 1.5 times the maximum design load. The load shall be held for 5 minutes, removed, and reapplied for a second period of 5 minutes. The bearing shall be visually examined while under the second loading. If the bearing exhibits three separate surface cracks which are greater than 2 mm wide and 2 mm deep or a single crack (deeper) or wider than 6 mm, the lot shall be rejected. For laminated bearings, if bulging patterns imply laminate placement which does not satisfy design criteria and manufacturing tolerances or if bulging suggests poor laminate bond, the lot shall be rejected.

8.8.3 For laminated bearings, a minimum of one sampled bearing per lot shall be tested for bond strength in accordance with Section 9.2 of this specification. Fabric reinforced pads shall have a minimum bond strength of 5.2 kN/m and steel reinforced pads a strength of 6.9 kN/m. If the testing bearing fails to meet the required minimum bond strength, the lot shall be rejected.

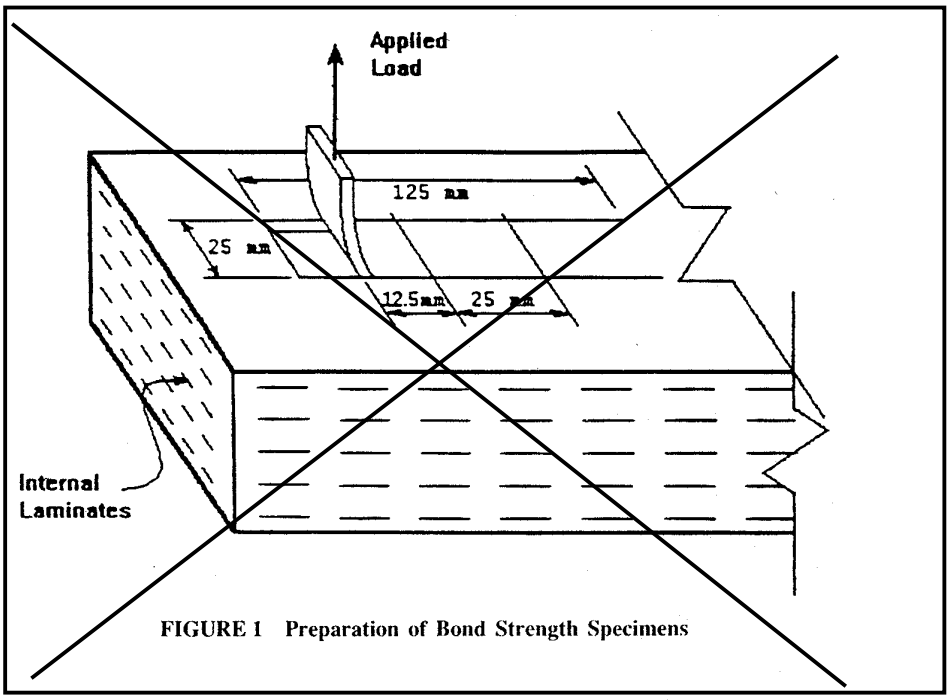

FIGURE 1 Preparation of Bond Strength Specimens

8.8.4 When required by the purchaser, a minimum of two pads per lot shall be tested for low temperature shear in accordance with the purchaser's requirements and Section 9.3 of this specification. Maximum allowable shear stresses will depend on the temperature at which the bearings are conditioned and the hardness of the elastomer. For bearings conditioned at −29° C and constructed with 50 durometer elastomer, shear stress shall not exceed 345 kPa for bearings constructed with polychloroprene (neoprene) or 207 kPa for bearings constructed with polyisoprene (natural rubber). If the measured shear stress exceeds the specified value, the lot shall be rejected.

8.9 Level II criteria shall include the following requirements:

8.9.1 The pads must meet all Level I criteria.

8.9.2 The shear modulus of the elastomer shall be determined at 23°C ± 1°C in accordance with Annex A1/ASTM D 4014. Shear modulus shall be determined by testing a specimen cut from the sampled bearings. Alternatively, at the purchaser's discretion, a comparable nondestructive stiffness test may be conducted on a pair of sampled bearings. If nondestructive stiffness test is performed, the shear modulus shall be computed from the measured shear stiffness of the bearings, taking into account the influence on shear stiffness of bearing geometry and compressive load. The shear modulus shall be within 15 percent of the value specified value, or within the limits listed in Table 3 for the specified nominal hardness. If shear modulus does not meet the specified minimum value, the lot shall be rejected.

8.9.3 For elastomer grades 2–5, additional shear modulus testing shall be performed on elastomer from the sampled bearings in accordance with Section 9.4 of this specification. If the measured stiffness at the specified temperature exceeds 4 times the stiffness measured at 23° C, the lot shall be rejected.

8.9.4 Elastomer from the sampled bearings shall be tested for instantaneous thermal stiffening in accordance with ASTM D 1043. The elastomer stiffness shall be measured at 23°C and at a lower

3 mm deep

Annex B

Annex A ,Annex B or Annex A1/ASTM D 4014

TABLE 3 Shear Modulus Requirements

Nominal hardness	50	60	70
Shear modulus at 23°C	0.62 – 0.90 MPa	0.90 – 1.40 MPa	1.40 – 2.05 MPa

modified as follows: the initial cycles shall be taken to a strain of 0.7 and on the last cycle the shear modulus shall be determined at 0.5 strain.

temperature corresponding to the specified grade of elastomer. The lower test temperatures for the various grades of elastomer shall be as follows:

Grades 0 & 2 Test @ −32°C
Grade 3 Test @ −40°C
Grade 4 Test @ −46°C
Grade 5 Test @ −54°C

If the stiffness of the elastomer measured at the specified lower temperature is more than four times the stiffness of the elastomer measured at 23°C, the lot shall be rejected.

~~**8.9.5** A sampled bearing from each lot of bearings shall be subjected to a long term compression test. This test shall be conducted in accordance with the requirements of Section 8.8.2 of this specification except that the second load shall be maintained for 15 hours. If the load drops below 90 percent of its target value during this time, the load shall be increased to the target value and the test duration shall be increased by the time for which the load was below the required value. The bearing shall be visually examined at the end of the test while it is still under load. If the bearing exhibits three separate surface cracks which are greater than 2 mm wide and 2 mm deep or a single crack deeper or wider than 6 mm, the lot shall be rejected. For laminated bearings, if bulging patterns imply laminate placement which does not satisfy design criteria and manufacturing tolerances or if bulging suggests poor laminate bond, the lot shall be rejected.~~

8.9.6 The purchaser may require more severe testing of pads such as fatigue or test to failure ~~under Level II criteria.~~

9. TESTS

9.1 *Determination of Compression Strain at Maximum Design Load:*

9.1.1 The bearing to be tested shall be placed in a test machine capable of applying a compressive load equal to the bearings maximum design dead plus live service load.

9.1.2 A pair of deflectometers shall be placed on opposite sides of the bearing in the test machine. The deflectometers shall be located as near as possible to the center of the bearing.

9.1.3 The bearing shall be loaded at a rate of 520 kPa/min. to a compression stress equal to 5 percent of the bearing's maximum design dead plus live service load. The 5 percent load shall be maintained for two minutes. At the end of the two minutes, the deflectometer readings shall be recorded.

9.1.4 The compressive load shall be increased at a rate of 520 kPa/min. to a compressive stress equal to the bearing's maximum design dead plus live service load. The load shall be maintained for a period of two minutes, at the end of which the deflectometer readings shall be recorded.

9.1.5 The total compressive deflection between the two loadings shall be calculated for each deflectometer. The bearing's compressive strain shall be calculated as the average of the compressive deflections indicated by the two deflectometers divided by the design effective rubber thickness of the tested bearing.

9.2 *Determination of Bond Strength:*

9.2.1 Bond strength shall be determined in accordance with ASTM D 429 Method B as modified herein.

9.2.2 The bond test shall be performed on sampled bearings by cutting the required strip from an elastomer layer bonded to an internal laminate. The strip size shall be 25 mm wide, 125 mm long, and at least 6.3 mm thick.

9.2.3 Peeling of the elastomer strip from the internal laminate shall be initiated by carefully cutting the elastomer back to create a tab long enough to install in the grips of the testing machine.

9.2.4 Draw lines across the strip 12.5 mm and 37.5 mm from where the peeled portion of the strip meets the internal laminate (see Figure 1). Install the specimen in the grips so that the angle between the elastomer tab and the surface of the bearing will be approximately 90° for the duration of the test.

9.2.5 Apply the tensile load at the required rate until the elastomer peels back beyond the 37.5 mm mark while recording the load as required. If the load reaches 270 N without the elastomer starting to peel from the laminate surface, end the test and record the bond strength as 10.5 ± kN/m. If the elastomer peels back to the 37.5 mm mark without reaching 270 N of load, record the bond strength as the average load in kilonewtons per meter of width required to peel the elastomer between the marks. If the elastomer tab rips off the bearing before reaching the 37.5 mm mark or reaching 270 N of load, retest in another area of the bearing.

9.3 *Low Temperature Shear Test:*

9.3.1 Two bearings shall be conditioned at a specified temperature for 96 ± 1 hours. Unless otherwise specified by the purchaser, the conditioning temperature shall be −29°C ± 0.5°C. After conditioning, the bearings shall be placed in a compression machine such that one bearing is on top of the other bearing with the top bearing upside down.

9.3.2 The bearings shall be loaded in compression to a stress of 3400 kPa based on the design net internal laminate area of the bearing.

9.3.3 The bearings shall be sheared to a total strain equivalent to 25 percent of the design effective rubber thickness. Shear stress, based on the design net plan area of the elastomer shall be recorded 15 minutes after reaching 25 percent shear strain. The total time lapse between removal from the conditioning environment and completion of the test shall not exceed 30 minutes.

9.4 *Additional Shear Modulus Testing for Elastomer Grades 2–5:*

9.4.1 Shear modulus testing shall be performed as described in Annex A1 of ASTM D 4014 except as modified below.

9.4.2 The test specimens shall be taken from sampled bearings. After preparing the test specimen, it shall be conditioned for a period of time at a specified temperature. Conditioning times and temperatures for the various elastomer grades shall be as follows:

Grade 2–7 days @ −18°C
Grade 3–14 days @ −26°C
Grade 4–21 days @ −37°C
Grade 5–28 days @ −37°C

9.4.3 Shear modulus testing shall be performed with the test specimen in an enclosed freezer unit capable of maintaining the specified conditioning temperature. A ±25 percent strain cycle shall be applied with a period of 100 seconds. The first $^3/_4$ cycle of strain shall be discarded and the stiffness shall be determined by the slope of the force deflection curve for the next $^1/_2$ cycle of loading.

Insert Appendices A, C,and D as Annex A, , Annex C and Annex B

The **Transportation Research Board** is a unit of the National Research Council, which serves the National Academy of Sciences and the National Academy of Engineering. The Board's mission is to promote innovation and progress in transportation by stimulating and conducting research, facilitating the dissemination of information, and encouraging the implementation of research results. The Board's varied activities annually draw on approximately 4,000 engineers, scientists, and other transportation researchers and practitioners from the public and private sectors and academia, all of whom contribute their expertise in the public interest. The program is supported by state transportation departments, federal agencies including the component administrations of the U.S. Department of Transportation, and other organizations and individuals interested in the development of transportation.

The National Academy of Sciences is a private, nonprofit, self-perpetuating society of distinguished scholars engaged in scientific and engineering research, dedicated to the furtherance of science and technology and to their use for the general welfare. Upon the authority of the charter granted to it by the Congress in 1863, the Academy has a mandate that requires it to advise the federal government on scientific and technical matters. Dr. Bruce M. Alberts is president of the National Academy of Sciences.

The National Academy of Engineering was established in 1964, under the charter of the National Academy of Sciences, as a parallel organization of outstanding engineers. It is autonomous in its administration and in the selection of its members, sharing with the National Academy of Sciences the responsibility for advising the federal government. The National Academy of Engineering also sponsors engineering programs aimed at meeting national needs, encourages education and research, and recognizes the superior achievements of engineers. Dr. William A. Wulf is president of the National Academy of Engineering.

The Institute of Medicine was established in 1970 by the National Academy of Sciences to secure the services of eminent members of appropriate professions in the examination of policy matters pertaining to the health of the public. The Institute acts under the responsibility given to the National Academy of Sciences by its congressional charter to be an adviser to the federal government and, upon its own initiative, to identify issues of medical care, research, and education. Dr. Kenneth I. Shine is president of the Institute of Medicine.

The National Research Council was organized by the National Academy of Sciences in 1916 to associate the broad community of science and technology with the Academy's purpose of furthering knowledge and advising the federal government. Functioning in accordance with general policies determined by the Academy, the Council has become the principal operating agency of both the National Academy of Sciences and the National Academy of Engineering in providing services to the government, the public, and the scientific and engineering communities. The Council is administered jointly by both the Academies and the Institute of Medicine. Dr. Bruce M. Alberts and Dr. William A. Wulf are chairman and vice chairman, respectively, of the National Research Council.

Abbreviations used without definitions in TRB publications:

AASHO	American Association of State Highway Officials
AASHTO	American Association of State Highway and Transportation Officials
ASCE	American Society of Civil Engineers
ASME	American Society of Mechanical Engineers
ASTM	American Society for Testing and Materials
FAA	Federal Aviation Administration
FHWA	Federal Highway Administration
FRA	Federal Railroad Administration
FTA	Federal Transit Administration
IEEE	Institute of Electrical and Electronics Engineers
ITE	Institute of Transportation Engineers
NCHRP	National Cooperative Highway Research Program
NCTRP	National Cooperative Transit Research and Development Program
NHTSA	National Highway Traffic Safety Administration
SAE	Society of Automotive Engineers
TCRP	Transit Cooperative Research Program
TRB	Transportation Research Board
U.S.DOT	United States Department of Transportation

THE NATIONAL ACADEMIES

Advisers to the Nation on Science, Engineering, and Medicine

National Academy of Sciences
National Academy of Engineering
Institute of Medicine
National Research Council